

Characterisation of ^{L597V}BRAF in cancer

Thesis submitted for the degree of

Doctor of Philosophy

At the University of Leicester

by

Lai-Kay Maggie Cheung (BMedSci. Hons. University of Birmingham)

Department of Biochemistry

University of Leicester

February 2013

Abstract

Characterisation of ^{L597V}BRAF in cancer

Lai-Kay Maggie Cheung

BRAF is a component of the RAF/MEK/ERK signalling cascade which controls fundamental cellular activities, including proliferation, cell survival, differentiation and motility. Deregulation of this pathway is common in cancer and ~7% of cancers have a mutation in *BRAF*. Leu597 is the fifth most commonly mutated residue in *BRAF*-mutated human cancers, and a substitution to a valine is one of only seven *BRAF* mutations that are found in both cancer and a group of developmental syndromes known as RASopathies. A major question is how the mutation can be associated with both diseases. In this study, using an autochthonous model and HEK 293^T cells, ^{L597V}BRAF was shown to have weak kinase and MEK/ERK-inducing activity. It did not induce morphological transformation or foci formation, nor confer a growth advantage or induce early immortalisation. Therefore, the mutation was found not to be a driver oncogene. ^{L597V}*BRAF* mutations are found to co-exist with other oncogenic mutations in human cancer. Using cells derived from a conditional knock-in mouse model, we showed that ^{L597V}Braf synergises with ^{G12D}Kras to induce cell changes more reminiscent of the high activity mutant ^{V600E}Braf. Double mutant ^{L597V}Braf and ^{G12D}Kras cells have higher Braf and Craf kinase activity than single mutants, which translates to higher Mek/Erk activity to a similar level to ^{V600E}Braf. These cells were more morphologically transformed than Braf^{+/L597V} and Kras^{+/G12D} cells alone. RAF inhibitors induced paradoxical activation of Erk in ^{L597V}Braf-expressing cells, and this was shown to be through heterodimerisation and activation of Craf. These results caution against the use of RAF inhibitors in treatment of RASopathy and cancer patients with the ^{L597V}*BRAF* mutation. Aged Braf^{+/L597V} mice developed some predisposition to tumour formation. The tumours were benign, and one out of eight tumours was heterozygous for ^{Q61L}*Hras*. This supports the idea that ^{L597V}BRAF is insufficient to induce cancer, but epistatically modifies other oncogenes to promote cancer progression by hyperactivation of the Erk pathway.

Acknowledgements

I would like to express my very great appreciation to my supervisor Professor Catrin Pritchard. Words cannot express my gratitude for the support, patient guidance, enthusiastic encouragement and expertise during the planning and development of this research work.

I would also like to thank my committee members Professor Andrew Fry and Dr Kayoko Tanaka for their encouragement, insightful comments and wise suggestions.

I am indebted to Dr Catherine Andreadi who has always been available for help and guidance. I have really enjoyed her company and really really appreciate the emotional support.

I would like to thank Ellie Karekla, Maria Aguilar-Hernandez, Pooyeh Farahmand, Hong Jin, Tamihiro Kamata and all past and present members of lab 3/43. Particular thanks go to Susan Giblett and Bipin Patel for help and assistance, and for creating a livelier atmosphere in the lab.

I would also like to thank Jenny Edwards for her histology expertise.

I wish to thank Ellie, not for the pinching, tripping and slapping, but for being a great friend and for providing delicious Cypriot food including chicken soup and a place to stay.

This thesis is dedicated to my parents and brothers for their continued support and encouragement throughout my study.

Abbreviations

AP-1	activating protein-1
ATF	activating transcription factor
bZIP	basic region leucine zipper
CDC42	cell-division cycle 42
CFC	Cardiofaciocutaneous syndrome
CRD	cysteine-rich domain
CRE	cAMP-responsive element
DNA	deoxyribonucleic acid
DUSP	dual specificity phosphatase
E	embryonic day
EMT	epithelial mesenchymal transition
ERK	extracellular-signal-regulated kinases
GAP	GTPase-activating protein
GEF	guanine nucleotide-exchange factor
HCC	hepatocellular carcinoma
HGF	hepatocyte growth factor
kDa	kilodalton(s)
KIM	kinase interaction motif
KSR	kinase suppressor protein
JMML	juvenile myelomonocytic leukaemia
LB	Luria Bertani
MAPK	mitogen-activated protein kinase
MAPKK	mitogen-activated protein kinase kinase
MAPKKK	mitogen-activated protein kinase kinase kinase

MBP	myelin-basic protein
MEF	mouse embryonic fibroblast
MKP	MAPK phosphatase
mRNA	messenger ribonucleic acid
NF1	neurofibromin 1 gene
NSCLC	non-small cell lung carcinoma
p90 ^{RSK}	p90 ribosomal S6 kinase
PAK	p21-activated kinase
PCR	polymerase chain reaction
PDK1	3-phosphoinositide-dependent protein kinase-1
PI3K	phosphatidylinositol 3-kinase
P-loop	glycine-rich ATP-phosphate-binding loop
PP2A	protein phosphatase 2
pRb	Retinoblastoma protein
RBD	Ras binding domain
RHO	Ras homologue
RKIP1	RAF kinase inhibitor protein 1
RNA	ribonucleic acid
RSK	90K-ribosomal S6 kinase
RTK	receptor tyrosine kinase
SEF	similar expression to FGF
SH2	Src homology-2 domain
SHP2	Src homology-2 domain-containing protein tyrosine phosphatase
siRNA	small interference RNA

SOS	Son of Sevenless
SPRY	sprouty
SPRED	SPROUTY-related enabled/vasodilator-stimulated phosphoprotein homology 1 domain-containing
SRE	serum response element
SRF	serum response factor
TCF	ternary complex factors
TPA	12-O-tetradecanoylphorbol-13-acetate
TRE	phorbol 12-O-tetradecanoate-13-acetate-response element

Contents

Title page	i
Abstract	ii
Acknowledgements	iii
Abbreviations	iv

1. Introduction	1
1.1. Cell signalling and Cancer	1
1.1.1. The Mitogen-Activated Protein Kinase (MAPK) pathway	1
1.1.2. ERK cascade.....	3
1.2. RAF isoforms	5
1.2.1. RAF family members	5
1.2.2. RAF protein structure	9
1.3. Activation of RAF	11
1.3.1. Activation of CRAF	11
1.3.2. Activation of BRAF	13
1.3.3. Different splice forms of BRAF	15
1.3.4. Heterodimerisation of RAFs.....	16
1.4. Downstream of RAF	18
1.4.1. Direct RAF substrates	18
1.4.2. Activation of MEK and ERK	20
1.4.3. Biological effects of ERK	20
1.4.4. Feedback regulation	25
1.5. Cancer	35
1.5.1. Mutations of MAPK pathway components in cancer	37
1.6. <i>BRAF</i> mutants	40
1.6.1. High kinase activity mutants	43
1.6.2. Intermediate kinase activity mutants	46

1.6.3. Impaired kinase activity mutants.....	47
1.7. RASopathies.....	48
1.7.1. Mutations of RAS/RAF pathway	50
1.8. Data on mouse models	54
1.8.1. Cre-LoxP system.....	55
1.8.2. Mouse models of cancer	57
1.8.3. Mouse models of RASopathies	62
1.9. Kinase inhibitors of the RAF/MEK/ERK pathway.....	66
1.9.1. MEK inhibitors	66
1.9.2. RAF inhibitors.....	70
1.9.3. Drug resistance	74
1.10. Aims.....	77
2. Materials and methods	78
2.1. Molecular biology	78
2.1.1. Plasmids.....	78
2.1.2. Transformation into DH5 α	78
2.1.3. Purification of plasmid DNA: Miniprep	80
2.1.4. Purification of plasmid DNA: Maxiprep.....	81
2.1.5. Purification of plasmid DNA: Caesium Chloride preparation	82
2.1.6. Diagnostic restriction digestion of plasmid DNA.....	83
2.1.7. Agarose gel electrophoresis	83
2.1.8. Genotyping.....	83
2.1.9. Sequencing	87
2.2. Cell lines and tissue culture	90
2.2.1. HEK 293 ^T	90
2.2.2. Production and maintenance of Mouse Embryonic Fibroblasts (MEFs)	91
2.2.3. Freezing down stocks of cells.....	91
2.2.4. Thawing out of cells.....	92
2.2.5. Transfection.....	92
2.2.6. Infection with Adenoviral Cre	93
2.2.7. Inhibition of RAF and MEK pathway	94
2.2.8. siRNA knock-down	94
2.2.9. 3T3 immortalisation assay	96
2.2.10. Cell Counting Assay	96
2.2.11. Metaphase spread.....	96
2.2.12. Focus forming assay	97

2.2.13. p53 function analysis	98
2.3. Protein Analysis	98
2.3.1. Preparation of Soluble protein lysates	98
2.3.2. Quantitation of protein lysates	98
2.3.3. Immunoprecipitation of protein lysates	99
2.3.4. SDS-polyacrylamide gel electrophoresis (SDS-PAGE)	100
2.3.5. Western blot – semi-dry transfer	102
2.3.6. Western blot - Treatment with antibodies	102
2.3.7. Quantitation of Western Blot signals	104
2.4. Preparation of RNA for microarray	104
2.5. Histology	106
2.5.1. Harvesting mouse tissue	106
2.5.2. Tissue processing	106
2.5.3. Preparation of glass slides for tissue sections	106
2.5.4. Sectioning of wax-embedded tissue samples	107
2.5.5. Haematoxylin and Eosin staining	107
2.6. Statistical analysis	108
3. Characterisation of ^{L597V}BRAF	109
3.1. Introduction	109
3.1.1. The classes of BRAF mutants	109
3.1.2. Heterodimerisation of BRAF and CRAF	110
3.1.3. Negative regulators of ERK	110
3.1.4. Generation of ^{Braf^{+/Lox-L597V}} mice	111
3.2. Aims	112
3.3. Results	112
3.3.1. ^{L597V} BRAF has intermediate activity towards the MEK/ERK pathway when overexpressed in HEK 293 ^T cells	112
3.3.2. CRAF forms a heterodimer with ^{L597V} BRAF in HEK 293 ^T	115
3.3.3. CRAF suppresses ^{L597V} BRAF-induced MAPK activation	118
3.3.4. Cre-induced recombination of LSL alleles in MEFs	120
3.3.5. ^{L597V} Braf has low kinase activity in MEFs	123
3.3.6. ^{L597V} Braf induces weak Mek/Erk activation in MEFs	125
3.3.7. ^{L597V} Braf does not transform MEFs	128
3.3.8. ^{L597V} Braf does not induce foci formation	130
3.3.9. ^{L597V} Braf does not confer growth advantage on MEFs	133
3.3.10. ^{L597V} Braf does not induce early immortalisation in MEFs	135
3.4. Conclusion	140

4. ^{L597V}Braf co-operates with ^{G12D}Kras	145
4.1. Introduction	145
4.1.1. Co-existence of ^{L597V} BRAF with mutations in other oncogenes in cancer samples	147
4.1.2. ^{G12D} KRAS	149
4.1.3. Generation of Kras ^{+/-Lox-G12D} mice	150
4.2. Aims.....	152
4.3. Results.....	152
4.3.1. Preparation of double mutant MEFs	152
4.3.2. ^{L597V} Braf induces further transformation of Kras ^{+/-G12D} MEFs	155
4.3.3. ^{L597V} Braf enhances ^{G12D} Kras-induced Mek/Erk activation.....	157
4.3.4. ^{L597V} Braf slows the growth rate of Kras ^{+/-Lox-G12D} MEFs	159
4.3.5. ^{L597V} Braf does not affect immortalisation profiles of Kras ^{+/-Lox-G12D} MEFs	162
4.3.6. Transcriptome profiling	166
4.4. Conclusion	169
5. ^{L597V}Braf signals through Braf and Crafa.....	173
5.1. Introduction	173
5.1.1. BRAF inhibitors induce paradoxical activation of the MAPK pathway in RAS-mutant cells	173
5.2. Aim	174
5.3. Results.....	175
5.3.1. ^{L597V} Braf enhances Crafa kinase activity in Kras ^{+/-G12D} MEFs	175
5.3.2. Optimisation of Braf and Crafa knock-down.....	177
5.3.3. Knock-down of Crafa does not affect ^{L597V} Braf signalling.....	181
5.3.4. BRAF inhibitors increase P-Erk and P-Mek in Braf ^{+/-Lox-L597V} and double mutant MEFs.....	185
5.4. Conclusion	191

6. $\text{Braf}^{+/Lox-L597V}$ mice develop tumours with age.....	193
6.1. Introduction	193
6.2. Aims.....	193
6.3. Results.....	193
6.3.1. $\text{Braf}^{+/Lox-L597V}$ mice had a shorter lifespan.....	194
6.3.2. Summary of abnormal growths identified so far	194
6.3.3. Histology of the abnormal growths.....	196
6.3.4. Screening for mutations in <i>Raf</i> and <i>Ras</i>	198
6.4. Conclusion	205
 7. Summary and Discussion	 208
7.1. L597V BRAF	208
7.2. Comparison of the overexpression and endogenous system	209
7.3. L597V Braf is an epistatic modifier of G12D Kras	212
7.4. L597V Braf signals through Braf and Crafa	217
7.5. RAF inhibitors induce paradoxical activation of the Mek/Erk pathway in L597V Braf-expressing cells	218
7.6. Genetic heterogeneity of tumours with the L597V BRAF mutation.....	219
7.7. Future work.....	221
 8. Appendix	 224
9. References	239

1.Introduction

1.1. Cell signalling and Cancer

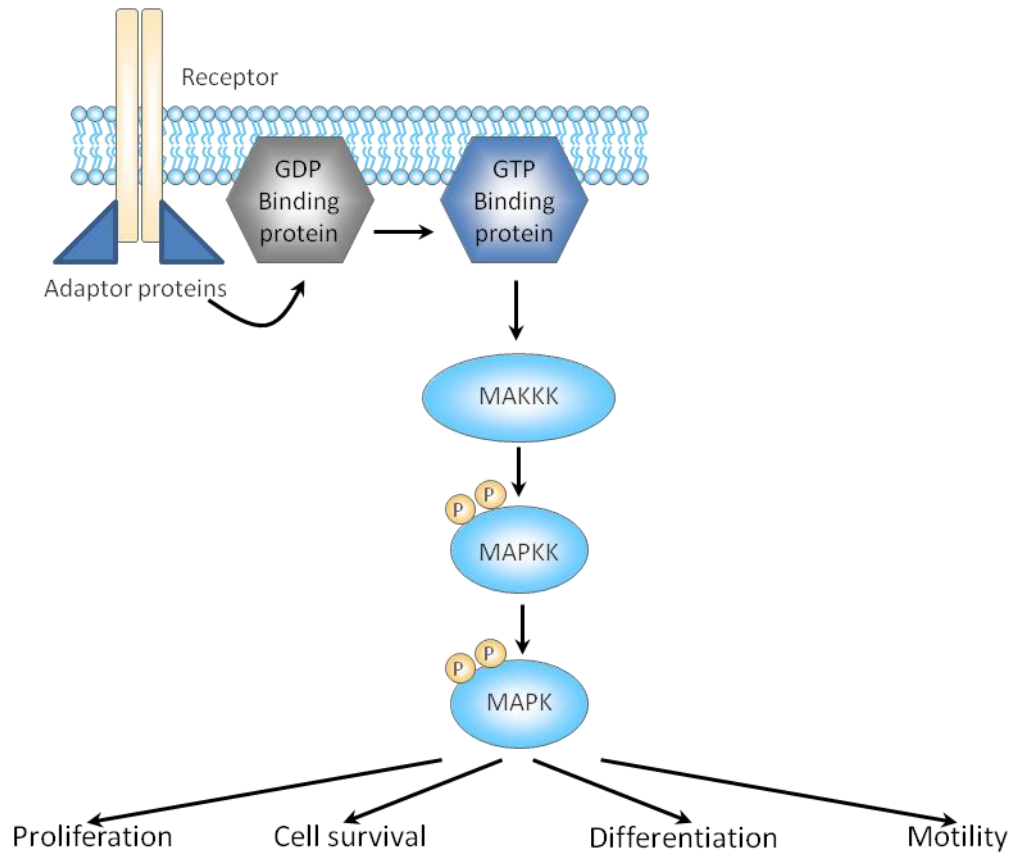
Cells send out and receive signals in response to the cellular environment. The combination of signals control processes such as proliferation, differentiation and apoptosis. The detection of small molecules secreted by neighbouring cells or the contact of plasma membrane-bound molecules involves a change in the cell surface receptor, which leads to a cascade of signalling events and eventually leads to production, modification and/or disruption of proteins that are used within the cell, or produced and secreted to neighbouring cells. Cell signalling pathways that are advantageous to cancer progression are often aberrantly regulated. These are usually pathways involved in control of cell proliferation and survival. One of the most studied pathways is the Mitogen-Activated Protein Kinase (MAPK) pathway, and this plays a critical role in the response of cells to extracellular environment, controlling multiple cellular processes.

1.1.1. The Mitogen-Activated Protein Kinase (MAPK) pathway

The MAPK pathway is a conserved pathway in eukaryotes that controls fundamental cellular activities, including proliferation, cell survival, differentiation and motility (Reviewed by Aksamitiene *et al.*, 2010; Reviewed by Plotnikov *et al.*, 2011). The prototypical MAPK pathway (Figure 1.1) involves a receptor protein, which may be a G-coupled Receptor or Receptor Tyrosine Kinase (RTK).

Figure 1.1 Schematic diagram of MAPK pathway

Extracellular stimulus binding to the receptor induces receptor dimerisation and autophosphorylation leading to activation of small-GTP binding molecules by exchange of GDP for GTP. Activated small GTP-binding proteins lead to the recruitment of MAPKKK to the plasma membrane where it is phosphorylated and activated. MAPKKK then activates MAPKK, and MAPKK activates MAPK which phosphorylates proteins within the cell.



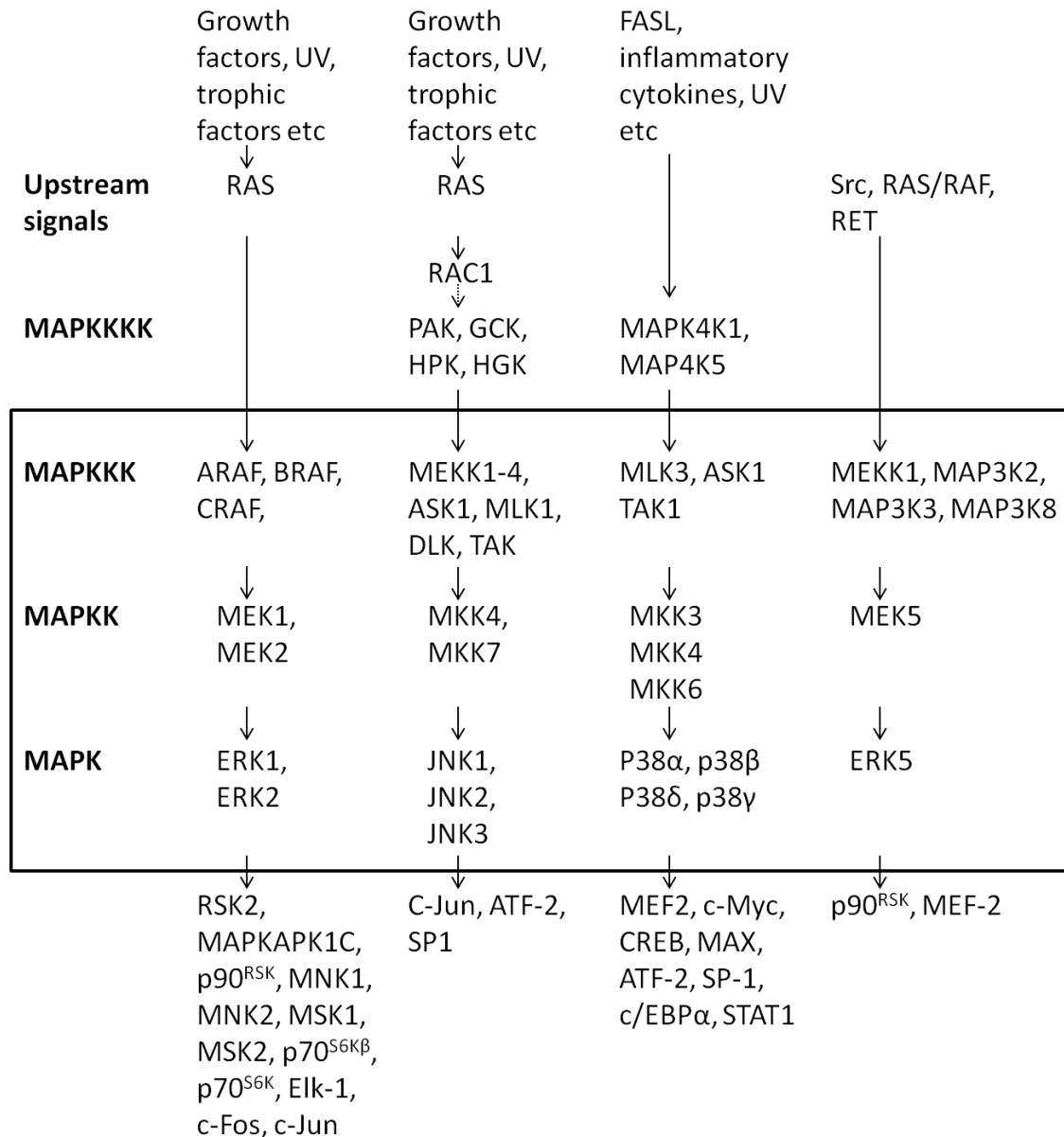
The Ras and Rho family of small GTP-binding proteins include Ras, Rho, Rac and Cdc42. All RTKs stimulate the exchange of GDP for GTP on the small-GTP binding protein RAS by SOS (Bar-Sagi & Hall, 2000; Pawson, 1995; Schlessinger, 1994), and this leads to the phosphorylation and activation of a mitogen-activated protein kinase kinase kinase (MAPKKK). The MAPKKKs are activated in part by phosphorylation of serine/threonine residues. When activated, the MAPKKKs phosphorylate and activate a mitogen-activated protein kinase kinase (MAPKK). MAPKKs are dual-specificity kinases that phosphorylate a Thr-Xxx-Tyr motif in the activation loops of a mitogen-activated protein kinase (MAPK). MAPKs phosphorylate substrates on serine and threonine residues. The main effectors include transcription factors, protein kinases, phospholipases and cytoskeletal-associated proteins. Each step of the cascade amplifies the signal with approximately a 10-fold increase at the end of the cascade (Roskoski, 2012a). Negative regulators at each step suppress this amplification. Several MAPK pathways exist in mammals, including the extracellular signal-regulated kinase 1 and 2 (ERK1/2), p38^{MAPK}, c-Jun N terminal kinase (JNK), and ERK5 pathways (Figure 1.2).

1.1.2. ERK cascade

RAS signals through multiple pathways including ERK, phosphatidylinositol 3-kinase (PI3K) (Rodriguez-Viciano *et al.*, 1994) and RalGDS pathways (Gonzalez-Garcia *et al.*, 2005). The best characterised RAS-induced pathway is the ERK pathway.

Figure 1.2 Multiple MAPK pathways exist (adapted from Yang et al., 2003a).

The major MAPK pathways include the ERK1/2, p38^{MAPK}, JNK and ERK5 pathways. G protein-coupled receptors and growth factor receptors transduce signals from the cell surface directly or via small G proteins such as RAS and RAC through levels of MAPKs. Notably, p21-associated kinases (PAKs) are not MAPKs, but participate in the JNK signalling pathway.



RAS is activated downstream of RTKs and other receptors. The RTK-dependent activation of RAS will be discussed here. The binding of an agonist to a RTK induces their dimerisation and autophosphorylation. Adaptor molecules, for example, Src homology 2 domain containing proteins (Shc) localise to the C-terminus of the activated RTK allowing Grb2 to bind. Grb2 is constitutively bound to the guanine nucleotide-exchange factor (GEF), Son of Sevenless (SOS), which when activated catalyses the dissociation of RAS-GDP, and upon release, RAS binds to the more abundant GTP, and becomes active. RAS-GTP recruits RAF to the plasma membrane where it becomes phosphorylated and adopts the active conformation. RAF recognises the carboxy-terminal domain of MEK1/2 that contains proline-rich sequences and catalyses its phosphorylation (Catling *et al.*, 1995). MEK1/2 are dual-specificity protein kinases that catalyse the phosphorylation of Tyr204/187 and then Thr202/185 on ERK1/2, which are their only known substrates (Roskoski, 2012a; Ray & Sturgill, 1988; Roskoski, 2012b). ERK1/2 are protein-serine/threonine kinases that catalyse the phosphorylation and activation of hundreds of substrates within the cytoplasm and nucleus (Roskoski, 2012a; Ray & Sturgill, 1988; Roskoski, 2012b). RAS is inactivated by GTPase-activating proteins (GAPs), such as p120GAP and NF1 that stimulate the intrinsic GTPase activity of RAS (Reviewed by Bos *et al.*, 2007).

1.2. RAF isoforms

1.2.1. RAF family members

The RAF family consists of three serine/threonine-specific protein kinases. They are ARAF, BRAF and RAF-1, of which RAF-1, also known as CRAF is the best

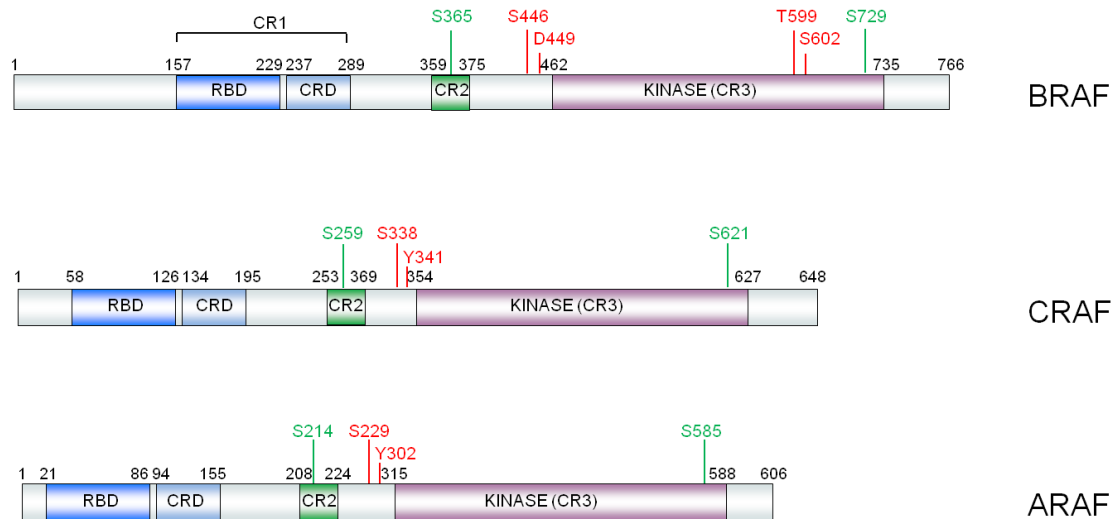
characterised. They share homology in three regions, known as conserved regions CR1, CR2 and CR3 (Figure 1.3). CR1 contains the Ras binding domain (RBD) (Scheffler *et al.*, 1994) and the cysteine-rich domain (CRD) (Mott *et al.*, 1996). The CR2 region is rich in serine and threonine residues. The CR3 region contains the kinase domain.

ARAF, located on the X chromosome, is expressed at high levels in tissues that comprise the urogenital system and is detectable in many other tissues (Storm *et al.*, 1990). *ARAF* knock-out mice on a C57 BL6 background show neurological defects and intestinal problems that may pose difficulties for survival, and these mice do not survive beyond 21 days (Pritchard *et al.*, 1996).

BRAF, located on human chromosome 7q34, was originally found to have a very restricted pattern of expression (Storm *et al.*, 1990). However, later it was shown that BRAF is expressed in most tissues (Barnier *et al.*, 1995; Wellbrock *et al.*, 2004). BRAF has a higher affinity (Papin *et al.*, 1998) and is more efficient in phosphorylating MEK (Pritchard *et al.*, 1995; Marais *et al.*, 1997) than CRAF. BRAF has been shown to be the main activator of MEK when transfected into NIH 3T3 cells (Pritchard *et al.*, 1995) and in primary mouse fibroblasts (Wojnowski *et al.*, 2000). This was shown by the significantly reduced ability of EGF treatment to phosphorylate ERK1/2, as measured by phosphorylation in *Braf*-null (*Braf*^{-/-}) fibroblasts (Wojnowski *et al.*, 2000). In contrast, ERK1/2 phosphorylation was unchanged in *Craf*^{-/-} fibroblasts (Wojnowski *et al.*, 1998). BRAF has been shown to signal exclusively through the ERK pathway. This has

Figure 1.3 Structure of the three RAF isoforms.

The RAF family of kinases share conserved regions CR1 (blue), CR2 (green), CR3 (purple). CR1 contains the RAS-binding domain (RBD) and the cysteine-rich domain (CRD). CR3 contains the kinase domain. Important sites are indicated in red, and 14-3-3 binding sites are indicated in green.



been supported by similar transcriptional profiles induced by inhibition of BRAF or inhibition of MEK in BRAF-mutant cells (Joseph *et al.*, 2010). Braf is also essential for survival, since Braf knock-out mice do not survive beyond embryonic day E12.5 (Wojnowski & Patkowski, 1997).

CRAF, located on human chromosome 3p25, is expressed ubiquitously at high levels in most tissues (Storm *et al.*, 1990). Craf knock-out mice die at mid-gestation, showing that Craf is essential for mouse development (Mikula *et al.*, 2001; Huser *et al.*, 2001). In an outbred strain, the mice die shortly after birth with general growth retardation and developmental defects, most pronounced in the placenta (Mikula *et al.*, 2001; Huser *et al.*, 2001), liver (Mikula *et al.*, 2001), lungs and skin (Wojnowski *et al.*, 1998). This was caused by excessive apoptosis in the absence of CRAF (Mikula *et al.*, 2001). CRAF transmits signals from oncogenic RAS to MEK (Blasco *et al.*, 2011; Dumaz *et al.*, 2006; Karreth *et al.*, 2011) but also interacts with non-MEK effectors which will be discussed later.

The RAF kinases are highly conserved across many organisms, including *Drosophila*, chicken and mice, with roles in organism development, apoptosis and regulation of the cell cycle (Wojnowski *et al.*, 2000). The three mammalian RAF isoforms have different levels of intrinsic ability to activate MEK (Marais *et al.*, 1997). Taken together the three RAF isoforms are important in early development, and are not functionally redundant.

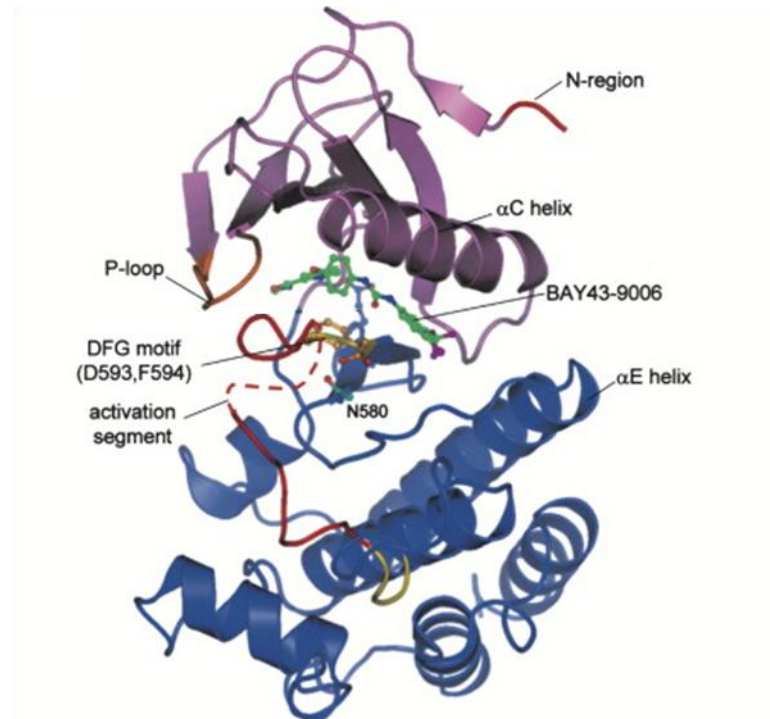
1.2.2. RAF protein structure

As mentioned earlier, all RAF members share three conserved regions. The RBD region is sufficient for translocation of CRAF to the plasma membrane, and CRD is essential for activation following their interaction with RAS (Hu *et al.*, 1997; Luo *et al.*, 1997; Roy *et al.*, 1997). CR2 is rich in serine and threonine residues, and contains an inhibitory site at Ser259 on CRAF that allows 14-3-3 binding when phosphorylated (Wellbrock *et al.*, 2004). CR3, the kinase domain is located near the C-terminus, adjacent to a stimulatory 14-3-3 binding site at Ser621 on CRAF (Wellbrock *et al.*, 2004).

The full crystal structure of BRAF and CRAF have not been solved, but the CRD region was solved by Mott *et al.* (1996) and, the kinase domain bound to the RAF inhibitors Sorafenib (Figure 1.4) (Wan *et al.*, 2004), CS292 (Xie *et al.*, 2009), PLX4720 (Tsai *et al.*, 2008) and GDC-0879 analogue (Hatzivassiliou *et al.*, 2010) was subsequently solved. The kinase domain has a small N-terminal lobe and a large C-terminal lobe that moves to open or close the cleft. The open form releases ADP from the catalytically active site, and allows access of ATP, while the closed form brings residues into the active site. The N-terminal lobe contains the glycine-rich ATP-phosphate-binding loop (P-loop) and anchors and orients ATP, while the C-terminal loop contains the activation loop that binds to ATP. In the unstimulated form, the glycine-rich P-loop and activation segment interact, displacing the activation loop and holding the kinase domain in an inactive conformation (Wan *et al.*, 2004). When active, Asp448 interacts with Arg506 of the α C helix, stabilising the active conformation (Wan *et al.*, 2004).

Figure 1.4 Crystal structure of the BRAF kinase domain when bound to Sorafenib (BAY43-9006) (Taken from Wan *et al.*, 2004).

The distal pyridyl ring of Sorafenib binds to the ATP binding pocket, whilst the lipophilic trifluoromethyl phenyl ring inserts into a hydrophobic pocket between the α C and α E helices and N-terminal regions of the DFG motif and catalytic loop of BRAF while in the inactive conformation. The kinase domain has a small N-terminal lobe and a large C-terminal lobe that move to open or close the cleft. In the inactive conformation, Asn581 (N580) and Phe595 (F594) interact to stabilise the kinase domain.



1.3. Activation of RAF

RAF activation involves activation of RAS that recruits RAF to the plasma membrane which is essential for RAF activation by other kinases. Both ARAF and CRAF require phosphorylation of conserved Ser259 and Ser338 and Tyr341 in the N-region for activation, but in BRAF, Ser446, which is equivalent to Ser259 in CRAF, is constitutively phosphorylated and Tyr341 in CRAF is substituted for an aspartic acid at residue 449 in BRAF. Therefore BRAF has a higher basal kinase activity and requires fewer phosphorylation steps for full activation (Reviewed by Roskoski, 2010). However, the high basal kinase activity in immunoprecipitation kinase assays is not translated to MEK activation in the basal state. It has been suggested that BRAF may be bound to an accessory factor that prevents BRAF from binding to MEK, or BRAF may not be within physical proximity of MEK until it is translocated to the plasma membrane (Reviewed by Mercer & Pritchard, 2003).

1.3.1. Activation of CRAF

CRAF has been shown to be cytoplasmic (Wartmann & Davis, 1994) and bound to 14-3-3 (Freed *et al.*, 1994) in unstimulated cells. CRAF is constitutively phosphorylated on Ser621, which forms a docking site for the phosphoserine-specific adaptor 14-3-3 (Muslin *et al.*, 1996) (binding sites are indicated in Figure 1.3). Tzivion *et al.* (1998) suggested that 14-3-3 binding to Ser259 and Ser621 retains CRAF in the inactive conformation, as shown by kinase assays on immunoprecipitated 14-3-3 bound to CRAF (Tzivion *et al.*, 1998). The use of synthetic phosphopeptides that displaced 14-3-3 from Ser621 deactivated

CRAF kinase activity, and the replacement of 14-3-3 restored kinase activity (Tzivion *et al.*, 1998). Therefore although inactive CRAF is bound to 14-3-3, 14-3-3 binding to Ser621 is required for CRAF activation.

A ^{R89L}CRAF mutant that failed to bind to RAS showed that RAS was responsible for CRAF recruitment to the plasma membrane (Marais *et al.*, 1995). RAS then displaces 14-3-3 from CRAF, a requirement for CRAF activity, as shown by increased kinase activity of a ^{S259A}CRAF mutant that does not bind 14-3-3 (Light *et al.*, 2002). Dephosphorylation of Ser259 and 14-3-3 displacement was suggested to be induced by Protein Phosphatase 2 (PP2A), that was identified to be associated with CRAF following EGF treatment, and PP2A was found to counteract Ser259 phosphorylation (Kubicek *et al.*, 2002). This is subsequently followed by Ser338 phosphorylation and Src-mediated phosphorylation of Tyr340 and Tyr341 (Mason *et al.*, 1999). Phosphorylation at both Ser338 and Tyr341 is a requirement for CRAF activation, as shown by the S338A and Y341A mutants that prevented phosphorylation and CRAF activation (Mason *et al.*, 1999). Several kinases have been reported to be candidates for Ser338 phosphorylation, including p21-activated kinase 3 (PAK3) (King *et al.*, 1998). PAK3 is activated by CDC42 and RAC at the plasma membrane, and dominant negative versions of PAK3 have been shown to block RAS-induced CRAF activation (King *et al.*, 1998). However, when both Ser338 and Tyr341 were mutated to aspartic acid residues, the basal kinase activity was not raised and could not be fully activated by RAS and EGF stimulation, suggesting the involvement of other residues (Chong *et al.*, 2001). Other potential phosphorylation sites include Thr491 and Ser494 within the activation segment.

A mutant that mimicked phosphorylation at Thr491 and Ser494 had higher MEK kinase activity than ^{WT}CRAF, and a mutant that mimicked phosphorylation at Thr491, Ser494, Ser338 and Tyr341 induced MEK kinase activity to levels similar to ^{G12V}HRAS-induced activity (Chong *et al.*, 2001).

Negative phosphorylation sites were identified by PDGF treatment followed by U0126 treatment, the latter preventing phosphorylation of Ser29, Ser289, Ser296, Ser301 and Ser642 on CRAF, suggesting them to be targets of ERK (Dougherty *et al.*, 2005). Hyperphosphorylated CRAF failed to dimerise with RAS, indicating that these negative phosphorylation sites inhibit signal propagation (Dougherty *et al.*, 2005).

1.3.2. Activation of BRAF

The tyrosine phosphorylation sites Tyr340 and Tyr341 present in CRAF are occupied by aspartic acid residues Asp448 and Asp449 in BRAF (Figure 1.3). Ser446, equivalent to Ser338 of CRAF, is also constitutively phosphorylated in BRAF (Mason *et al.*, 1999). This negative charge in the N-region is thought to contribute to the high basal kinase activity of BRAF, which is 15-20 times higher than CRAF kinase activity (Mason *et al.*, 1999).

Inactive BRAF has been proposed to be bound to 14-3-3 proteins at Ser365 and Ser729 in the cytoplasm according to sequence homology with CRAF (Reviewed by Mercer *et al.*, 2003). Crystallographic analysis of the BRAF kinase domain, shows that the aspartate, phenylalanine and glycine (DFG) motif within the activation segment orients the region of activation towards the

glycine-rich P-loop, bringing the glycine-rich segments Gly595-Val600 near to Gly463-Val470, which form hydrophobic interactions, rendering the catalytic cleft inaccessible and the ATP and peptide recognition segments disorganised (Wan *et al.*, 2004).

Immunofluorescence microscopy of cells overexpressing RAS showed that RAS-GTP was essential for recruitment of BRAF to the plasma membrane (Marais *et al.*, 1997). Mutation of Asp448 to phenylalanine greatly reduced RAS-GTP-induced BRAF activity, suggesting that RAS binds to Asp448 on BRAF for BRAF activation (Marais *et al.*, 1997). RAS-GTP binding is followed by displacement of 14-3-3 and the subsequent dephosphorylation of Ser365 (Reviewed by Mercer *et al.*, 2003), and exposure of Thr599 and Ser602 (Reviewed by Dibb *et al.*, 2004). Zhang & Guan (2000) showed that when cells were transfected with BRAF and RAS, BRAF was phosphorylated at Thr599 and Ser602, and immunoprecipitation kinase assays show that ^{T599A}BRAF and ^{S602A}BRAF have a reduced oncogenic RAS-induced activity. This suggested that active RAS leads to phosphorylation of Thr599 and Ser602 and BRAF activation (Zhang & Guan, 2000). Crystallography data indicated that phosphorylation of Thr599 and Ser602 disrupts the interactions between Val600 and residues in the glycine-rich P-loop, destabilising the inactive conformation (Wan *et al.*, 2004). BRAF changes to the active conformation with the Phe side chain rotated out of the ATP-binding pocket, and the Asp side chain facing into the ATP-binding pocket. This active conformation exposes the ATP binding site (Wan *et al.*, 2004). Once in the active conformation, salt bridges may form

between Lys507 and Arg575 that further stabilise the active conformation (Xie *et al.*, 2009).

U0126 treatment prevented phosphorylation of Ser365, Ser419, Ser429, Ser446 and Ser729 on BRAF. Therefore these were suggested to be ERK phosphorylation sites. When these sites were mutated to alanines, BRAF remained bound to RAS (Ritt *et al.*, 2010). Therefore these phosphorylation sites are proposed to inhibit signal transmission.

1.3.3. Different splice forms of BRAF

BRAF is differentially spliced to produce at least 10 different splice variants ranging in size from 67 to 99 kDa (Barnier *et al.*, 1995). These are produced by alternative splicing of exons 8b and 10a and by the presence of two different N-termini for BRAF. Splice variants that contain exon 10 were found to have a higher affinity and basal kinase activity towards MEK resulting in increased cell growth and colony formation (Papin *et al.*, 1998), and splice variants that contained exon 8b had a lower basal kinase activity without any change in affinity for MEK (Papin *et al.*, 1998). Variants that contained both exons 8b and 10 had activity between the two variants (Papin *et al.*, 1998). Differential splicing was also found to change RAF dimerisation preference which is important in drug resistance as will be discussed in Section 1.9.3.2

1.3.4. Heterodimerisation of RAFs

Dimerisation is essential for RAF activation (Rajakulendran *et al.*, 2009), as shown by the increase in P-MEK levels induced by ^{E558K}CRAF that promoted kinase domain dimerisation, and ablation of P-MEK levels by the dimer-interface mutant ^{R481H}CRAF (Rajakulendran *et al.*, 2009). RAS not only recruits RAF to the plasma membrane, but is also crucial for the homodimerisation or heterodimerisation of BRAF and CRAF as shown by immunoprecipitation (Weber *et al.*, 2001; Packer *et al.*, 2011; Heidorn *et al.*, 2010; Poulikakos *et al.*, 2010).

Mutation of Ser621 to alanine in CRAF not only disrupts 14-3-3 binding, but also the binding to BRAF, suggesting the involvement of 14-3-3 in heterodimerisation (Ritt *et al.*, 2010; Weber *et al.*, 2001; Garnett *et al.*, 2005; Fischer *et al.*, 2007; Rushworth *et al.*, 2006). Peptide arrays show that BRAF binds to amino acids 301-315 and amino acids 365-387 between the ATP-binding site and activation loop of CRAF, while CRAF binds to amino acids 737-766 in BRAF, which contains the amino acid phosphorylation site Thr753 for ERK-dependent destabilisation of dimerisation (Rushworth *et al.*, 2006). Dimerisation is inhibited by phosphorylation of Thr753 on BRAF, as shown by prolonged heterodimerisation of ^{T753A}BRAF with CRAF (Ritt *et al.*, 2010). Hence why RAF (Wan *et al.*, 2004; Heidorn *et al.*, 2010) and MEK inhibitors stabilise heterodimer levels (Wan *et al.*, 2004; Rushworth *et al.*, 2006).

CRAF was found to be activated by BRAF on dimerisation, which is important in ERK activation by impaired activity BRAF mutants (Wan *et al.*, 2004; Garnett *et*

al., 2005). Kinase assays show that BRAF:CRAF heterodimers have the highest level of activity, and heterodimers of ^{WT}CRAF or ^{WT}BRAF and kinase-dead BRAF or CRAF mutants displayed elevated kinase activity, indicating one kinase-competent RAF isoform is sufficient to induce kinase activity (Rushworth *et al.*, 2006). However, CRAF was found to reduce the P-ERK levels, and cell proliferation and colony formation capability of ^{V600E}BRAF upon heterodimerisation (Karreth *et al.*, 2009). Since RAS induces heterodimerisation, this may be why oncogenic RAS and ^{V600E}BRAF do not co-exist in the same cells. Moreover, dimerisation was found to be mutation-specific. Both ^{V600E}BRAF and ^{G469A}BRAF had potent homodimerising capacity, and ^{V600E}BRAF had been shown to signal as a monomer (Roring *et al.*, 2012).

Both BRAF and CRAF are able to form a heterodimer with ARAF upon binding to RAS, and unlike CRAF, the defective RAS-binding ^{R52L}ARAF mutant was able to form a heterodimer with BRAF, indicating the ability of ARAF to heterodimerise with BRAF without binding to RAS, but the defective RAS-binding ^{R188L}BRAF was unable to form a heterodimer with ARAF (Rebocho & Marais, 2012). siRNA depletion of ARAF caused a strong reduction in BRAF:CRAF heterodimers (Rebocho & Marais, 2012). This showed that each RAF isoform has a different ability to heterodimerise and contribute to MEK/ERK output.

1.4. Downstream of RAF

1.4.1. Direct RAF substrates

All RAF isoforms have activity towards MEK, with BRAF having the strongest activity, and ARAF the weakest, as shown by IP kinase assays (Bosch *et al.*, 1997). CRAF in particular has been shown to bind to other mediators independently of MEK, such as MEKK1. The use of dominant negative-versions of MEK showed that CRAF was able to enhance MEKK1-mediated NF- κ B dependent gene expression independently of MEK (Baumann *et al.*, 2000). Mediators in addition to MEKs have been shown to be direct targets of CRAF in particular for cell survival.

Pull-down assays showed that CRAF interacts with pRb following serum stimulation. The direct binding of CRAF to pRb prevented pRb inhibitory activity on E2F-mediated transcription. This was shown by reporter assays, where a truncated CRAF mutant that is unable to bind pRb failed to prevent pRb from inhibiting E2F-mediated transcription (Wang *et al.*, 1998).

CRAF has been shown to associate with the mitochondria in several studies. The mitochondrial anti-apoptotic factor BCL-2 has been shown to target CRAF to the mitochondria. The apoptotic factor BAD was phosphorylated only in cells transfected with CRAF and not in cells transfected with a CRAF plasmid fused with the plasma membrane-targeting sequence. This suggested that BAD was directly phosphorylated by CRAF at the mitochondria (Wang *et al.*, 1996). However, the effect of phosphorylation of BAD has not been examined in full detail, but CRAF translocation to the mitochondria correlated with improved cell

survival (Wang *et al.*, 1996). Grb10 had been shown to bind closely to the RAS-binding domain of CRAF at the mitochondria, and may therefore play a role in the anti-apoptotic activity of CRAF at the mitochondria (Nantel *et al.*, 1999).

Although CRAF has not been shown to directly bind to Caspase-1, active Caspase-1 appeared faster in CRAF deficient macrophages following *Salmonella* treatment (Jesenberger *et al.*, 2001). This was not accompanied by alterations to P-ERK levels or localisation of CRAF to mitochondria, therefore CRAF was proposed to antagonise Caspase-1-induced cell death independently of MEK (Jesenberger *et al.*, 2001). The use of MEK inhibitors and MEK overexpression showed that CRAF interacts with apoptosis signal-regulating kinase 1 (ASK1), and inhibits apoptosis independently of MEK. Kinase-defective CRAF mutants still had the capability of inhibiting ASK1, which supported the MEK-independent activity of CRAF (Chen *et al.*, 2001).

CRAF has also been shown to mediate cell migration independently of MEK by binding to Rok- α . CRAF knock-out fibroblasts, in which Rok- α was not associated with the vimentin cytoskeleton, were less efficient at migration shown in a transwell assay. Cell migration was restored when CRAF was re-expressed (Ehrenreiter *et al.*, 2005). CRAF could also bind to and phosphorylate myosin-binding subunit, inhibiting the phosphatase activity (Broustas *et al.*, 2002), which normally acts to dephosphorylate myosin light chain. The sustained phosphorylated state of myosin light chain is required for filopodia extension.

In contrast to CRAF, there is no current evidence for BRAF operating through any other pathway other than MEK/ERK (Kolch, 2000). BRAF binding partners other than MEK and CRAF have not been found as yet.

1.4.2. Activation of MEK and ERK

The only common downstream substrates for the three RAFs are MEK1/2 (Mercer & Pritchard, 2003). MEK1 and MEK2 contain a proline-rich sequence, which is thought to be required for recognition by RAF proteins (Catling *et al.*, 1995). MEK1 is activated by phosphorylation of Ser218 and Ser222 in the activation loop (Alessi *et al.*, 1994; Yan & Templeton, 1994; Zheng & Guan, 1994) and MEK2 is activated by phosphorylation of Ser222 and Ser226 (Roskoski, 2012b). ERK1 and ERK2 are the only known MEK1/2 substrates (Robbins *et al.*, 1993). Activated MEK1/2 phosphorylate Thr185 and Tyr187 in ERK1 and Thr202 and Tyr204 in ERK2, causing a conformational change in the activation loop and the neighbouring regions of ERK, inducing ERK activation.

1.4.3. Biological effects of ERK

The ERK cascade is important in many cellular processes, including cell proliferation, cell-cycle arrest, cell adhesion, cell migration, terminal differentiation, metabolism and apoptosis (Reviewed by Plotnikov *et al.*, 2011). The outcome is determined by the duration and intensity of ERK signalling (Marshall, 1995; Sewing *et al.*, 1997; Woods *et al.*, 1997b), and co-operation with other pathways (Peyssonnaud *et al.*, 2000; Sahai *et al.*, 2001). The effect of ERK duration has been extensively studied in PC12 cells, which, when treated with nerve growth factor (NGF), caused sustained ERK activation

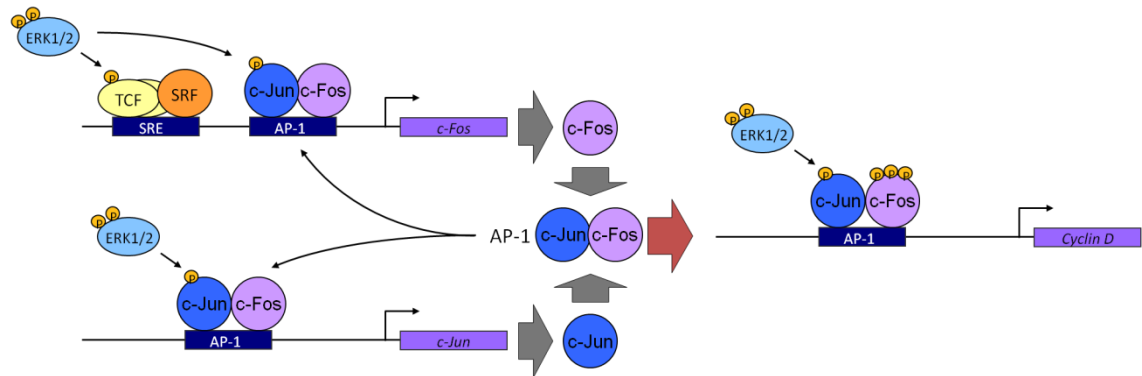
(Muroya *et al.*, 1992) and lead to differentiation and cessation of cell division (Greene & Tischler, 1976). PC12 treated with EGF, which gives a transient burst of ERK1/2 phosphorylation (Muroya *et al.*, 1992) lead to induction of cell proliferation (Huff *et al.*, 1981). Studies in other cell types, such as in the hamster CCL39 fibroblast cell line (Balmano & Cook, 1999), Swiss 3T3 cells (Murphy *et al.*, 2002; Murphy *et al.*, 2004), macrophages (Whalen *et al.*, 1997) and T lymphocytes (Sharp *et al.*, 1997) have shown similar findings. Low intensity ERK1/2 signalling had been found to induce Cyclin D1 and Cyclin E expression, with a reduction in p27^{Kip1} and subsequent proliferation (Woods *et al.*, 1997a). On the other hand, high intensity ERK1/2 signalling had been found to induce p21^{Cip1}, which lead to cell cycle arrest in mouse cells (Sewing *et al.*, 1997; Woods *et al.*, 1997a; Pumiglia & Decker, 1997a; Pumiglia & Decker, 1997b) and senescence in human fibroblasts (Peyssonnaud *et al.*, 2000; Zhu *et al.*, 1998).

ERK1/2-induced Cyclin D expression had been shown to involve Elk-1, Sap-1 and RSKs that lead to Fos expression, which is involved in regulating Cyclin D expression (Figure 1.5). Growth factor induced ERK1/2 phosphorylation was also shown to modify Elk-1 and SAP-1, which have DNA binding properties identical to p62^{TCF}, and were subsequently identified to be Ternary Complex Factors (TCF) (Hipskind *et al.*, 1994). Serum Response Factors (SRF) direct TCF to the c-Fos Serum Response Element (SRE) and induce c-Fos expression (Gille *et al.*, 1992; Marais *et al.*, 1993). When Ser383 and Ser389 of Elk-1 were mutated to Alanines, ERK failed to phosphorylate Elk-1, and reporter

Figure 1.5 MAPK regulate Cyclin D expression

MAPK modify Ternary Complex Factors (TCF), which are directed to the c-Fos Serum Response Element (SRE) by Serum Response Factors (SRF) and induce c-Fos expression.

The activating protein-1 (AP-1) family of transcription factors consist of homodimers or heterodimers of Jun, Fos, activating transcription factor or bZIP proteins that bind to a common palindromic DNA motif and induce transcription of delayed response genes including Cyclin D.



assays showed a marked decrease in SRE promoter activity induced by single mutants and virtually a complete loss of reporter activity when both were mutated (Marais *et al.*, 1993). This suggested phosphorylation of Elk-1 at these residues by ERK, enabled Elk-1 binding to SRE of the c-Fos promoter or enhanced its transcriptional activity.

Another important ERK-induced activation family of proteins is the 90K-ribosomal S6 kinase (RSK) family (Murphy *et al.*, 2002). The family members include RSK1, RSK2 and RSK3 (Cargnello & Roux, 2011). The C-terminal kinase domain of RSK1/2/3 are constitutively bound to ERK and upon stimulation are phosphorylated at residues Thr359, Ser363 and Thr573 by ERK (Dalby *et al.*, 1998; Ranganathan *et al.*, 2006) leading to Ser380 autophosphorylation, creating a docking site for 3-phosphoinositide-dependent protein kinase-1 (PDK1). PDK1 phosphorylates the N-terminal kinase domain and activates RSK (Frodin *et al.*, 2000; Vik & Ryder, 1997). Activated RSK proteins have been shown to phosphorylate CREB, which induces transcription of c-Fos (Ginty *et al.*, 1994), c-Jun and NUR77 (Davie & Spencer, 1999; Davis *et al.*, 1993).

This links ERK to activation of the activating protein-1 (AP-1) family of transcription factors that consist of homodimers or heterodimers of the Jun (v-Jun, c-Jun, JunB, JunD), Fos (v-Fos, c-Fos, FosB, Fra1, Fra2), or activating transcription factor (ATF2, ATF3/LRF1, B-ATF) family of bZIP (basic region leucine zipper) proteins that bind to a common palindromic DNA motif (5'TGAG/CTCA-3') (Vogt & Bos, 1990; Angel & Karin, 1991; Ameyar *et al.*, 2003). Antibodies directed at Fos and Jun prevented DNA synthesis and S-

phase entry of the cell cycle, indicating the requirement of Fos and Jun in DNA synthesis (Kovary & Bravo, 1991). Reporter assays have shown that AP1 proteins including c-Jun, JunB, c-Fos and ATFs bind to Cyclin D1 gene regulatory sequences, and c-Jun induce Cyclin D1 transcription (Albanese *et al.*, 1995; Herber *et al.*, 1994). Cyclin D proteins bind to CDK4 and phosphorylate and inactivate the retinoblastoma tumour suppressor protein enabling cell cycle progression (Sherr, 1996). Reporter assays showed that c-fos^{-/-}; fosB^{-/-} double mutant fibroblasts had reduced Cyclin D1-promoter-driven luciferase activity (Brown *et al.*, 1998). c-fos^{-/-}; fosB^{-/-} fibroblasts also failed to proliferate, which was restored upon Cyclin D1 transfection. This suggested that Fos proteins induce Cyclin D1 expression and cell cycle entry (Brown *et al.*, 1998) and provides a link between ERK signalling and cell proliferation.

The RAS/MEK/ERK pathway is not the only pathway involved in control of cell proliferation. In some cell types cooperation with the RAC/RHO pathway was required for cell proliferation (Peyssonnaud *et al.*, 2000), and RHO was found to reduce p21^{Cip1} levels to that enable the process (Sahai *et al.*, 2001). This was further complicated by the upstream activator RAS that signals to other pathways. For example, the phospholipid products from PI3K have been shown to activate RAC, which binds to and activates p21Cdc42/Rac1-activated serine/threonine kinase (PAK) (Sun *et al.*, 2000). PAK then phosphorylates CRAF on Ser338 (King *et al.*, 1998), a requirement for CRAF activation. Furthermore, the Janus kinase (JAK) family tyrosine kinases also induce CRAF activation (Stancato *et al.*, 1997; Xia *et al.*, 1996). However, PI3K also has negative effects on the ERK pathway. PI3K/AKT phosphorylates Ser259, and

may suppress CRAF activity (Zimmermann & Moelling, 1999). The level of AKT was found to be important in the progression of melanoma (Cheung *et al.*, 2008) and tumourigenesis in advanced stage melanomas (Stahl *et al.*, 2004; Madhunapantula *et al.*, 2007). AKT was found to be elevated in dysplastic nevi and 60-70% of melanomas (Dhawan *et al.*, 2002). The high levels of AKT are thought to be important in suppression of the high levels of ^{V600E}BRAF-induced ERK activity, to levels that enable cell proliferation.

1.4.4. Feedback regulation

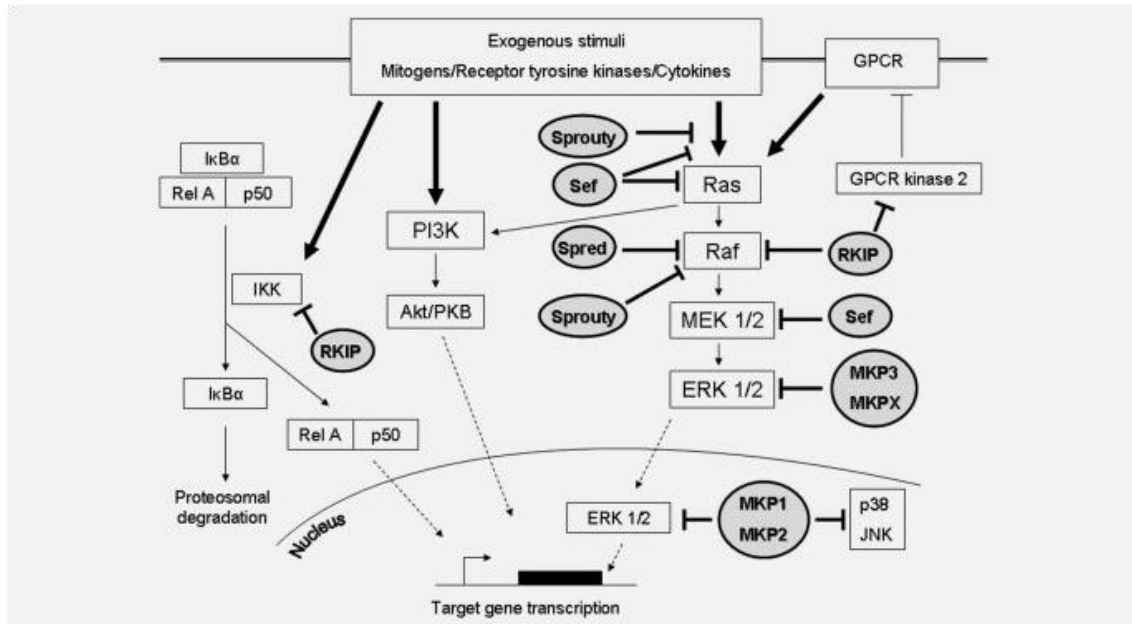
Tight regulation of the MAPK pathway is critical for normal cell homeostasis. Disruption of this regulation leads to pathway hyperactivation, and is disastrous for the cell. Studies have shown that apart from inducing ERK activation through the RAS/MEK/ERK pathway, the pathway is also subjected to negative feedback regulation as briefly mentioned in Section 1.3. Several different negative regulators have been identified including RAF kinase inhibitor protein 1 (RKIP1), SEF, DUSP, Sprouty (SPRY) and SPROUTY-related enabled/vasodilator-stimulated phosphoprotein homology 1 domain-containing (SPRED) family of proteins (Figure 1.6). Since these negative regulators inhibit the MEK/ERK pathway, they may function as tumour suppressor proteins (Julien *et al.*, 2011).

RKIP1 was identified as a RAF-interacting protein through a yeast 2 hybrid screen, and shown to colocalise with CRAF and MEK, disrupting their interaction and the subsequent MEK-induced activities. Depletion of RKIP1 by

Figure 1.6 Direct negative feedback of the ERK pathway (Taken from Murphy et al., 2010)

DUSP6 expression is induced by P-ERK, and is activated on binding to P-ERK. DUSP6 dephosphorylates and inactivates P-ERK. DUSP1 and DUSP4 are induced by signals that activate the MAPK pathway. They reside mainly in the nucleus, and inactivate ERK1/2.

SPRY gene expression is induced by high P-ERK levels, and is activated by tyrosine phosphorylation by RTK. They have been proposed to uncouple the tyrosine receptor activation of RAS or induce GTPase activity on RAS and inactivating RAS.



antisense RNA and antibody injection enabled MEK-, ERK- and AP-1- induced transcription (Yeung *et al.*, 1999).

There are two isoforms of SPRED, which are SPRED1 and SPRED2. They were identified to contain a C-terminal SPROUTY domain and an amino-terminal Ena/Vasodilator-stimulated phosphoprotein homology-1 domain (Prehoda *et al.*, 1999), and subsequently named Sprouty-related protein with EVH-1 domain (SPRED). Platelet-derived growth factor (PDGF), EGF and stem cell factor (SCF) were found to induce SPRED-1 tyrosine phosphorylation, which became localised to the plasma membrane (Wakioka *et al.*, 2001). A study found that SPRED1 and SPRED2 levels were lower in human hepatocellular (HCC) tissue than in the neighbouring normal tissue, and forced SPRED expression reduced HCC cell proliferation (Yoshida *et al.*, 2006). The level of P-ERK and metalloproteinase-9 and 2, which are associated with tumour invasion and metastasis were also reduced (Yoshida *et al.*, 2006), suggesting a tumour suppressor role for SPREDs.

SPRED overexpression was found to sustain RAS activity measured by kinase assays, but promoter assays showed inhibition of RAS-induced Elk-1 activation. Increased amounts of RAF co-precipitated with RAS and, RAF was retained at the plasma membrane for longer, and was not phosphorylated on Ser338 when SPRED-1 was co-expressed, suggesting that SPRED increases the RAS-RAF interaction, preventing the phosphorylation and activation of RAF (Wakioka *et al.*, 2001).

1.4.4.1. Dual-specificity protein tyrosine phosphatases

The dual-specificity protein tyrosine phosphatases (DUSPs) are the major group of phosphatases that dephosphorylate one or both of the conserved threonine and tyrosine residues in the activation loop of the MAPKs (Boutros *et al.*, 2008). There are three families of DUSPs based on their substrate specificity and sub-cellular localisation. DUSP6, DUSP7 and DUSP9 are ERK1/2 specific and reside in the cytoplasm (Dowd *et al.*, 1998; Muda *et al.*, 1997). DUSP8, DUSP10 and DUSP16 are p38 MAPK/JNK specific and shuttle between the nucleus and cytoplasm (Tanoue *et al.*, 1999; Muda *et al.*, 1996; Masuda *et al.*, 2001). DUSP1, DUSP2, DUSP4 and DUSP5 are induced by signals that activate MAPK signalling and reside in the nucleus (Tanoue *et al.*, 1999; Noguchi *et al.*, 1993; Keyse & Emslie, 1992; Mandl *et al.*, 2005). Although DUSP8, 10 and 16 are p38 MAPK/JNK specific, they have been shown to have weak activity towards ERK (Reviewed by Boutros *et al.*, 2008). DUSPs that affect ERK signalling, namely DUSP1, DUSP6, DUSP7 and DUSP9 will be discussed in more detail in this section.

DUSP1, also known as MAPK phosphatase 1 (MKP1) is a nuclear phosphatase encoded on chromosome 5. Loss of DUSP1 expression is commonly reported in advanced and aggressive tumours, including prostate cancer where an increase in expression is observed in early disease, but reduced in advanced cancer (Loda *et al.*, 1996; Rauhala *et al.*, 2005). However, increased DUSP1 expression has also been associated with poor survival. For example in ovarian cancer, patients with high DUSP1 levels had shorter progression-free survival

(Denkert *et al.*, 2002), and high levels of DUSP1 were reported in poorly differentiated and advanced stage breast cancer (Loda *et al.*, 1996).

The promoter region of DUSP1 contains AP1, AP2, *trans*-acting transcription factor 1, cAMP-response element, and nuclear factor 1 binding sites (Kwak *et al.*, 1994; Pursiheimo *et al.*, 2002). Many factors have been shown to induce DUSP1 protein expression, including but not limited to insulin in rat smooth muscle and hepatoma cells (Takehara *et al.*, 2000), EGF and serum (Wu *et al.*, 2005; Metzler 1998). Although DUSP1 and DUSP4 inhibit p38 MAPK activity, p38 MAPK does not induce their activation, as shown by the same levels of DUSP1 and DUSP4 following serum stimulation with or without pre-treatment of the p38 MAPK inhibitor SB203580 (Brondello *et al.*, 1997). ERK1 or ERK2 did not phosphorylate a ^{S359A; S364A}DUSP1 mutant, suggesting that these two residues are phosphorylation sites, but both phosphorylated and non-phosphorylated forms of DUSP1 had equal activity in ERK dephosphorylation. Phosphorylated DUSP1 had a lower degradation rate, suggesting ERK1/2-mediated phosphorylation of DUSP1 prevented its degradation (Brondello *et al.*, 1999).

DUSP1 was shown to have highest affinity for p38 MAPK followed by JNK and ERK1/2 (Franklin & Kraft, 1997; Camps *et al.*, 2000; Farooq & Zhou, 2004), and DUSP1 binding to the different MAPKs involved different residues of the phosphatase (Reviewed by Boutros *et al.*, 2008). For example, yeast two-hybrid analysis showed that when Arg53 to 55 were mutated to alanine, serine and alanine respectively, the mutant could not bind to ERK1/2 and p38 α , but was

still able to bind to JNK1 (Slack *et al.*, 2001). Overexpression of the N-terminus of DUSP1 did not change the levels of P-ERK, but inhibited ERK1/2-induced Elk-1 phosphorylation of Ser338, and SRE-mediated gene expression. This suggested that DUSP1 competes with Elk-1 in binding to MAPK, preventing Elk-1 activation, which is one of the key mediators of ERK1/2 and p38 (Wu *et al.*, 2005). Both DUSP1 and DUSP4 prevented ERK1/2-induced myelin-basic protein (MBP) phosphorylation, JNK-induced c-Jun phosphorylation, and p38 MAPK-induced ATF-2 phosphorylation in co-transfection assays (Brondello *et al.*, 1997). DUSP1 and DUSP4 also prevented colony formation (Brondello *et al.*, 1997).

DUSP6, DUSP7 and DUSP9 have a high degree of selectivity for ERK1/2 (Muda *et al.*, 1996; Groom *et al.*, 1996). The N-region of DUSP6 contains a conserved nuclear export signal for cytoplasmic localisation, and a kinase interaction motif (KIM) that recognises the negative aspartate residues within a common docking site of the target MAPK (Karlsson *et al.*, 2004; Nichols *et al.*, 2000).

DUSP6, also known as MKP3 is encoded on chromosome 12 (Reviewed by Murphy *et al.*, 2010). DUSP6 expression was found to be upregulated in dysplastic carcinoma cells, but down-regulated in invasive carcinoma (Furukawa *et al.*, 2003). The mechanism of downregulation differs depending on tumour cell type. For example, in pancreatic cancer, it was due to hypermethylation of the gene promoter (Xu *et al.*, 2005), and in lung cancer, loss of heterozygosity was a potential mechanism (Okudela *et al.*, 2009). FGF-

induced DUSP6 protein levels were not affected by the treatment of LY294002, a PI3K inhibitor, rapamycin, a TOR pathway inhibitor, and U-73122, a phospholipase C inhibitor, suggesting that these pathways do not directly induce DUSP6 expression (Ekerot *et al.*, 2008). But the treatment of the MEK inhibitor PD184352 blocked FGF-induced DUSP6 mRNA and protein expression (Ekerot *et al.*, 2008). Further analysis showed that the DUSP6 promoter contained binding sites for several transcriptional factors, which include Forkhead, ETS family of transcriptional factors, NF- κ B, and pre-B-cell leukaemia transcription factor 1 (PBX1)-related homeobox factor SOX5, but reporter assays show that only mutation of the ETS-1 binding site prevented FGF-mediated DUSP6 transcription (Ekerot *et al.*, 2008). Knock-down of DUSP6 has been shown to result in an increase in P-ERK levels (Chan *et al.*, 2008), and DUSP6 overexpression had been shown to inhibit ERK kinase activity (Tanoue *et al.*, 2000), but overexpression of the mutated DUSP6 that does not bind ERK did not affect ERK kinase activity (Tanoue *et al.*, 2000). Therefore, DUSP6 binding to ERK is crucial.

Re-introducing DUSP6 into pancreatic cell lines reduced P-ERK levels and suppressed cell growth (Furukawa *et al.*, 2003). Therefore DUSP6 acts a tumour suppressor by suppressing the levels of P-ERK and inducing cell death. Interestingly, IGF-1 stimulated the phosphorylation of p70 S6K, the target of mTOR, and this led to degradation of DUSP6, suggesting involvement of DUSP6 in cross-talk between the ERK and mTOR pathways (Bermudez *et al.*, 2008). However, ERK1/2 has also been shown to target DUSP6 for degradation by the proteasome following phosphorylation of DUSP6 at Ser159 and Ser197

(Marchetti *et al.*, 2005). This further highlights the importance of the duration and intensity of ERK signalling.

DUSP7, also known as MKP-X is located on chromosome 3 (Reviewed by Keyse, 2008). DUSP7 mRNA is consistently higher in peripheral blood mononuclear cells from leukaemia patients than healthy blood donors (Levy-Nissenbaum *et al.*, 2003b). Activation of ERK1/2 by 12-O-tetradecanoylphorbol-13-acetate (TPA) induced DUSP7 RNA and protein expression, and inhibition of MEK by PD098059 inhibited TPA-induced DUSP7 expression (Levy-Nissenbaum *et al.*, 2003a). This showed that ERK1/2 activation lead to DUSP7 protein expression. Furthermore, serum-induced ERK1/2 phosphorylation induced DUSP7 expression (Dowd *et al.*, 1998). Immunoprecipitation kinase assays showed that DUSP7 suppressed ERK1/2 activity towards MBP, and to a much lower extent, suppressed JNK activity towards Jun, and p38 MAPK activity towards MBP (Dowd *et al.*, 1998).

DUSP9 is the only dual specificity phosphatase to map to the X-chromosome (Muda *et al.*, 1997). Semi-quantitative analysis of yeast two-hybrid showed strong interaction between DUSP9 and ERK1 and ERK2, weak interaction with p38 α , and very weak interaction with JNK1 and ERK5 (Dickinson *et al.*, 2002). Overexpression of DUSP9 inhibited ERK and p38 MAPK activity towards MBP (Muda *et al.*, 1997; Dickinson *et al.*, 2002), and induced cell death (Liu *et al.*, 2007). DUSP9 expression in tumour xenografts induced tumour shrinkage (Liu *et al.*, 2007b). Immunostaining of renal tumour samples showed that DUSP9 protein expression was higher in the adjacent normal tissue, and a high

percentage of patients with low DUSP9 expression had metastatic cancer with a shorter survival (Wu *et al.*, 2011).

Overall, these studies show that ERK1/2 induce or stabilise DUSP proteins, thereby inhibiting ERK1/2-induced effects. Therefore DUSPs act as negative regulators of ERK1/2 signalling.

1.4.4.2. Sprouty

Sprouty proteins (SPRY) were first identified as antagonists of FGF-induced branching of the *Drosophila* airways (Hacohen *et al.*, 1998), and overexpression of SPRY impaired eye and wing development, both of which require EGF signalling (Kramer *et al.*, 1999). Unlike *Drosophila*, which only has one SPRY protein, at least four SPRY proteins have been identified in mammals which inhibit basic fibroblast growth factor (bFGF)- and vascular endothelial growth factor A (VEGF)- induced ERK activation (Sasaki *et al.*, 2003; Sasaki *et al.*, 2001; Taniguchi *et al.*, 2007). SPRY was found to inhibit serum-, EGF-, FGF- and PDGF-stimulated cell migration, serum-stimulated cell proliferation (Yigzaw *et al.*, 2001), and reduce cell growth by limiting DNA synthesis required for cell division (Gross *et al.*, 2001). These effects required an intact conserved C-terminus (Yigzaw *et al.*, 2001), which is required for plasma membrane translocation (Sasaki *et al.*, 2003). Of the four isoforms, SPRY2 overexpression was found to inhibit ERK2 phosphorylation, SPRY1 had a smaller impact on inhibition of ERK phosphorylation than SPRY2, and neither SPRY isoform inhibited JNK or p38 MAPK phosphorylation (Yusoff *et al.*, 2002).

SPRY proteins are repressed mainly by DNA methylation or loss of heterozygosity in many cancers, including breast cancer (Lo *et al.*, 2004), prostate cancer (Kwabi-Addo *et al.*, 2004; McKie *et al.*, 2005) and liver cancer (Yoshida *et al.*, 2006; Lo *et al.*, 2004; Fong *et al.*, 2006), and are therefore considered to be tumour repressors. SPRY gene expression is induced by high ERK1/2 activity (Hanafusa *et al.*, 2002; Ozaki *et al.*, 2001), and is activated by tyrosine phosphorylation by RTK (Hanafusa *et al.*, 2002).

SPRY was suggested to act at the RAS level, where it prevents the activation of RAS by uncoupling receptor tyrosine kinase activation of RAS or by inducing the GTPase activity (Gross *et al.*, 2001; Hanafusa *et al.*, 2002; Cabrita & Christofori, 2008; Casci *et al.*, 1999). However, SPRY has been shown to be unable to act at the RAS level by co-transfection of FGFR1 and SPRY2, where SPRY2 failed to reduce the levels of RAS-GTP induced by FGFR1 (Yusoff *et al.*, 2002). Moreover, VEGF activates ERK1/2 via phospholipase C gamma and protein kinase C pathway where protein kinase C activates CRAF independently of RAS (Takahashi *et al.*, 2001). Therefore SPRY-mediated inhibition of VEGF-stimulated ERK1/2 activation could be independent of RAS. SPRY has been shown to act at the RAF level in several studies, where transfection of SPRY1/2/4 inhibited RAF kinase activity (Yusoff *et al.*, 2002). A SPRY4 mutant that carried a mutation in the RAF-binding motif still localised to the plasma membrane, but failed to bind to CRAF, did not disrupt VEGF-induced ERK activation, suggesting SPRY4 inhibits CRAF activity (Sasaki *et al.*, 2003). However, the activation loop mutants L597V, V600D, V600E, K601E (Tsavachidou *et al.*, 2004), and P-loop BRAF mutants G466A, G466E and

G466V do not bind to SPRY2 or SPRY4 (Brady *et al.*, 2009), and are therefore not sensitive to the SPRY-induced negative regulation, whereas ^{WT}BRAF and the non-activating mutants K438Q and T439O are able to bind SPRY (Tsavachidou *et al.*, 2004). Also, the knockdown of SPRY2 in ^{V600E}BRAF cells did not affect P-ERK levels or cell growth (Tsavachidou *et al.*, 2004), and MEK inhibition by PD0325901 in ^{V600E}BRAF xenografts did not reduce the levels of P-MEK (Pratilas *et al.*, 2009), suggesting ^{V600E}BRAF to be unresponsive to negative regulators.

Spry2 expression has been observed in a $Kras^{+/G12D}$ mouse model that exhibited a branching defect in the lungs. $G12D$ Kras was found to induce Spry2 expression in MEFs, which correlated with reduced P-Erk levels. The developing lungs of wild-type mice had variable expression of Spry2 with high levels at the leading edge of branching tips, whereas the lungs of $Kras^{+/G12D}$ mice had high uniform expression of Spry2 with reduced P-Erk levels throughout the epithelium. The lungs of $Kras^{+/G12D}; Spry2^{-/-}$ double mutants had high levels of P-Erk1/2, exhibited increased bronchi branching with a higher tumour burden (Shaw *et al.*, 2007). This suggested that oncogenic Kras induces Spry2 expression which regulates ERK1/2 activity during lung development and opposes $G12D$ Kras-induced tumourigenesis (Shaw *et al.*, 2007).

1.5. Cancer

Control of ERK1/2 signalling is crucial for normal cell homeostasis. Hyperactivation of the ERK1/2 can cause cancer and has been linked to a group of developmental syndromes known as RASopathies.

Cancer is a broad group of diseases that all involve the abnormal overgrowth of cells. It can be hereditary, is influenced by environmental factors, and increases in predisposition with age, although some cancers occur early in life. Mutations accumulate over years of DNA damage to genes involved in cell cycle progression. Different factors such as UV radiation and DNA-binding chemicals contribute to gene mutations that may cause a cell to proliferate out of control, forming a large mass. Additional mutations are required for the cells to invade neighbouring tissues and grow at distant places within the body. This phenomenon is known as metastasis and makes the management and treatment of the disease much more challenging. Cancerous cells normally develop their own blood supply, starving surrounding normal cells of oxygen. This results in the death of neighbouring cells and loss of function of the affected organs.

The Human Genome Project (HGP) has helped unravel driver mutations in cancer. HGP began in 1990 coordinated by the US Department of Energy and the National Institutes of Health, and finished in 2003. The aim of the project was to determine the nucleotide sequence of all the 20,000-25,000 genes in human DNA. The goal was achieved by mapping human and mouse genomes for study in inherited diseases, by sequencing organisms with smaller, simpler genomes to serve as guides for method development and for assisting in interpreting the human genome (International Human Genome Sequencing Consortium, 2004). This project helped with identification of genes that are deregulated in cancer. The hallmarks of cancer include sustained proliferative

signals, ability to evade growth suppressors, ability to resist cell death, induction of immortality, ability to induce angiogenesis, and ability to invade and metastasise (Hanahan & Weinberg, 2011) (Figure 1.7).

Oncogenes are mutated genes that cause cancer. Oncogenes are therefore genes that encode proteins that are involved in the hallmarks of cancer. Genes involved in the ERK1/2 pathway are common oncogenes which will be discussed later. RAS also activates the PI3K pathway, which is involved in cell growth, proliferation, differentiation, motility and survival (Reviewed by Workman *et al.*, 2006).

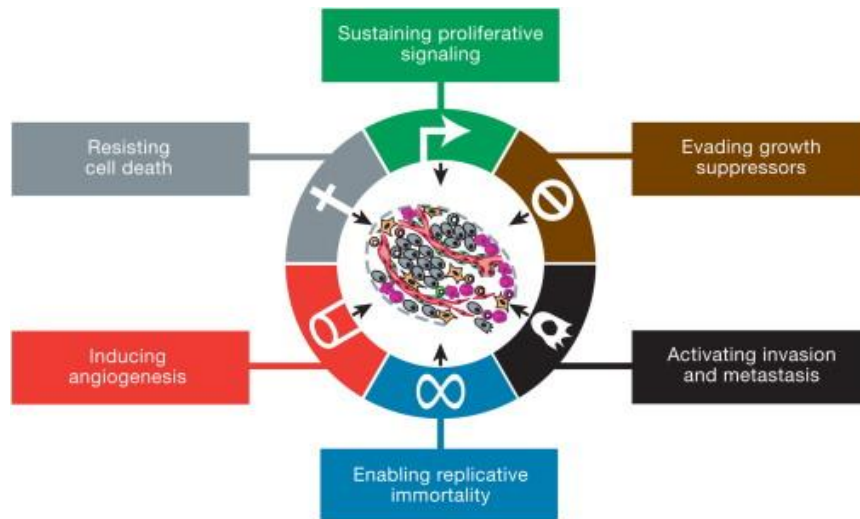
1.4.5. Mutations of ERK1/2 pathway components in cancer

Components of the ERK1/2 pathway are frequently mutated in melanomas, gastrointestinal tract, lung, thyroid, ovarian, cervical, endometrial pancreatic and prostate cancer (<http://cancer.sanger.ac.uk/cosmic/gene/analysis?ln=BRAF>). Most tumours deregulate the ERK1/2 pathway, demonstrating the importance of regulation of the pathway.

RTKs form the largest family of oncogenes (Reviewed by Easty *et al.*, 2011). There are 20 subfamilies in humans with 58 members, which share a common overall composition, consisting of an extracellular ligand-binding domain, a single-pass transmembrane domain and an intracellular tyrosine kinase domain (Sugiura *et al.*, 2007).

Figure 1.7 Hallmarks of Cancer (Taken from Hanahan & Weinberg, 2011).

The six hallmarks of cancer have been described by Hanahan and Weinberg originally proposed in 2000, and revised in 2011.



Mutations in each *RAS* isoform are specific to particular cancers. *HRAS* mutations are commonly found in bladder, head and neck and skin cancers, *KRAS* mutations are commonly found in lung, colon and pancreatic cancers, and *NRAS* mutations predominate in melanoma (Reviewed by Bos, 1989). *KRAS* is the most commonly mutated isoform, accounting for ~85% of *RAS* mutations in human cancers (Downward, 2003).

Mutations are more commonly found in *BRAF* than *ARAF* or *CRAF*, and this is thought to be due to the fact that *BRAF* activation requires fewer steps for activation as mentioned in Section 1.3. Mutations in *ARAF* are rare, and the mutants G331C and A451T have low activity with no transforming ability, suggesting that they are passenger mutations (Rebocho & Marais, 2012). ~25,000 human cancers have been found to contain a mutation in *BRAF* (<http://cancer.sanger.ac.uk/cosmic/gene/analysis?ln=BRAF>), representing ~7% of human cancers (Davies *et al.*, 2002; Garnett & Marais, 2004; McCubrey *et al.*, 2008).

CRAF mutations in human cancer are rare. 31 base substitutions and 7 fusion mutations have been reported (<http://cancer.sanger.ac.uk/cosmic/gene/analysis?ln=BRAF>). The same mutations are rarely reported more than once. Two *SRGAP3-CRAF* fusion proteins have been reported in pilocytic astrocytoma, but their activity was not assessed (Cin *et al.*, 2011). 4 of the 545 cancer cell lines studied by Emuss *et al.* (2005) were found to contain a base-substitution in *CRAF*, including P207S, V226I, Q335H and E478K. Immunoprecipitation kinase assays in cells

overexpressing these mutations showed that they did not significantly change CRAF activity (Emuss *et al.*, 2005). The most common *RAF* mutation is $V600E$ *BRAF*, which has high kinase activity as will be discussed later. When the equivalent of $V600E$ *BRAF* mutation was introduced into *CRAF*, the kinase activity was only weakly increased, and *CRAF* was not converted to an oncogene (Emuss *et al.*, 2005). Moreover, when the tyrosine phosphorylation sites Tyr340 and Tyr341 of *CRAF* were converted to aspartic residues as in *BRAF*, and the equivalent of $V600E$ mutation were introduced into *CRAF*, *CRAF* activity was increased by over 1,000 fold and was able to transform COS cells (Emuss *et al.*, 2005) showing the importance of the negative charge in the N-termini of *BRAF* in transforming ability.

BRAF mutations rarely coincide with *RAS* mutations, and $V600E$ *BRAF* is mutually exclusive from *RAS* mutations at the single cell level (Dadzie *et al.*, 2009). Cancers with *BRAF* and *RAS* mutations share some similarities, and therefore it has been suggested that either mutation is sufficient to drive cancer. Interestingly, studies have shown that $V600E$ *BRAF*-mutant cancers do not require *RAS* to drive proliferation, although other *BRAF*-mutant cells still depend on *RAS* signalling (Davies *et al.*, 2002). This may be due to the potent transforming capability of $V600E$.

1.6. *BRAF* mutants

Insertions, deletion and fusion mutations in *BRAF* have been identified in human cancers, but the most common type of mutation is a base substitution, which accounts for 99% of *BRAF* mutations in human cancer

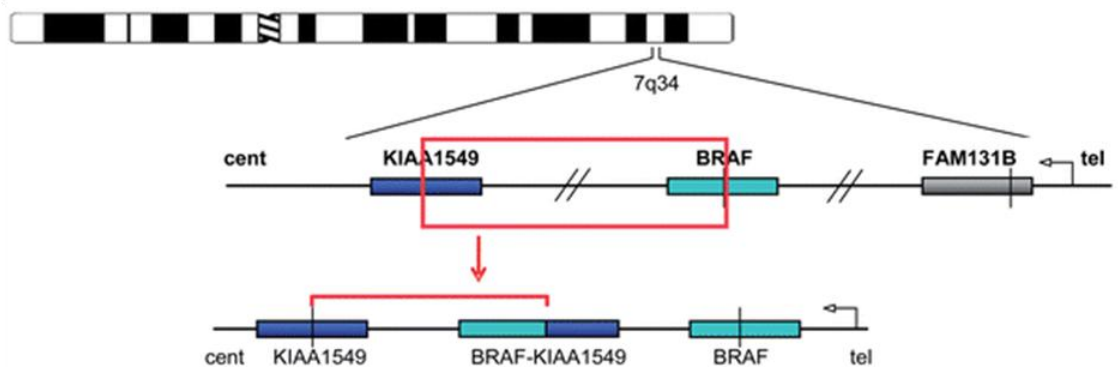
(<http://cancer.sanger.ac.uk/cosmic/gene/analysis?In=BRAF>). *BRAF* mutations are found in ~7% of human cancers, and are most commonly found in melanomas, accounting for ~90% of the mutations (Davies *et al.*, 2002). *BRAF* mutations are also found in a number of other cancers, including thyroid, colorectal and lung cancers, and in sarcomas and ovarian carcinomas (<http://cancer.sanger.ac.uk/cosmic/gene/analysis?In=BRAF>). Almost all base substitutions cluster within the activation segment or the glycine-rich P-loop, disrupting the inactive conformation, resulting in a more active protein. Insertions and deletions are rare, but fusion mutations are not uncommon with the majority containing an in-frame fusion of *KIAA1549* and *BRAF* (<http://cancer.sanger.ac.uk/cosmic/gene/analysis?In=BRAF>).

KIAA1549 is expressed in many tissues and contains two transmembrane domains, but little is known about the protein (Nagase *et al.*, 2000). The fusion protein arises as a result of copy number gain of approximately 2Mb of chromosome 7q34, which is inserted back into the *KIAA1549* or *BRAF* gene, resulting a transcript that codes for the *BRAF* kinase domain adjacent to *KIAA1549*, which replaces the N-terminus (Figure 1.8) (Forsheew *et al.*, 2009; Jones *et al.*, 2008; Sievert *et al.*, 2009). Without autoinhibition by the N-terminus, the fusion protein is constitutively active, as shown by kinase assays and transforms NIH-3T3 cells (Jones *et al.*, 2008). The fusion protein is commonly found in pilocytic astrocytomas, a common pediatric brain tumour (Forsheew *et al.*, 2009; Jones *et al.*, 2008; Sievert *et al.*, 2009). In addition to the *KIAA1549*-*BRAF* fusion protein, an in-frame deletion of ~2.5Mb that forms a *BRAF* fusion protein with *FAM131B* has been identified in pilocytic astrocytoma

Figure 1.8 A schematic of BRAF fusion proteins (Taken from Cin et al., 2011)

- A) KIAA1549-BRAF fusion protein arises as a result of duplication of a tandem repeat of ~2Mb of chromosome 7q34, which is re-inserted to produce a fusion protein of KIAA1549 and the kinase domain of BRAF.
- B) FAM131B-BRAF fusion protein arises as a result of deletion of ~2.5Mb from chromosome 7q34 to produce fusion protein of FAM131B and the kinase domain of BRAF.

A) KIAA1549-BRAF fusion protein



B) FAM131B-BRAF fusion protein

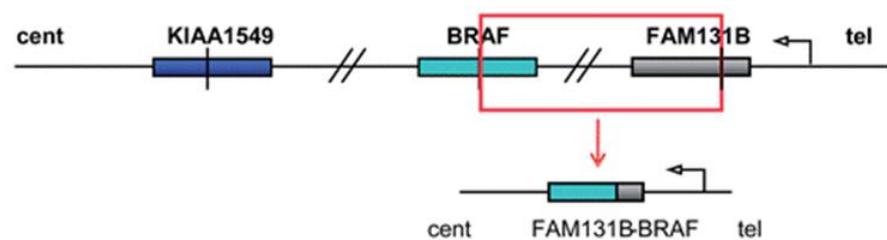


(Figure 1.8). Again, the fusion protein lacks the N-terminus of BRAF, with potent MEK/ERK activity and transforming capability in NIH 3T3 cells (Cin *et al.*, 2011).

In order of prevalence, the most commonly mutated residues from single base substitution include: V600, K601, G469, D594, L597 and G466 (<http://cancer.sanger.ac.uk/cosmic/gene/analysis?ln=BRAF>), all of which are within the activation segment or glycine-rich P-Loop (Figure 1.9).

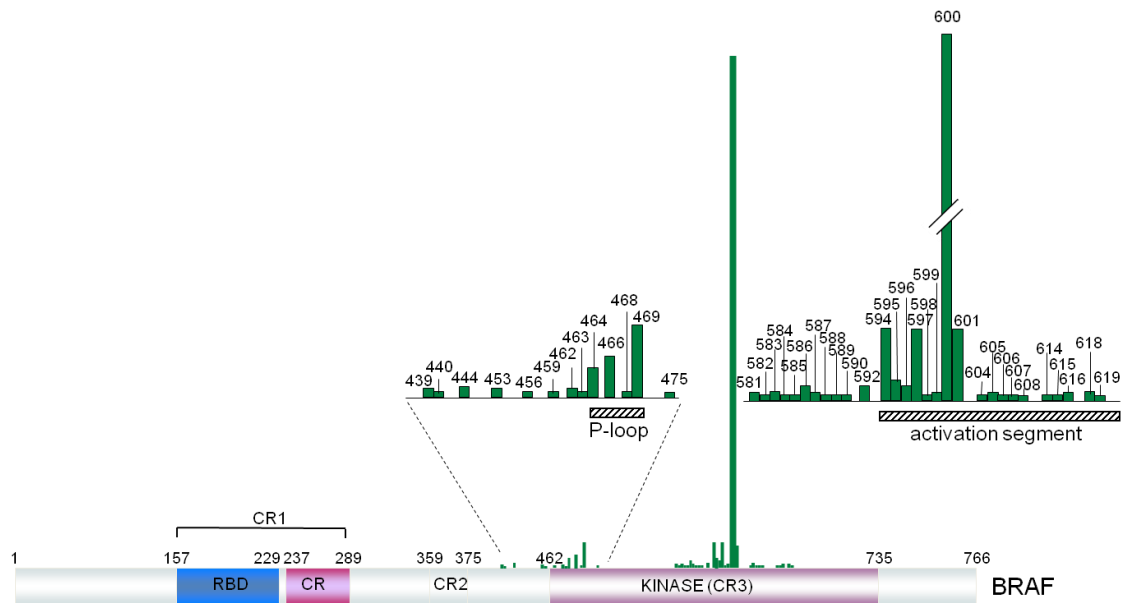
Not all *BRAF* mutations result in an increase in kinase activity. To examine the *BRAF* mutants more directly, they were classified into 3 groups according to their level of intrinsic kinase activity (Wan *et al.*, 2004). High kinase activity mutants have a basal kinase activity above oncogenic RAS-induced ^{WT}*BRAF* activity. Intermediate kinase activity mutants have basal kinase activity in between ^{WT}*BRAF* activity and oncogenic RAS-induced ^{WT}*BRAF* activity. Impaired kinase activity mutants have basal kinase activity lower than ^{WT}*BRAF* activity (Wan *et al.*, 2004).

1.6.1. High kinase activity mutants

High activity mutants include G469A, E586K, V600E, V600E, V600K, V600R and K601E. All of these mutants lie within the glycine-rich P-loop and DFG motif except ^{E586K}*BRAF*, which lies on the opposite surface of the kinase domain from the DFG motif. The crystal structure of the *BRAF* kinase domain suggests that this mutation disrupts the interdomain interactions, thereby relieving N-terminal domain autoinhibition (Wan *et al.*, 2004). High activity mutants adopt the conformational changes of the active protein kinase activity (Wan *et al.*, 2004).

Figure 1.9 Oncogenic *BRAF* mutations (adapted from Wellbrock et al., 2004).

The majority of mutations in *BRAF* lie within the activation segment or glycine rich loop. The frequency of mutations at each residue is represented by green bars.



The majority of *BRAF* mutants in human cancer have high kinase activity, and all translated to elevated levels of P-ERK1/2 when overexpressed in COS cells (Wan *et al.*, 2004).

The most frequently occurring *BRAF* mutation in human cancers is ^{V600E}*BRAF*, which involves a 1799T>A transversion, resulting in a valine being substituted with glutamic acid at residue 600. Mutations at this residue account for 98% of the 24,000 base substitutions in *BRAF* (<http://cancer.sanger.ac.uk/cosmic/gene/analysis?ln=BRAF>). ^{V600E}*BRAF* can signal as a monomer and is constitutively active independently of RAS activation and dimerisation (Poulikakos *et al.*, 2011). A substitution of the medium sized valine for the larger and negatively charged glutamic acid is thought to mimic the phosphorylating events required for BRAF activation, and disrupts the Val600 interaction with Phe467, resulting in a constitutively active conformation with approximately 500 fold increase in activity. However, this cannot explain how all other activation loop mutants cause an increase in BRAF activity, since they do not all introduce a negative charge within the glycine-rich P-loop of BRAF.

^{V600E}*BRAF* is detected in nevi (Pollock *et al.*, 2003; Yazdi *et al.*, 2003), and in the early stages of colorectal cancer (Rajagopalan *et al.*, 2002; Yuen *et al.*, 2002), suggesting it to be a founder mutation. However, ^{V600E}*BRAF* may not be sufficient for cancer progression on its own, as suggested by the high percentage of nevi with ^{V600E}*BRAF*, and a significantly lower percentage of metastatic melanomas with the mutation (Pollock *et al.*, 2003).

1.6.2. Intermediate kinase activity mutants

Intermediate kinase activity mutants include F595L, L597V, T599L, G466A and G469E (Wan *et al.*, 2004). They are most likely to be caused by a disruption in the inactive conformation of the DFG motif, but the substitution is unable to provide optimal catalytic activity (Wan *et al.*, 2004). Our knowledge on intermediate kinase activity BRAF mutants is limited because they are rarely reported.

A mutation at Leu597 constitutes for <0.5% of the total BRAF mutations, but is the 5th most commonly mutated residue in BRAF in human cancers (<http://cancer.sanger.ac.uk/cosmic/gene/analysis?ln=BRAF>). To date, 12 cancer samples (<http://cancer.sanger.ac.uk/cosmic/gene/analysis?ln=BRAF>) have been identified to carry the ^{L597V}BRAF mutation. The mutation involves a 1789C>G transversion resulting in a leucine being substituted for a valine at residue 597. Leu597 lies within the activation segment and contacts Val471, Gly464 and Gly466 of the glycine-rich P-loop (Wan *et al.*, 2004). It is intriguing how both leucine and valine have similar properties, but a substitution from leucine to the more hydrophobic valine can elevate the kinase activity to 64-fold higher than ^{WT}BRAF (Wan *et al.*, 2004).

Other ^{L597}BRAF mutants have been briefly described. ^{L597Q}BRAF has been reported in acute lymphocytic leukaemia (Gustafsson *et al.*, 2005), melanoma (Cruz *et al.*, 2003), lung, ovarian and other cancers (<http://cancer.sanger.ac.uk/cosmic/gene/analysis?ln=BRAF>). Overexpression of

^{L597Q}BRAF in NIH 3T3 cells was found to induce foci formation and P-ERK to similar levels of ^{V600E}BRAF overexpressing cells (Hou *et al.*, 2007). ^{L597S}BRAF has only been reported in melanoma (<http://cancer.sanger.ac.uk/cosmic/gene/analysis?ln=BRAF>). The level of P-ERK in melanoma cell lines expressing ^{L597S}BRAF were equivalent to melanoma cell lines harbouring ^{V600E}BRAF (Daniotti *et al.*, 2004), and the cells formed networks in matrigel (Zipser *et al.*, 2011). Therefore unlike L597V, substitution of the neutral leucine to the polar amino acids glycine or serine resulted in a more active mutant and became a high kinase activity mutant.

^{L597}BRAF has been found to be co-expressed with other driver mutations, including other BRAF mutations, most commonly V600E and mutations in ATM, EGFR, FGFR, NRAS, TP53 etc (<http://cancer.sanger.ac.uk/cosmic/gene/analysis?ln=BRAF>). This suggested that mutations at this residue are insufficient to drive tumourigenesis, but it is unknown whether L597 mutations arise as a result of cancer or are involved in cancer development.

1.6.3. Impaired kinase activity mutants

Only a handful of impaired activity mutants have been identified in cancer, including G466E, G466V, G596R and D594V. They are a result of amino acid substitution of highly conserved or invariant residues that are required for optimal protein kinase catalytic reaction activity (Wan *et al.*, 2004). These mutants have between 30-80% of basal ^{WT}BRAF activity, but ERK activity is higher than cells transfected with ^{WT}BRAF (Wan *et al.*, 2004).

The D594 residue is the most commonly mutated residue to produce impaired kinase activity mutants. Wan et al (2004) showed that D594V did not activate ERK in COS cells, unlike other impaired kinase activity mutants. Kinase assays showed that D594V failed to activate CRAF, whereas other impaired kinase activity mutants maintained CRAF and ERK kinase activity (Wan *et al.*, 2004). In a separate study, a ^{D594G}BRAF mutant cell line relied on CRAF activity for ERK activation and cell survival, shown by cell death and inhibition of P-ERK levels by treatment of the CRAF-inhibitor Sorafenib (Smalley *et al.*, 2009). Further studies have shown the importance of CRAF in ERK signalling induced by impaired kinase activity mutants in a $\text{Braf}^{+/D594A}$ transgenic mouse model. D594A involves a 1781A>C transversion resulting in an aspartic acid being substituted for an alanine at residue 594. $\text{Braf}^{+/Lox-D594A}$ mouse embryonic fibroblasts (MEFs) immortalised without loss of p19^{ARF} or p53 function and maintained P-Erk levels, which were consistently higher in immortalised MEFs, and this was dependent on Crf (Kamata *et al.*, 2010). Another feature of $\text{Braf}^{+/Lox-D594A}$ MEFs was aneuploidy (Kamata *et al.*, 2010). Introduction of the kinase-dead Crf, ^{D486A}Craf into $\text{Braf}^{+/Lox-D594A}$ MEFs did not induce early immortalisation, and MEFs remained diploid, suggesting the importance of Crf in ^{D594A}Braf-induced aneuploidy and early immortalisation (Kamata *et al.*, 2010).

1.7. RASopathies

As mentioned, hyperactivation of the MAPK pathway has been linked to a group of developmental syndromes known as RASopathies. The group of RASopathy syndromes include Autoimmune lymphoproliferative syndrome,

Cardiofaciocutaneous syndrome (CFC), Capillary malformation-AV malformation syndrome, Costello syndrome, Hereditary Gingival fibromatosis type 1, Legius syndrome, LEOPARD Syndrome, Neurofibromatosis Type 1 and Noonan Syndrome (ras-pathway-syndromes.com/about). Patients share neurological, cardiovascular, facial and cutaneous disorders to different degrees, depending on the mutation that they carry. Medical geneticists can usually distinguish between syndromes by the characteristics presented. Due to the phenotypic and pathogenetic similarities these disorders have been termed neurocardiofacialcutaneous syndromes or RASopathies (Bentires-Alj *et al.*, 2006; Tidyman & Rauen, 2009). Even within the same syndrome, there is a diverse range of symptoms and this is dependent on the difference in gene mutations directing the different disorders. The most common RASopathies will be discussed in more extent below.

CFC, Costello and Noonan syndrome share similar characteristics, including short stature, mental retardation, fine sparse curly hair, relative macrocephaly, palpebral ptosis, downward-slanting palpebral fissures, strabismus and skin defects including café-au-lait spots and pigmented nevi. Other facial, skin and cardiac features are more syndrome-specific. CFC and Noonan syndrome patients have a large head with a tall forehead, and narrowing at the temples. Noonan syndrome patients have a small face behind a small cranium, and both CFC and Costello patients have a tall forehead with a small chin and a short broad nasal base. CFC patients have dry hyperkeratotic skin, Costello patients have loose skin with excessive wrinkling, and Noonan syndrome patients have thin transparent skin. The common cardiac defects in CFC, Costello and

Noonan patients include hypertrophic cardiomyopathy, and pulmonic stenosis which is less frequently detected in Costello patients. Skeletal deformities are also evident and seizures are common in patients with CFC and Noonan syndrome (Roberts *et al.*, 2006; Costello, 1977; Hennekam, 2003; Noonan, 1968; Noonan, 1994; Allanson, 2007; van der Burgt, 2007).

Patients with LEOPARD syndrome develop symptoms similar to Noonan syndrome, with cranial dimorphism, but milder, short neck without the characteristic wide webbed neck and progressive myocardial hypertrophy. Other symptoms include growth retardation, lentigo which develop into café-au-lait spots, webbed fingers, ECG conduction abnormalities, ocular hypertelorism, pulmonic stenosis, abnormal genitalia, and sensorineural deafness (Gorlin *et al.*, 1971).

Neurofibromatosis type 1 patients are presented with at least 2 features, which include café-au-lait spots, intertriginous freckling, lisch nodules affecting the eyes, neurofibromas, optic pathway gliomas, and distinctive bony lesions (Williams *et al.*, 2009).

1.7.1. Mutations of RAS/RAF pathway

Many studies have now shown that RASopathy patients have germline mutations in transducers of the RAS pathway (Table 1.1), and inhibition of the pathway using the MEK inhibitor PD0325901 can reduce or prevent characteristics of the syndrome in zebrafish models expressing BRAF^{Q257R}, BRAF^{G596V} or BRAF^{S467A} (Anastasaki *et al.*, 2009; Anastasaki *et al.*, 2012).

Table 1.1 Mutations found in RASopathies.

The majority of RASopathy patients carry a mutation in genes that code for proteins involved in the RAS pathway.

Syndrome	Gene	Protein function
Cardiofaciocutaneous Syndrome	KRAS	GTPase
	BRAF	Kinase
	MEK1	Kinase
	MEK2	Kinase
Costello Syndrome	HRAS	GTPase
	KRAS	GTPase
	BRAF	Kinase
	MEK1	Kinase
Leopard Syndrome	BRAF	Kinase
	CRAF	Kinase
	PTPN11	Phosphatase
Neurofibromatosis type 1	NF1	RASGAP
Noonan Syndrome	SOS1	RASGEF
	KRAS	Kinase
	NRAS	Kinase
	BRAF	Kinase
	CRAF	Kinase
	MEK1	Kinase
	PTEN11	Phosphatase

Studies have shown that the RASopathy-causing germline mutations are rarely found in cancer, suggesting that cancer-causing lesions may severely affect embryonic or foetal development (Sarkozy *et al.*, 2009).

Almost all cases of CFC are sporadic (<http://www.cfcsyndrome.org>). ~75% of mutation-positive CFC patients have a mutation in *BRAF*, and a smaller proportion of NS and LS patients have a mutation in *BRAF* (Sarkozy *et al.*, 2009; Rodriguez-Viciano *et al.*, 2006). Only 7 *BRAF* mutations, which are G469E, F468S, L485F, L597V, F595L, V600G and K601E have been found in both cancer and CFC (Rodriguez-Viciano *et al.*, 2006; Champion *et al.*, 2011) with L597V being detected in both CFC and NS (Sarkozy *et al.*, 2009; Pierpont *et al.*, 2010). However, not all of the syndromes are linked to a higher risk in cancer. Only several patients with CFC have developed neoplasms in different tissues including acute lymphocytic leukaemia (Rauen *et al.*, 2011). Therefore it is still uncertain whether CFC patients have a higher risk of malignancies or not (Tidyman & Rauen, 2008).

Costello syndrome is an autosomal dominant inherited disorder of which most cases are sporadic (Hennekam, 2003). ~17% of patients with Costello syndrome develop cancer, the most common being embryonic rhabdomyosarcoma (Rauen *et al.*, 2011). The clinical symptoms overlap with CFC syndrome, making a clinical diagnosis challenging, but individuals with a *HRAS* mutation are considered to have Costello syndrome (Rauen, 2006; Kerr *et al.*, 2008). Patients typically have a mutation in exon 12 or 13 that disrupt

guanine-nucleotide binding, resulting in reduction of intrinsic and GAP-induced GTPase activity, causing RAS to remain in the active form (Gibbs *et al.*, 1984; McGrath *et al.*, 1984; Sweet *et al.*, 1984).

LEOPARD syndrome is an autosomal disorder. The syndrome is rare and many of the patients have a mutation in *PTPN11*, which may account for the similarity of the characteristics shared between these patients and Noonan syndrome patients (Digilio *et al.*, 2006). Mutations in *BRAF* or *CRAF* are less frequent (Koudova *et al.*, 2009; Kuburovic *et al.*, 2011). Several cases of malignancies have been recorded, including acute myeloid leukaemia, acute lymphoblastic leukaemia, neuroblastoma and melanoma (Kratz *et al.*, 2011). However, cases of LEOPARD syndrome are rare, making it hard to draw conclusions as to whether patients are prone to develop cancer or not (Kratz *et al.*, 2011).

Neurofibromatosis type 1 is one of the most common autosomal dominant disorders. All patients have a germline mutation in one copy of the neurofibromin 1 (NF1) gene, which is responsible for the GTPase activity of HRAS, and approximately half of these are *de novo* mutations. Patients are predisposed to developing benign and malignant neoplasias (Williams *et al.*, 2009), and individuals carrying this mutation develop Juvenile myelomonocytic leukemia at an incidence that is elevated to ~200-fold higher than patients without the mutation (Stiller *et al.*, 1994; Bader & Miller, 1978).

Noonan syndrome is an autosomal dominant disease with a high proportion of sporadic cases arising from *de novo* mutations. Noonan syndrome patients

have a higher risk of developing juvenile myelomonocytic leukaemia (JMML). Although the disorder may regress without treatment, it may progress to acute myeloid leukaemia. ~75% of patients carry a mutation as so far detected, but the cause for the remaining 25% is unknown. The majority of patients have a mutation that causes an increase in RAS signalling. Most patients have a mutation in *PTPN11*, a gene that codes for the Src homology-2 domain-containing protein tyrosine phosphatase (PTP) SHP2. Other less frequent mutations include mutations in *KRAS* that causes a reduction in the intrinsic GTPase activity of RAS (Schubbert *et al.*, 2006), mutations in the residues responsible for stabilising the SOS1 protein in an inhibited conformation (Roberts *et al.*, 2007; Tartaglia *et al.*, 2007), or one of several gain-of-function mutations in *CRAF* (Pandit *et al.*, 2007; Razzaque *et al.*, 2007). Interestingly, one patient harboured a mutation within the activation segment of CRAF which caused a loss of function (Pandit *et al.*, 2007).

Since the majority of the mutations are activating mutations, inhibitors that have been shown to be successful in blocking their activity and limiting tumour growth may be useful in ameliorating the disease phenotypes. However, this may be limited to before birth as shown in mouse models (Schuhmacher *et al.*, 2008), which will be discussed in Section 1.8.3.

1.8. Data on mouse models

Mice have proven to be a useful tool in modelling diseases, due to the capability of genetically modifying the mouse genome. Pluripotent embryonic stem (ES) cells can be cultured on a layer of Mouse Embryonic Fibroblasts (MEFs) that provide the ES cells with nutrients and anchorage. Exogenous DNA can be

incorporated into cultured ES cells by electroporation, and following homologous recombination between exogenous and endogenous DNA, the exogenous DNA can be incorporated into the genome. Bacterial cloning is used to produce targeting vectors which include exogenous DNA and a selectable marker, flanked by homologous DNA sequences such that homologous recombination occurs at the point of interest, replacing endogenous DNA with the exogenous DNA. This is a rare event, and the selectable marker allows selection for ES cells that carry the targeting vector.

1.8.1. Cre-LoxP system

Many genes are essential for survival. For example, *Braf*^{-/-} embryos do not survive beyond E12.5. As a result, the function of the gene cannot be investigated past embryonic stage. To circumvent this problem, conditional 'knock-out' mouse models have been developed. One of the most commonly used systems is the Cre-LoxP system.

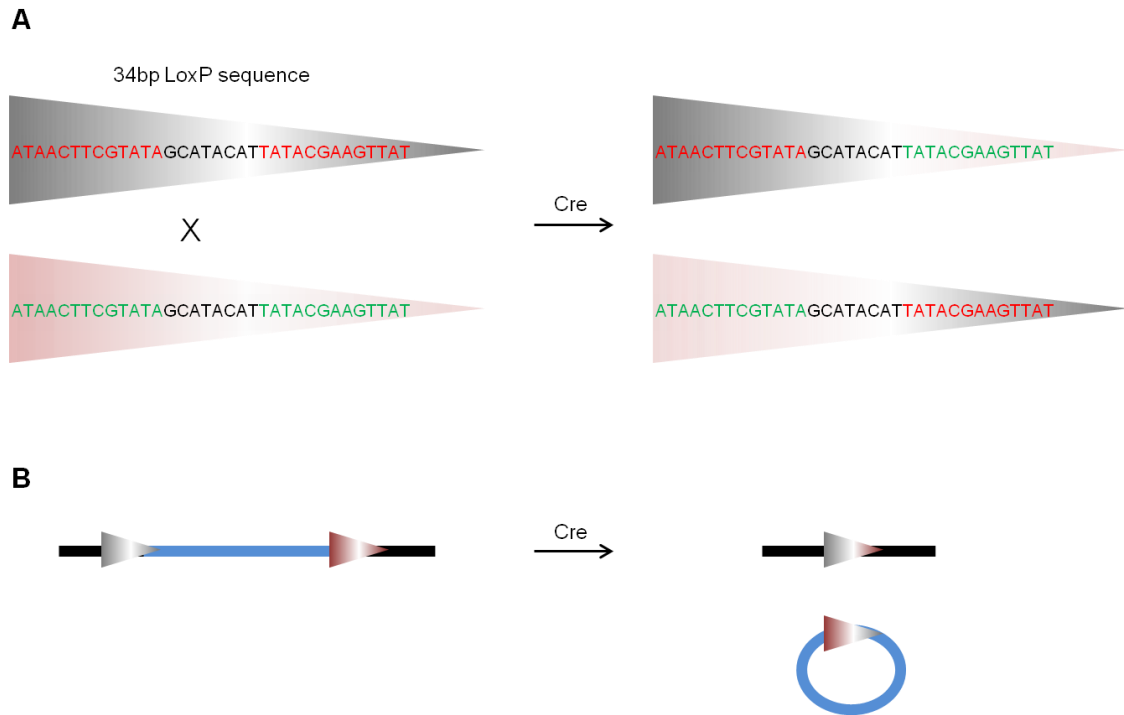
The Cre-Lox mechanism was first discovered in P1 bacteriophage which uses Cre-Lox recombination to circularize and facilitate replication of its DNA during reproduction (Figure 1.10) (Sauer & Henderson, 1988; Sternberg *et al.*, 1981).

The LoxP site is a 34bp consensus sequence that carries a core spacer sequence flanked by two 13bp palindromic sequences. A single Cre recombinase molecule binds to each palindromic half of a LoxP site, and then the recombinase forms a tetramer bringing the two LoxP sites together, and recombination occurs within the spacer area of the LoxP sites. Recombination

Figure 1.10 Cre-LoxP system to show the LoxP site

The LoxP site is a 34bp consensus sequence that carries a core spacer sequence flanked by two 13bp palindromic sequences. A single Cre recombinase molecule binds to each palindromic half of a LoxP site, and then the recombinase forms a tetramer bringing the two LoxP sites together. Recombination occurs within the spacer area of the LoxP sites.

- A) LoxP sequence.
B) Schematic of excision.



results in excision, inversion or translocation depending on the relative orientation of the two LoxP sites (Reviewed by Nagy, 2000).

$Braf^{+/LSL-L597V}$, $Braf^{+/LSL-V600E}$ and $Braf^{+/LSL-D594A}$ mice were produced by homologous recombination of a mutated exon 15. To prevent expression of the mutation in all cells, a Lox-Stop-Lox cassette that expresses wild-type exons 15 to 18 of Braf and a neo^R cassette were inserted in between exons 14 and 15. The cassette was flanked by wild-type exon 14 and the mutated exon 15 to target the cassette for successful homologous recombination (Figure 1.11).

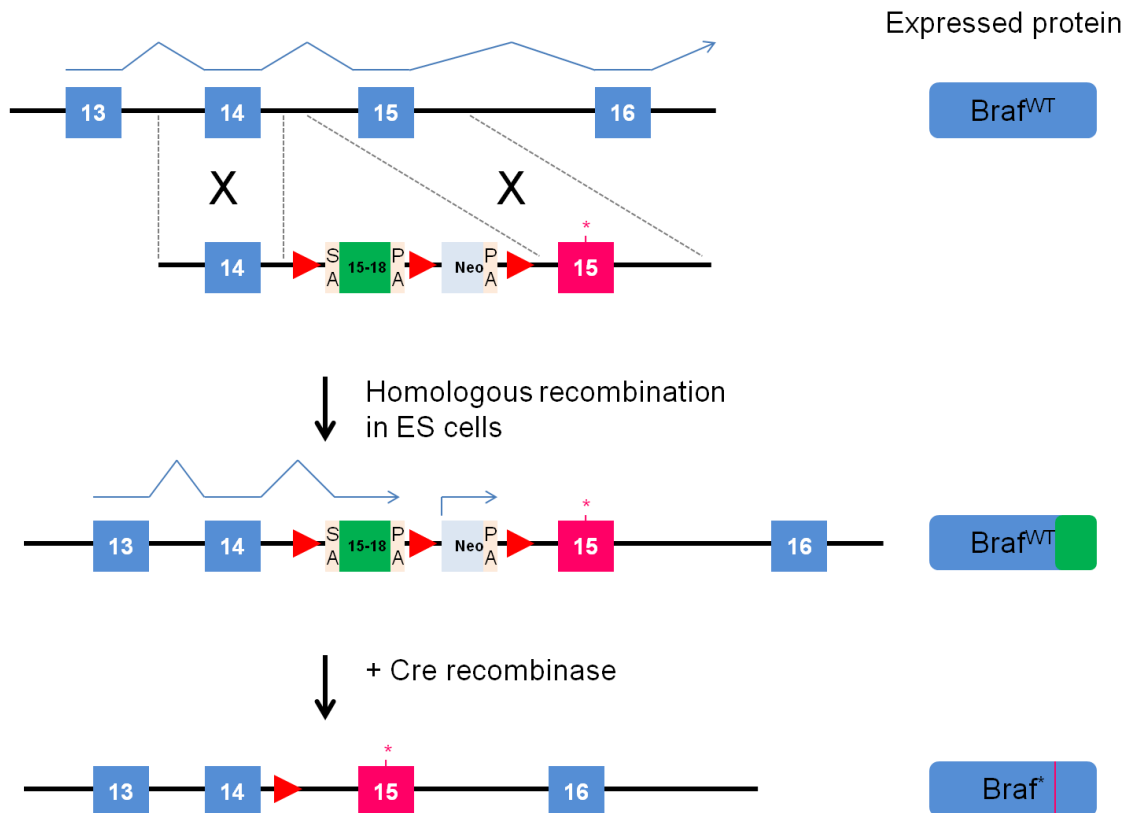
Splice acceptor and polyadenylation sequences were cloned on either side of the minigene. In the absence of Cre recombinase, mice express $^{WT}Braf$. In the presence of Cre recombinase, the LoxP sites come together and following recombination, the cassette is released. This leaves the mutated exon 15 intact and the mutant Braf protein is expressed. $Kras^{+/LSL-G12D}$ mice were generated in a similar way, and will be discussed later.

1.8.2. Mouse models of cancer

Human tumours have been xenografted into mice to examine the effectiveness of drug treatment. Cancer cells have been injected into mice to examine metastasis. For example, mice injected with $G12V$ KRAS melanoma cells developed lung tumours (Milagre *et al.*, 2010). Injection of $V600E$ BRAF melanoma cells that have had BRAF knocked-down into mice tail veins resulted in fewer lung tumours, in comparison with mice injected with $V600E$ BRAF positive melanoma cells without BRAF knock-down (Sharma *et al.*, 2006). This suggests

Figure 1.11 Conditional knock-in mouse models

Braf-mutant mice were generated from ES cells that contained the modified allele. A Lox-Stop-Lox cassette that contains a minigene expressing wild-type exons 15 to 18 of Braf and a neo^R cassette was inserted between exons 14 and 15. Splice acceptor (SA) and polyadenylation (PA) sequences were cloned on either side of the minigene. In the absence of Cre recombinase, mice express ^{WT}Braf. In the presence of Cre recombinase, recombination occurs between the LoxP sequence (large red arrows) and the LSL cassette is released. Following recombination, the mutated exon 15 (*) is transcribed and the mutant Braf is expressed.



the importance of ^{V600E}BRAF in metastasis. Many mouse models of human cancers have been established, including mouse models harbouring mutations of the RAS/RAF/MEK/ERK pathway. To study the effect of gene modification *in vivo*, animal models have been extensively used to examine human diseases, including cancer. This has been a break-through in examination of individual and combinations of mutations in tumour development. The most common ways to model human cancer are to activate oncogenes or inactivate tumour suppressor genes, using the conditional knock-in or knock-out models. Most of these have been generated using the Cre-Lox technology mentioned above.

A Cre-controlled $Kras^{+/LSL-G12D}$ mouse strain was subsequently reported (Tuveson *et al.*, 2004). $Kras^{+/LSL-G12D}$ mice were generated by insertion of a Lox-Stop-Lox cassette containing the splice acceptor, polyadenylation site and the selection marker Pur^R . The targeting vector contained the LSL cassette at the 5' end of *Kras* exon 1 containing the G35A mutation, and was flanked by homologous regions of the introns 3' and 5' to exon 1, which targeted the vector to the *Kras* gene. In the absence of Cre, the polyA-tail within the LSL cassette halts transcription, and ^{WT}*Kras* is transcribed by the other allele. Cre was introduced by Adenovirus expressing Cre recombinase (AdCre) by nasal inhalation to target recombination and ^{G12D}*Kras* expression in the lungs (Jackson *et al.*, 2001). Atypical adenomatous hyperplasia (AAH), epithelial hyperplasia (EH) and adenomas were observed. The tumour burden increased with AdCre dose and with age (Jackson *et al.*, 2001), enabling synchronisation and control of tumour burden.

$Braf^{+/Lox-V600E}$ mice were generated by the Cre-Lox system mentioned above. $Braf^{+/LSL-V600E}$ mice were intercrossed with mice heterozygous for the CMV-Cre transgene, but no viable $Braf^{+/Lox-V600E}$; CMV-Cre offspring were born (Mercer *et al.*, 2005), indicating $V600E$ Braf induces embryonic lethality (Mercer *et al.*, 2005). Subsequent studies used a targeted approach to study the mutation in different cancers. A melanoma model was generated by intercrossing $Braf^{+/LSL-V600E}$ mice to a tamoxifen-controlled Cre strain (Dhomen *et al.*, 2009). Tamoxifen was applied to the skin of the mice to induce recombination. Tamoxifen-treated mice developed nevi, the early precursor of melanoma, and the majority of these mice developed melanoma following a latency period of ~10 months (Dhomen *et al.*, 2009). These results suggest that $V600E$ Braf is a founder mutation. The long latency period involved senescence where cells entered quiescence. Senescence was also observed in the lungs of $Braf^{+/V600E}$ mice, where adenomas fail to progress to cancer without loss of the senescence markers p16^{INK4A}, p19^{Arf} or p53, and $Braf^{+/V600E}$ mice that were engineered to lack p16^{INK4A}, p19^{Arf} or p53 developed spontaneous adenocarcinomas (Dankort *et al.*, 2007). Furthermore, a gastrointestinal $Braf^{+/V600E}$ mouse model showed crypt hyperplasia followed by $V600E$ Braf-induced hypermethylation of p16^{INK4a} and senescence (Carragher *et al.*, 2010). Therefore the $V600E$ Braf mutation drives cancer, but cooperates with tumour suppressor genes in this process.

$Braf^{+/D594A}$ mice were generated by the Cre-Lox system as mentioned above. Cre was introduced by intercrossing $Braf^{+/LSL-D594A}$ mice with mice heterozygous for the CMV-Cre transgene. In contrast, $Braf^{+/Lox-D594A}$ mice were born at a frequency of ~13%, and mice survived for at least 6 months (Kamata *et al.*,

2010). Splenomegaly was observed in all mice, and arose as a result of accelerated proliferation of myeloid and lymphoid lineages (Kamata *et al.*, 2010). Other abnormalities that were not consistently observed in animals included strokes, genital warts and ovarian cysts (Kamata *et al.*, 2010). In a separate publication, $\text{Braf}^{+/LSL-D594A}$ mice were intercrossed with $\text{Tyr}::\text{CreERT2}$ mice, in which the tyrosinase promoter drives expression of the tamoxifen-regulated Cre recombinase in melanocytes (Heidorn *et al.*, 2010). $\text{Braf}^{+/Lox-D594A}$ mice did not have skin hyperpigmentation, nevi or tumours, except for weak tail darkening (Heidorn *et al.*, 2010), but when combined with $\text{G}^{12D}\text{Kras}$ in melanocytes, the mice developed hyperpigmentation with large, rapidly growing oligo-pigmented tumours with features of malignancy (Heidorn *et al.*, 2010). The features were shown to be due to $\text{D}^{594A}\text{Braf}$ binding to $\text{G}^{12D}\text{Kras}$ and inducing transactivation of Craf (Heidorn *et al.*, 2010).

$\text{Braf}^{+/L597V}$ mice were generated using the Cre/Lox system as mentioned above. $\text{Braf}^{+/Lox-L597V}$ mice were generated by intercrossing $\text{Braf}^{+/LSL-L597V}$ mice with mice heterozygous for the CMV-Cre transgene. Animals were born at the Mendelian ratio, and ~70% of mice survived to adulthood (Andreadi *et al.*, 2012). Mice displayed variable penetrance of benign tumours, including skin papillomas and intestinal polyps. AdCre introduction to the lungs did not induce recombination, suggesting a limited or absent growth advantage by $\text{L}^{597V}\text{Braf}$, and the lungs were normal, which could be due to the weak Mek/Erk activity of $\text{L}^{597V}\text{Braf}$. However, introduction of $\text{L}^{597V}\text{Braf}$ to $\text{Kras}^{+/Lox-G12D}$ mice increased the lung tumour burden with a faster progression to adenocarcinoma, and the range of hyperplasias were more similar to lungs of $\text{Braf}^{+/Lox-V600E}$ mice (Andreadi *et al.*,

2012). Therefore, like $\text{Braf}^{+/Lox-D594A}$ mice, $\text{Braf}^{+/Lox-L597V}$ mice showed some predisposition to benign tumours, and showed some contribution to cancer in the presence of the G^{12D} *Kras* oncogene.

1.8.3. Mouse models of RASopathies

Zebrafish models have been developed to study RASopathies. These models showed that developmental problems arise before birth. Developmental problems of zebrafish embryos after being injected with the CFC-causing BRAF^{Q257R} and BRAF^{G596V} DNA include elongation and lack of tail formation (Anastasaki *et al.*, 2009). Early MEK-inhibition by CI-1040 or PD0325901 prevented abnormal development, supporting the cause of CFC syndrome to be associated with MEK activity (Anastasaki *et al.*, 2009; Anastasaki *et al.*, 2012). However, high doses and MEK inhibition for long periods had serious additional developmental defects. To examine the underlying deregulation of the RAS pathway *in vivo*, and to examine the use of potential drugs in prevention of developmental abnormalities, transgenic mouse models have been a useful tool.

V^{600E} *Braf* causes embryonic lethality when constitutively expressed in mice (Mercer *et al.*, 2005), which is probably why this mutation is not found in RASopathies. A mouse strain that expressed very low levels of V^{600E} *Braf* was born alive and displayed the symptoms of CFC (Urosevic *et al.*, 2011). These included lower weight to age ratio, cranial abnormality associated with facial dysmorphia, increased heart to body weight ratio characterised by an increased number of cardiomyocytes per area and an increased heart ejection fraction

(Urosevic *et al.*, 2011). However, a CFC patient has been identified with a $V600G$ *BRAF* mutation, which has lower activity than $V600E$ *BRAF*, demonstrating that a mutation at this residue is compatible with development (Champion *et al.*, 2011).

Although $G12V$ *HRAS* is rare amongst patients with Costello syndrome, a mouse model that constitutively expressed $G12V$ Hras developed characteristics of Costello syndrome. Features include facial dysmorphia characterised by depression of the anterior frontal bone, nasal bridge and premaxillar bone, and cardiomyopathies with large heart chambers caused by increased cardiomyocytes (Schuhmacher *et al.*, 2008).

A $Ptpn11^{+/Q79R}$ mouse model of Noonan syndrome revealed that $Q79R$ Shp2 during embryogenesis caused cardiac defects. Mice developed atrial and ventricular dilation, chronic left atrial thrombi and increased heart weight to body weight and lung weight to body weight ratios, but expression of $Q79R$ Shp2 after birth did not cause heart defects. Knock-out of Erk1 or Erk2 in the embryos reduced the proliferation marker Ki-67 to normal levels, and mice were born and developed a normal heart (Nakamura *et al.*, 2007). This model nicely shows that a germline mutation causes RASopathy, while sporadic mutations do not. Phenotypic features of Noonan syndrome were also present in $Ptpn11^{+/D61G}$ mice. $Ptpn11^{+/Y279C}$ mice have been shown to develop characteristics of LEOPARD syndrome, and in particular cardiac defects, which could be reversed by the mTOR inhibitor, Rapamycin (Marin *et al.*, 2011).

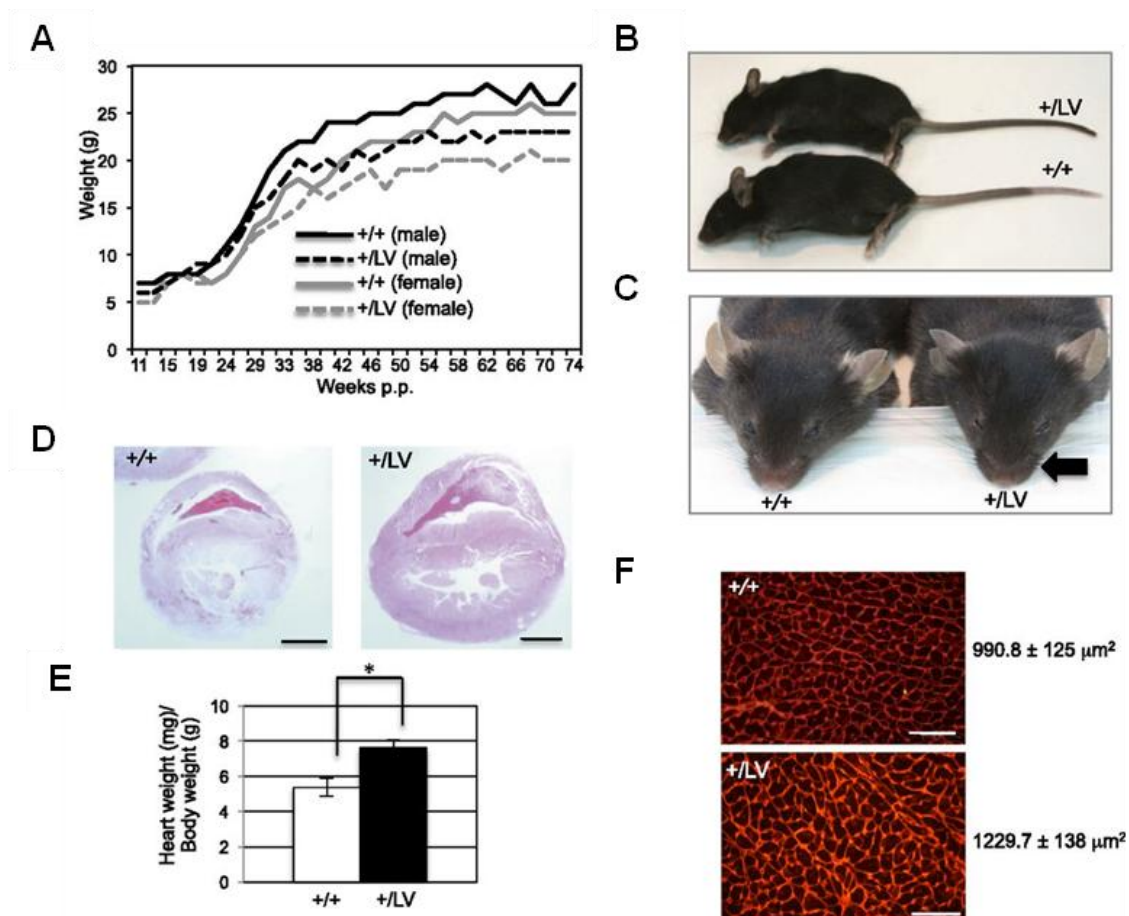
Previous work in the lab showed that $\text{Braf}^{+/Lox-L597V}$ mice, produced by the Cre-LoxP system as outlined in Section 1.8.1 developed some characteristics of CFC. These included lower weight to age ratio, stunted growth, facial dysmorphia, an enlarged heart with thickening of the ventricular wall and septum, a higher heart to weight ratio and increased cardiomyocyte cross-sectional area, which is indicative of cardiac hypertrophy (Figure 1.12) (Andreadi *et al.*, 2012). The mice did not develop advanced cancers but a proportion of aged mice developed benign tumours, which will be discussed in Chapter 6.

A $\text{Sos1}^{+/E846K}$ mouse model showed symptoms of Noonan syndrome (Chen *et al.*, 2010). Homozygous expression of $E846K\text{Sos1}$ was embryonic lethal. Embryos died of cardiovascular defects, which were reversed with MEK inhibition by PD0325901. $\text{Sos1}^{E846K/E846K}$ Embryos injected with PD0325901 were born at the expected Mendelian ratio, developed a normal heart structure and showed improvement of their facial dysmorphia (Chen *et al.*, 2010).

Studies in mouse models have provided an insight into the effects of mutations in transducers of the RAS pathway in development in which *in vitro* studies cannot provide. These models have provided a basement for the effect of drug treatment in relieving symptoms.

Figure 1.12 $\text{Braf}^{+/Lox-L597V}$ mice show characteristics of RASopathies
(Taken from Andreadi et al., 2012).

- A) Weight comparison of $\text{Braf}^{+/+}$ (+/+) and $\text{Braf}^{+/Lox-L597V}$ (+/LV) mice.
 B) Gross appearance of 3 month old $\text{Braf}^{+/+}$ and $\text{Braf}^{+/Lox-L597V}$ female mice.
 C) Gross facial appearance of 3 month old $\text{Braf}^{+/+}$ and $\text{Braf}^{+/Lox-L597V}$ female mice. Arrowhead illustrates the blunt nose of mutant mice.
 D) $\text{Braf}^{+/Lox-L597V}$ mice have an enlarged heart. H&E stained cross sections of hearts of $\text{Braf}^{+/+}$ and $\text{Braf}^{+/Lox-L597V}$ mice at 3 months of age.
 E) A bar chart of heart weight/body weight ratio of 3 month old $\text{Braf}^{+/+}$ (n=6) and $\text{Braf}^{+/Lox-L597V}$ (n=3) mice. (*) - $P < 0.05$, 2-tailed Student's t test.
 F) Wheat germ agglutinin-stained cross-sections of cardiomyocytes from $\text{Braf}^{+/+}$ and $\text{Braf}^{+/Lox-L597V}$ mice. Bars, 100 μm . Cross-sectional areas were measured (n=3, with 100 cells counted per sample). The average areas were given.



1.9. Kinase inhibitors of the RAF/MEK/ERK pathway

The importance of the RAS pathway, in particular the RAF/MEK/ERK pathway in cancer progression and developmental abnormalities has been highlighted above. Kinase inhibitors of the pathway are already in clinical use for cancer treatment. However, specificity is important for targeting tumour cells without targeting normal cells. The ideal drug would be orally available, to solely inhibit cells harbouring the mutation, and induce cell death.

1.9.1. MEK inhibitors

U0126 (1,4-diamino-2,3-dicyano-1, 4-bis[2-aminophenylthio]butadiene) was identified from a screen of 40,000 components to functionally antagonise AP-1-driven gene activation (Favata *et al.*, 1998). U0126 inhibited the kinase activity of MEK1 and MEK2 without affecting the kinase activity of other kinases, including protein kinase C, Abl, Raf, MEKK, ERK, JNK, MKK3, MKK6, Cdk2 and Cdk4. Further examination showed that U0126 has a high affinity for both MEK1 and MEK2, and had the same affinity for free MEK and MEK coupled to ERK or ATP (Favata *et al.*, 1998). U0126 is therefore a non-competitive inhibitor. Crystal studies showed that U0126 binds to the inhibitor pocket adjacent to the ATP binding site (Fischmann *et al.*, 2009) locking the kinase into a catalytically inactive form (Ohren *et al.*, 2004). U0126 had a lower affinity for RAF-activated MEK. Therefore U0126 is thought to prevent conformation change required for activation of MEK1 (Favata *et al.*, 1998). BRAF-mutant melanoma cell lines have an elevated level of P-ERK, and U0126 has been shown to reduce P-ERK, block their ability to synthesise DNA and induce apoptosis. However, U0126 did not have any effect on ^{WT}BRAF cells which had low levels of P-ERK

(Karasarides *et al.*, 2004), suggesting selectivity to BRAF-mutant cells. However, U0126 is limited to *in vitro* use due to its lack of oral availability.

PD184352, also known as CI-1040 is an inhibitor of the MAPK pathway that was the first MEK inhibitor to enter clinical trials. Crystal studies showed that PD184352 binds to the same non-competitive binding site as U0126 (Fischmann *et al.*, 2009), forming van der Waal interactions within a deep hydrophobic pocket, forcing the two lobes of the MEK1 enzyme to adopt a closed conformation (Ohren *et al.*, 2004; Sebolt-Leopold *et al.*, 1999). PD184352 inhibits MEK with a half-maximal inhibitory concentration (IC₅₀) of 100-500nM in melanoma cell lines (Solit *et al.*, 2006) depending on *BRAF* mutational status (Solit *et al.*, 2006). A study showed that *BRAF* mutants are more reliant on MEK/ERK signalling, and PD184352 suppressed P-ERK in all cell lines, but failed to reduce Cyclin D levels in ^{WT}*BRAF* cell lines. In *BRAF*-mutant cell lines, MEK inhibition resulted in upregulation of p27^{Kip1}, downregulation of Cyclin D1 and hypophosphorylation of pRb leading to growth arrest, differentiation, senescence, and apoptosis (Solit *et al.*, 2006). PD184352 failed to progress any further than a Phase II trial where none of the patients with breast, colon, NSCLC or pancreatic cancer had a complete or partial response (Rinehart *et al.*, 2004). However, patients were not rationalised according to their *BRAF* status, therefore the poor response might be due to ineffective patient selection. Instead, PD325901 the second-generation more potent allosteric inhibitor of MEK1 and MEK2 with improved oral bioavailability and a longer duration of target suppression was developed.

The MEK1/2 inhibitor PD0325901 has more than 50-fold increased potency against MEK, improved oral availability and longer duration of target suppression in comparison with PD184352, and has been shown in several studies to prevent ^{V600E}BRAF-induced tumourigenesis (Dankort *et al.*, 2007; Ohren *et al.*, 2004; Rinehart *et al.*, 2004; Sebolt-Leopold, 2004). PD0325901 treatment suppressed the growth of ^{V600E}BRAF xenografts in mice. The xenografts were characterised by a loss of Cyclin D, an increase in p27^{Kip1} levels and hypophosphorylation of pRb (Solit *et al.*, 2006). PD0325901 treatment has also been shown to induce tumour regression in mice bearing papillary thyroid tumours and ^{V600E}Braf-driven adenomas in a transgenic mouse model, characterised by reduction in P-Erk levels (Henderson *et al.*, 2010; Trejo *et al.*, 2012). PD0325901 also dramatically suppressed formation of lung metastases in nude mice injected with ^{V600E}BRAF positive melanoma cells (Sharma *et al.*, 2006). However, PD0325901 only managed to suppress P-ERK levels, without any delay in growth of complete wild-type tumours, and only delayed the growth, without inducing tumour shrinkage of ^{Q61R}NRAS tumour xenografts in mice (Solit *et al.*, 2006). PD0325901 incompletely blocked ^{G12D}Kras-induced lung tumourigenesis (Trejo *et al.*, 2012) unless the PI3-kinase pathway was inhibited concurrently (Engelman *et al.*, 2008), due to the ability of RAS to signal through other pathways.

PD0325901 is absorbed quickly on an empty stomach and reached peak plasma concentrations within 1 to 2 hours (Lorusso *et al.*, 2005). Clinical trials of PD0325901 in patients with previously treated melanoma, breast cancer and colon cancer showed efficacy of drug (Boasberg *et al.*, 2011; Lorusso *et al.*,

2005). However, a Phase II study on NSCLC patients who have been previously treated did not show anti-tumour activity, and only seven out of thirty-four patients showed stable disease. Therefore it was concluded that as in preclinical studies, MEK inhibition is unlikely to cause growth arrest in non-^{V600E}BRAF tumours, and patients must be rationalised prior to treatment (Haura *et al.*, 2010).

Mechanistic enzymology studies on AZD6244 shows that it is a potent, selective non-competitive inhibitor of MEK1/2 (Yeh *et al.*, 2007). AZD6244 failed to inhibit P-ERK levels in human cancer cell lines that were wild-type for either *BRAF* or *KRAS*, but inhibited P-ERK levels in BRAF- or KRAS-mutant human cancer cell lines (Yeh *et al.*, 2007), and when serum-starved, induced BIM expression, which was accompanied by cell death (Wickenden *et al.*, 2008). However, it has been shown that a mutation in *BRAF* or *KRAS* do not necessarily correlate with sensitivity, and inhibition of P-ERK levels did not necessarily correlate with drug-induced cell death as will be discussed in Section 1.9.3 (Balmanno *et al.*, 2009). AZD6244 given orally to ^{V600E}BRAF or ^{G12V}KRAS human colon carcinoma mouse xenograft models showed tumour regression, with inhibition of P-ERK (Yeh *et al.*, 2007; Davies *et al.*, 2007), as well as with increased levels of cleaved PARP and cleaved forms of caspase-3, an indication of apoptosis (Huynh *et al.*, 2007).

Phase I and II studies showed that AZD6244 is well tolerated and is successful in the treatment of lung and thyroid cancer and melanoma (Adjei, 2005; Hayes *et al.*, 2012; Kirkwood *et al.*, 2012; Patel *et al.*, 2012). Nineteen out of twenty

lung biopsies showed inhibition of ERK phosphorylation and reduced Ki-67 staining after at least seven days of continuous treatment (Adjei, 2005). This was also seen in patients with a mutation in *KRAS* (Adjei, 2005). Inhibition of P-ERK was also seen in peripheral blood mononuclear cells 15 or 22 days after treatment, providing a useful method of monitoring (Adjei, 2005). However, AZD6244 did not show increase in efficacy compared to drugs already approved for therapy (Kirkwood *et al.*, 2012; Hainsworth *et al.*, 2010), and it was suggested that patients should be tested positive for *BRAF* or *KRAS* mutations before treatment, since the majority of patients that showed response to therapy were tested positive for these mutations as in preclinical studies (Hayes *et al.*, 2012; Kirkwood *et al.*, 2012; Hainsworth *et al.*, 2010).

1.9.2. RAF inhibitors

Sorafenib, also known as BAY 43-9006 was the first RAF inhibitor to enter clinical trials. Sorafenib is FDA approved for use in renal cell carcinoma and hepatocellular carcinoma (Escudier *et al.*, 2007), but is ineffective in treating ^{V600E}BRAF positive melanomas (Sharma *et al.*, 2006; Ratain *et al.*, 2006). It is a multi-kinase inhibitor that binds to the inactive conformation of kinases. Targets include BRAF even though is four times more effective at inhibiting CRAF (Smalley *et al.*, 2009). The distal pyridyl ring of Sorafenib binds to the ATP binding pocket, while the lipophilic trifluoromethyl phenyl ring inserts into a hydrophobic pocket between the α C and α E helices and N-terminal regions of the DFG motif and catalytic loop (Wan *et al.*, 2004). Its interaction with Phe594 of the DFG motif and insertion of the lipophilic trifluoromethyl phenyl ring into a site occupied by Phe594 in the active site prevents activation of BRAF (Wan *et*

et al., 2004). Although Sorafenib inhibited DNA synthesis and induced cell death in melanoma cell lines, Sorafenib treatment induced growth retardation but failed to induce tumour regression in mice with human melanoma xenografts possibly because Sorafenib is not potent enough to induce a complete response when used in monotherapy (Karasarides *et al.*, 2004). Clinical trials of Sorafenib in combination with other agents have shown some success in overall survival of patients of renal-cell carcinoma (Escudier *et al.*, 2007), metastatic nasopharyngeal carcinoma (Xue *et al.*, 2012), and advanced thyroid carcinoma (Schneider *et al.*, 2012).

PLX4720, a compound analogue of Vemurafenib (PLX4032) is a kinase inhibitor that preferentially binds to and inhibits the open conformation of BRAF, which is also adopted by ^{V600E}BRAF. PLX4720 can bind to both the inactive and active conformation of BRAF, but preferentially binds to the active conformation, possibly due to a displacement of the A-loop away from the ATP-binding pocket, which is where PLX4720 binds to (Tsai *et al.*, 2008). The propyl group of PLX4720 binds to the RAF-selective pocket, which is present in very few other kinases in the exact location, and this pocket is the reason for selectivity towards ^{V600E}BRAF, since it is significantly different to ^{WT}BRAF (Tsai *et al.*, 2008).

In vitro studies showed that PLX4032 and PLX4720 blocked MAPK signalling and proliferation of ^{V600E}BRAF cell lines (Tsai *et al.*, 2008; Sondergaard *et al.*, 2010). *In vivo* studies show that PLX4032 treatment of mice bearing ^{V600E}BRAF tumour xenografts regressed on PLX4032 treatment (Yang *et al.*, 2010).

Tumour biopsies of PLX4032-treated patients suggest that PLX4032 inhibits MAPK activity, leading to a reduction in Cyclin D1 levels and reduced proliferation (Flaherty *et al.*, 2010). A clinical study showed that there was a 69% response rate amongst ^{V600E}BRAF positive melanoma patients, with a median progression-free survival of over 7 months, but patients bearing ^{WT}BRAF melanomas had progressive disease within months of treatment (Flaherty *et al.*, 2010). Vemurafenib was FDA approved for therapy of patients with unresectable or metastatic melanoma, harbouring the ^{V600E}BRAF mutation in 2011 (<http://www.fda.gov/AboutFDA/CentersOffices/OfficeofMedicalProductsandTobacco/CDER/ucm268301.htm>).

SB590885 is a low molecular weight compound that binds to the ATP-binding pocket of the active conformation of BRAF, forming a stable complex (King *et al.*, 2006). The drug was found to be ^{V600E}BRAF-specific and blocked G₁ phase cell cycle progression, causing a reduction in cell proliferation, without apoptosis, and inhibited anchorage-independent growth (King *et al.*, 2006). SB590885 decreased tumourigenesis in mice xenografted with ^{V600E}BRAF melanoma cells, but failed to reduce tumour mass due to lack of apoptotic effect (King *et al.*, 2006).

1.9.2.1. RAF inhibitor-induced heterodimerisation

Heterodimers consisting of BRAF and CRAF have been identified when RAS-mutant cells were treated with RAF inhibitors Sorafenib, PLX4072 or SB590885. Although Sorafenib is a RAF inhibitor, it has been found to induce dimerisation, and at low doses, induces homodimerisation, causing an increase in CRAF

activity and transient ERK activation (Karreth *et al.*, 2009; Arnault *et al.*, 2012). At higher doses in ^{V600E}BRAF cell lines, it induces heterodimerisation, and this inhibits ^{V600E}BRAF activity, inhibiting P-ERK levels (Karreth *et al.*, 2009).

It has been proposed that BRAF-specific inhibitors inhibit the auto-inhibition of BRAF by its amino-terminal domain (Heidorn *et al.*, 2010), enabling BRAF to translocate to the plasma membrane and form a complex with CRAF (Hatzivassiliou *et al.*, 2010; Heidorn *et al.*, 2010). Knock-down of NRAS or CRAF prevented RAF-inhibitor induced P-ERK upregulation in NRAS-mutant cells, suggesting that active NRAS and CRAF are crucial for P-ERK induction by RAF inhibitors (Heidorn *et al.*, 2010). Inhibitor-binding to BRAF was a requirement. “Gatekeeper mutations” that prevent drug binding were introduced into BRAF and CRAF. The BRAF-mutants were unable to heterodimerise with CRAF, but CRAF-mutants were still able to bind BRAF with SB590885 treatment (Heidorn *et al.*, 2010). However, a study using GDC-0879 and PLX4720 showed that inhibitor binding to the CRAF nucleotide-binding pocket was required for CRAF translocation to the plasma membrane, and activation and phosphorylation of MEK (Hatzivassiliou *et al.*, 2010). This was shown by reduction in P-MEK levels when cells were transfected with the “gatekeeper” mutant ^{T421N}CRAF (Hatzivassiliou *et al.*, 2010). This paradoxical MEK/ERK activation could be why a fifth of Vemurafenib-treated patients develop keratoacanthoma or cutaneous squamous cell carcinoma (Keating, 2012; Su *et al.*, 2012b).

1.9.3. Drug resistance

There are two forms of resistance. One form is intrinsic, in which cells are resistant to inhibitors without prior exposure, and the other is acquired resistance in which cells develop resistance following exposure to the drug. The latter is more studied and is a limiting factor to overall survival.

1.9.3.1. Resistance to MEK inhibitors

For all of the MEK inhibitors discussed, preclinical and clinical data have suggested that only cells dependent on ERK signalling, as indicated by basal levels of P-ERK are sensitive to MEK inhibitors (Karasarides *et al.*, 2004; Balmano *et al.*, 2009). MEK inhibitor-resistant cells expressed low levels of P-ERK or high levels of PKB or P-AKT, indicating activation of PI3-K pathway (Balmano *et al.*, 2009; Corcoran *et al.*, 2010; Wang *et al.*, 2005; Won *et al.*, 2012). These results show that RAS- or BRAF-mutant cells or tumours that are likely to be dependent on ERK signalling are therefore sensitive to MEK inhibitors, whereas cells that are wild-type for *RAS* or *BRAF* are less likely to be ERK-dependent and are therefore not sensitive to MEK inhibitors, but resistance can be overcome by treatment concomitantly with PI3-K inhibitors.

Acquired resistance to MEK inhibitors has been proposed to be due to mutations in *MEK* as identified in patients presented with relapse following MEK-inhibitor treatment (Emery *et al.*, 2009), or amplification of BRAF or KRAS, the oncogenic driver of the pathway (Corcoran *et al.*, 2010; Wang *et al.*, 2005).

1.9.3.2. Resistance to RAF inhibitors

Preclinical and clinical data have shown that only ^{V600E}BRAF-positive cells or tumours respond to Vemurafenib (Tsai *et al.*, 2008; Sondergaard *et al.*, 2010). This is because the drug preferentially binds to the active form of BRAF (Wan *et al.*, 2004). ^{V600E}BRAF-negative melanomas are likely to harbour a mutation in *RAS*, which induce P-ERK levels and drive cell proliferation in the presence of RAF inhibitors through drug-induced heterodimerisation (Hatzivassiliou *et al.*, 2010; Heidorn *et al.*, 2010; King *et al.*, 2006; Su *et al.*, 2012b).

Patients with metastatic melanoma have a median survival of 6-10 months (Atkins *et al.*, 2008; Chapman *et al.*, 1999; Falkson *et al.*, 1998; Middleton *et al.*, 2000; Tsao *et al.*, 2004), which is improved to 15.9 months with Vemurafenib treatment (Sosman *et al.*, 2012). Patients respond quickly to treatment, but resistance occurs after ~7 months and the patient enters relapse (Flaherty *et al.*, 2010). Although relapse is likely to be due to drug-resistant *RAS*-mutant cells repopulating the tumour (Su *et al.*, 2012b; Diaz *et al.*, 2012), *in vitro* studies suggest resistance to occur through acquisition of mutations in *RAS*. PLX4032-resistant melanoma cell lines were identified to carry ^{Q61K}*NRAS* mutation, previously not identified in the parental cell line (Nazarian *et al.*, 2010).

Studies have shown that drug-resistant cells arise following long-term treatment (Poulikakos *et al.*, 2011). Drug-resistant clones were identified to have developed mutations in *MEK* (Wagle *et al.*, 2011), which activated the ERK pathway and, mutations in *PI3K* (Su *et al.*, 2012a) and *PTEN* (Chen *et al.*,

2011) which activated the PI3-K pathway and sustained the ERK pathway (Chen *et al.*, 2011; Blivet-Van Eggelpoel *et al.*, 2012). Maintenance of P-ERK levels enabled cell survival.

A RAF-inhibitor-resistant alternatively-spliced form of BRAF that was more efficient in forming heterodimers emerged following drug treatment. The splice variant that lacked exons 4-8, which contains the RAS binding domain and cysteine-rich domain, was not found in patients that had not been treated with Vemurafenib, and was still sensitive to the MEK inhibitor PD0325901 (Poulikakos *et al.*, 2011; Smalley *et al.*, 2006).

Cancer cells typically express multiple RTKs, and increased levels of PDGFR were found in PLX4032-resistant melanoma clones, which, when knocked-down induced cell cycle arrest (Nazarian *et al.*, 2010). Autocrine or paracrine RTK ligand production was also suggested to contribute to drug-resistant (Wilson *et al.*, 2012). Hepatocyte Growth Factor (HGF) treatment was shown to attenuate PLX4032 sensitivity in BRAF-mutant melanoma cell lines, and increased plasma HGF correlated with lower progression-free survival in the BRIM2 clinical trial (*BRAF*-mutant metastatic melanoma patients treated with PLX4032) (Wilson *et al.*, 2012), supporting the hypothesis that drug resistance arose from repopulation of HGF-responsive cells.

1.10. Aims

The aim of this project is to characterise the ^{L597V}BRAF mutant and to determine its involvement in cancer. This was accomplished by:

- Characterisation of ^{L597V}BRAF mutant in HEK 293^T cells transfected with the mutant plasmid and in MEFs endogenously expressing the mutation.
- Investigation in cooperation of ^{L597V}Braf with ^{G12D}Kras in MEFs.
- Examination of the response of Braf^{+/-Lox-L597V} MEFs to RAF and MEK inhibitors.
- Identification of other cooperating mutations involved in tumours with ^{L597V}Braf mutations.

2. Materials and methods

The H₂O used in all methods (including those requiring RNase-free H₂O) was always MilliQ water, dispensed in sterile containers.

2.1. Molecular biology

All chemicals and reagents were supplied by Fisher Scientific or Sigma unless otherwise stated. All restriction endonucleases were supplied by New England Biolabs.

2.1.1. Plasmids

The plasmids used are detailed below and in Figure 2.1. All of the plasmids were gifts from Professor Richard Marais (Institute of Cancer Research, London, UK).

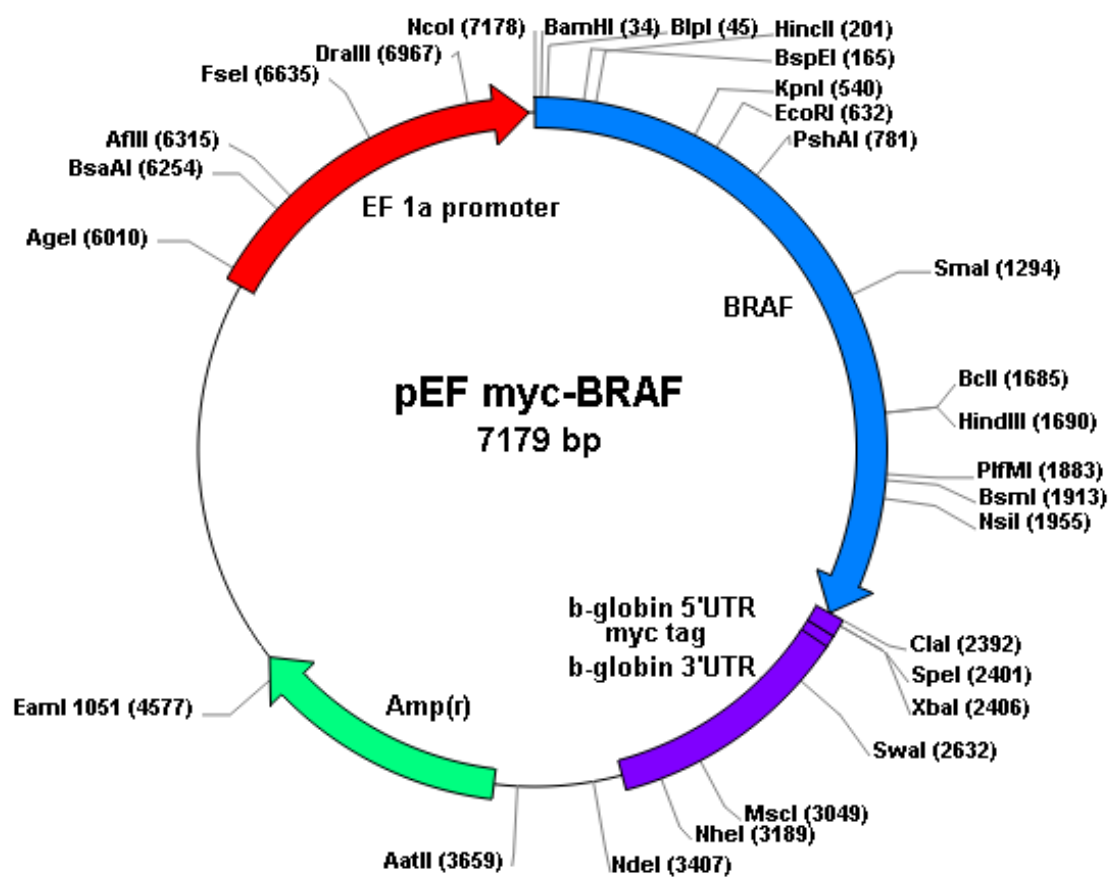
- pEF myc-BRAF^{WT}
- pEF myc-BRAF^{L597V}
- pEF myc-BRAF^{V600E}
- pEF myc-BRAF^{D594A}
- pEF myc-CRAF^{WT}

2.1.2. Transformation into DH5α

Plasmids were transformed into Library DH5α cells (18263-012, Invitrogen). Briefly, 50μl of competent DH5α cells were incubated with 1ng of plasmid on ice for 30 minutes. Cells were then subjected to heat-shock at 42°C for 1 minute.

Figure 2.1 Plasmid map of pEF myc-BRAF

In the pEF myc-CRAF plasmid the BRAF cDNA was substituted for the CRAF cDNA.



After a five minute incubation on ice 200µl of Luria Broth (LB) (dH₂O containing 1% [w/v] Bacto Tryptone, 0.5% [w/v] Bacto Yeast Extract, 1% [w/v] NaCl) was added, and incubated at 37°C with shaking at 225rpm for 45 minutes. 10-200µl of the mixture was diluted with LB to a total volume of 100-200µl and spread onto LB-agar plates (1% [w/v] Bacto Tryptone, 0.5% [w/v] Bacto Yeast Extract, 1% [w/v] NaCl, 1.5% [w/v] agar, dH₂O) containing 50µg/ml of ampicillin for selection and allowed to grow overnight at 37°C.

2.1.3. Purification of plasmid DNA: Miniprep

Colonies were inoculated and allowed to grow in 3ml of LB with 50µg/ml ampicillin at 37°C shaking at 225rpm overnight. Cells were harvested by centrifugation at >8000rpm for 3 minutes. The bacterial pellets were resuspended in 100µl of Buffer P1 (25mM Tris-HCl, 10mM EDTA, 50mM glucose) containing 100µg/ml of RNase A to digest any RNA that may interfere with future reactions. Cells were lysed using 200µl of Buffer P2 (200mM NaOH, 1% [w/v] SDS), and 150µl of Buffer P3 (1.2M potassium acetate, 11.5% [v/v] glacial acetic acid) was added to precipitate out cell constituents. Samples were centrifuged at 13,000rpm for 10 minutes. The supernatant was collected and placed into a clean tube. DNA was precipitated by the addition of 350µl of isopropanol. DNA was collected by centrifugation at 13,000rpm for 5 minutes. Isopropanol was removed and the DNA pellet washed with 200µl of 70% [v/v] ethanol. Following centrifugation at 13,000rpm for 2 minutes, ethanol was removed and the DNA pellet air-dried at 37°C. The DNA pellet was resuspended in 50µl of TE buffer (10mM Tris [pH 8.0], 1mM EDTA)

supplemented with 1µl of RNase A to a final concentration of 0.2 µg/µl. The DNA was confirmed to be the plasmid of interest as in Section 2.1.6.

2.1.4. Purification of plasmid DNA: Maxiprep

100µl of an overnight culture was grown in 100ml of LB with 50µg/ml of ampicillin shaking at 225rpm at 37°C overnight. DNA was extracted using the MaxiPrep Kit (12162, Qiagen). Briefly, bacterial cells were harvested by centrifugation at 6000rpm at 4°C for 15 minutes and resuspended in 10ml of Buffer P1 (provided by manufacturer). Cells were lysed by the addition of 10ml Buffer P2 (provided by manufacturer). The lysate was neutralised with 10ml chilled Buffer P3 (provided by manufacturer) and incubated on ice for 20 minutes. The lysate was mixed and centrifuged at 20,000rpm for 30 minutes at 4°C. The supernatant was removed promptly and centrifuged again at 20,000rpm for 15 minutes. Meanwhile, a QIAGEN-tip 500 was equilibrated with Buffer QBT (provided by manufacturer). The supernatant was poured into the QIAGEN-tip 500 and allowed to enter the resin. The QIAGEN-tip 500 was washed twice with Buffer QC (provided by manufacturer). DNA was eluted with 15ml Buffer QF (provided by manufacturer) and precipitated by the addition of 10.5ml of isopropanol and centrifuged at 15,000rpm for 30 minutes at 4°C. The pellet was washed with 5ml of 70% [v/v] ethanol and DNA collected by centrifugation at 15,000rpm for 10 minutes at 4°C and air-dried before dissolving in 100-500µl of TE Buffer. The DNA was confirmed to be the plasmid of interest as in Section 2.1.6.

2.1.5. Purification of plasmid DNA: Caesium Chloride preparation

To produce a higher yield of DNA, Caesium Chloride preparation was also used. 2ml of a 5ml overnight culture was allowed to grow in 400ml of LB containing 50µg/ml of ampicillin overnight. Bacterial cells were harvested by centrifugation at 6000rpm for 10 minutes and the pellet resuspended in 10ml of buffer P1. 20ml of buffer P2 was added and cells lysed by gentle shaking until viscous. 15ml of buffer P3 was added to neutralise the lysate, and the debris removed by centrifugation at 9000rpm for 15 minutes. The supernatant containing plasmid DNA was filtered into a new tube. DNA was precipitated by the addition of 50ml of ice-cold isopropanol followed by centrifugation at 9000rpm for 15 minutes. The pellet was air-dried for 20 minutes and resuspended in 6ml of TE buffer. Then 6g of caesium chloride was added. Working in foil to avoid the light, 2.75mg of Ethidium Bromide was added and the excess Ethidium Bromide removed by centrifugation at 4000rpm for 5 minutes. The supernatant was loaded and sealed into two Beckman Quickseal centrifuging tubes. The tubes were then centrifuged at 100,000rpm for 16 hours at 20°C to separate DNA according to density. The band of plasmid DNA was collected and Ethidium Bromide removed by adding water-saturated Isobutanol and shaking to mix. Ethidium Bromide formed a pink-coloured upper layer and was removed. The process was repeated until the upper layer was clear. The clear layer was removed and DNA was precipitated with 6x volume of 70% [v/v] ethanol and centrifuged at 11,000rpm for 15 minutes at 4°C. The pellet was washed with 70% [v/v] ethanol, air-dried and resuspended in 250µl of TE buffer. The DNA was confirmed to be the plasmid of interest as in Section 2.1.6.

2.1.6. Diagnostic restriction digestion of plasmid DNA

To confirm that the plasmid DNA was the plasmid of interest, restriction enzyme digestion was carried out. A reaction mixture consisting of 11µl of DNA, NE Reaction Buffer 4 (provided by New England Biolabs), 20µg of BSA, and 10 units of *NcoI* and *XbaI*, which cut specifically in the pEF plasmid in a total volume of 15µl were incubated at 37°C for 1 hour. Products were resolved by agarose gel electrophoresis on a 1% [w/v] agarose gel.

2.1.7. Agarose gel electrophoresis

The appropriate weight of agarose was heated in TAE buffer (40mM Tris, 1% [v/v] acetic acid, 1.3mM EDTA) in a microwave until fully dissolved, then poured into a tray with a gel comb. Once set, the comb was removed and submerged into TAE buffer in a gel electrophoresis tank. Samples were mixed with 6x loading dye and loaded into the wells adjacent to a 1kb plus ladder (10787-018, Invitrogen). The gel was electrophoresed for 50 minutes, and the gel viewed under a transilluminator.

2.1.8. Genotyping

2.1.8.1. DNA extraction from tissues

To genotype mice, tissue samples were collected. Samples were incubated with 100µl of GNTK lysis buffer (50mM KCl, 10mM Tris-HCl at pH 8.3, 2.5mM MgCl₂, 0.1mg/ml gelatin) supplemented with 40ng of Proteinase K (P2308, Sigma) and heated at 65°C for 2 hours. This was followed by a heat inactivation step at 95°C for 5 minutes. The DNA samples were stored at 4°C.

2.1.8.2. DNA extraction from cells

To confirm MEF genotypes, MEFs were washed with PBS and collected in 0.5ml of DNA lysis buffer (50mM Tris-HCl at pH 7.6, 1mM EDTA, 100mM NaCl, 0.2% SDS) supplemented with 50ng of Proteinase K and heated at 65°C for 1 hour. DNA was precipitated using 1ml of 100% ethanol and collected by centrifugation at 13,000rpm for 1 minute. The pellet was washed with 1ml of 70% [v/v] ethanol and resuspended in 100-500µl of dH₂O. The DNA samples were stored at 4°C.

2.1.8.3. DNA extraction from paraffin embedded tissue sections

After Haematoxylin and Eosin staining, if tissues were confirmed to contain tumours, DNA was extracted from the paraffin-embedded block. Immediately after tissue sections were cut as mentioned in Section 2.5.4, the tumour was microdissected using a fine needle and collected in a sterile tube. DNA was extracted using GNTK buffer as described in Section 2.1.8.1.

2.1.8.4. Polymerase Chain Reaction (PCR)

To check genotyping, PCR was performed in a final volume of 20µl consisting of 16µl of Reddymix PCR Master mix (PCR 300-610D, ABgene), 40nM of each primer and 2µl of DNA. The reactions were carried out in a G-Storm™ PCR machine using the following conditions:

	94°C for 10 minutes
35 cycles	{ 94°C for 1 minute 60°C for 1 minute 72°C for 1 minute
	72°C for 10 minutes

The primers used are shown in Table 2.1.

Table 2.1 Primers used for genotyping

Gene name	Primers	Sequence
Braf WT allele	A	AGTCAATCATCCACAGAGACCT
	C	GCCCAGGCTCTTTATGAGAA
Braf LSL allele	A	GCCCAGGCTCTTTATGAGAA
	B	GCTTGGCTGGACGTAAACTC
Braf Lox recombined allele	A	AGTCAATCATCCACAGAGACCT
	C	GCCCAGGCTCTTTATGAGAA
Cre	OCP 84	GTTGCAAGAACCTGATGGACA
	OCP 85	CTAGAGCCTGTTTTGCACGTTT
Kras WT allele	OCP 260	GTCGACAAGCTCATGCGGGTG
	OCP 262	CCTTTACAAGCGCACGCAGACTGTAGA
Kras LSL allele	OCP 261	AGCTAGCCACCATGGCTTGAGTAAGTCTGCG
	OCP 262	CCTTTACAAGCGCACGCAGACTGTAGA
Kras Lox recombined allele	D	TGACACCAGCTTCGGCTTCCT
	E	TCCGAATTCAGTGACTACAGATGTACAGA

2.1.9. Sequencing

For identification of mutations in the mouse tumour samples, primers were designed to flank mutation hotspots in *Braf*, *Craf*, *Hras*, *Kras* and *Nras*. Primers were designed using Primer-blast (<http://www.ncbi.nlm.nih.gov/tools/primer-blast/>).

2.1.9.1. Polymerase Chain Reaction

Following DNA extraction, DNA was subjected to PCR amplification. For relevant genes: primers for *Braf* exons 11 and 15, *Craf* exons 7 and 10, *Hras* exon 1 and exon 2, *Kras* exons 1 and 2, and *Nras* exons 2 and 4 were designed using Primer-BLAST (<http://www.ncbi.nlm.nih.gov/tools/primer-blast/>). PCR was performed in a final volume of 20µl consisting of 16µl of PuReTaq ready-to-go PCR beads (27-9558-01, GE Healthcare) resuspended in MilliQ water, 40nM of each primer and 2µl of DNA. The reaction was carried out in a G-StormTM PCR machine using the following conditions:

	94°C for 10 minutes
35 cycles	{ 94°C for 1 minute
	{ 60°C for 1 minute 20 seconds
	{ 72°C for 1 minute
	{ 72°C for 10 minutes

The primers used are shown in Table 2.2.

Table 2.2 Primers used for PCR amplification and sequencing

Primer description	Sequence
Braf Exon 11 Forward	TGAACTATCTCTCCAGCACCAA
Braf Exon 11 Reverse	GTGTGGGGAATATCGGAGTG
Braf Exon 15 Forward	GGTCCCCCATAGGCTTGGAA
Braf Exon 15 Reverse	CCTGTGAGTAGTGGGAACTGT
Craf Exon 7 Forward	CTTTTCAGAGGGATGGCAAG
Craf Exon 7 Reverse	CCAGCCCAAAGAAATCACAT
Craf Exon 10 Forward	CTGTGCCAGCACAAAGAGAG
Craf Exon 10 Reverse	GCACCACGGGGATTTTATTA
Hras Exon 1 Forward	TAGCCGTCTCAAGTGGCAAG
Hras exon 1 Reverse	GACCACCTGTTTCCGGTAGG
Hras Exon 2 Forward	AGGGTGTAGGCTGGTTCTGT
Hras Exon 2 Reverse	AGGGGGATGGGGTGGATATG
Kras Exon 1 Forward	TGGCTCCAACACAGATGTTC
Kras Exon 1 Reverse	GGATGGCATCTTGGACCTTA
Kras Exon 2 Forward	TGCTTTGCCTGTTTTGAATG
Kras Exon 2 Reverse	CAACCCCTTCTCCCTAAACC
Nras Exon 2 Forward	GGTTTGCAGGAATTGGAAGA
Nras Exon 2 Reverse	GCAAGAGAAAGCCCAAAGTG
Nras Exon 4 Forward	GTTAGCGGGTTGAGGGTAAA
Nras Exon 4 Reverse	AAAGGTGTGCACCATCACTG

2.1.9.2. PCR purification

PCR products were subjected to PCR purification using QIAquick PCR Purification kit (28106, Qiagen). Briefly, the PCR products were resuspended in 5 volumes of Buffer PB (provided by the manufacturer) to allow optimal binding of DNA to the column. DNA was allowed to bind to the column by centrifugation at 13,000rpm for 1 minute. Unwanted impurities were washed away by applying 750µl of Buffer PE (provided by manufacturer) to the column and centrifugation at 13,000rpm for 1 minute. Excessive Buffer PE was removed by centrifugation of the columns at 13,000rpm for 1 minute. DNA was eluted by the addition of 30µl of Buffer EB (provided by the manufacturer) and centrifugation at 13,000rpm for 1 minute into a clean eppendorf tube. Samples were stored at 4°C.

2.1.9.3. Gel purification

Bands of the correct size were subjected to gel purification using QIAquick Gel Purification kit (28704, Qiagen). Briefly, gel slices were weighed and 3 volumes of Buffer QG (provided by manufacturer) added. The gel slices were dissolved by heating at 50°C with gentle vortexing every 3 minutes for 10 minutes. DNA was bound to the column by centrifugation at 13,000rpm for 1 minute. Agarose was removed by the addition of Buffer QG followed by centrifugation at 13,000rpm for 1 minute. Impurities were washed with Buffer PE (provided by manufacturer), and excessive buffer PE removed by centrifugation at 13,000rpm for 1 minute. DNA was eluted by the addition of 30µl of Buffer EB and centrifugation at 13,000rpm for 1 minute. Samples were stored at 4°C.

2.1.9.4. Level 2 Sequencing

20ng of DNA in a total volume of 16µl and 10µl of forward and reverse primers at 1pmol/µl were sent to The Protein Nucleic Acid Chemistry Laboratory (PNACL) for sequencing. PNACL is part of the School of Medicine, Biological Sciences and Psychology at the University of Leicester, who specialise in DNA Sequencing, SNP Genotyping, Proteomics and Mass Spectrometry, and Protein Sequencing. Sequencing data was provided as a .SEQ file.

2.2. Cell lines and tissue culture

All procedures were performed in a class I tissue culture hood unless otherwise stated. All tissue culture reagents plastic ware were provided by Invitrogen unless otherwise stated.

2.2.1. HEK 293^T

Human Embryonic Kidney (HEK) 293^T cells were kindly provided by Dr Sue Shackleton. Cells were maintained in Dulbecco's Modified Eagle Medium (DMEM) (High glucose, 41965, Invitrogen) supplemented with 10% [v/v] Foetal Bovine Serum (FBS) (10270, Gibco Ltd) and 1% [v/v] Penicillin Streptomycin (10000 units of penicillin and 10000 µg of streptomycin/ml, 15140, Invitrogen). Cells were passaged at a split ratio of 1:15 twice a week and re-fed every day. Cells were cultured in 10cm plates and maintained at 37°C in 10% CO₂.

2.2.2. Production and maintenance of Mouse Embryonic Fibroblasts (MEFs)

Mouse Embryonic Fibroblasts (MEFs) were prepared from embryos of intercrosses between $\text{Braf}^{+/LSL-L597V}$ and $\text{Kras}^{+/LSL-G12D}$ mice at E13.5. The embryos were isolated under Home Office regulated procedures. The head and liver were removed. A fresh scalpel blade was used to finely chop each embryo, and the tail was removed for genotyping (Section 2.1.8.1). The tissue was left in 0.25% [v/v] trypsin for 16 hours at 4°C. Then, the trypsin was removed and the cells were resuspended in 10ml DMEM supplemented with 10% [v/v] FBS and 1% [v/v] Penicillin Streptomycin. The cell suspension was allowed to adhere to a 10cm plate at 37°C in 10% CO₂ overnight. The media was removed and replaced 24 hours following plating to remove dead cells. MEFs were maintained in 10ml DMEM supplemented with 10% [v/v] FBS and 1% [v/v] Penicillin Streptomycin in a 10cm plate at 37°C in 10% CO₂. MEFs were passaged at a split ratio of 1:2 when confluent.

2.2.3. Freezing down stocks of cells

The media of a confluent 10cm plate of cells was aspirated, and the cells rinsed with PBS (140mM NaCl, 8mM Na₂HPO₄, 2.7mM KCl, 1.5mM KH₂PO₄). Cells were collected by the addition of 0.05% [v/v] trypsin for 2 minutes at 37°C and gentle pipetting. Trypsin was neutralised with an equal volume of DMEM media. The cell suspension was centrifuged at 1,100rpm for 5 minutes to allow the cells to form a pellet. The supernatant was removed and the pellet resuspended in 3ml of FBS supplemented with 10% [v/v] DMSO. The suspension was

transferred to 3 cryovials. The cryovials were stored at -80°C for 24 hours and then transferred to liquid Nitrogen for permanent storage.

2.2.4. Thawing out of cells

A cryovial containing cells was thawed in a 37°C water bath. The cell suspension was transferred to a 15ml falcon tube containing 6ml DMEM supplemented with 10% [v/v] FBS and 1% [v/v] Penicillin Streptomycin. This was centrifuged at 1,100rpm for 5 minutes. The supernatant was removed, and the cell pellet resuspended in the appropriate culture media, and then plated into a 10cm plate and grown under appropriate conditions.

2.2.5. Transfection

HEK 293^T cells were transfected using Lipofectamine 2000 (VX11668019, Invitrogen). 24 hours before transfection, one 10cm plate of confluent cells were trypsinised and centrifuged to remove debris. One tenth of the cells was plated with the aim of reaching a confluency of ~60% on the day of transfection in a total volume of 5ml of DMEM media in a 6cm dish in DMEM supplemented with 10% [v/v] FCS. On the day of transfection, cells were re-fed with DMEM supplemented with 10% [v/v] FCS 2 hours prior to transfection.

Per transfection, 5µg of each construct was diluted in 500µl OPTI-MEM medium (31985-047, Invitrogen), and 10µl of Lipofectamine 2000 was diluted in OPTI-MEM medium for 10 minutes to allow complexes to form. The Lipofectamine 2000 reaction was added to the DNA reaction and 20 minutes was allowed for the Lipofectamine 2000 mixture to form a complex with the DNA. The reaction

was then added to the plate of cells already containing 4ml of DMEM supplemented with 10% FBS, and mixed by gentle swirling. 4-6 hours post-transfection, the medium was replaced with DMEM supplemented with 10% [v/v] FBS and 1% [v/v] Penicillin Streptomycin. 48 hours post-transfection, the cells were rinsed with PBS and lysed as detailed in Section 2.3.

2.2.6. Infection with Adenoviral Cre

All of the following procedures were carried out in a Class II hood.

To induce the expression of ^{L597V}Braf, ^{V600E}Braf or ^{G12D}Kras, MEFs containing the ^{Braf}^{+/LSL-L597V}, ^{Braf}^{+/LSL-V600E} or ^{Kras}^{+/LSL-G12D} alleles were infected with Adenovirus carrying Cre recombinase (AdCre) (Ad5CMVCre, Gene Transfer Vector Core, University of Iowa Carver College of Medicine, USA). As a control for viral infection, MEFs were infected with Adenovirus carrying β -Galactosidase (Ad5CMVntLacZ, Gene Transfer Vector Core, University of Iowa Carver College of Medicine, USA). One day before infection, 2×10^5 MEFs were seeded into 6cm plates. Before infection, FBS and Penicillin Streptomycin were removed, and cells were rinsed twice with DMEM media without FBS and Penicillin Streptomycin. 2ml of DMEM media without FBS and Penicillin Streptomycin was left on the plate, and 2 μ l (8×10^7 pfu) of virus was added to the media. 2 hours after the addition of the virus, 3ml of DMEM supplemented with 10% [v/v] FBS and 1% [v/v] Penicillin Streptomycin was added, and the cells were cultured at 37°C in 10% CO₂ for relevant periods.

2.2.7. Inhibition of RAF and MEK pathway

The suppliers of the drugs are listed in Table 2.3. All drugs were constituted in DMSO. U0126 was stored at -20°C. All other drugs were stored in the dark at room temperature. On the day of treatment, cells were aimed at being ~95% confluent. Cells were treated with the drugs listed in Table 2.3 for 4 hours at the concentrations given. Cells were lysed as in Section 2.3.

2.2.8. siRNA knock-down

Lipofectamine 2000 was used to transfect 100nM of BRAF (L-040325-00-0010, Dharmacon) or CRAF (L-040149-00-0010, Dharmacon) siRNA into immortalised MEFs to knock-down either isoform, or a total of 100nM of both BRAF and CRAF siRNA was used to knock-down both isoforms. As a control, 100nM of scrambled gene pool 2 siRNA (D-001206-14-20, Dharmacon) was used. MEFs were plated one day before transfection with the aim of reaching a confluency of ~70% on the day of transfection in 5ml of DMEM supplemented with 10% [v/v] FBS in a 6cm dish. On the day of transfection, the media was replaced with 4ml of fresh DMEM supplemented with 10% [v/v] FBS. 10µl of Lipofectamine 2000 was diluted in 500µl of OPTI-MEM, and siRNA was diluted to 200mM in 500µl of OPTI-MEM. The Lipofectamine 2000 mixture was then added to the siRNA mixture and incubated for 20 minutes at room temperature to allow Lipofectamine 2000: siRNA complexes to form. The mixture was then added to cells. 24 hours post-transfection, the media was replaced, and the cells lysed for protein extraction 48 hours post-transfection.

Table 2.3 Drugs used

Drug	Working concentration	Supplier / catalogue number
U0126	10µM	Cell signalling / 9903
PD184352	1µM	Dr Simon Cook, Babraham Institute, UK
PLX 4720	0.3µM	Prof. Richard Marais, Institute of Cancer Research, UK
SB590885	1µM	Prof. Richard Marais, Institute of Cancer Research, UK
Sorafenib	10µM	Prof. Richard Marais, Institute of Cancer Research, UK

2.2.9. 3T3 immortalisation assay

To examine the immortalisation profile of MEFs, MEFs were infected as mentioned in Section 2.2.6, and then cultured at 37°C in 10% CO₂. After one day of culture, they were trypsinised and counted using a haemocytometer and 3x10⁵ cells replated. After every three days of culture, they were trypsinised and counted using a haemocytometer and 3x10⁵ cells replated. This procedure was repeated for a total of 20 passages. The population doubling per passage was calculated by the following equation:

Population doublings = $\log_2 N_H - \log_2 N_1$, where N_H is the number of cells counted on the day, and N_1 is the number of cells replated the passage before (Kamata *et al.*, 2010). Cumulative population was obtained by adding the population doublings for each passage.

2.2.10. Cell Counting Assay

To monitor short-term cell growth, MEFs were infected with Adenoviral Cre as mentioned in Section 2.2.6 for 72 hours to allow complete recombination. Cells were plated at 3x10⁵ per 12-well plate in triplicate. The number of cells was counted in triplicate every 2 days for 8 days using a haemocytometer.

2.2.11. Metaphase spread

MEFs were allowed to grow to ~50% confluency. Media was replaced with fresh DMEM supplemented with 10% [v/v] FBS and 1% [v/v] Penicillin Streptomycin and MEFs were treated with 2µg/ml Nocodoxole (M1404, Sigma) for two hours. The media was collected. Cells were rinsed with PBS, and trypsinised and combined with the supernatant cells. Cells were harvested by centrifugation at

1,000rpm for 5 minutes. The cell pellet was resuspended in 300µl of DMEM supplemented with 10% [v/v] FBS and 1% [v/v] Penicillin Streptomycin. 3.5ml of 0.075M KCl at 37°C which was added dropwise while gently shaking the tube. The cell suspension was incubated in a 37°C water bath for 20 minutes to allow water to enter the cells by osmosis. The cells were centrifuged at 1,000rpm for 5 minutes. The supernatant was removed, and cells resuspended in 1ml of fixative (25% [v/v] acetic acid, 75% [v/v] methanol) added dropwise. Cells were transferred to a 1.5ml eppendorf tube and cells were collected by centrifugation at 2,500rpm for 3 minutes. The supernatant was removed and cells were resuspended in 1ml of fixative. This was repeated twice more and the cells were resuspended in 200µl of fixative. Cells were dropped onto a slide from 20cm high using a Gilson pipette, allowed to dry for 10 minutes and stained with Giemsa. Giemsa stain was prepared by adding 15 drops of Giemsa (350864X, Gurr) to 10ml of PBS (331922B, Gurr). Slides were immersed in stain for 10 minutes and then carefully washed with tap water. The slides were viewed under a Leica (DM 5000B) microscope and the number of chromosomes per cell were counted.

2.2.12. Focus forming assay

1×10^6 cells per 10cm dish were plated in DMEM supplemented with 10% [v/v] FBS and 1% [v/v] Penicillin Streptomycin. Cell were replenished with fresh DMEM supplemented with 10% [v/v] FBS and 1% [v/v] Penicillin Streptomycin every 2-3 days. Cells were cultured for 14 days at 37°C in 10% CO₂. Cells were rinsed with PBS, and stained with Giemsa (350864X, Gurr) for 5 minutes at

room temperature. Excess stain was washed in tap water. Plates were allowed to dry and photographed using a Canon EOS 7D camera.

2.2.13. p53 function analysis

To assess for the function of the p53 pathway, MEFs were allowed to grow to a confluency of ~80%. MEFs were treated with 0.2µg/ml of the DNA damaging agent adriamycin (D1515, Sigma) for 24 hours. For comparison purposes, untreated MEFs were also prepared. Protein lysates were analysed for p19^{ARF} and p53 by western blotting.

2.3. Protein Analysis

2.3.1. Preparation of Soluble protein lysates

Media was removed from plates and cells were rinsed once in cold PBS, and then the plates were transferred to ice. Cells were lysed using 50µl of GLB (1% [v/v] Triton X-100, 0.5% NP-40, 50mM Tris [pH 7.5], 150mM NaCl, 5mM EDTA, 5mM EGTA, 10mM NaF, 1mM sodium orthovanadate, corrected to pH 7.0 at room temperature and stored at 4°C. Immediately before use, 1mM AEBSF, 250µg/ml Aprotinin, and 50µg/ml Leupeptin were added. The insoluble fraction was removed by spinning at 13,000rpm at 4°C for 10 minutes, and the supernatants were collected into a fresh tube. The lysates were stored at -20°C.

2.3.2. Quantitation of protein lysates

1µl of cell lysate was mixed with 1ml of Bradford's Reagent (23200, Thermo Scientific). Immediately after mixing by inverting, the optical density was

measured by a spectrophotometer (Biophotometer, Eppendorf) at 595nm. The concentration of protein was determined by comparing the optical density of a standard curve produced by measuring a series of known concentrations of BSA (23209, Thermo Scientific). 0.5µl (1µg), 1µl (2µg), 1.5µl (3µg), 2µl (4µg) and 2.5µl (5µg) BSA was added to separate cuvettes containing 1ml of Bradford's Reagent, and measured by a spectrophotometer.

2.3.3. Immunoprecipitation of protein lysates

50µl of Dynabeads Protein G (100.04D, Invitrogen) were placed into an eppendorf tube, and were washed in Tris-buffered saline (10mM Tris, 0.9% [w/v] NaCl, pH 7.6) with 0.1% [v/v] Tween (TBST). Tubes were placed into a Dynamag-2 magnet and the supernatant removed. The Dynamag-2 magnet was provided by the manufacturer of the Dynabeads. The magnet attracts the magnetic beads, separating the beads from the solution, allowing the beads to be isolated and washed. Beads were coupled to BRAF antibody by incubation with 25µl (5µg) of BRAF antibody (Table 2.5) in a total volume of 200µl TBST for 30 minutes at room temperature on rotation. The beads were then washed 3 times in TBST, and the TBST was removed without discarding the beads by placing the tube into a Dynamag-2 magnet. The beads were incubated with 200µg of protein lysate on rotation at 4°C for 4 hours. As a negative control the beads were incubated with 5µg of mouse IgG (sc-2025) for 30 minutes at room temperature in the absence of BRAF antibody, and then incubated with 200µg of protein lysate for 4 hours at 4°C. The beads were then washed 5 times in TBST and boiled at 95°C with 50µl of 4x SDS loading buffer (62.5M Tris, 10% [v/v] glycerol, 2% [w/v] SDS, 0.05% [v/v] β-Mercaptoethanol, 0.05% [w/v]

bromophenol blue) for 5 minutes. The tubes were placed into a Dynamag-2 magnet, and the supernatant was collected into a fresh tube. 10µl of the supernatant was loaded per lane in an SDS-page gel and preceded as stated in Section 2.3.4.

2.3.4. SDS-polyacrylamide gel electrophoresis (SDS-PAGE)

SDS-PAGE gels of the appropriate percentages (Table 2.4) were prepared with a 5% stacking gel (2.1ml H₂O, 0.5ml 30% [w/v] acrylamide, 380µl 1M Tris-HCl at pH 6.8, 30µl 10% [w/v] SDS, 30µl 10% [w/v] APS, 3µl TEMED) in a Miniprotean III cell (BioRad). The gel was placed in a cassette, and the whole apparatus was immersed into a running tank containing SDS-PAGE running buffer (192mM glycine, 25mM Tris-base, 0.1% [w/v] SDS). Protein lysates were thawed and 5µl of 4x SDS loading buffer was added to 10µg of protein and denatured by boiling at 95°C for 5 minutes prior to loading. The samples were loaded adjacent to pre-stained molecular weight SDS-PAGE markers (All Blue Precision Plus Protein Standards, BioRad) and electrophoresed at 100 volts until the 4x SDS loading buffer had reached the bottom of the gel.

Table 2.4 Composition of SDS-PAGE gel

% gel	H₂O (ml)	30% Acrylamide (ml)	1.5M Tris- HCl, pH 8.8 (ml)	10% SDS (μl)	10% APS (μl)	TEMED (μl)	Size of protein to resolve (kDa)
6	5.3	2	2.5	100	100	8	55-200
8	4.6	2.7	2.5	100	100	8	36-97
10	4	3.3	2.5	100	100	8	22-66
12	3.3	4	2.5	100	100	8	14-50

2.3.5. Western blot – semi-dry transfer

A sheet of 0.2µm nitrocellulose membrane (Schleicher & Schuell) was pre-soaked in transfer buffer (192mM glycine, 25mM Tris, 0.01% [w/v] SDS) prior to transfer. Proteins were electroblotted to the nitrocellulose membrane using a semi-dry blotter (BioRad) following the manufacturer's instructions. A sheet of 3mm blotting paper was soaked in transfer buffer, and placed on the semi-dry blotter. Air bubbles were removed by rolling the paper using a stripette. The sheet of 0.2µm nitrocellulose membrane was placed on top, and air bubbles were removed. The gel was taken out from the Miniprotean III cell, and the stacking gel removed using a scalpel blade. The gel was briefly rinsed in transfer buffer and placed on top of the 0.2µm nitrocellulose membrane and the air bubbles were removed. A sheet of 3mm blotting paper was soaked in transfer buffer and placed on top, and air bubbles were removed. The semi-dry blotter was assembled and proteins were electroblotted to the nitrocellulose membrane at 10 volts for 1 hour and 20 minutes.

2.3.6. Western blot - Treatment with antibodies

Membranes were blocked in 5% [w/v] milk made in TBST for 1 hour, and then incubated with the appropriate antibody (see Table 2.5) diluted in the correct diluent as detailed in Table 2.5 overnight at 4°C with gentle shaking. Membranes were washed 5 times in TBST and then incubated in secondary antibody (Table 2.6) diluted 1:2000 [v/v] in 5% [w/v] milk for 1 hour at room temperature. Following a further 5 washes in TBST, products were visualised using SuperSignal West Pico Chemiluminescent Substrate kit (Pierce). The two reagents in the kit were mixed at an equal ratio and added to the blots for 5

Table 2.5 Primary antibodies used for immunoblotting

Antibody	Size (kDa)	species	dilution	diluent	company	Catalogue number
BRAF	90	Mouse	1:1000	Milk	Santa-Cruz	Sc-5284
Bim	23	Rabbit	1:1000	Milk	Millipore	AB17003
CRAF	74	Mouse	1:200	Milk	BD Biosciences	610153
Cyclin D1	36	Mouse	1:200	Milk	Cell Signalling	2926
Cyclin D2	34	Rabbit	1:1000	Milk	Santa-Cruz	Sc-593
Cyclin D3	31	Mouse	1:500	Milk	Cell Signalling	2936
DUSP-6	42, 44	Rabbit	1:500	Milk	Abcam	ab76310
ERK 2	42, 44	Mouse	1:1000	Milk	Santa-cruz	Sc-1647
GAPDH	37	Mouse	1:2000	Milk	Millipore	MAB374
Myc-tag (9B11)	+6kD	Mouse	1:1000	Milk	Cell signalling	2276
p19^{ARF}	19	Rabbit	1:1000	BSA	Abcam	Ab80
p21	21	Rabbit	1:1000	Milk	Santa-Cruz	Sc-471
p27	27	Rabbit	1:1000	Milk	Cell Signalling	2552
p53	53	Mouse	1:500	Milk	Cell Signalling	2524
P-ERK	42, 44	Rabbit	1:500	BSA	Cell signalling	9101S
P-MEK	45	Rabbit	1:500	BSA	Cell signalling	9154S
P-RSK	90	Rabbit	1:1000	BSA	Cell signalling	9346S
SPRY-2	34	Rabbit	1:500	Milk	Abcam	ab50317
SPRY-4	43	Rabbit	1:200	Milk	Santa-Cruz	Sc-1200

Table 2.6 Secondary antibodies used for western blotting

Species	Company	Catalogue number
Rabbit HRP	Sigma	A6154
Mouse HRP	Sigma	A4416

minutes. The blots were wrapped in Saranwrap, and placed into a cassette. Membranes were exposed to photographic film (Fuji) in the dark.

2.3.7. Quantitation of Western Blot signals

To ensure equal loading, blots were re-probed with an antibody for a house-keeping gene, for example ERK 2 or GAPDH. Autoradiographs were scanned and the intensity of the bands was measured using Image J. Image J is a Java-based image processing program developed at the National Institutes of Health. To normalise for each sample, the intensity of the band of the protein of interest was divided by the intensity of the band of the house-keeping gene. Fold induction was calculated by dividing the normalised intensity of the sample of interest by the normalised intensity of the wild-type sample or untreated sample.

2.4. Preparation of RNA for microarray

RNA was extracted from cells at ~80% confluency. Cells were trypsinised and then collected into a tube. The trypsin was neutralised with DMEM supplemented with 10% [v/v] FBS and 1% [v/v] Penicillin Streptomycin. Cells were counted using a haemocytometer, and the remaining cells were collected by centrifugation at 1,100rpm for 5 minutes. The supernatant was removed and the pellet was snap frozen in liquid Nitrogen. Pellets were stored at -80°C until ready for RNA extraction using a RNeasy mini kit (74104, Qiagen) following the manufacturer's instructions. Briefly, pellets were thawed out in ice, and gently rinsed with cold PBS. A maximum of 1×10^7 cells were resuspended in 600µl of Buffer RLT (provided by manufacturer) and homogenised by centrifugation at

13,000rpm for 2 minutes in a QIAshredder homogeniser (79654, Qiagen). 600µl of 70% [v/v] ethanol was added to the lysate and mixed by pipetting. The sample was pipetted into a RNeasy spin column (provided by manufacturer) and centrifuged at 10,000rpm for 15 seconds. The flow-through was discarded and impurities were removed with 700µl of Buffer RW1 (provided by manufacturer) and centrifuged at 10,000rpm for 15 seconds. The spin column was washed with 500µl of Buffer RPE (provided by manufacturer) and centrifuged at 10,000rpm for 15 seconds to wash the spin column. The spin column was washed again with 500µl of Buffer RPE and centrifuged at 10,000rpm for 15 seconds to wash the spin column. The spin column was placed into a fresh eppendorf tube, and 50µl of RNase-free water (provided by the manufacturer) was added to the spin column. RNA was eluted by centrifugation at 10,000rpm for 1 minute.

RNA was quantitated using a Bioanalyser 2100 (Agilent). RNA labelling and hybridization to Affymetrix GeneChip Mouse Gene 1.0ST arrays were performed by the Microarray facility at the Gladstone Institute using standard protocols

(<http://www.gladstone.ucsf.edu/gladstone/site/genomicscore/section/380>). Data was subjected to Bioinformatic analysis by Alexander Williams at the Gladstone Institute.

2.5. Histology

2.5.1. Harvesting mouse tissue

Mice were sacrificed according to Home Office guidelines. Organs and abnormal growths were dissected, rinsed in PBS and fixed in 10x volume of paraformaldehyde (4% [w/v] paraformaldehyde, 80mM Na_2HPO_4 , 20mM NaH_2PO_4) (PFA) shaking at room temperature for 24 hours. PFA was removed and replaced with 70% [v/v] ethanol, and then stored in 70% [v/v] ethanol at 4°C. The small intestine and large intestine were flushed out with PBS. The small intestine was divided into 6 sections. Both the large intestine and small intestine were opened up and swiss-rolled and then fixed in PFA for 24 hours and stored in 70% [v/v] ethanol at 4°C.

2.5.2. Tissue processing

Tissues were impregnated with wax using a Shandon Citadel 2000 following the manufacturer's protocol by J. Edwards (MRC Toxicology Unit, Leicester). Following processing, tissues were embedded in a paraffin wax block by placing the tissue in a metal case, in the correct orientation and adding warm wax, and then allowing the wax to cool down, forming a solid block.

2.5.3. Preparation of glass slides for tissue sections

Uncoated glass microscopic slides (631-0907, VWR) were placed into polyacetyl racks and soaked overnight in 5% [v/v] Decon. The slides were washed in running hot water for 30 minutes and then rinsed in MilliQ H_2O five times for 5 minutes each time. The slides were dried in a 60°C incubator, then

submerged and agitated in subbing solution (2% [v/v] 3-aminopropyltriethoxysilane in acetone) for 2 minutes, and then in acetone twice for 2 minutes. They were rinsed twice in H₂O for 2 minutes each. The slides were dried in a 60°C incubator.

2.5.4. Sectioning of wax-embedded tissue samples

Paraffin blocks were cooled to 4°C, and then sectioned by S. Giblett (Biochemistry, Leicester) using a Leica RM2135 microtome. The sections were floated in a 40°C waterbath and then transferred to pre-treated slides. The slides were placed in a polyacetal rack and allowed to dry in a 37°C incubator.

2.5.5. Haematoxylin and Eosin staining

The slides were placed into a polyacetal rack and dewaxed by placing into two consecutive tanks of xylene for 10 minutes each, followed by two tanks of 100% ethanol, 90% [v/v] ethanol and finally 70% [v/v] ethanol. The slides were washed in running tap water for 3 minutes, and then stained in Haematoxylin (GHS-132, Sigma-Aldrich) for 5 minutes. They were rinsed under a running tap for 3 minutes. The excess staining was removed by submerging the slides in 1% acid alcohol (70% [v/v] ethanol, 1% [v/v] HCl) for 10 seconds. The slides were then washed for 1 minute, allowing the haematoxylin-stained cell nuclei to turn blue. The cytoplasm was stained by 1% Eosin (9619, RA Lamb) for 1 minute and then washed in water immediately and dehydrated by submerging in 70% [v/v] ethanol for 30 seconds, followed by 90% [v/v] ethanol for 10 minutes, 100% [v/v] ethanol twice for 10 minutes each and finally xylene twice for 10 minutes. The slides were mounted with DPX. The slides were viewed under

Leica (DM 5000 B) microscope, and photographed using a Leica DFC 420 C camera.

2.6. Statistical analysis

The fold induction from western blot quantitation was subjected to statistical analysis by a two-tailed Student T-test, using Microsoft Excel 2010 package.

3. Characterisation of ^{L597V}BRAF

3.1. Introduction

Among the *BRAF* mutants found in human cancers, ^{V600E}*BRAF* is the most common mutation in cancer. However, it is important to characterise other mutants that may provide further insight into the role of BRAF in cancer development. *BRAF* mutations are also found in RASopathies, but *BRAF* mutations found in cancers are rarely found in RASopathies. ^{L597V}*BRAF* is an example of a *BRAF* mutant that is found in both.

3.1.1. The classes of BRAF mutants

BRAF mutants detected in human cancer were classified into high, intermediate and impaired kinase activity mutants by Wan et al (2004) as mentioned in Section 1.6. The study by Wan et al (2004) showed that the BRAF kinase level as measured by MEK1/2 phosphorylation by ^{L597V}BRAF when overexpressed in COS cells was in between the kinase activity of ^{WT}BRAF and ^{G12V}RAS-activated BRAF, and the P-ERK levels in ^{L597V}BRAF-transfected cells were also in between those levels in ^{WT}BRAF- and ^{G12V}RAS-transfected cells (Wan *et al.*, 2004). However, the small increase in BRAF and ERK kinase activity of intermediate kinase activity mutants do not translate to a higher transforming ability, as shown by focus forming assays of NIH 3T3 cells transfected with an intermediate activity mutant (Sarkozy *et al.*, 2009). The level of P-ERK in COS cells transfected with a high kinase activity mutant was similar to cells transfected with ^{G12V}RAS (Wan *et al.*, 2004). However, the level of P-ERK was

slightly lower in COS cells transfected with intermediate kinase activity mutants in comparison to cells transfected with high kinase activity mutants (Wan *et al.*, 2004). Impaired kinase activity mutants were shown to induce ERK activation through CRAF (Wan *et al.*, 2004). However, these experiments were carried out by transfection that allowed overexpression at high levels. It is important to examine the effects of the mutants when expressed endogenously, as this may generate different results.

3.1.2. Heterodimerisation of BRAF and CRAF

Impaired kinase activity mutants have been found to form a heterodimer and transactivate CRAF, inducing activation of MEK and ERK (Farrar *et al.*, 1996; Luo *et al.*, 1996; Weber *et al.*, 2001). However, CRAF was found to inhibit ^{V600E}BRAF-induced ERK activation (Karreth *et al.*, 2009), and ^{V600E}BRAF-expressing melanoma cell lines have been shown to have reduced CRAF expression (Karreth *et al.*, 2009), as a proposed means to counteract the negative effects of CRAF. Therefore, this leads to the question as to whether CRAF can form a heterodimer with the intermediate kinase activity mutants and, if so, whether CRAF suppresses or enhances MEK/ERK output by intermediate kinase activity mutants.

3.1.3. Negative regulators of ERK

Recent studies have shown that SPRY2 and DUSP6 are transcriptional targets of the MEK/ERK pathway and act as negative regulators of the ERK pathway. Emerging evidence shows that they may be important for the tumour phenotype. Their role downstream of intermediate mutants has not yet been

studied extensively. In overexpression studies it has been shown that ^{L597V}BRAF does not bind to SPRY2 or SPRY4, and is therefore not inhibited by SPRY (Tsavachidou *et al.*, 2004), in a similar way to ^{V600E}BRAF. The role of negative regulators, if any, in regulating output of pathway in cells expressing ^{L597V}BRAF needs to be examined.

3.1.4. Generation of *Braf*^{+Lox-L597V} mice

Cre-LoxP technology was used to produce mice that conditionally express ^{L597V}Braf as mentioned in Section 1.8.1. *Braf*^{+LSL-L597V} mice were generated by insertion of a Lox-Stop-Lox cassette containing a minigene cassette coding for the wild-type exons 15 to 18 and the selection marker neo^R cassette (Figure 3.1). These were flanked by 3 LoxP sites. Splice acceptor (SA) and polyadenylation (PA) sequences were cloned on either side of the minigene cassette. The targeting vector was inserted by homologous recombination. Homologous regions of wild-type exon 14 on the left hand side of the LSL cassette and exon 15 containing the C1789G mutation on the right hand side of the LSL cassette target the vector to the *Braf* gene, and the neo^R marker allows for selection.

In the absence of Cre recombinase, the polyA-tail at the end of the minigene and at the end of the neo^R halts transcription, and mice express ^{WT}Braf. A single Cre recombinase molecule binds to each palindromic half of a LoxP site, and then the recombinase forms a tetramer bringing the two LoxP sites together. Recombination occurs within the spacer area of the LoxP sites. The LoxP sites are in the same orientation, which allows excision of the minigene cassette

following recombination. This leaves the mutated exon 15 intact and the mutant Braf protein is expressed. However, there are three LoxP sites, and in rare cases, mosaic recombination occurs. The primers used for genotyping are indicated in Figure 3.1.

3.2. Aims

Previous studies have mainly focussed on ^{V600E}BRAF and its role in cancer development. Unlike ^{V600E}BRAF, ^{L597V}BRAF is expressed constitutively in 3 cases of RASopathies (Sarkozy *et al.*, 2009; Pierpont *et al.*, 2010). These patients suffer developmental abnormalities and do not develop cancer. The oncogenic potential of L597V thus remains to be addressed. The aim of this chapter was to examine the effects of ^{L597V}BRAF in ERK signalling and whether this is affected by CRAF. The effect of ^{L597V}BRAF on cell proliferation and immortalisation were also studied.

3.3. Results

3.3.1. ^{L597V}BRAF has intermediate activity towards the MEK/ERK pathway when overexpressed in HEK 293^T cells

The MAPK output induced by ^{L597V}BRAF was first examined in the Human Embryonic Kidney cell line (HEK 293^T). HEK 293^T were transfected with vectors expressing myc-tagged ^{WT}BRAF, ^{L597V}BRAF, or ^{V600E}BRAF using Lipofectamine 2000 for 6 hours and lysed 48 hours post-transfection. Protein expression was examined by western blotting (Figure 3.2). Untransfected and mock-transfected cells were used as controls.

Figure 3.1 Conditional knock-in mouse model

$Braf^{f+/LSL-L597V}$ mice were generated from ES cells that contained the modified allele. A Lox-Stop-Lox cassette that contains a minigene expressing WT exons 15 to 18 of Braf and a neo^R cassette was inserted before the mutated exon 15. Splice acceptor (SA) and polyadenylation (PA) sites have been indicated.

In the absence of Cre recombinase, mice express ^{WT}Braf. In the presence of Cre recombinase, LoxP sites come together and recombination occurs between the LoxP sequences, and the LSL cassette is released. Following recombination, the mutated exon 15 is transcribed and ^{L597V}Braf is expressed. (A-C) genotyping primers and their orientation are shown.

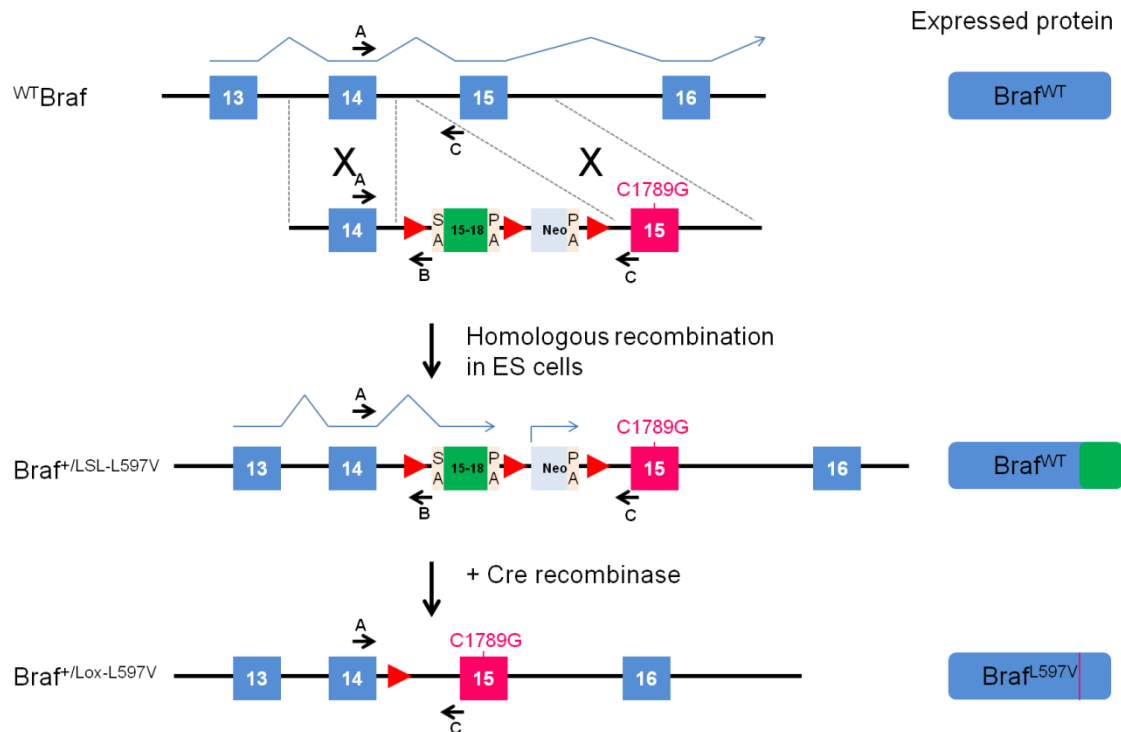
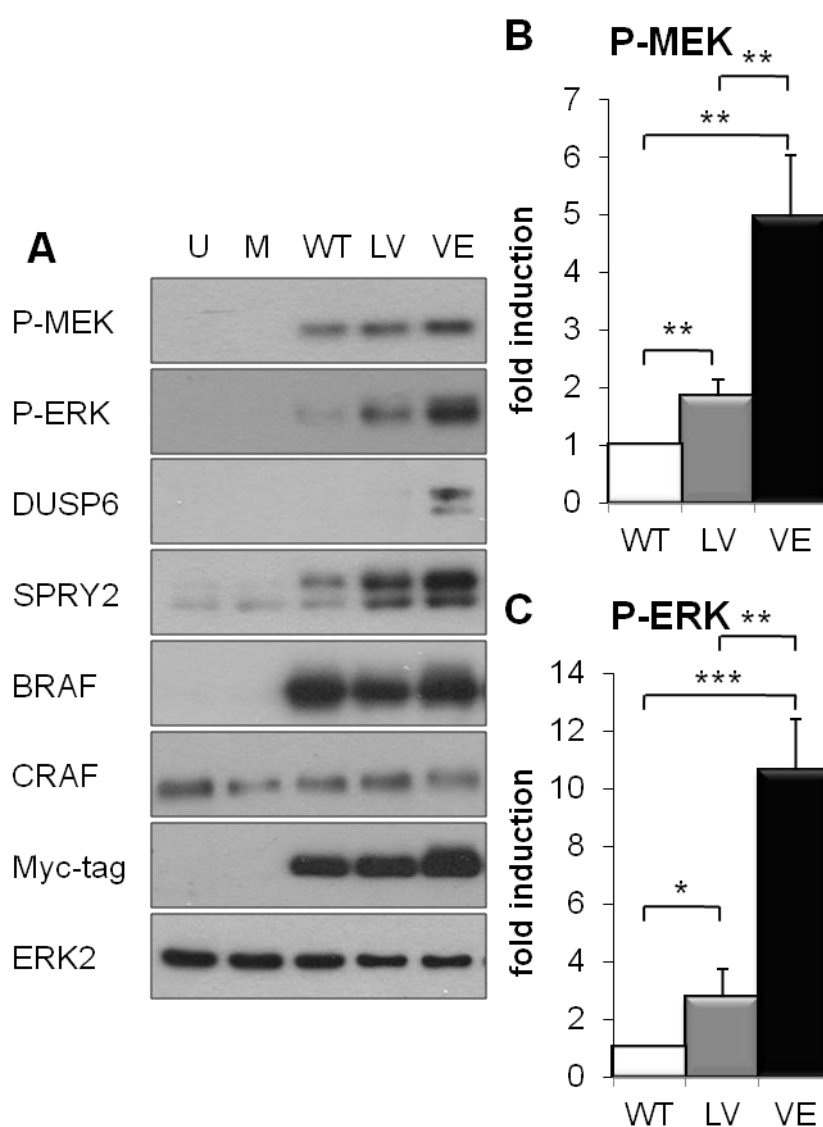


Figure 3.2 L^{597V} BRAF is an intermediate level mutant towards the MEK/ERK pathway.

HEK 293^T cells were untransfected, mock-transfected, or transfected with expressing vectors myc-tagged WT BRAF (WT), L^{597V} BRAF (LV) or V^{600E} BRAF (VE) using Lipofectamine 2000 for 6 hours and lysed 48 hours post-transfection.

- A) Protein expression was analysed by western blotting. Shown are representative western blots (n=3).
- B) Bar chart showing the level of P-MEK quantitated using ImageJ and normalised with respect to ERK2. The fold changes compared with cells transfected with WT BRAF are shown. Bars indicate mean of 3 experiments, error bars indicate standard error. (*) $P < 0.05$ (**) $P < 0.01$ (***) $P < 0.001$ with respect to WT BRAF-transfected cells.
- C) Bar chart showing the level of P-ERK quantitated using ImageJ and normalised with respect to ERK2. The fold changes compared with WT BRAF are shown. Bars indicate mean of 3 experiments, error bars indicate standard error. (*) $P < 0.05$ (**) $P < 0.01$ (***) $P < 0.001$ with respect to WT BRAF-transfected cells.



Results show that the levels of both P-ERK and P-MEK in ^{L597V}BRAF-transfected cells were in between cells transfected with ^{WT}BRAF and the high kinase activity mutation ^{V600E}BRAF (Figure 3.2). This shows that the intermediate kinase activity ^{L597V}BRAF mutant induces MEK and ERK phosphorylation in between levels induced by ^{WT}BRAF and the high kinase activity mutant ^{V600E}BRAF. The western blots were quantitated using ImageJ, and a Student's t-test was performed on three separate sets of results for statistical analysis. Results show that the level of P-MEK and P-ERK of ^{L597V}BRAF-transfected cells was significantly different to ^{WT}BRAF- and ^{V600E}BRAF-transfected cells (Figure 3.2).

The negative regulators SPRY2 and DUSP6 should also be taken into consideration when analysing the MAPK output. Both are induced by P-ERK, and negatively regulate the MAPK pathway, although ^{L597V}BRAF and ^{V600E}BRAF do not bind to SPRY2 (Tsavachidou *et al.*, 2004).

SPRY2 levels were induced by ^{L597V}BRAF and ^{V600E}BRAF, although to a greater extent by ^{V600E}BRAF, whereas only ^{V600E}BRAF-transfected cells induced DUSP6. This shows that ^{V600E}BRAF has a much higher activity towards the MAPK pathway and indeed the P-ERK levels would be even higher if DUSP6 was not expressed.

3.3.2. CRAF forms a heterodimer with ^{L597V}BRAF in HEK 293^T

Heterodimerisation has been shown to be important in activation of the ERK pathway (Rushworth *et al.*, 2006), and in particular in cells harbouring impaired

kinase activity mutants (Wan *et al.*, 2004). Previous studies have shown that, as well as ^{V600E}BRAF, intermediate kinase activity mutants ^{G465A}BRAF and ^{G468E}BRAF, and impaired kinase activity mutants ^{G465E}BRAF, ^{G465V}BRAF and ^{G595R}BRAF (Wan *et al.*, 2004), can also form a heterodimer with CRAF.

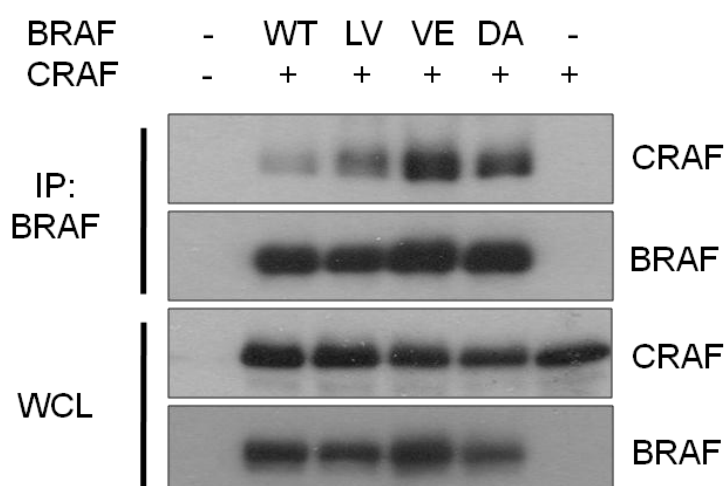
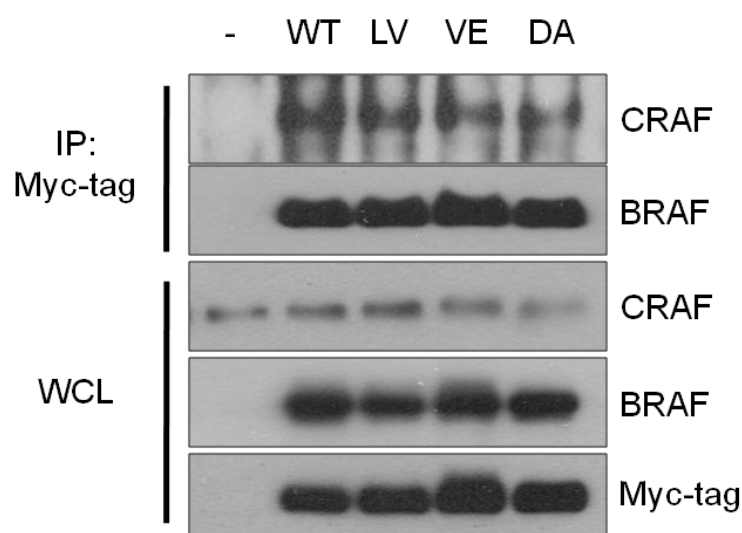
Since the ability of ^{L597V}BRAF to heterodimerise is not known to have been examined before, in order to determine whether exogenous ^{L597V}BRAF can form a heterodimer with exogenous CRAF, ^{L597V}BRAF was immunoprecipitated from HEK 293^T cells, co-transfected with plasmids expressing myc-tagged CRAF and ^{L597V}BRAF, and the immunoprecipitated proteins were western blotted for CRAF (Figure 3.3A). ^{WT}BRAF, ^{V600E}BRAF and ^{D594A}BRAF were used as controls, since all have been shown to heterodimerise with CRAF. To determine whether exogenous ^{L597V}BRAF can form a heterodimer with endogenous CRAF, myc-tagged BRAF was also immunoprecipitated from HEK 293^T cells transfected with a plasmid expressing ^{L597V}BRAF alone and the immunoprecipitated proteins were western blotted for CRAF (Figure 3.3B).

Results show that ^{L597V}BRAF, like ^{WT}BRAF and the other BRAF mutants such as ^{V600E}BRAF and ^{D594A}BRAF, were all able to form a heterodimer with CRAF when overexpressed in cells (Figure 3.3A). The level of CRAF co-immunoprecipitated with BRAF varied somewhat between samples but also varied between experiments, for unknown reasons (data not shown).

All BRAF mutants and ^{WT}BRAF, when overexpressed, formed a heterodimer with endogenous CRAF in HEK 293^T cells (Figure 3.3B). In this experiment,

Figure 3.3 ^{L597V}BRAF forms a heterodimer with ^{WT}CRAF in HEK 293^T cells

- A) HEK 293^T cells were mock-transfected, transfected with ^{WT}CRAF or co-transfected with ^{WT}CRAF and either ^{WT}BRAF (WT), ^{L597V}BRAF (LV), ^{V600E}BRAF (VE) or ^{D594A}BRAF (DA) using Lipofectamine 2000 for 6 hours and lysed 48 hours post-transfection. Cells were lysed and immunoprecipitated for BRAF using antibodies toward BRAF. The immunoprecipitated proteins were analysed by western blotting for the indicated antibodies. Shown are representative western blots (n=3).
- B) HEK 293^T cells were mock-transfected or transfected with myc-tagged ^{WT}BRAF (WT), ^{L597V}BRAF (LV), ^{V600E}BRAF (VE) or ^{D594A}BRAF (DA) using Lipofectamine 2000 for 6 hours and lysed 48 hours post-transfection. Cells were lysed and immunoprecipitated for the myc-tag. The immunoprecipitated protein was analysed by western blotting. Shown are representative western blots (n=2).

A**B**

again the level of CRAF co-immunoprecipitated with BRAF was slightly different, but the same difference was not seen in all experiments. Therefore we cannot conclude whether different BRAF mutants were able to form a more stable complex with CRAF or not from these data.

3.3.3. CRAF suppresses ^{L597V}BRAF-induced MAPK activation

Since RAS binds to both BRAF and CRAF and, as mentioned above, BRAF can heterodimerise with CRAF, the effect of CRAF on BRAF-induced activation of the MAPK pathway was studied. CRAF has been found to reduce the ability of ^{V600E}BRAF to activate MEK and ERK1/2 signalling (Karreth *et al.*, 2009), but enhance the activity of ^{WT}BRAF (Rushworth *et al.*, 2006) and the impaired kinase activity mutant ^{G466V}BRAF (Karreth *et al.*, 2009).

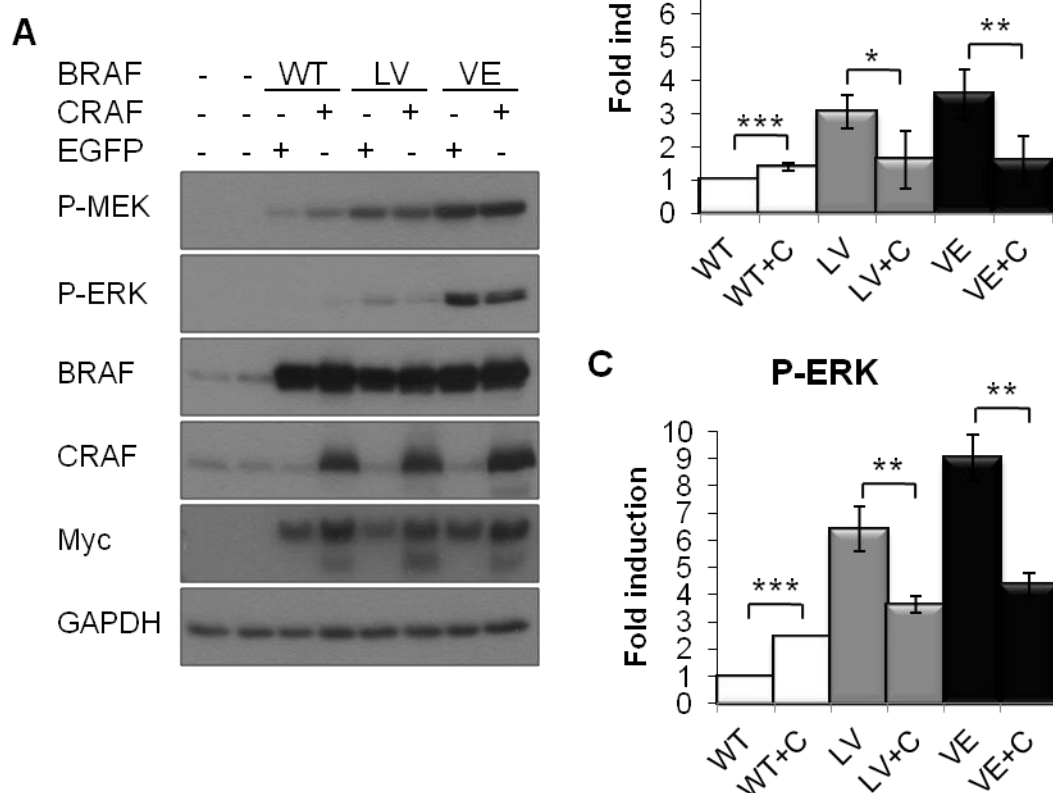
To examine whether CRAF affects the MAPK activity of ^{L597V}BRAF, HEK 293^T cells were transiently co-transfected with myc-tagged BRAF and myc-tagged CRAF plasmid. P-ERK and P-MEK levels were examined by western blotting (Figure 3.4). For comparison purposes, HEK 293^T cells were transfected with a vector expressing BRAF alone. To eliminate the possibility of MAPK activity being suppressed by an excessive DNA load, cells that were transfected with BRAF alone were also transfected with the empty vector expressing EGFP. ^{WT}BRAF and ^{V600E}BRAF were included as a control for successful enhancement or suppression of P-MEK and P-ERK by CRAF respectively.

As shown by Karreth *et al* (2009), when cells were co-transfected with ^{WT}CRAF and ^{WT}BRAF, there was an increase in P-ERK and P-MEK levels in comparison

Figure 3.4 CRAF suppresses ^{L597V}BRAF-induced ERK activation

HEK 293^T cells were untransfected, mock-transfected or transfected with a combination of EGFP, ^{WT}CRAF, ^{WT}BRAF (WT), ^{L597V}BRAF (LV) or ^{V600E}BRAF (VE) using Lipofectamine 2000 for 6 hours and lysed 24 hours post-transfection.

- A) Protein expression was analysed by western blotting. Shown are representative western blots (n=3).
- B) Bar chart showing the levels of P-MEK quantitated using ImageJ and normalised with respect to GAPDH. The fold changes compared with ^{WT}BRAF are shown. Bars indicate mean of 3 experiments, error bars indicate standard error. (*) P<0.05 (**) P<0.01 (***) P<0.001 with respect to ^{WT}BRAF-transfected cells.
- C) Bar chart showing the levels of P-ERK quantitated using ImageJ and normalised with respect to GAPDH. The fold changes compared with ^{WT}BRAF are shown. Bars indicate mean of 3 experiments, error bars indicate standard error. (*) P<0.05 (**) P<0.01 (***) P<0.001 with respect to ^{WT}BRAF-transfected cells.



to cells transfected with ^{WT}BRAF alone (Figure 3.4). Also, when cells were transfected with both ^{WT}CRAF and ^{V600E}BRAF, there was a reduction in P-ERK and P-MEK levels in comparison to cells transfected with ^{V600E}BRAF alone as shown by Karreth et al (2009). When ^{L597V}BRAF was co-transfected with CRAF, the levels of P-ERK and P-MEK were suppressed in comparison with ^{L597V}BRAF alone. The western blots were quantitated using ImageJ and a Student's t-test show that the results were significant (Figure 3.4). Therefore CRAF enhanced ^{WT}BRAF-induced ERK activation, but suppressed ^{L597V}BRAF- and ^{V600E}BRAF-induced ERK activation.

3.3.4. Cre-induced recombination of LSL alleles in MEFs

All of the previous work on ^{L597V}BRAF was performed using transfection techniques resulting in overexpression, which may perturb the cell system and give different results to expression of mutants endogenously. Only one human cancer cell line is available that carries the ^{L597V}BRAF mutation endogenously, and this cell line also contains many other mutations including mutations in *NRAS* and *TP53*. Therefore, to study the ^{L597V}BRAF mutation in isolation, a conditional knock-in mouse model was used.

As mentioned in Section 3.1.4, the conditional mouse model was previously generated in the Pritchard lab and expresses ^{WT}Braf in the absence of Cre recombinase but ^{L597V}Braf following Cre-induced recombination. Primary MEFs were isolated from mouse embryos at E13.5 resulting from intercrosses between *Braf*^{+/LSL-L597V} mice and *Braf*^{+/+} mice. MEFs were isolated and genotyped as described in Section 2.1.8. To induce recombination and

expression of the mutant protein, primary MEFs at passage 1 were seeded at 2×10^5 MEFs per 6cm plate. 24 hours later, MEFs were infected with Adenovirus expressing Cre recombinase (AdCre) (Tuveson *et al.*, 2004) for 24 hours. To test whether infection induced recombination, DNA was isolated and analysed by PCR to test for the recombined allele using the primers indicated in Figure 3.1. To test for efficiency of AdCre-mediated recombination, primary MEFs were infected with AdCre over a time course of 0-96 hours. DNA was harvested at each time point and then analysed by PCR. As controls, $\text{Braf}^{+/+}$ MEFs were infected as well as MEFs containing the same conditional knock-in allele of ^{V600E}Braf. Also as controls, MEFs were infected with Adenovirus expressing β -galactosidase (Ad β gal). DNA was also analysed by PCR for Cre recombinase. PCR results are shown in Figure 3.5.

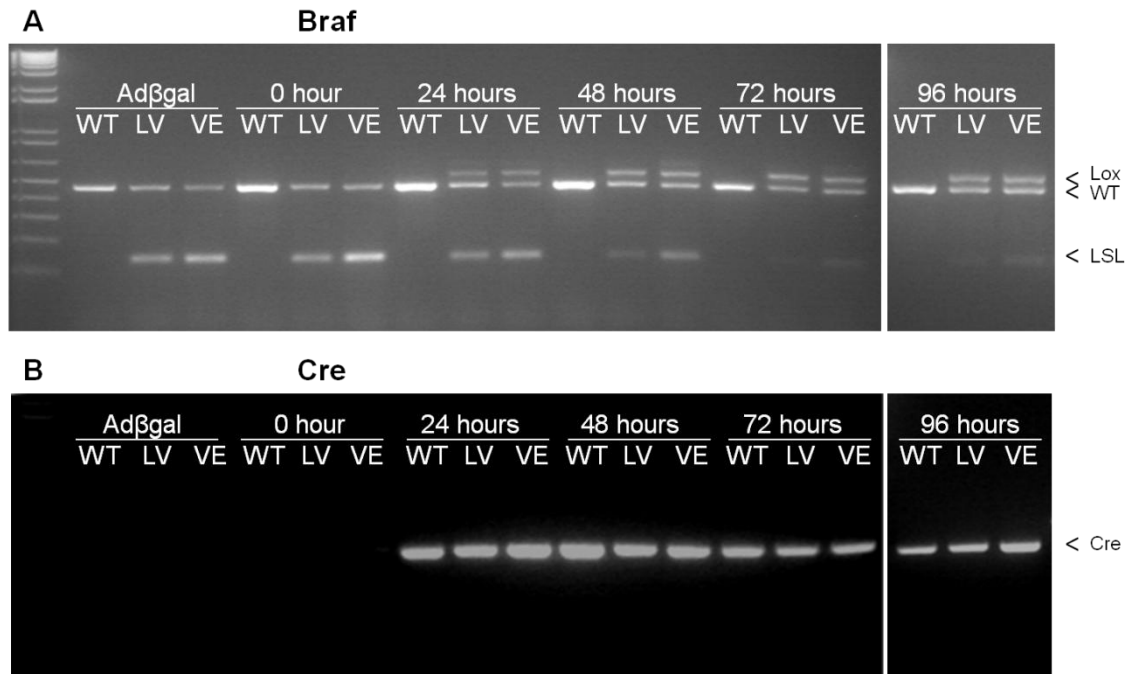
Ad β gal-infected mutant MEFs and $\text{Braf}^{+/+}$ MEFs only contained the ^{WT}Braf band at 466bp as expected (Figure 3.5). Both $\text{Braf}^{+/LSL-L597V}$ and $\text{Braf}^{+/LSL-V600E}$ MEFs are heterozygous and have both a ^{WT}Braf band and an LSL band at 140bp. Following 24 hours of AdCre infection, recombination was detected in both $\text{Braf}^{+/LSL-L597V}$ and $\text{Braf}^{+/LSL-V600E}$ MEFs by the presence of a band at 518bp. Recombination continued to increase with time. It was virtually complete by 72 hours, as indicated by loss of the LSL band. The recombination rate was approximately the same in $\text{Braf}^{+/LSL-L597V}$ and $\text{Braf}^{+/LSL-V600E}$ MEF lines. Ad β gal did not induce recombination.

Figure 3.5 Time course of AdCre-induced LSL recombination

Braf^{+/+} (WT), Braf^{+/LSL-L597V} (LV) and Braf^{+/LSL-V600E} (VE) MEFs were infected with AdCre for 0-96 hours and lysed for DNA extraction. As controls, MEFs were infected with Adβgal for 96 hours. DNA was amplified by PCR, and then PCRs run on an agarose gel and photographed.

A) Braf PCR amplification using Primers A-C.

B) Cre PCR amplification using Primers OCP84 and OCP85 shows that only infected cells contain DNA for the Cre recombinase.



3.3.5. ^{L597V}Braf has low kinase activity in MEFs

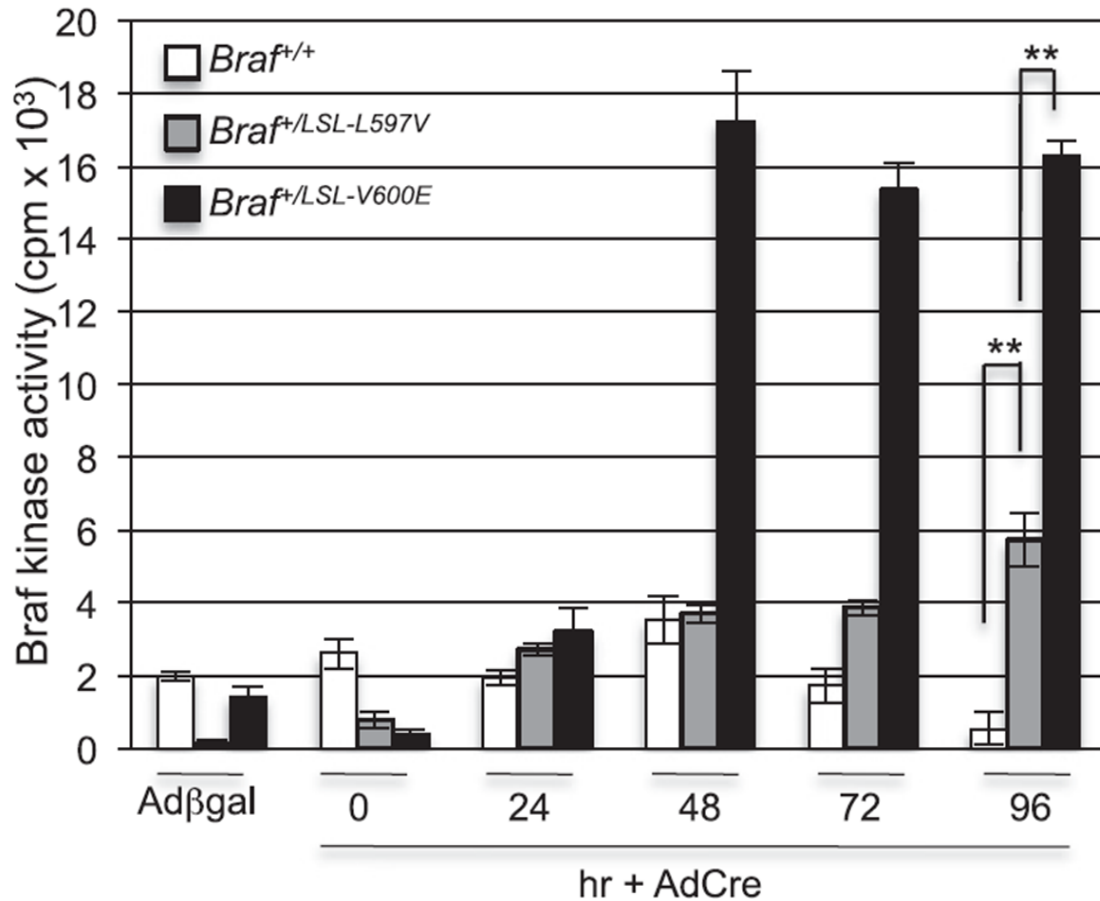
The BRAF kinase activity of ^{V600E}BRAF and various impaired and intermediate kinase activity mutants was determined in a previous study (Wan *et al.*, 2004). However, these activities were measured in cells overexpressing the BRAF mutants.

To determine the kinase activity of ^{L597V}Braf when endogenously expressed, primary MEFs were seeded at a density of 3×10^5 MEFs per 6cm plate. 24 hours later, MEFs were infected with AdCre over a 96 hour time course. Cells were lysed at 24 hour time points. As controls, MEFs were either uninfected or infected with Ad β gal. Braf^{+/+} and Braf^{+/LSL-V600E} MEFs infected with AdCre over the same time course were included for comparison. Protein lysates were subjected to immunoprecipitation kinase assays using the kinase cascade assay (Wan *et al.*, 2004) (Figure 3.6). Braf was immunoprecipitated, and incubated with glutathione S-transferase (GST)-MEK, GST-ERK and MBP with [γ -³²P]ATP as sequential substrates, and the radioactivity measured. These assays were undertaken by Bipin Patel (Biochemistry, Leicester).

Results show a slight variation of ^{WT}Braf kinase activity following AdCre infection and in control MEFs infected with Ad β gal (Figure 3.6). Braf kinase activity of ^{V600E}Braf only slightly increased at 24 hours, but changed significantly after 48 hours of AdCre infection and reached a peak of ~8-fold greater than ^{WT}Braf kinase activity. This level of activity stayed the same up to 96 hours. ^{L597V}Braf kinase activity was slightly increased after 24 hours of AdCre infection, but increased with time to ~2-fold greater than ^{WT}Braf kinase activity at 96 hours

Figure 3.6 ^{L597V}Braf kinase activity in MEFs

MEFs of the genotypes indicated were infected with AdCre to induce recombination. As controls, MEFs were either uninfected (0) or infected with Ad β gal. MEFs were lysed at 24 hour time points. Proteins were isolated and subjected to Braf kinase assays. Bars indicate mean of 3 experiments and, error bars indicate standard deviation (**) $P < 0.01$ with respect to $Braf^{+/+}$ MEFs. Assays performed by Bipin Patel (Biochemistry, Leicester)



after AdCre infection. Statistical analysis by Student's t-test showed that the difference in fold activation between ^{WT}Braf and ^{L597V}Braf, and ^{L597V}Braf and ^{V600E}Braf after 96 hours of AdCre infection was statistically significant. Thus ^{L597V}Braf induces Braf activity in between ^{WT}Braf and ^{V600E}Braf.

3.3.6. ^{L597V}Braf induces weak Mek/Erk activation in MEFs

The level of MEK/ERK activation in COS cells overexpressing ^{L597V}BRAF has been shown to be slightly elevated when compared with cells overexpressing ^{WT}BRAF (Wan *et al.*, 2004) and HEK 293^T cells (Section 3.3.1). To test activation of the downstream Mek/Erk pathway following endogenous ^{L597V}Braf expression, primary MEFs were seeded at 3x10⁵ MEFs per 6cm plate. 24 hours later, MEFs were infected with AdCre over a 96 hour time course. Cells were lysed at 24 hour time points. As controls, MEFs were either uninfected or infected with Adβgal. Braf^{+/+} and Braf^{+/LSL-V600E} MEFs were included for comparison. Protein lysates were analysed by western blotting (Figure 3.7).

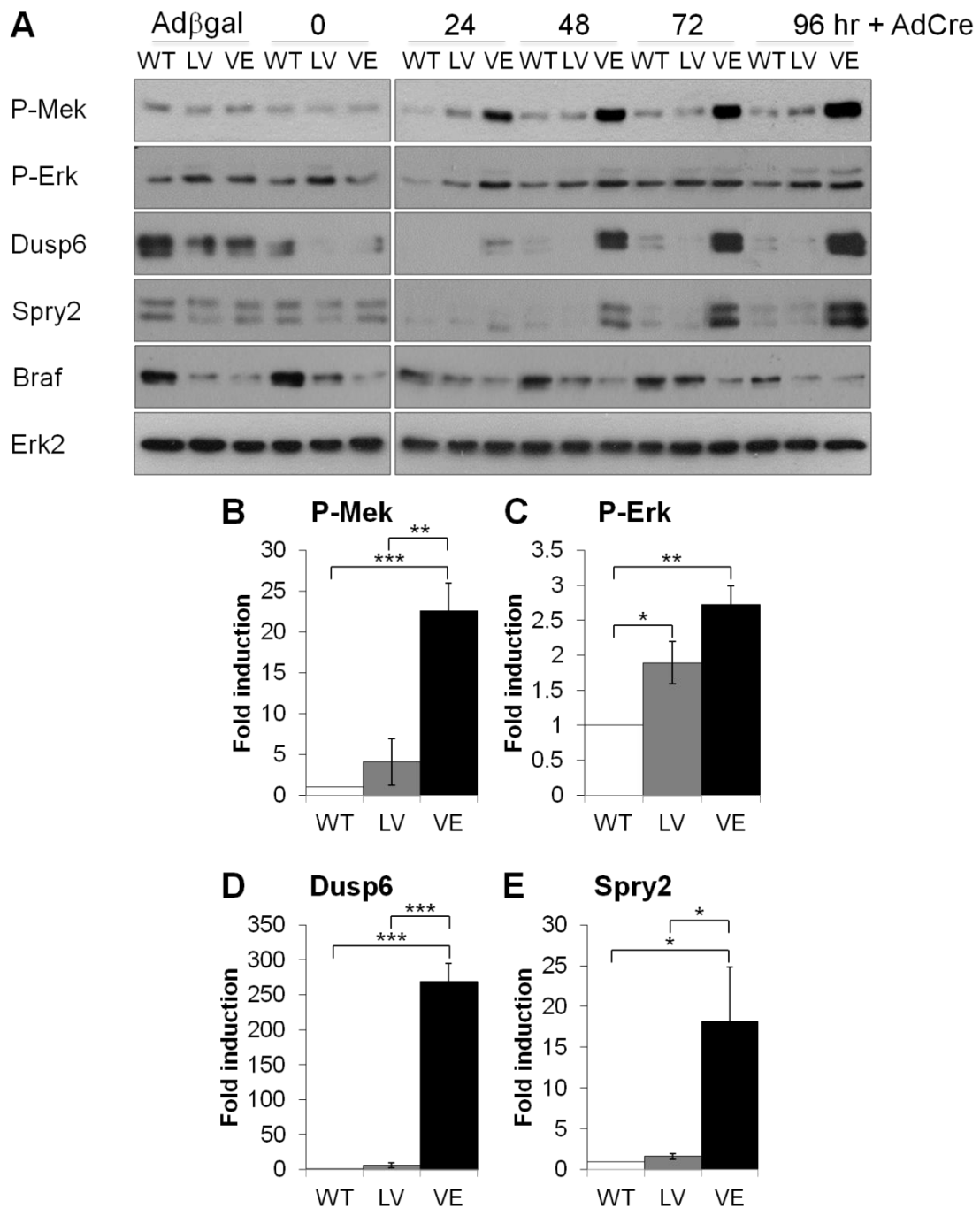
The levels of P-Mek, P-Erk, Dusp6 and Spry2 in Braf^{+/Lox-L597V} MEFs were all in between those of Braf^{+/+} and Braf^{+/Lox-V600E} MEFs (Figure 3.7). Like the kinase activity, the levels of the proteins fluctuated over the time course in Braf^{+/+} MEFs. The levels of P-Mek, P-Erk, Dusp6 and Spry2 of Braf^{+/LSL-V600E} MEFs increased following 24 hours of AdCre infection, and continued to increase over the time course. This was not due to changes in Braf expression.

Figure 3.7 ^{L597V}Braf induces weak MEK/ERK activity

Braf^{+/+} (WT), Braf^{+/LSL-L597V} (LV) and Braf^{+/LSL-V600E} (VE) MEFs were infected with AdCre for 0-96 hours. As controls, MEFs were infected with Adβgal.

A) Protein expression was analysed by western blotting. Shown are representative western blots (n=3).

B-E) Bar charts showing the levels of P-Mek, P-Erk, Dusp6 and Spry2 after 96 hours of AdCre infection, quantitated using ImageJ and normalised with respect to Erk2. The fold changes with respect to Braf^{+/+} at 96 hours are shown. Bars indicate mean of 3 experiments, error bars indicate standard error. (*) P<0.05 (**) P<0.01 (***) P<0.001 with respect to Braf^{+/+} MEFs.



The level of proteins at 96 hours was quantitated using ImageJ, and a Student's t-test revealed that the level of expression of each protein in $\text{Braf}^{+/Lox-V600E}$ MEFs was significantly different to $\text{Braf}^{+/+}$ MEFs. The level of P-Mek in $\text{Braf}^{+/Lox-V600E}$ MEFs was ~22-fold greater than in $\text{Braf}^{+/+}$ MEFs. However, the level of P-Erk was only ~2-fold greater than in $\text{Braf}^{+/+}$ MEFs. This could be due to the high level of Dusp6 at ~270-fold higher than in $\text{Braf}^{+/+}$ MEFs. Although ^{V600E}Braf is not negatively regulated by Spry2, the level of Spry2 was ~17-fold higher than in $\text{Braf}^{+/+}$ MEFs. Results therefore show that ^{V600E}Braf-induced Mek/Erk activity is significantly higher than ^{WT}Braf and ^{L597V}Braf.

The levels of P-Mek and P-Erk in $\text{Braf}^{+/LSL-L597V}$ MEFs were slightly increased over $\text{Braf}^{+/+}$ MEFs, but showed no change in the levels of Dusp6 and Spry2. The level of proteins quantitated at 96 hours show that the level of P-Mek, Dusp6 and Spry2 of $\text{Braf}^{+/Lox-L597V}$ MEFs was significantly different to $\text{Braf}^{+/Lox-V600E}$ MEFs, but not always that different to $\text{Braf}^{+/+}$ MEFs. Therefore ^{L597V}Braf induces weak Mek/Erk activity, which is slightly higher than ^{WT}Braf, but significantly lower than ^{V600E}Braf.

The level of P-Erk in $\text{Braf}^{+/Lox-L597V}$ MEFs was approaching that in $\text{Braf}^{+/Lox-V600E}$ MEFs. To test whether this was due to high levels of negative feedback regulators induced by $\text{Braf}^{+/Lox-V600E}$ cells, immortalised $\text{Braf}^{+/Lox-V600E}$ MEFs were seeded to reach a confluency of ~70%. MEFs were transfected with Dusp6 siRNA or Spry2 siRNA for 24 hours. As controls, MEFs were transfected with

scrambled siRNA. Protein lysates were analysed by western blotting (Figure 3.8).

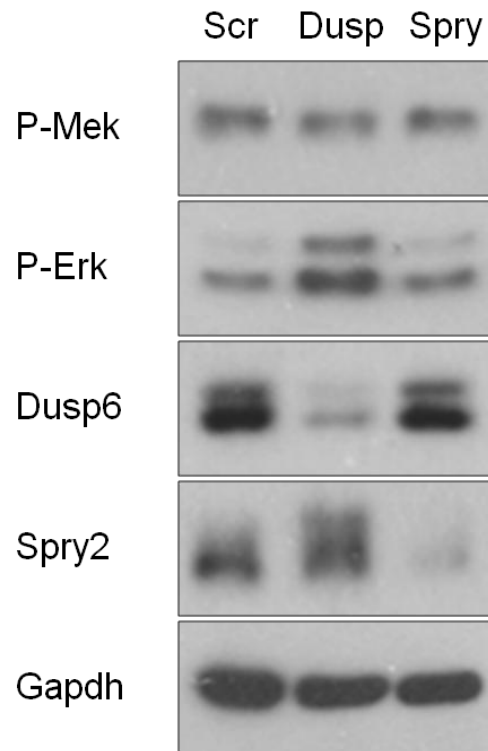
Dusp6 and Spry2 siRNA depleted the majority of Dusp6 and Spry2 levels respectively (Figure 3.8). Spry2 knock-down did not affect the levels of P-Mek or P-Erk, which supports a previous study that showed SPRY2 knock-down in cells harbouring ^{V600E}BRAF did not affect P-ERK levels and cell growth (Tsavachidou *et al.*, 2004). P-Erk levels were much higher in cells where Dusp6 had been knocked-down. This shows that Dusp6 reduced the high P-Erk levels in *Braf*^{+/-Lox-V600E} MEFs. The level of P-Mek following Dusp6 knock-down could also be observed to be slightly reduced. This could be as a result of induction of other negative regulators of the pathway that may act upstream. These results show that the high MAPK activity induced by ^{V600E}Braf induces activation or stabilisation of MAPK negative regulators, including Dusp6 and Spry2, but ^{V600E}Braf is insensitive to Spry2 regulation.

3.3.7. ^{L597V}Braf does not transform MEFs

The high kinase activity mutant ^{V600E}Braf has been shown to induce morphological transformation of MEFs (Mercer *et al.*, 2005; Roring *et al.*, 2012). However, the transforming ability of ^{L597V}Braf has not been examined. To examine the potential of ^{L597V}Braf in cell transformation, primary *Braf*^{+/-LSL-L597V} MEFs were seeded at 3x10⁵ MEFs per 6cm dish. 24 hours later, MEFs were infected with AdCre to induce recombination and expression of ^{L597V}Braf.

Figure 3.8 Knock-down of Dusp6 in Brf^{+/-Lox-V600E} MEFs elevates P-Erk levels

Immortalised Brf^{+/-Lox-V600E} MEFs were transfected with Scrambled control (Scr), Dusp6 (Dusp) or Spry2 (Spry) siRNA using Lipofectamine 2000 for 24 hours. Western blots were analysed with the antibodies indicated. Shown are representative western blots (n=2).



Following seven passages, MEFs were photographed (Figure 3.9). $\text{Braf}^{+/+}$ and $\text{Braf}^{+/LSL-V600E}$ MEFs infected with AdCre were used for comparison of cell morphology, and Ad β gal-infection was used as controls.

All three MEF lines exhibited a flat untransformed morphology before infection (Figure 3.9). Ad β gal infection had no effect on cell morphology. Following AdCre infection, $\text{Braf}^{+/Lox-V600E}$ changed the most in appearance. Cells appeared bright and displayed a refractile, long, spindle-shaped morphology showing the typical morphology of transformed cells. Both $\text{Braf}^{+/+}$ and $\text{Braf}^{+/Lox-L597V}$ MEFs retained a flat, untransformed morphology. Therefore, unlike ^{V600E}Braf, ^{L597V}Braf does not transform MEFs.

3.3.8. ^{L597V}Braf does not induce foci formation

It has been shown that ^{L597V}BRAF overexpression in NIH3T3 cells induces foci formation (Ritt *et al.*, 2010), but the number of foci formed was not different to overexpressed ^{WT}BRAF (Sarkozy *et al.*, 2009). However, this does not equate to endogenous expression of ^{L597V}BRAF. To examine whether ^{L597V}Braf can induce focus formation when endogenously expressed, immortalised $\text{Braf}^{+/Lox-L597V}$ MEFs were plated at 1×10^6 cells per 10cm plate, and allowed to grow for 14 days with a media change every 2-3 days. Cells were then stained with Giemsa and photographed (Figure 3.10). Immortalised $\text{Braf}^{+/Lox-V600E}$ and $\text{Braf}^{+/+}$ MEFs were included for comparison.

Figure 3.9 ^{L597V}Braf does not transform MEFs

Braf^{+/+} (WT), Braf^{f+/LSL-L597V} (LV) and Braf^{f+/LSL-V600E} (VE) MEFs were infected with AdCre to induce recombination and expression of ^{WT}Braf, ^{L597V}Braf or ^{V600E}Braf respectively. As controls, MEFs were infected with Adβgal. MEFs were photographed 7 passages following AdCre infection. Shown are representative photographs (n=3).

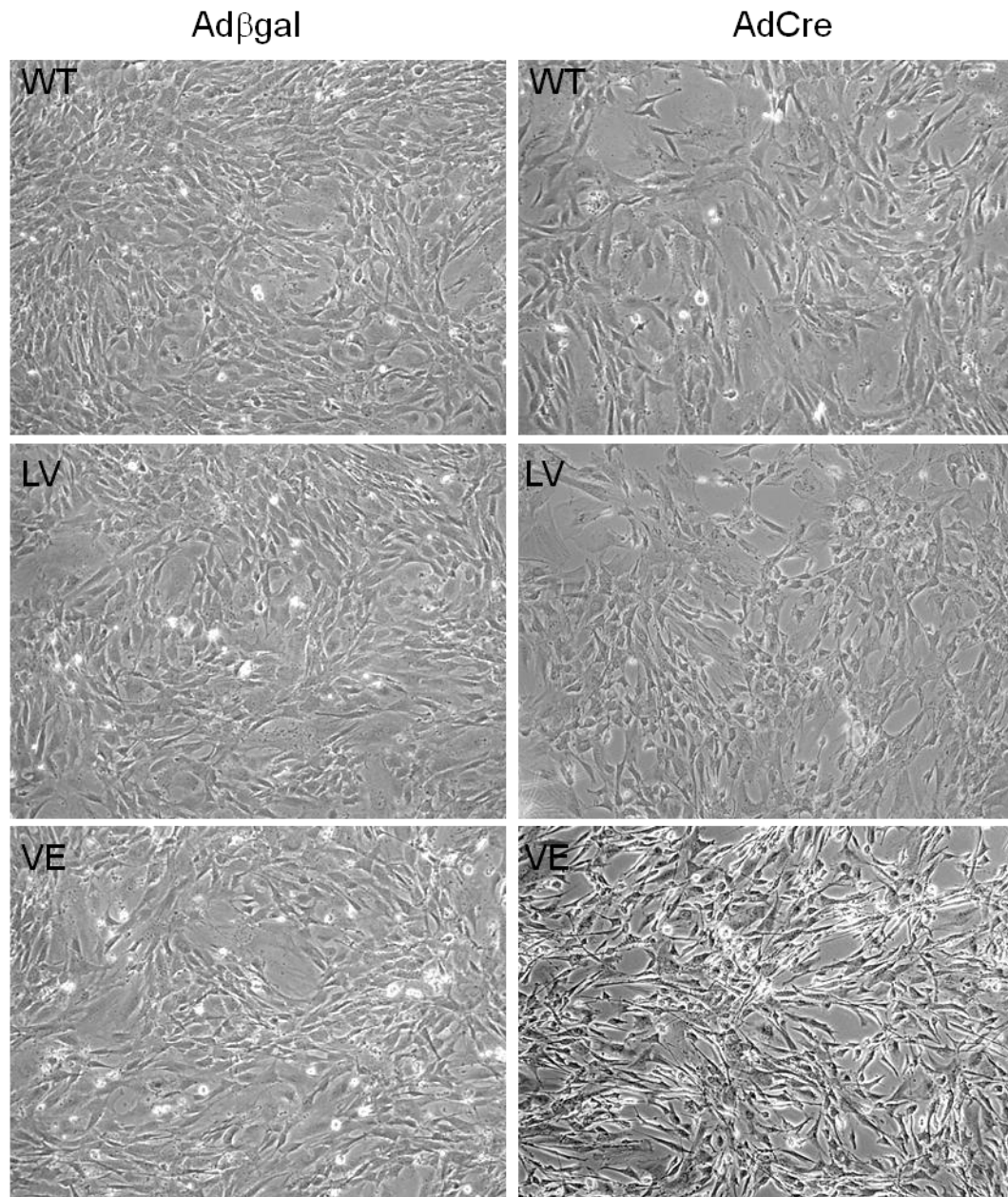
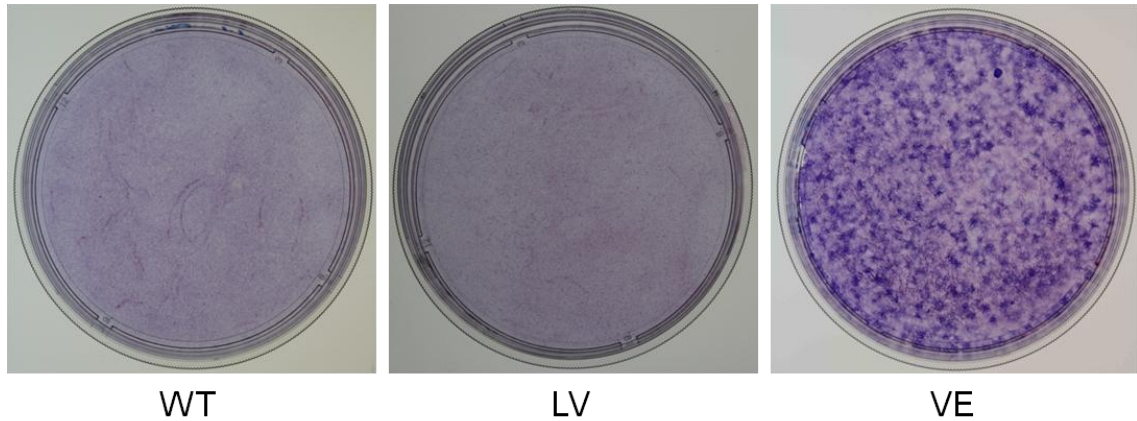


Figure 3.10 ^{L597V}Braf does not induce focus formation

Immortalised $\text{Braf}^{+/+}$ (WT), $\text{Braf}^{+/Lox-L597V}$ (LV) and $\text{Braf}^{+/Lox-V600E}$ (VE) MEFs were plated at 1×10^6 cells per 10cm plate and allowed to grow for 14 days. Media was replenished every 2-3 days. Cells were rinsed with PBS, and stained with Giemsa. Excess stain was removed by rinsing gently with tap water. Plates were photographed. Shown are representative photographs (n=3).



In contrast to previous studies that showed foci formation of NIH 3T3 cells overexpressing ^{L597V}BRAF (Sarkozy *et al.*, 2009), endogenously expressed ^{L597V}Braf did not induce focus formation (Figure 3.10). Giemsa stained plates of ^{Braf^{+/Lox-L597V}} MEFs were identical to plates of ^{Braf^{+/+}} MEFs in that no foci were observed. In contrast, ^{Braf^{+/Lox-V600E}} MEFs were able to grow without contact inhibition and were able to grow on top of each other, forming foci. This has also been shown in NIH 3T3 cells overexpressing ^{V600E}BRAF (Wan *et al.*, 2004; Sarkozy *et al.*, 2009; Ritt *et al.*, 2010) and in Cre-infected ^{Braf^{+/LSL-V600E}} MEFs (Mercer *et al.*, 2005). This shows that the ^{L597V}Braf mutation does not confer resistance to contact inhibition, and suggests that it is not an oncogene.

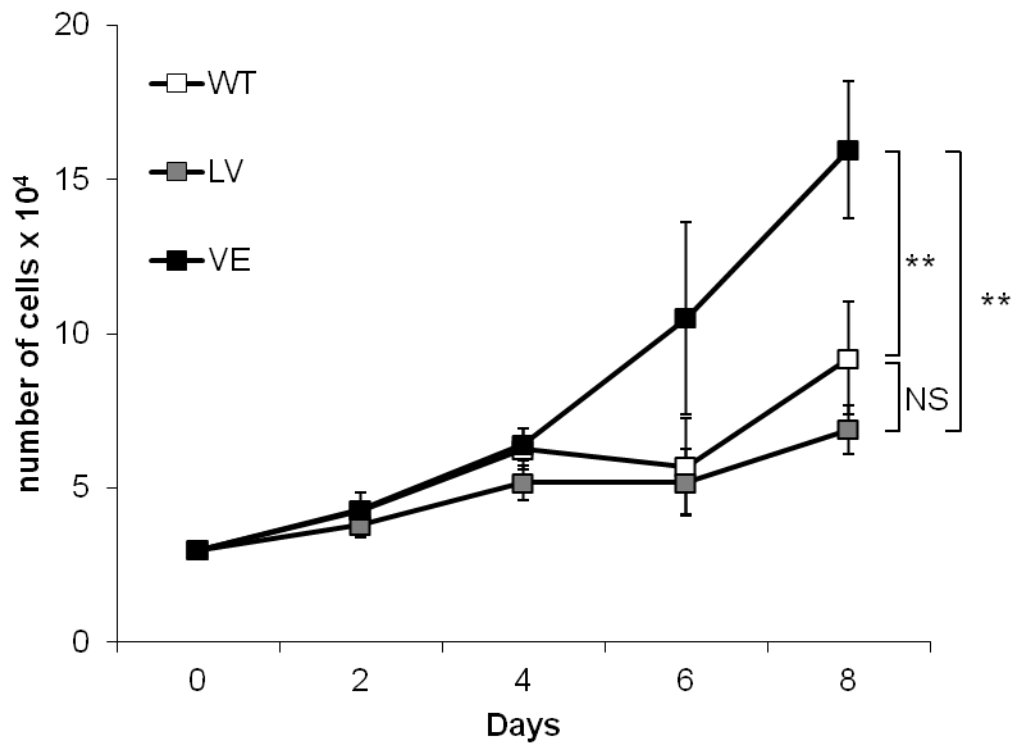
3.3.9. ^{L597V}Braf does not confer growth advantage on MEFs

The importance of ERK signalling in inducing cell proliferation is well studied. To examine whether ^{L597V}Braf provides a growth advantage given the weak Mek/Erk activity it induces, growth curves were generated. Primary ^{Braf^{+/LSL-L597V}} MEFs were seeded at 3×10^5 MEFs per 6cm plate. 24 hours later, MEFs were infected with AdCre for 72 hours to allow full recombination, and then plated at 3×10^4 cells per 12-well plate. The media was replenished every 2 days and the number of cells was counted in triplicate every two days for eight days (Figure 3.11). ^{Braf^{+/+}} and ^{Braf^{+/LSL-V600E}} MEFs infected with AdCre were included for comparison.

Each MEF line was derived from a single embryo, and individual variation can arise in growth rates between MEFs, even of the same genotype. Pooling data across MEFs was thus very difficult. Therefore, the results presented are of a

Figure 3.11 $\text{Braf}^{+/Lox-L597V}$ MEFs do not have a growth advantage

$\text{Braf}^{+/+}$ (WT), $\text{Braf}^{+/LSL-L597V}$ (LV) and $\text{Braf}^{+/LSL-V600E}$ (VE) MEFs were infected with AdCre for 72 hours to allow full recombination. After this, MEFs were plated at 3×10^4 cells per 12-well plate, and the number of cells was counted in triplicate every two days for eight days. Shown are representative counts in triplicates from $n=3$, error bars indicate standard deviation between triplicates. (NS) not significant, (**) $P < 0.01$.



single line for each genotype counted in triplicate (Figure 3.11). This is representative of three experiments with MEFs derived from different embryos. A Student's t-test at day 8 showed that the number of $\text{Braf}^{+/Lox-V600E}$ MEFs was significantly different to the number of $\text{Braf}^{+/+}$ and $\text{Braf}^{+/Lox-L597V}$ MEFs, but the number of $\text{Braf}^{+/Lox-L597V}$ MEFs was not significantly different to $\text{Braf}^{+/+}$ MEFs. Therefore ^{L597V}Braf does not confer a growth advantage on MEFs, unlike ^{V600E}Braf.

3.3.10. ^{L597V}Braf does not induce early immortalisation in MEFs

In primary cells, ^{L597V}Braf does not provide a growth advantage. It has previously been shown that ^{G12D}Kras and ^{D594A}Braf can induce early immortalisation of MEFs and so this was examined for ^{L597V}Braf. To test whether $\text{Braf}^{+/L597V}$ MEFs are able to immortalise, the 3T3 assay was used. Primary $\text{Braf}^{+/LSL-L597V}$ MEFs were seeded at 2×10^5 MEFs per 6cm plate. 24 hours later, MEFs were infected with AdCre for 24 hours and 3×10^5 MEFs were replated, and this was repeated for a total of 20 passages. The number of MEFs was counted every 3 days and 3×10^5 MEFs replated. The number of population doublings was worked out at each passage and a growth curve was produced (Figure 3.12). As controls $\text{Braf}^{+/+}$ and $\text{Braf}^{+/LSL-V600E}$ MEFs were infected with AdCre, and primary MEFs were also uninfected (data not shown) or infected with Ad β gal (Figure 3.12).

The immortalisation profiles of Ad β gal-infected MEFs were similar in that MEFs did not immortalise regardless of the genotype (Figure 3.12). However, since Cre is known to induce DNA damage, AdCre-infected $\text{Braf}^{+/+}$ MEFs formed a

Figure 3.12 L^{597V} Brf does not induce early immortalisation

Braf^{+/+} (WT), Braf^{+/LSL-L597V} (LV) and Braf^{+/LSL-V600E} (VE) MEFs were infected with Ad β gal or AdCre for 24 hours and 3×10^5 MEFs were replated. The number of MEFs was counted every 3 days and 3×10^5 MEFs replated to obtain the number of population doublings at every passage. Shown are three separate lines of each genotype. For comparison purposes, each line has been given an ID (WT 1-3, VE 1-3, LV 1-3).

- Population doublings for AdCre-infected MEFs.
- Population doublings for Ad β gal-infected MEFs.
- Population doublings of one representative immortalisation curve for each genotype.

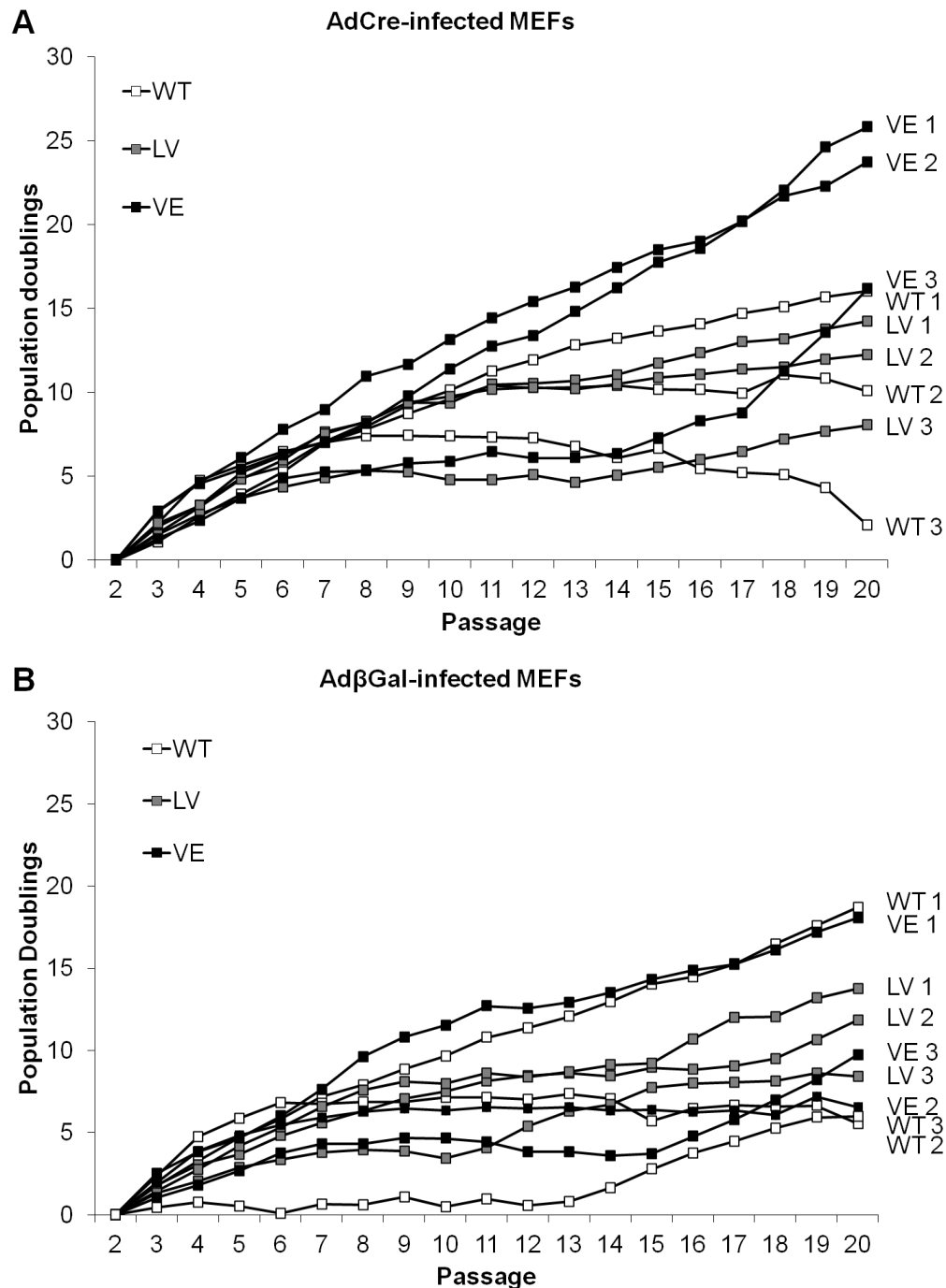
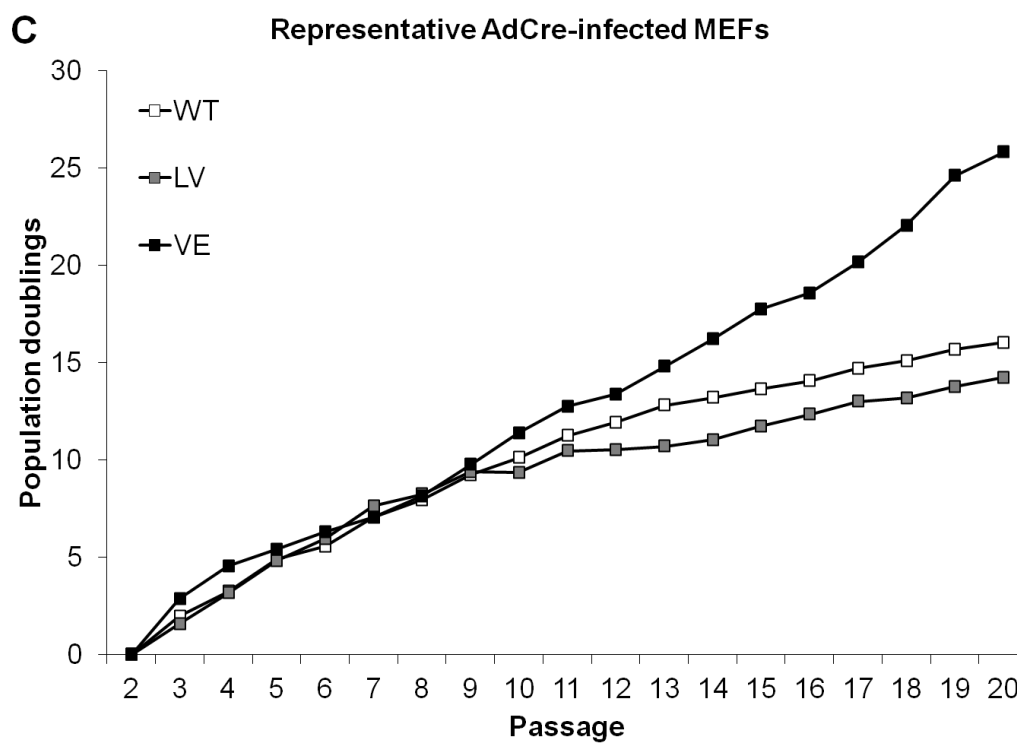


Figure 3.12 continued

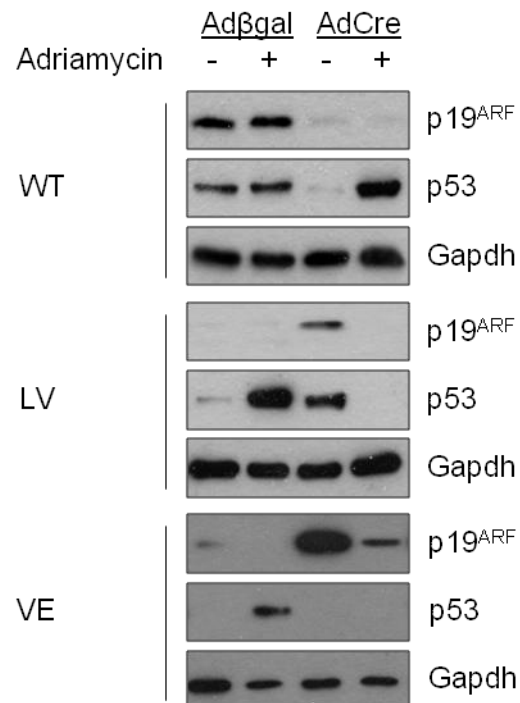


better control. Two out of three $\text{Braf}^{+/Lox-V600E}$ MEF lines underwent early immortalisation, and the third line immortalised at a slightly later passage (Figure 3.12). This supports previous unpublished work by Hong Jin (Biochemistry, Leicester) who induced ^{V600E}Braf expression in MEFs using tamoxifen in a tamoxifen-inducible Cre-ER mouse model, and observed early immortalisation induced by ^{V600E}Braf. None of the examined $\text{Braf}^{+/+}$ or $\text{Braf}^{+/Lox-L597V}$ MEF lines underwent early immortalisation (Figure 3.12). Thus, although $\text{Braf}^{+/Lox-V600E}$ MEFs show evidence of early immortalisation, this is not the case for $\text{Braf}^{+/Lox-L597V}$ MEFs.

It is known that immortalisation of wild-type mouse fibroblasts is associated with inactivation of $p19^{\text{ARF}}$ or $TP53$ (Kamata *et al.*, 2010). To test if the immortalised cells have lost $p19^{\text{ARF}}$ or p53 function, MEFs were treated with or without the DNA damaging agent adriamycin and western blots prepared and analysed with antibodies toward $p19^{\text{ARF}}$ and p53 (Figure 3.13). Loss of function was indicated by the loss of $p19^{\text{ARF}}$ levels, loss of p53 levels, increased levels of p53 in the absence of adriamycin treatment, an indication of a defective negative feedback mechanism, or unchanged levels of p53 or $p19^{\text{ARF}}$ following adriamycin treatment, an indication of unresponsiveness to DNA damage. Representative blots are shown in Figure 3.13. All $\text{Braf}^{+/+}$ immortalised MEFs either lost $p19^{\text{ARF}}$ expression or p53 function (Figure 3.13). The same was also observed in $\text{Braf}^{+/Lox-L597V}$ MEFs, and, surprisingly also $\text{Braf}^{+/Lox-V600E}$ MEFs.

Figure 3.13 Immortalisation of MEFs is associated with loss of p19^{ARF} or p53 function

Braf^{+/+} (WT), Braf^{+/LSL-L597V} (LV) and Braf^{+/LSL-V600E} (VE) MEFs were infected with Adβgal or AdCre and allowed to immortalise. Immortalised MEFs were either untreated (-), or treated with adriamycin (+) to induce DNA damage. Protein lysates were collected 24 hours after treatment. Western blots were analysed using the antibodies shown. Shown is a selection of western blots from each genotype (n=3).



3.4. Conclusion

Little is known about the ^{L597V}BRAF mutant, aside from it having intermediate BRAF kinase activity when overexpressed in COS cells (Wan *et al.*, 2004). Western blots of HEK 293^T cells overexpressing ^{L597V}BRAF confirmed that the mutant has intermediate activity towards the MEK/ERK pathway in which the levels of P-MEK and P-ERK in ^{L597V}BRAF-transfected cells were in between ^{WT}BRAF- and ^{V600E}BRAF-transfected cells. Although ^{L597V}BRAF has been shown to be unable to bind to SPRY2 (Tsavachidou *et al.*, 2004), SPRY2 levels act as an indication of MEK/ERK output, and results showed that SPRY2 levels of ^{L597V}BRAF-transfected cells were in between ^{WT}BRAF- and ^{V600E}BRAF-transfected cells. ^{L597V}BRAF however, failed to induce DUSP6 expression. This showed that the level of ^{L597V}BRAF-induced MAPK activity was much lower than that induced by ^{V600E}BRAF.

Studies have shown that the activity of BRAF can be modified by CRAF, through heterodimerisation. Transfection of ^{L597V}BRAF and immunoprecipitation of BRAF showed that ^{L597V}BRAF is capable of forming a heterodimer with CRAF. Co-transfection of ^{L597V}BRAF with CRAF resulted in a reduction in P-MEK and P-ERK levels in comparison with cells transfected with ^{L597V}BRAF alone, suggesting that CRAF can inhibit ^{L597V}BRAF-induced activation of MEK and ERK1/2 as with ^{V600E}BRAF (Karreth *et al.*, 2009).

Studies using overexpression can perturb the cell system and give different results to expression of mutants endogenously. However, the only human cell line that harbours ^{L597V}BRAF mutation also contains many other mutations.

Therefore, a conditional knock-in mouse model was used. However, knock-in mouse models are not without disadvantages. Adenoviral infection was required to introduce Cre recombinase for recombination and expression of the mutant protein. Cre recombinase can introduce DNA damage (Loonstra *et al.*, 2001) which can affect cell signalling and cell growth, which are the properties being examined. Furthermore, individual variation poses an additional complication. To circumvent these problems, each experiment was repeated twice and a range of controls were used.

Using the knock-in mouse model, we could examine the Braf kinase activity of endogenous ^{L597V}Braf, unlike the previous study which tested the BRAF kinase activity of overexpressed BRAF (Wan *et al.*, 2004). We showed slight variation in the Braf kinase activity of ^{L597V}Braf following AdCre infection, which could be as a result of recombination efficiency. After 96 hours of AdCre infection, recombination was complete, and the kinase activity of ^{L597V}Braf was at ~2-fold in comparison with ^{WT}Braf. The kinase activity of ^{L597V}Braf was also statistically different to ^{V600E}Braf, which was at ~8-fold. This supports the findings by Wan *et al* (2004) that ^{L597V}BRAF is an intermediate kinase activity mutant. Both of the mutants have significantly lower Braf kinase activity than when overexpressed.

The intermediate kinase activity also translated to weak Mek/Erk activity. The level of P-Mek in Braf^{+/Lox-L597V} MEFs increased following 24 hours of AdCre infection, and was stable for up to 96 hours following AdCre infection, and the levels were statistically different to the levels observed in Braf^{+/Lox-V600E} MEFs, but not Braf^{+/+} MEFs. The small increase in P-Mek levels was sufficient to

induce phosphorylation of Erk, which continued to increase over the time course to levels equivalent to $\text{Braf}^{+/Lox-V600E}$ MEFs. However, it failed to induce expression of the negative regulators Dusp6 and Spry2, and the levels remained statistically different to $\text{Braf}^{+/Lox-V600E}$, but not to $\text{Braf}^{+/+}$ MEFs.

The level of P-Erk in $\text{Braf}^{+/Lox-L597V}$ MEFs was similar to $\text{Braf}^{+/Lox-V600E}$ MEFs probably because P-Erk was negatively regulated in $\text{Braf}^{+/Lox-V600E}$ MEFs. The major MAPK negative regulators are the Dusps and Spry family of negative regulators. As shown by Tsavachidou et al (2004), knock-down of Spry2 did not restore P-Erk levels, whereas knock-down of Dusp6 did. Therefore P-Erk in $\text{Braf}^{+/Lox-V600E}$ MEFs is at least partly regulated by Dusp6.

Following AdCre infection, $\text{Braf}^{+/Lox-L597V}$ MEFs maintained a flat untransformed morphology as in $\text{Braf}^{+/+}$ MEFs, whereas $\text{Braf}^{+/LoxV600E}$ MEFs were highly transformed (Mercer *et al.*, 2005). This shows that the weak MAPK activity induced by ^{L597V}Braf was insufficient to induce cell transformation. The ability of ^{L597V}Braf to induce cell growth without contact inhibition was examined by focus forming assays. ^{L597V}BRAF overexpression in NIH 3T3 cells has been shown to induce foci formation, but the number of foci formed was not different to cells overexpressing ^{WT}BRAF (Sarkozy *et al.*, 2009). However, when ^{L597V}Braf was expressed endogenously, we failed to detect foci, unlike $\text{Braf}^{+/Lox-V600E}$ MEFs which proliferated without contact inhibition to form many foci. This suggests that the weak Mek/Erk activity induced by ^{L597V}Braf was insufficient for foci formation. ERK signalling is important for cell survival and proliferation, which are hallmarks of cancer. The ability of the weak Mek/Erk signalling to induce cell

proliferation was examined. There was some variation between MEFs of the same genotype, but the number of $\text{Braf}^{+/Lox-L597V}$ MEFs was consistently similar to counts of $\text{Braf}^{+/+}$ MEFs, and was much lower than $\text{Braf}^{+/Lox-V600E}$ MEFs. Therefore ^{L597V}Braf did not confer growth advantage. Overall, the data show that ^{L597V}Braf is not a driver oncogene.

It has been shown that wild-type MEFs enter a senescent stage until MEFs develop a mutation in $p19^{\text{ARF}}$ or $p53$, rendering the tumour suppressor inactive (Kamata *et al.*, 2010). However, $\text{Braf}^{+/Lox-D594A}$ MEFs were shown to enter early immortalisation through aneuploidy induced by Craf (Kamata *et al.*, 2010). The immortalisation profile of $\text{Braf}^{+/Lox-L597V}$ MEFs was examined by a 3T3 counting assay. There was some variation between MEFs of the same genotype, but overall $\text{Braf}^{+/Lox-L597V}$ MEFs failed to enter early immortalisation unlike $\text{Braf}^{+/Lox-V600E}$ MEFs. $\text{Braf}^{+/Lox-L597V}$ MEFs like $\text{Braf}^{+/+}$ MEFs lost $p19^{\text{ARF}}$ or $p53$ function following immortalisation. Therefore loss of tumour suppressor function is required for immortalisation of cells of these genotypes. Surprisingly, immortalised $\text{Braf}^{+/Lox-V600E}$ MEFs also lost $p19^{\text{ARF}}$ or $p53$ function, even though they underwent early immortalisation. Ras and Raf oncogenes have been shown previously to affect $p19^{\text{ARF}}$ and $p53$ biology which may contribute to the early immortalisation induced by these oncogenes (Palmero *et al.*, 1998). ^{V600E}Braf may also have the ability to enhance DNA damage and so promote mutations within these tumour suppressors, which would confer the early immortalisation phenotype.

Overall, ^{L597V}Braf is an intermediate kinase activity mutant and, does not confer a growth advantage, does not induce early immortalisation or induce foci formation. Therefore it does not have oncogenic-driving properties.

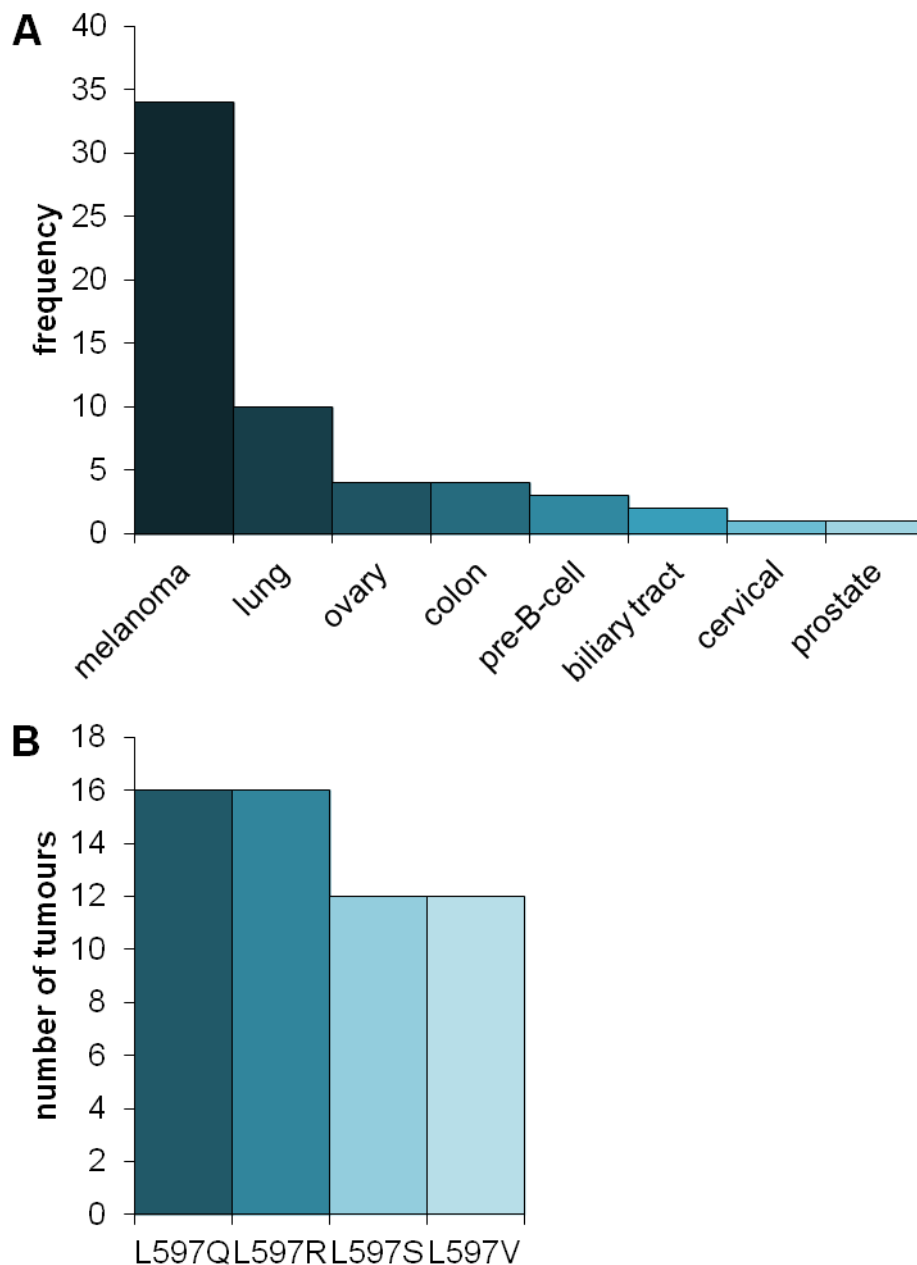
4. ^{L597V}Braf co-operates with ^{G12D}Kras

4.1. Introduction

To date, 59 cancer samples with a base-substitution at the Leu597 residue of *BRAF* (^{L597}*BRAF*) have been detected. The Leu597 residue has been found to be mutated to four different amino acids and the frequency of these is shown in Figure 4.1. A mutation at this residue has been found in a range of human cancers including lung, ovarian, colorectal, haematological, cervical, prostate and biliary tract cancers with melanoma being the most frequent (Figure 4.1). A leucine substitution to a valine at this residue has been shown to have intermediate kinase activity as mentioned in Chapter 1. However, in a separate study, the level of P-ERK in ^{L597Q}*BRAF*-transfected NIH 3T3 cells and in ^{L597S}*BRAF* melanoma cells was found to be similar to ^{V600E}*BRAF*-transfected cells (Hou *et al.*, 2007) or ^{V600E}*BRAF*-harbouring melanoma cells (Daniotti *et al.*, 2004) respectively. Overexpression of ^{L597Q}*BRAF* in NIH 3T3 cells induced foci formation (Hou *et al.*, 2007), and ^{L597S}*BRAF* melanoma cells also formed networks in matrigel (Zipser *et al.*, 2011). This has been taken to indicate that L597Q and L597S are high activity mutants but their intrinsic kinase activities have not yet been tested.

Figure 4.1 Mutations at Leu597 are found in a variety of cancers (data from <http://cancer.sanger.ac.uk/cosmic/gene/analysis?ln=BRAF>)

- A) Leu597 mutations have been identified in melanomas, lung, ovarian, colon, pre-B-cells, biliary tract, cervical and prostate cancers. The number of absolute samples for each given cancer is shown.
- B) Leu597 have been identified to be mutated to glutamine, arginine, serine and valine. The numbers mutated to each of four amino acids is shown.



4.1.1. Co-existence of *L597V* *BRAF* with mutations in other oncogenes in cancer samples

38 of the 59 cancer samples have also been tested for mutations in at least one other oncogene, of which 10 have been found to be accompanied with mutations in other driver oncogenes, including other mutations in *BRAF* (Table 4.1). Only one *L597Q* *BRAF*-harbouring melanoma was coincident with *V600E* *BRAF*. One *L597R* *BRAF*-harbouring ovarian cancer sample had *N857S* *ERBB2* and *S259A* *CRAF* mutations, and one melanoma sample had the *K601E* *BRAF* as well as *L597R* *BRAF*. One *L597S* *BRAF*-harbouring melanoma sample had a *G12S* *NRAS* mutation, a second sample had *PTEN* deletion, and another melanoma sample had a *R759Q* *FGFR2* mutation. Of the *L597V* *BRAF*-harbouring samples, one lung sample was coincident with *Q61R* *NRAS*, another lung sample had *Q61K* *NRAS*, *Q335H* *CRAF* and many other mutations including checkpoint regulators *E848Q* *ATM* and *V157F* *TP53* mutation, and two *L597V* *BRAF*-mutated melanomas also had the *V600E* *BRAF* mutation (<http://cancer.sanger.ac.uk/cosmic/gene/analysis?ln=BRAF>). This is a significant enrichment for coincident mutations and suggests that *L597V* *BRAF* acts in concert with other driver oncogenes in cancer development and progression. This is in contrast to *V600E* *BRAF*, which is coincident with other mutations, but is never co-expressed with *RAS* mutations in human cancers. *L597Q* *BRAF* and *L597S* *BRAF* mutations were documented to be high kinase activity mutants based on P-ERK levels they induced, but these mutants are also co-expressed with mutations in other oncogenes, albeit at lower incidences.

Table 4.1 Other mutations that co-exist with Leu597 mutations (data from <http://cancer.sanger.ac.uk/cosmic/gene/analysis?ln=BRAF>).

Leu597 mutation	tissue	Other mutations
L597Q	skin	<i>V600E</i> <i>BRAF</i>
L597R	ovary	<i>N857S</i> <i>ERBB</i> , <i>S259A</i> <i>CRAF</i>
L597R	skin	<i>K601E</i> <i>BRAF</i>
L597S	skin	<i>G12S</i> <i>NRAS</i>
L597S	skin	<i>PTEN</i> deletion
L597S	skin	<i>F759Q</i> <i>FGFR2</i>
L597V	lung	<i>Q61R</i> <i>NRAS</i>
L597V	lung	<i>Q61K</i> <i>NRAS</i> , <i>Q335H</i> <i>CRAF</i> , <i>E848Q</i> <i>ATM</i> , <i>V15F</i> <i>TP53</i>
L597V	skin	<i>V600E</i> <i>BRAF</i>
L597V	skin	<i>V600E</i> <i>BRAF</i>

Next-generation sequencing and comparative genomic hybridisation studies have revealed the extent of intra-tumour heterogeneity (Navin *et al.*, 2010; Shah *et al.*, 2009; Torres *et al.*, 2007), and comparison of the mutational status of primary and metastatic tumours support a branched evolutionary pattern of tumour growth and metastases (Shah *et al.*, 2009; Gerlinger *et al.*, 2012). Gerlinger *et al.* (2012) observed that only ~35% of mutations were observed in all regions of the tumours from the same patient, and some mutations were only found in the primary or metastatic tumour (Gerlinger *et al.*, 2012; Reviewed by Fisher *et al.*, 2013). These results suggest subclonal evolution. In Chapter 3 it was shown that ^{L597V}Braf did not have oncogenic-driving properties. However, mutations at this residue appear to be too common for a passenger mutation in human cancer, and in Chapter 3, it has been shown that ^{L597V}BRAF had some effect on MAPK pathway, albeit weakly. Since ^{L597V}BRAF is frequently coincident with other mutations, the effect of ^{L597V}BRAF on another common oncogene was studied here to assess if it is a “cooperating mutation”.

4.1.2. ^{G12D}KRAS

KRAS mutations are more frequently found than mutations in NRAS or HRAS. G12D is the most frequently observed mutation in KRAS (<http://cancer.sanger.ac.uk/cosmic/gene/analysis?ln=BRAF>). The change from glycine to an aspartate residue results in a reduction of the affinity of RAS for GTP, but also a reduction in the intrinsic GTPase activity, and the mutation renders the protein refractory to GTPase activation by GAP binding (Al-Mulla *et al.*, 1999). The mutant accumulates in the GTP-bound active form (Dail *et al.*,

2010; Shields *et al.*, 2000), signalling mainly through the downstream RAF/MEK/ERK and PI3K pathways.

Knock-in mutations in the *Ras* genes in mice were previously generated in the Tyler Jacks lab, including Cre-controlled *Kras*^{+/G12D} mice which have been mentioned in Section 1.8.2, and *Nras*^{+/G12D} mice. *Nras*^{+/LSL-G12D} mice were generated in a similar way to *Kras*^{+/Lox-G12D} mice. *G12D**Nras* was embryonic lethal, but somatic expression of heterozygous *Nras* has not been reported to induce any change in phenotype. However, homozygous expression of *G12D**Nras* was examined to induce excessive proliferation of myeloid progenitors and symptoms of myeloproliferative disease (Wang *et al.*, 2011).

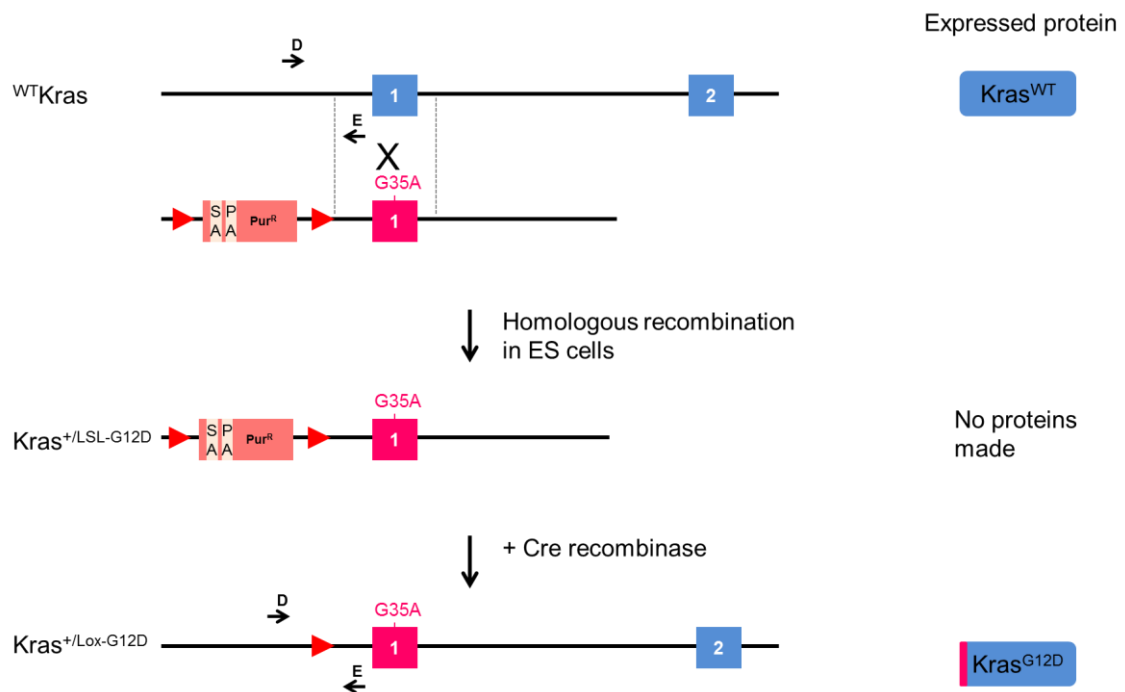
4.1.3. Generation of *Kras*^{+/Lox-G12D} mice

Cre-LoxP technology was used to produce mice that conditionally express *G12D**Kras* in a similar way to *Braf*^{+/Lox-L597V} mice. Mice were generated in the Tyler Jacks lab. *Kras*^{+/LSL-G12D} mice were generated by insertion of a Lox-Stop-Lox cassette containing the splice acceptor, polyadenylation and the selection marker *Pur*^R. The targeting vector contained the LSL cassette to the 3' end of exon 1 containing the G35A mutation, and was flanked by homologous regions of the introns 3' and 5' to exon 1, which targeted the vector to the endogenous *Kras* gene (Figure 4.2).

Figure 4.2 Conditional knock-in *Kras*^{+/LSL-G12D} mouse model

Kras^{+/LSL-G12D} mice were generated from ES cells that contained the modified allele. The targeting vector contained the LSL cassette adjacent to the 3' end of exon 1 containing the G35A mutation, and was flanked by homologous regions of the introns 3' and 5' to exon 1, which targeted the vector to the *Kras* gene. The LSL cassette contained a splice acceptor (SA), polyadenylation (PA) and Puromycin resistance gene (Pur^R).

In the absence of Cre recombinase, the polyA-tail within the LSL cassette halts transcription, and *Kras*^{WT} is transcribed by the other allele. In the presence of Cre recombinase, the LoxP sites come together and, following recombination, the LSL cassette is released, and *Kras*^{G12D} is expressed. (D and E) genotyping primers and their orientation are shown.



In the absence of Cre recombinase, the polyA-tail within the LSL cassette halts transcription, and ^{WT}Kras is transcribed by the other allele. In the presence of Cre recombinase, the LoxP sites come together and, following recombination, the LSL cassette is released, transcription is not stopped and ^{G12D}Kras is expressed.

4.2. Aims

^{L597}BRAF mutations co-exist with mutations in other oncogenes in human cancers. Therefore ^{L597V}BRAF may synergise with other oncogenes in the progression of cancer. BRAF signals exclusively through the MEK/ERK pathway, and ^{L597}BRAF mutations have been found to be co-expressed with NRAS mutations in human cancers, including ^{Q61K}NRAS and ^{Q61R}NRAS, suggesting that ^{L597}BRAF may direct RAS signalling through the MEK/ERK pathway. The aim of this chapter is to examine the effects of combining ^{L597V}BRAF with oncogenic RAS and ^{G12D}KRAS was examined here. The effect of ^{L597V}Braf on ^{G12D}Kras with respect to cell morphology, foci formation, kinase activity, cell growth and immortalisation was studied.

4.3. Results

4.3.1. Preparation of double mutant MEFs

Three cancer samples have been identified to contain ^{L597V}BRAF and ^{Q61K}NRAS or ^{Q61R}NRAS mutations. Nras-mutant mouse models were not available in the lab and consequently, the ^{Kras^{+/G12D}} mouse model (Tuveson *et al.*, 2004) was utilised. Leu597 mutations were frequently co-expressed with V600E mutations, but the effect of ^{L597V}Braf in combination with ^{V600E}Braf was not examined. This

was due to previous work within the lab showing that ^{L597V}Braf and ^{V600E}Braf homozygous mice died in utero, which will be discussed in Chapter 7.

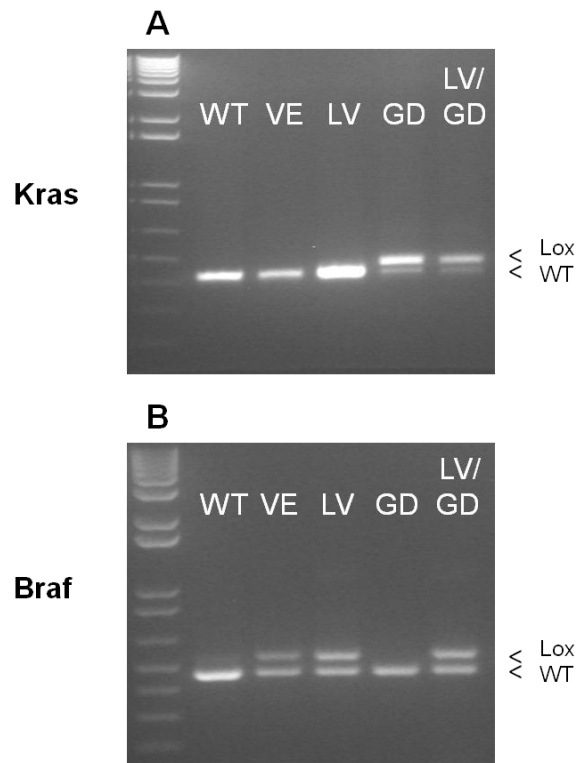
To examine the co-operation of ^{L597V}Braf with ^{G12D}Kras, primary MEFs were isolated from mouse embryos at E13.5 resulting from intercrosses between *Braf*^{+/^{LSL-L597V} mice and *Kras*^{+/^{LSL-G12D} mice. MEFs were isolated and genotyped as described in Section 2.1.8. Recombination was induced by AdCre infection as in Chapter 3. To test whether infection induced recombination, primary MEFs were infected with AdCre for 72 hours, DNA was isolated and analysed by PCR to test for the *Braf* and *Kras* recombined alleles using the primers indicated in Figure 3.1 and Figure 4.2 respectively.}}

PCR analysis of AdCre-infected *Braf*^{+/+}, *Braf*^{+/^{LSL-V600E} and *Braf*^{+/^{LSL-L597V} MEFs only showed the presence of a ^{WT}*Kras* band (Figure 4.3A). Analysis of *Kras*^{+/^{LSL-G12D} and double mutant (*Braf*^{+/^{Lox-L597V}; *Kras*^{+/^{Lox-G12D}) MEFs showed the presence of the ^{WT}*Kras* band and the Lox-recombined band. PCR analysis of AdCre-infected *Braf*^{+/+} and *Kras*^{+/^{LSL-G12D} MEFs only showed the presence of a ^{WT}*Braf* band (Figure 4.3B), while analysis of AdCre-infected *Braf*^{+/^{LSL-V600E}, *Braf*^{+/^{LSL-L597V} and double mutant MEFs displayed ^{WT}*Braf* and the Lox-recombined band. As in Chapter 3, the LSL band was lost (data not shown), indicating complete recombination. Thus, the recombination of *Kras* and *Braf* alleles occurred in double mutant MEFs following AdCre infection after 72 hours.}}}}}}}}

Figure 4.3. *Kras* recombination occurs after 72 hours of AdCre infection

Braf^{+/+} (WT), *Braf*^{f/+LSL-V600E} (VE), *Braf*^{f/+LSL-L597V} (LV), *Kras*^{+/LSL-G12D} (GD) and double mutant (LV/GD) MEFs were infected with AdCre for 72 hours. Genomic DNA was isolated and analysed by PCR for:

- A) *Kras* LSL recombination PCR amplification using primers D and E.
 B) *Braf* LSL recombination PCR amplification using primers A-C.



4.3.2. ^{L597V}Braf induces further transformation of ^{+G12D}Kras MEFs

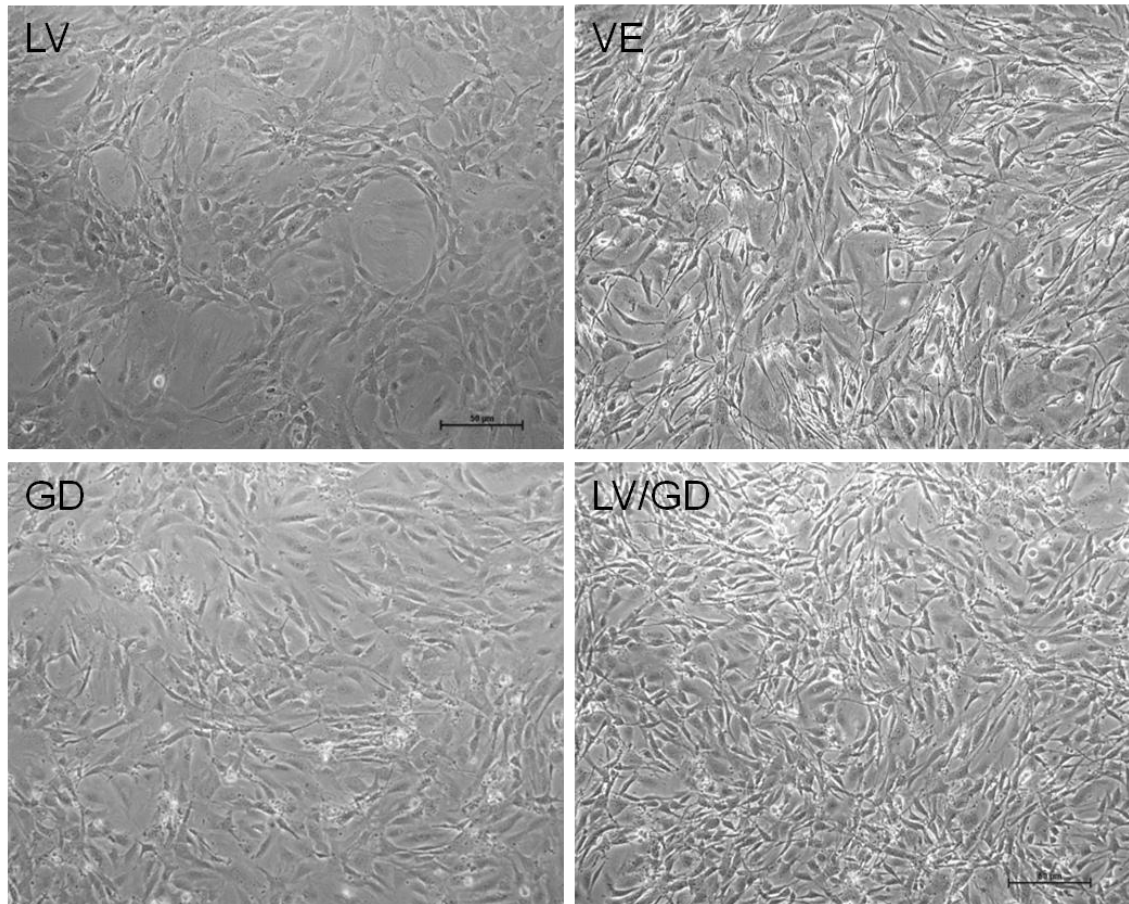
Tuveson et al (2004) have shown that ^{+Lox-G12D}Kras MEFs display morphological transformation 2-3 days following AdCre infection. In Chapter 3 it was shown that ^{V600E}Braf but not ^{L597V}Braf induces morphological transformation of MEFs. It would therefore be interesting to assess the morphological changes in MEFs expressing both ^{L597V}Braf and ^{G12D}Kras.

Primary double mutant MEFs were seeded at 3×10^5 MEFs per 6cm dish. 24 hours later, MEFs were infected with AdCre to induce recombination and expression of ^{L597V}Braf and ^{G12D}Kras. MEFs were replated every 3 days and allowed to immortalise. MEFs were photographed at ~90% confluency (Figure 4.4). ^{Braf^{+Lox-L597V}}, ^{Braf^{+Lox-V600E}} and ^{Kras^{+Lox-G12D}} MEFs were included for comparison.

As shown in Chapter 3, ^{Braf^{+Lox-V600E}} MEFs exhibited a transformed morphology, but the morphology of ^{Braf^{+Lox-L597V}} MEFs were unchanged following AdCre infection. ^{Kras^{+Lox-G12D}} MEFs appeared more transformed than ^{Braf^{+Lox-L597V}} MEFs, but considerably less transformed than ^{Braf^{+Lox-V600E}} MEFs in terms of refractility and shape changes (Figure 4.4). MEFs that expressed both ^{L597V}Braf and ^{G12D}Kras appeared to be more transformed than ^{Kras^{+Lox-G12D}} MEFs and appeared more similar to ^{Braf^{+Lox-V600E}} MEFs. This suggests that ^{L597V}Braf may co-operate with ^{G12D}Kras to induce morphological transformation.

Figure 4.4. ^{L597V}Braf co-operates with ^{G12D}Kras to induce morphological transformation

$\text{Braf}^{+/LSL-L597V}$ (LV), $\text{Braf}^{+/LSL-V600E}$ (VE), $\text{Kras}^{+/LSL-G12D}$ (GD) and double mutant (LV/GD) MEFs were infected with AdCre to induce recombination and expression of the mutant protein. MEFs were photographed after immortalisation.



4.3.3. ^{L597V}Braf enhances ^{G12D}Kras-induced Mek/Erk activation

The level of MEK/ERK activation of ^{L597V}BRAF has been shown to be slightly elevated in comparison with ^{WT}BRAF when overexpressed in COS cells (Wan *et al.*, 2004) and HEK 293^T cells (Section 3.3.1), and when expressed endogenously in MEFs (Section 3.3.6). Oncogenic RAS has previously been shown to induce high ERK kinase activity and exhibit high P-ERK levels when transfected into COS cells (Wan *et al.*, 2004). It was important to assess the effect of ^{L597V}Braf on signalling through the ERK pathway, in the context of Ras transformation.

To test activation of the Mek/Erk pathway in MEFs expressing ^{L597V}Braf and ^{G12D}Kras, primary Braf^{f+/LSL-L597V}, Kras^{+/-LSL-G12D} and double mutant MEFs were seeded at 2x10⁵ MEFs per 6cm plate. 24 hours later, MEFs were infected with AdCre for 72 hours. Braf^{f+/+} and Braf^{f+/LSL-V600E} MEFs were included for comparison. Protein lysates were analysed by western blotting (Figure 4.5).

As shown in Section 3.3.6, the levels of P-Mek, P-Erk, Dusp6 and Spry2 in Braf^{f+/Lox-V600E} MEFs were significantly higher than in Braf^{f+/+} and Braf^{f+/Lox-L597V} MEFs (Figure 4.5). As expected, the levels of P-Mek and P-Erk of Braf^{f+/Lox-L597V} MEFs were in between those in Braf^{f+/+} and Braf^{f+/Lox-V600E} MEFs.

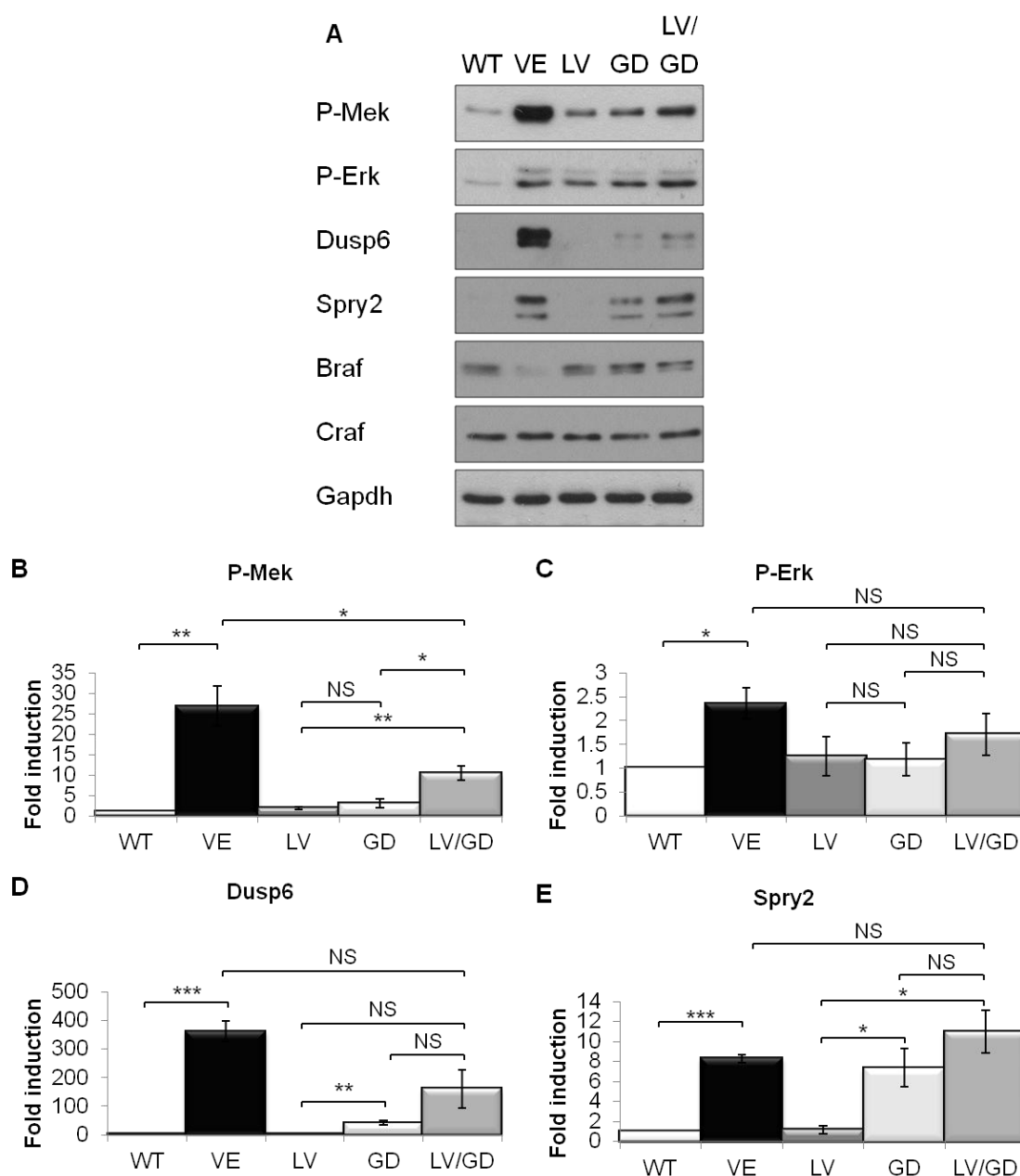
The level of P-Mek in Kras^{+/-Lox-G12D} MEFs was increased by ~3-fold in comparison with Braf^{f+/+}, and was slightly higher than in Braf^{f+/Lox-L597V} MEFs, but was significantly lower than in Braf^{f+/Lox-V600E} MEFs (Figure 4.5). However, this small increase in P-Mek levels did not translate to higher P-Erk levels. The P-

Figure 4.5. *L597V* *Braf* cooperates with *G12D* *Ras* to induce Mek/Erk activity

Braf^{+/+} (WT), *Braf*^{+/LSL-V600E} (VE), *Braf*^{+/LSL-L597V} (LV), *Kras*^{+/LSL-G12D} (GD) and double mutant (LV/GD) MEFs were infected with AdCre for 72 hours to allow recombination and expression of the mutant protein. Western blots were analysed with the antibodies indicated.

B) Protein expression was analysed by western blotting. Shown are representative western blots (n=3).

B-E) Bar charts showing the levels of P-Mek, P-Erk, Dusp6 and Spry2 quantitated using ImageJ and normalised with respect to Gapdh. The fold changes compared with cells expressing ^{WT}*Braf* are shown. Bars indicate mean of 3 experiments, error bars indicate standard error. (*) *P*<0.05 (**) *P*<0.01 (***) *P*<0.001.



Erk levels in $Kras^{+/Lox-G12D}$ was approximately the same as in $Braf^{+/+}$ and $Braf^{+/Lox-L597V}$ MEFs. This was probably due to upregulation of Dusp6 in the Ras-mutant cells.

The level of P-Mek in double mutant MEFs was significantly higher than in $Kras^{+/Lox-G12D}$ and $Braf^{+/Lox/L597V}$ MEFs, but lower than in $Braf^{+/Lox-V600E}$ MEFs. However, the level of P-Erk was only slightly elevated and was not statistically different because of the induction of Dusp6. Overall, these results suggest $L597V$ Braf and $G12D$ Kras cooperate to induce higher levels of signalling towards the MAPK pathway and to a greater extent than $G12D$ Kras alone, but not to the levels induced by $V600E$ Braf.

4.3.4. $L597V$ Braf slows the growth rate of $Kras^{+/Lox-G12D}$ MEFs

It has been shown that $Kras^{+/Lox-G12D}$ MEFs outgrow $Kras^{+/+}$ MEFs (Tuveson *et al.*, 2004), and in Chapter 3 it was shown that $Braf^{+/Lox-V600E}$ MEFs grow at a higher rate than $Braf^{+/+}$ and $Braf^{+/Lox-L597V}$ MEFs (Chapter 3, Figure 3.11). It was therefore important to assess whether the addition of $L597V$ Braf would affect the growth of $Kras^{+/Lox-G12D}$ MEFs.

Primary double mutant MEFs were seeded at 3×10^5 MEFs per 6cm plate. 24 hours later, MEFs were infected with AdCre for 72 hours to allow full recombination, and then plated at 3×10^4 cells per 12-well plate. The media was replenished every 2 days and the number of cells was counted in triplicate every two days for eight days (Figure 4.6). $Braf^{+/+}$, $Braf^{+/LSL-L597V}$, $Braf^{+/LSL-V600E}$ and $Kras^{+/LSL-G12D}$ MEFs infected with AdCre were included for comparison. As

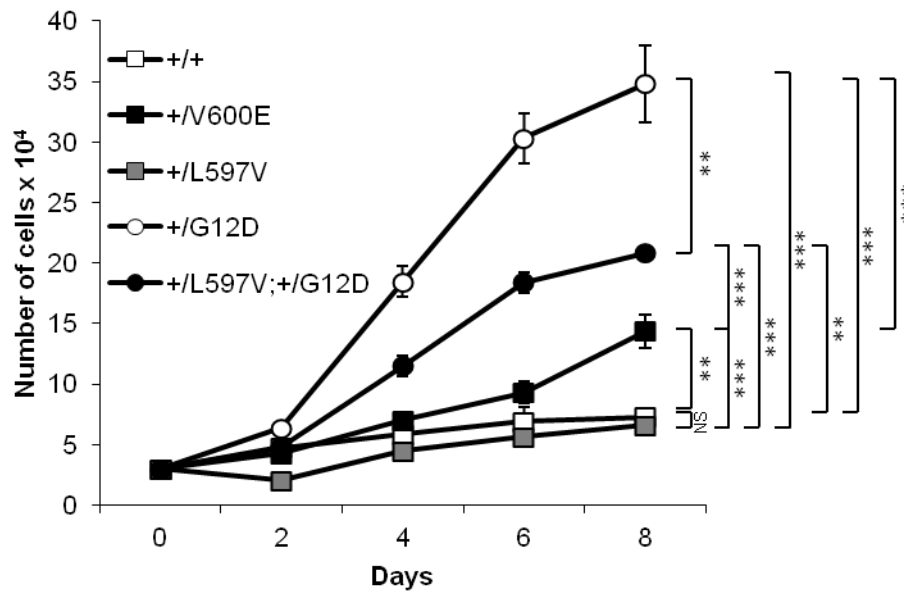
in Chapter 3, the results presented are of a single line for each genotype counted in triplicate (Figure 4.6). This is representative of three experiments using different MEF lines.

As expected, the growth of $\text{Braf}^{+/Lox-V600E}$ MEFs was significantly greater than $\text{Braf}^{+/+}$ and $\text{Braf}^{+/Lox-L597V}$ MEFs. These cells grew at a slower rate than $\text{Kras}^{+/Lox-G12D}$ and double mutant MEFs. Thus G12D Kras confers a growth advantage above V600E Braf . However, the addition of L597V Braf to $\text{Kras}^{+/Lox-G12D}$ MEFs slowed down growth to levels in between $\text{Braf}^{+/Lox-V600E}$ and $\text{Kras}^{+/Lox-G12D}$ MEFs.

The slower growth of $\text{Braf}^{+/Lox-V600E}$ and double mutant MEFs in comparison with $\text{Kras}^{+/Lox-G12D}$ MEFs might be due to excessively high MAPK signalling which has been shown to be suppressive of cell growth through induction of p21^{Cip1} and inhibition of Cyclin-CDK2 complexes (Woods *et al.*, 1997). At low levels of MAPK signalling, Cyclin D and Cyclin E expression were found to be induced with a reduction in p27^{Kip1} , which resulted in cell proliferation, but at high levels, p21^{Cip1} was also induced, leading to cell cycle arrest (Woods *et al.*, 1997). D-Cyclins form a complex with CDK4 or CDK6, and the complex phosphorylates pRB and pRB-like p107 and p130 proteins, alleviating the suppression of E2F transcription factors or activating E2F transcription factors that become available to induce transcription of the target genes required for entry to S phase (Trimarchi & Lees, 2002; Sherr & Roberts, 2004). The complexes also sequester p21^{Cip1} and p27^{Kip1} , leading to the activation of CDK2-containing complexes (Sherr & Roberts, 2004).

Figure 4.6. *L597V* *Braf* slows the growth rate of *Kras*^{+/-Lox-G12D} MEFs

Braf^{+/+} (WT), *Braf*^{+/-LSL-V600E} (VE), *Braf*^{+/-LSL-L597V} (LV), *Kras*^{+/-LSL-G12D} (GD) and double mutant (LV/GD) MEFs were infected with AdCre for 72 hours to allow full recombination. After this, MEFs were plated at 3×10^4 cells per 12-well plate, and the number of cells was counted in triplicate every two days for eight days. Shown are representative counts in triplicates from $n=3$, error bars indicate standard deviation between triplicates. (NS) Not significant, (*) $P < 0.05$, (**) $P < 0.01$, (***) $P < 0.001$.



To examine whether the high MAPK activity of double mutant and other MEFs suppressed cell proliferation via alterations in cell cycle proteins, lysates were generated and western blotted for p21^{Cip1} and D-Type Cyclins (Figure 4.7). For comparison purposes, *Braf*^{+/+} and *Braf*^{+/*LSL*-L597V} MEFs were included. Data are presented for two different MEF lines of each genotype.

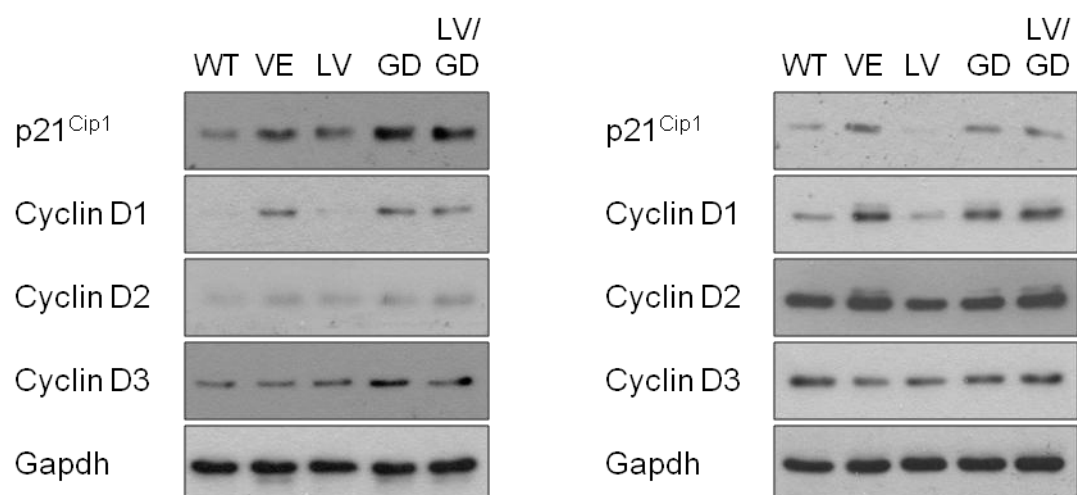
The levels of p21^{Cip1}, Cyclin D1 and Cyclin D2 were consistently higher in *Braf*^{+/*Lox*-V600E}, *Kras*^{+/*Lox*-G12D} and double mutant MEFs than *Braf*^{+/+} and *Braf*^{+/*Lox*-L597V} MEFs (Figure 4.7). The level of Cyclin D3 was slightly higher in *Kras*^{+/*Lox*-G12D} MEFs in the first set, but this was not reproducible in the second set. Overall, it is clear that *Kras*^{+/*Lox*-G12D} and double mutant MEFs proliferate at a higher rate than *Braf*^{+/*Lox*-V600E} MEFs, but it is difficult to conclude whether the difference is related to MAPK output and regulation of the expression of D-Type Cyclins and p21^{Cip1}.

4.3.5. *L597V* *Braf* does not affect immortalisation profiles of *Kras*^{+/*Lox*-G12D} MEFs

It has been shown that MEFs expressing *G12D* *Kras* undergo early immortalisation without loss of p19^{ARF} or p53 function (Tuveson *et al.*, 2004). It was therefore important to assess whether *L597V* *Braf* changes the immortalisation profile of *Kras*^{+/*Lox*-G12D} MEFs.

Figure 4.7. p21^{Cip1} and D-Type Cyclin expression in MEFs

Braf^{+/+} (WT), *Braf*^{+/LSL-V600E} (VE), *Braf*^{+/LSL-L597V} (LV), *Kras*^{+/LSL-G12D} (GD) and double mutant (LV/GD) MEFs were infected with AdCre for 72 hours. Western blots were analysed with the antibodies indicated (n=2). Shown are results for two different primary MEF lines of each genotype.

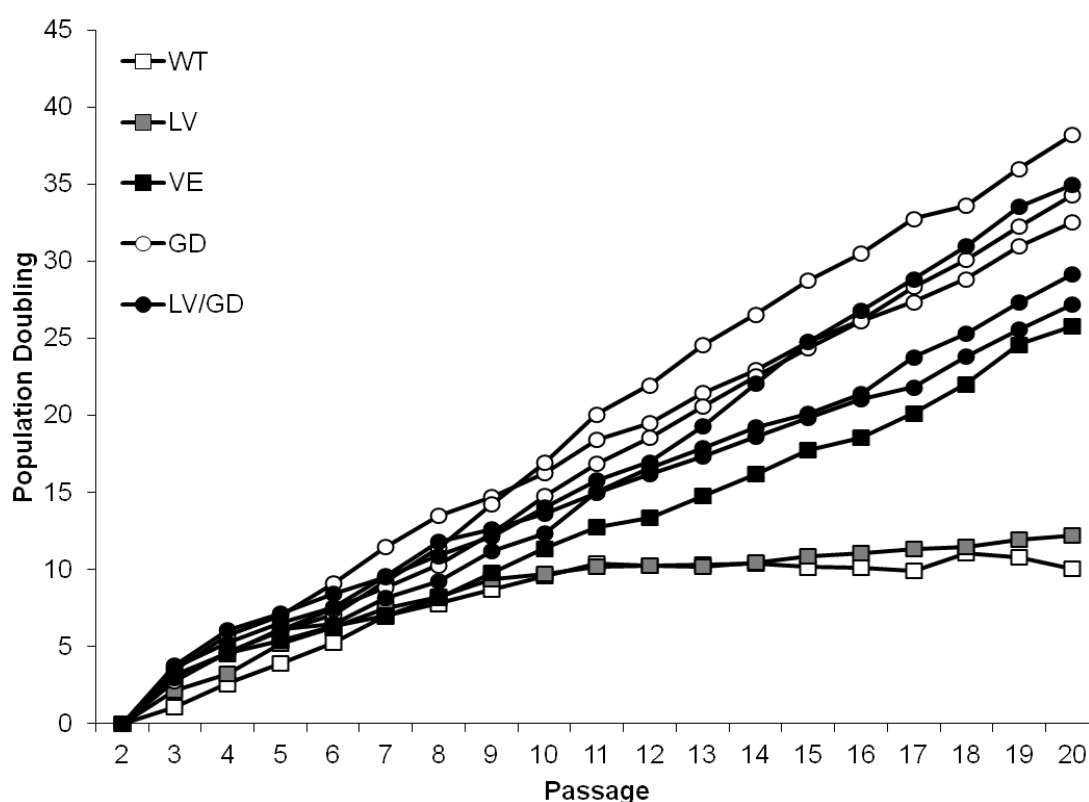


Primary Kras^{+/-LSL-G12D} and double mutant MEFs were seeded at 2×10^5 MEFs per 6cm plate. 24 hours later, MEFs were infected with AdCre for 24 hours and 3×10^5 MEFs were replated, and this was repeated for a total of 20 passages. The number of MEFs was counted every 3 days and 3×10^5 MEFs replated. The number of population doublings were calculated at each passage and a growth curve was produced (Figure 4.8). As controls, Braf^{+/+}, Braf^{+/-LSL-V600E} and Braf^{+/-LSL-L597V} MEFs were infected with AdCre, and primary MEFs were also uninfected (data not shown) or infected with Adβgal (data not shown).

The immortalisation profiles of Kras^{+/-Lox-G12D} and double mutant MEFs was compared with Braf^{+/-Lox-V600E} MEFs (Figure 4.8). As in Chapter 3, some differences in growth between MEFs of the same genotype were observed. However, Kras^{+/-Lox-G12D} and double mutant MEFs reproducibly grew at a higher rate than Braf^{+/-Lox-V600E} MEFs (Figure 4.8) and, as shown by Tuveson and colleagues (2004), Kras^{+/-Lox-G12D} MEFs did not enter senescence, immortalising very early. Two out of three double mutant MEF lines grew at a slower rate than Kras^{+/-Lox-G12D} MEFs, and the third grew at a slower rate than Kras^{+/-Lox-G12D} MEFs at early passages until passage 14. These results show that L597V Braf in combination with G12D Kras does not affect early immortalisation but slows down the growth rate of Kras^{+/-Lox-G12D} MEFs somewhat as shown in Section 4.3.4.

Figure 4.8. ^{L597V} Braf does not affect immortalisation profile of Kras^{+/-Lox-G12D} MEFs

Braf^{+/+} (WT), Braf^{+/LSL-L597V} (LV), Braf^{+/LSL-V600E} (VE), Kras^{+/-LSL-G12D} (GD) and double mutant (LV/GD) MEFs were infected with AdCre for 24 hours and 3x10⁵ MEFs were replated. The number of MEFs was counted every 3 days and 3x10⁵ MEFs replated to obtain the number of population doublings at every passage. Shown are three separate lines of Kras^{+/-LSL-G12D} (GD) and double mutant (LV/GD) MEFs. For comparison purposes, one representative Braf^{+/+} (WT), Braf^{+/LSL-L597V} (LV) and Braf^{+/LSL-V600E} (VE) MEF line were included.



4.3.6. Transcriptome profiling

It is clear from the above data that *L597V* *Braf* affects *G12D* *Kras*-induced MAPK signalling. It may also affect *G12D* *Kras* signalling through alternative pathways as well. To examine the gene changes induced by each mutation, immortalised *Braf*^{+/+}, *Braf*^{+/Lox-V600E}, *Braf*^{+/Lox-L597V}, *Kras*^{+/Lox-G12D} and double mutant MEFs were subjected to microarray analysis. MEFs were plated to reach a confluency of ~80% in 48 hours. RNA was extracted from three MEF lines of each genotype and quantitated using a Bioanalyser 2100 (Agilent). RNA labelling and hybridization to Affymetrix GeneChip Mouse Gene 1.0ST arrays were performed by the Microarray facility at the Gladstone Institute using standard protocols

(<http://www.gladstone.ucsf.edu/gladstone/site/genomicscore/section/380>). Data was subjected to Bioinformatics analysis by Alexander Williams at the Gladstone Institute. Microarray data was normalised and analysis of variance (ANOVA) with a 0.01 false discovery rate (FDR) threshold was used to identify genes significantly altered in comparison with *Braf*^{+/+} controls to produce a heat map (Figure 4.9).

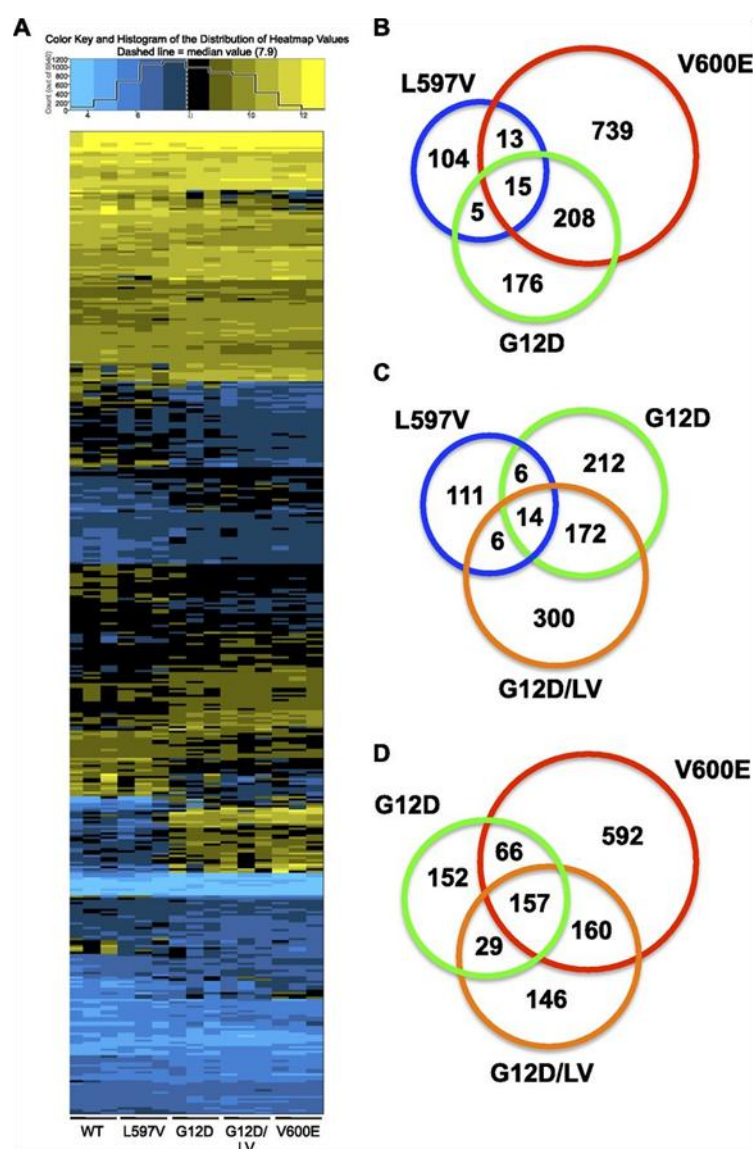
More genes were upregulated than downregulated in all of the examined genotypes (Figure 4.9A). The number of gene changes observed in *Braf*^{+/Lox-L597V} was 137, 404 in *Kras*^{+/Lox-G12D}, 492 in double mutant and 975 in *Braf*^{+/Lox-V600E} MEFs. This suggests that *L597V* *Braf* has the weakest molecular effect, while *V600E* *Braf* had the highest effect, and *L597V* *Braf* in combination with *G12D* *Kras* induced a stronger change than *G12D* *Kras* alone. Since *V600E* *BRAF* had been shown to signal exclusively through the ERK1/2 pathway (Packer *et al.*, 2009),

Figure 4.9 Microarray analysis

Immortalised *Braf*^{+/+}, *Braf*^{+/Lox-V600E} (V600E), *Braf*^{+/Lox-L597V} (L597V), *Kras*^{+/Lox-G12D} (G12D) and double mutant (G12D/LV) MEFs were plated to reach a confluency of ~80% in 48 hours. RNA was extracted and quantitated. RNA labelling and hybridization to Affymetrix GeneChip Mouse Gene 1.0ST arrays were performed by the Microarray facility at the Gladstone Institute (<http://www.gladstone.ucsf.edu/gladstone/site/genomicscore/section/380>). Microarray data was normalised and analysis of variance (ANOVA) with a 0.01 false discovery rate (FDR) threshold was used to identify genes significantly altered in comparison with *Braf*^{+/+} controls.

A) Heat map of 436 genes significantly differentially expressed in double mutant MEFs compared with *Braf*^{+/+} MEFs at a cutoff raw P-value of <0.01 in each of the biological samples. Values were generated through Affymetrix RMA normalisation of all the arrays and the absolute expression is represented. The scale is log₂, and the median expression level for the whole genome is ~7.9. Genes are ordered by magnitude of differential expression.

B-D) Venn diagrams of numbers of shared genes differentially expressed in each genotype compared with *Braf*^{+/+} MEFs at a cutoff raw P-value of <0.01.



it is thought that the 975 gene changes induced by ^{V600E}Braf were entirely induced through MAPK signalling, although this would need to be formerly proven for our cells using BRAF or MEK inhibitors.

^{Braf^{+/Lox-L597V}} MEFs only shared 28 gene changes with ^{Braf^{+/Lox-V600E}} MEFs. This result shows that ^{L597V}Braf induces little MAPK activity. ^{Kras^{+/Lox-G12D}} MEFs shared 223 gene changes with ^{Braf^{+/Lox-V600E}} MEFs, but also had 181 gene changes that were not shared with ^{Braf^{+/Lox-V600E}} MEFs (Figure 4.9B). Thus ^{G12D}Kras induces significant signalling through the MAPK pathway, but about half of ^{G12D}Kras activity induced Mek-independent pathways. Double mutant MEFs shared the most gene changes in common with ^{Braf^{+/Lox-V600E}} MEFs, which was more than ^{Braf^{+/Lox-L597V}} and ^{Kras^{+/Lox-G12D}} MEFs put together (Figure 4.9D). This suggests that ^{L597V}Braf may subvert some of the Ras signalling through the MAPK pathway. But there were also 175 gene changes, constituting ~30% of the total gene changes that were not shared with ^{Braf^{+/Lox-V600E}} MEFs. Therefore ^{L597V}Braf may act to induce gene changes in Mek/Erk-dependent and independent signalling pathways. One possibility is through hyperactivation of CraF, which has been previously shown to activate MAPK-dependent and MAPK-independent pathways (Broustas *et al.*, 2002; Ehrenreiter *et al.*, 2005; Jesenberger *et al.*, 2001; Chen *et al.*, 2001; Nantel *et al.*, 1999; Wang *et al.*, 1996). 300 gene changes that were not observed in ^{Braf^{+/Lox-L597V}} or ^{Kras^{+/Lox-G12D}} MEFs were observed in double mutant MEFs, constituting ~60% of the gene changes in double mutants. Thus, when the two mutations were combined, additional molecular changes occurred (Figure 4.9C).

4.4. Conclusion

L597V BRAF appears to be enriched in the coexistence of other oncogenic mutations in human cancer samples, including mutations in NRAS. However, only one BRAF^{+/L597V} human cancer cell line is available, and this cell line also contains many other mutations, and proved impossible to grow in our lab. Therefore a conditional mouse knock-in model was used. The cooperation of *L597V* Braf with *G12D* Kras rather than a Nras-mutant was examined due to the availability of this model in our lab. Recombination and expression of *G12D* Kras was observed after 72 hours of AdCre infection in Kras^{+/LSL-G12D} and double mutant MEFs. Loss of the LSL band was also observed (data not shown), indicating total recombination. Excision of the LSL cassette 72 hours after AdCre infection has been shown previously by southern blotting (Tuveson *et al.*, 2004). Recombination and expression of *L597V* Braf was also observed after 72 hours of AdCre infection in Braf^{+/LSL-L597V} and double mutant MEFs.

The cell morphology of Braf^{+/Lox-L597V} was shown to be the same as Braf^{+/+} MEFs in Chapter 3. Morphological transformation of Kras^{+/Lox-G12D} MEFs has been previously shown (Tuveson *et al.*, 2004). In this Chapter, Kras^{+/Lox-G12D} MEFs were shown to be less transformed than Braf^{+/Lox-V600E} MEFs, in that MEFs were less refractile and less bright, but were more morphologically transformed than Braf^{+/Lox-L597V} MEFs. Double mutant MEFs were more transformed than Kras^{+/Lox-G12D} MEFs, but less transformed than Braf^{+/Lox-V600E} MEFs. This suggests that *L597V* Braf may enhance *G12D* Kras-induced cell transformation.

The stronger morphological transformation of double mutant MEFs could be as a result of increased MAPK signalling by *G12D* *Kras* directed by *L597V* *Braf*. Unsurprisingly, the level of P-Mek in *Kras*^{+/-Lox-G12D} MEFs was slightly higher than in *Braf*^{+/-+} and *Braf*^{+/-Lox-L597V} MEFs, but was significantly lower than in *Braf*^{+/-Lox-V600E} MEFs. The level of P-Mek in double mutant MEFs was higher than in *Kras*^{+/-Lox-G12D} MEFs and more than single mutants put together, but lower than in *Braf*^{+/-Lox-V600E} MEFs indicating the additive effect of *L597V* *Braf* and *G12D* *Kras*.

Kras^{+/-Lox-G12D} MEFs grew at a high rate as shown previously (Tuveson *et al.*, 2004). However, the addition of *L597V* *Braf* slowed down the growth rate. *Braf*^{+/-Lox-V600E} MEFs grew at a lower rate than *Kras*^{+/-Lox-G12D} and double mutant MEFs. This prompted a suggestion that the high MAPK signalling might slow down the growth rate of MEFs. Previous studies have shown that high MAPK signalling is suppressive of cell growth through induction of p21^{Cip1} and inhibition of Cyclin-CDK2 complexes (Woods *et al.*, 1997), leading to cell cycle arrest in mouse cells (Woods *et al.*, 1997; Pumiglia & Decker, 1997a; Pumiglia & Decker, 1997b; Sewing *et al.*, 1997). However, western blotting of the D-type Cyclins and p21^{Cip1} levels was inconclusive with regard to whether there is a similar mechanism operating here.

Kras^{+/-Lox-G12D} and double mutant MEFs all underwent early immortalisation and grew at a higher rate than *Braf*^{+/-Lox-V600E} MEFs and, as shown by Tuveson and colleagues (2004), *Kras*^{+/-Lox-G12D} MEFs did not enter senescence, immortalising very early. Double mutant MEFs grew at a slower rate than *Kras*^{+/-Lox-G12D} MEFs after immortalisation but the profile of immortalisation was not affected.

Microarray analysis showed that the most number of gene changes in comparison to $\text{Braf}^{+/+}$ MEFs was found in $\text{Braf}^{+/Lox-V600E}$ MEFs, followed by double mutant, $\text{Kras}^{+/Lox-G12D}$ and $\text{Braf}^{+/Lox-L597V}$ MEFs. $\text{Braf}^{+/Lox-L597V}$ MEFs had very few gene changes, and only ~20% of these gene changes were shared with $\text{Braf}^{+/Lox-V600E}$ MEFs. This confirms that ^{L597V}Braf has very weak biological effect.

Double mutant MEFs shared the most number of gene changes with $\text{Braf}^{+/Lox-V600E}$ MEFs, which was more than the total number of gene changes shared between $\text{Braf}^{+/Lox-V600E}$ MEFs and $\text{Braf}^{+/Lox-L597V}$ and $\text{Kras}^{+/Lox-G12D}$ MEFs put together. This suggests that ^{L597V}Braf has an added effect on directing Kras-signalling through the MAPK pathway. Double mutant MEFs had gene changes that were not observed in $\text{Braf}^{+/Lox-L597V}$, $\text{Kras}^{+/Lox-G12D}$ or $\text{Braf}^{+/Lox-V600E}$ MEFs. Possibly, when the two mutations are combined, ^{L597V}Braf may act to induce further gene changes in Mek/Erk-dependent as well as independent signalling pathways. One possibility is through hyperactivation of Cra, which is known to have Mek/Erk-independent effects (Broustas *et al.*, 2002; Ehrenreiter *et al.*, 2005; Jesenberger *et al.*, 2001; Chen *et al.*, 2001; Nantel *et al.*, 1999; Wang *et al.*, 1996). This is examined further in Chapter 5.

Overall, ^{L597V}Braf is not a driver mutation possibly owing to its weak Mek/Erk activity, but significantly enhances ^{G12D}Kras-induced MAPK signalling, as judged by increased levels of P-MEK but the levels of P-ERK were unchanged due to

negative regulation, increased ERK1/2-dependent gene changes, and increased morphological transformation. This suggests that ^{L597V}Braf acts as an epistatic modifier of ^{G12D}Kras.

5. ^{L597V}Braf signals through Braf and Crafr

5.1. Introduction

Activated RAS has been shown to induce activation of all three RAF isoforms (Reviewed by Wellbrock *et al.*, 2004). However, studies in mice show a different role for each Raf isoform, and only mice deficient in Araf are born alive (Pritchard *et al.*, 1996). Moreover, each RAF isoform is expressed at different levels in different tissues. Of the three isoforms, Braf has been identified as the main activator of Mek in mice (Pritchard *et al.*, 1996; Wojnowski *et al.*, 2000; Huser *et al.*, 2001; Mikula *et al.*, 2001) and was found to have a higher affinity (Papin *et al.*, 1998) and efficiency at phosphorylating Mek (Pritchard *et al.*, 1995; Marais *et al.*, 1997) than Crafr. However, melanomas harbouring a RAS mutation were found to signal predominantly through CRAF (Dumaz *et al.*, 2006).

5.1.1. BRAF inhibitors induce paradoxical activation of the MAPK pathway in RAS-mutant cells

Small molecule inhibitors targeting BRAF are now in clinical use as anticancer drugs (Chapman *et al.*, 2011), and MEK inhibitors have been effective in ameliorating disease phenotypes in RASopathies (Anastasaki *et al.*, 2009; Schuhmacher *et al.*, 2008; Chen *et al.*, 2010). Although PLX4720 was first developed as a BRAF-specific inhibitor, Poulikakos *et al.* (2010) showed that all RAF inhibitors have the potential to inhibit BRAF and CRAF at high concentrations. However, when PLX4720 and SB590885 were used at concentrations to inhibit BRAF specifically, the level of P-ERK was suppressed

in BRAF^{V600E} cells, but P-ERK was induced in RAS-mutant cells (Heidorn *et al.*, 2010). Two models of paradoxical MAPK activation by BRAF inhibitors in RAS-mutant cells have been proposed.

The first model was proposed by Poulikakos *et al* (2010), in which inhibitor binding to the ATP-binding pocket induces BRAF binding to CRAF in RAS-mutant cells, and transactivates CRAF. The second model was proposed by Heidorn *et al* (2010), where inhibition of BRAF *per se* but not inhibitor binding, induces BRAF:CRAF heterodimerisation in RAS-mutant cells, transactivation of CRAF and MAPK activation. It is therefore important to examine whether these inhibitors also have the same effects in cells carrying ^{L597V}BRAF with ^{G12D}KRAS mutations.

5.2. Aim

In Chapter 3, it was shown that ^{L597V}Braf only has slightly higher Braf kinase activity compared to ^{WT}Braf, and this translates to a small increase in MAPK activity which is insufficient to transform cells. Also in Chapter 3, CRAF was shown to inhibit ^{L597V}BRAF-induced MAPK activity when overexpressed in HEK 293^T cells. The aim of this chapter was to determine whether ^{L597V}Braf signals through its own intrinsic activity or transactivates CraF. This was important to understand as it would provide useful information for determining best therapeutic approaches for treating cancers and RASopathies with the ^{L597V}BRAF mutation.

5.3. Results

5.3.1. ^{L597V}Braf enhances Craf kinase activity in Kras^{+G12D} MEFs

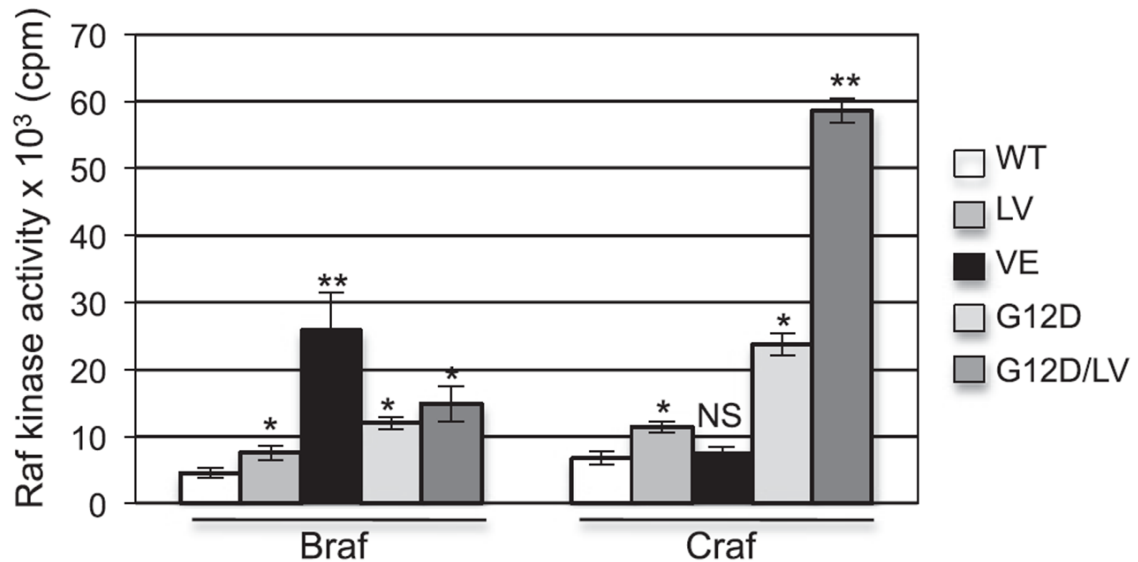
To determine the activity of Braf and Craf in MEFs of each genotype, kinase assays were performed. Immortalised Braf^{+/Lox-L597V}, Braf^{+/Lox-V600E}, Kras^{+Lox-G12D} and double mutant MEFs were plated to reach a confluency of ~80%. Braf^{+/+} MEFs were included as controls. Protein lysates were subjected to immunoprecipitation kinase assays using the kinase cascade assay (Figure 5.1). These assays were undertaken by Bipin Patel (Biochemistry, Leicester).

All of the Braf kinase activities were significantly different to activities in Braf^{+/+} MEFs, and the Craf kinase activity of all mutants except for ^{V600E}Braf was statistically increased compared to activities in Braf^{+/+} MEFs (Figure 5.1). As shown previously, Braf activity in Braf^{+/Lox-L597V} MEFs was in between that in Braf^{+/+} and Braf^{+/Lox-V600E} MEFs. Braf activity was also weakly induced in Kras^{+Lox-G12D} and double mutant MEFs over Braf^{+/+} MEFs.

The Craf kinase activity in Braf^{+/Lox-L597V} MEFs was significantly higher than in Braf^{+/+} MEFs whereas, in Braf^{+/Lox-V600E} MEFs, it was not changed. In support of previous studies that showed oncogenic RAS induces CRAF activity (Emuss *et al.*, 2005; Dumaz *et al.*, 2006), the Craf kinase activity in Kras^{+Lox-G12D} MEFs was elevated by ~3-fold compared to wild-type. Interestingly, the Craf kinase activity in double mutant MEFs was elevated by ~7-fold compared to wild-type, which was higher than the Craf kinase activity of Braf^{+/Lox-L597V} and Kras^{+Lox-G12D} MEFs put together. This suggests that ^{L597V}Braf and ^{G12D}Kras cooperate to induce Craf activity.

Figure 5.1 *L597V* **Braf enhances Craf kinase activity in *Kras*^{+G12D} MEFs**

Immortalised *Braf*^{+/+} (WT), *Braf*^{+/Lox-L597V} (LV), *Braf*^{+/Lox-V600E} (VE), *Kras*^{+Lox-G12D} (G12D) and double mutant (G12D/LV) MEFs were plated to reach a confluency of ~80%. MEFs were lysed after 48 hours. Protein lysates were subjected to *Braf* or *Craf* kinase assays by Bipin Patel. Bars indicate mean Raf kinase activity of 3 experiments and, error bars indicate standard deviation. (NS) Not significant, (*) $P < 0.05$, (**) $P < 0.01$ with respect to activities in wild-type MEFs.



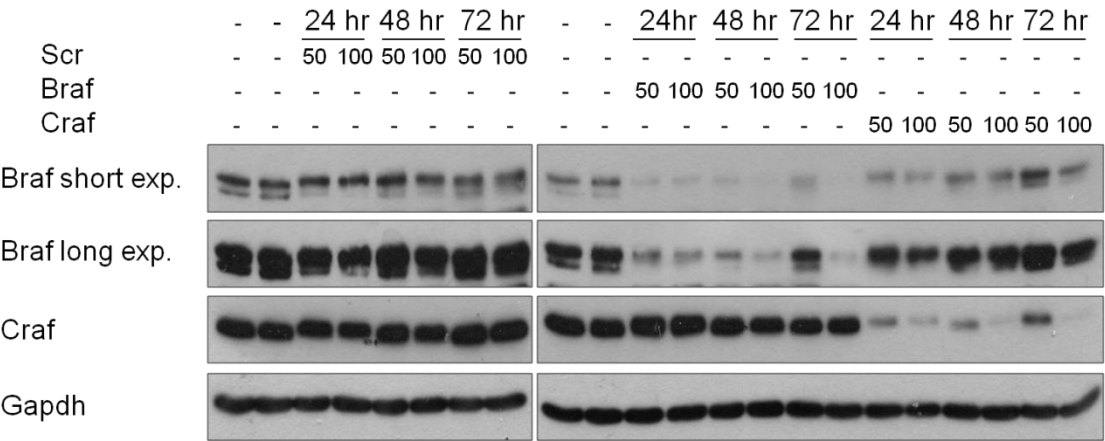
5.3.2. Optimisation of Braf and Cra knock-down

As mentioned in Chapter 1, CRAF has been shown to inhibit the MAPK activity of ^{V600E}BRAF (Karreth *et al.*, 2009), while impaired BRAF activity mutants have been shown to transactivate CRAF (Kamata *et al.*, 2010; Wan *et al.*, 2004). Knock-down studies have shown that BRAF is required for MEK/ERK signalling in ^{V600E}BRAF-harbouring melanocytes (Montagut *et al.*, 2008) and in wild-type melanocytes, but not in RAS-mutant melanocytes (Dumaz *et al.*, 2006). Instead, CRAF has been shown to be required for MEK/ERK signalling in these cells (Dumaz *et al.*, 2006). Given the result above showing high Cra activity in *Braf*^{+/Lox-L597V} MEFs, it is important to assess the contribution Cra makes to MAPK activity in these cells.

To determine which Raf isoform each mutant signals through, siRNA technology was utilised. The conditions for knock-down were first tested in double mutant MEFs. Immortalised double mutant MEFs were seeded to reach a confluency of ~70% on the day of transfection. MEFs were transfected with 50nM or 100nM of Braf or Cra siRNA. As controls, MEFs were untransfected, mock-transfected or transfected with a scrambled control. Media was replenished every 24 hours. Protein lysates were made every 24 hours after transfection up to 72 hours. Protein lysates were analysed by western blotting (Figure 5.2).

Figure 5.2 Time course of Braf or Cra knock-down

Immortalised double mutant MEFs were seeded to reach a confluency of ~70% on the day of transfection. MEFs were untransfected, mock-transfected, or transfected with 50nM (50) or 100nM (100) of scrambled (Scr), 50nM or 100nM of Braf, or 50nM or 100nM of Cra siRNA. Media was replenished every 24 hours. Protein lysates were made every 24 hours after transfection up to 72 hours. Protein lysates were analysed by western blotting.



Transfection of MEFs with a scrambled control did not affect the levels of Braf or Cra (Figure 5.2). Braf siRNA transfection did deplete the levels of Braf, but did not change the levels of Cra. The amount of Braf siRNA transfected for 24 or 48 hours did not differ in the ability to deplete Braf protein levels. However, 50nM for 72 hours failed to deplete Braf expression. This could be due to untransfected cells outgrowing the transfected cells and allowing Braf expression.

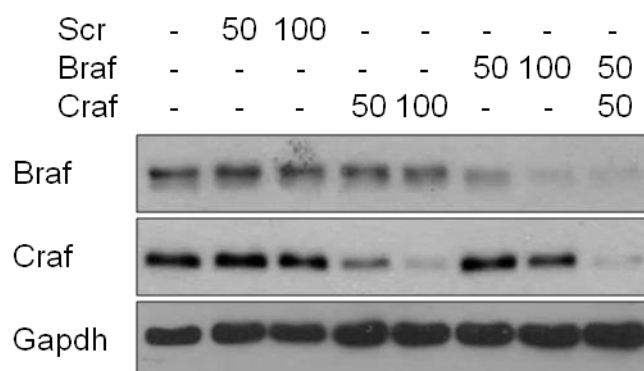
Cra expression was successfully depleted by Cra siRNA but, as with Braf siRNA, 50nM for 72 hours incompletely depleted Cra (Figure 5.2). Therefore the optimum time for knock-down was determined to be 48 hours, but the concentration was not yet chosen.

To determine the concentration of siRNA to transfect into cells, immortalised double mutant MEFs were seeded to reach a confluency of ~70% on the day of transfection. MEFs were transfected with 50nM or 100nM of Braf or Cra siRNA, or 50nM of Braf and 50nM of Cra siRNA for 48 hours. As controls, MEFs were mock-transfected or transfected with a scrambled control. Protein lysates were analysed by western blotting (Figure 5.3).

Transfection of the scrambled control did not affect Braf or Cra protein levels. 100nM of Braf or Cra siRNA efficiently depleted the majority of Braf or Cra protein levels respectively. Interestingly, 50nM of each Braf and Cra siRNA together was sufficient to deplete the levels of Braf and Cra protein to levels equivalent of using 100nM of each siRNA. These experiments suggest that the

Figure 5.3 50nM of each siRNA is sufficient for efficient knock-down

Immortalised double mutant MEFs were seeded to reach a confluency of ~70% on the day of transfection. MEFs were mock-transfected or transfected with 50nM (50) or 100nM (100) of scrambled (Scr), 50nM or 100nM of Braf, 50nM or 100nM of Cra siRNA, or 50nM of Braf and 50nM of Cra siRNA for 48 hours. As controls, MEFs were untransfected, mock-transfected or transfected with a scrambled control. Protein lysates were analysed by western blotting.



optimal conditions were transfection for 48 hours using 100nM of siRNA in total to deplete Braf or Cra protein levels. Using 100nM of siRNA for single knock-down was more complete, and these conditions also eliminated the possibility of off-target effects by using different amounts of siRNA.

5.3.3. Knock-down of Cra does not affect ^{L597V}Braf signalling

Immortalised Braf^{+/Lox-L597V}, Braf^{+/Lox-V600E}, Kras^{+/Lox/G12D} and double mutant MEFs were plated one day before transfection with the aim of reaching a confluency of ~70% on the day of transfection. Braf or Cra or both Braf and Cra were knocked down by siRNA transfection for 48 hours using a total of 100nM siRNA. As controls, MEFs were untransfected or transfected with a scrambled control. Protein lysates were examined by western blotting.

The levels of protein were quantitated and normalised to the scrambled control to take into account the effects of non-specific knock-down. Transfection of the Braf siRNA in all experiments significantly depleted or completely abolished Braf levels. Transfection of Cra siRNA in all experiments significantly depleted or completely abolished Cra levels. Co-transfection of Braf and Cra siRNA knocked-down Braf and Cra levels, and almost completely depleted both isotopes.

As mentioned in previous chapters, the best read-out of MAPK output is P-Mek levels, since P-Erk levels are affected by the expression of negative regulators such as Dusps. Western blots of the negative regulators were not included since the levels mirrored the levels of P-Mek (data not shown).

Effects of knock-down were first examined in Braf^{f+/Lox-V600E} MEFs. As expected, Braf siRNA reduced the levels of P-Mek and P-Erk in Braf^{f+/Lox-V600E} MEFs (Figure 5.4A). P-Mek and P-Erk levels were reduced to ~0.3-fold and ~0.4-fold respectively and this was statistically significant. With Crafa depletion, a tendency for P-Mek and P-Erk levels to increase was observed, which is consistent with previous studies that suggest CRAF to have inhibitory effects on ^{V600E}BRAF-driven MAPK activation (Karreth *et al.*, 2009).

In Braf^{f+/Lox-L597V} MEFs, Braf siRNA reduced the levels of P-Mek to ~0.5-fold and P-Erk to ~0.8-fold (Figure 5.4B). Crafa siRNA also reduced the levels of P-Mek and P-Erk somewhat, but the reduction was not statistically significant. This is in contrast with the results in Chapter 3 that showed Crafa inhibits ^{L597V}Braf-induced MAPK activation. The combined knock-down of Braf and Crafa gave a further reduction in P-Mek levels than Braf knock-down alone, which suggests that both are involved in signalling to Mek/Erk in these cells.

In Kras^{+Lox-G12D} MEFs, Braf and Crafa siRNA individually reduced P-Mek as well as when used together (Figure 5.5A). Braf and Crafa siRNA reduced the level of P-Mek even further to ~0.3-fold and the level of depletion was more statistically significant in comparison with single knock-down in Kras^{+Lox-G12D} MEFs. These results suggest that ^{G12D}Kras signals through both Braf and Crafa, but the loss of either Raf isoform can be compensated by the other isoform to some extent.

Figure 5.4. Knock-down of *Braf* and *Craf* in MEFs

Immortalised *Braf*^{f+/Lox-V600E} (VE) and *Braf*^{f+/Lox-L597V} (LV) MEFs were either untransfected, or transfected with 100nM of Scrambled control (Scr), 100nM of *Braf* (*Braf*), 100nM of *Craf* (*Craf*), or 50nM of *Braf* and 50nM of *Craf* siRNA for 48 hours.

Protein expression was analysed by western blotting. Shown are representative blots (n=3). Bar charts show the levels of P-Mek and P-Erk quantitated using ImageJ and normalised with respect to Gapdh. Bars indicate mean of fold changes of 3 experiments with respect to scrambled control, error bars indicate standard error. (NS) Not significant (*) P<0.05 (**) P<0.01 (***) P<0.001 with respect to MEFs transfected with the scrambled control.

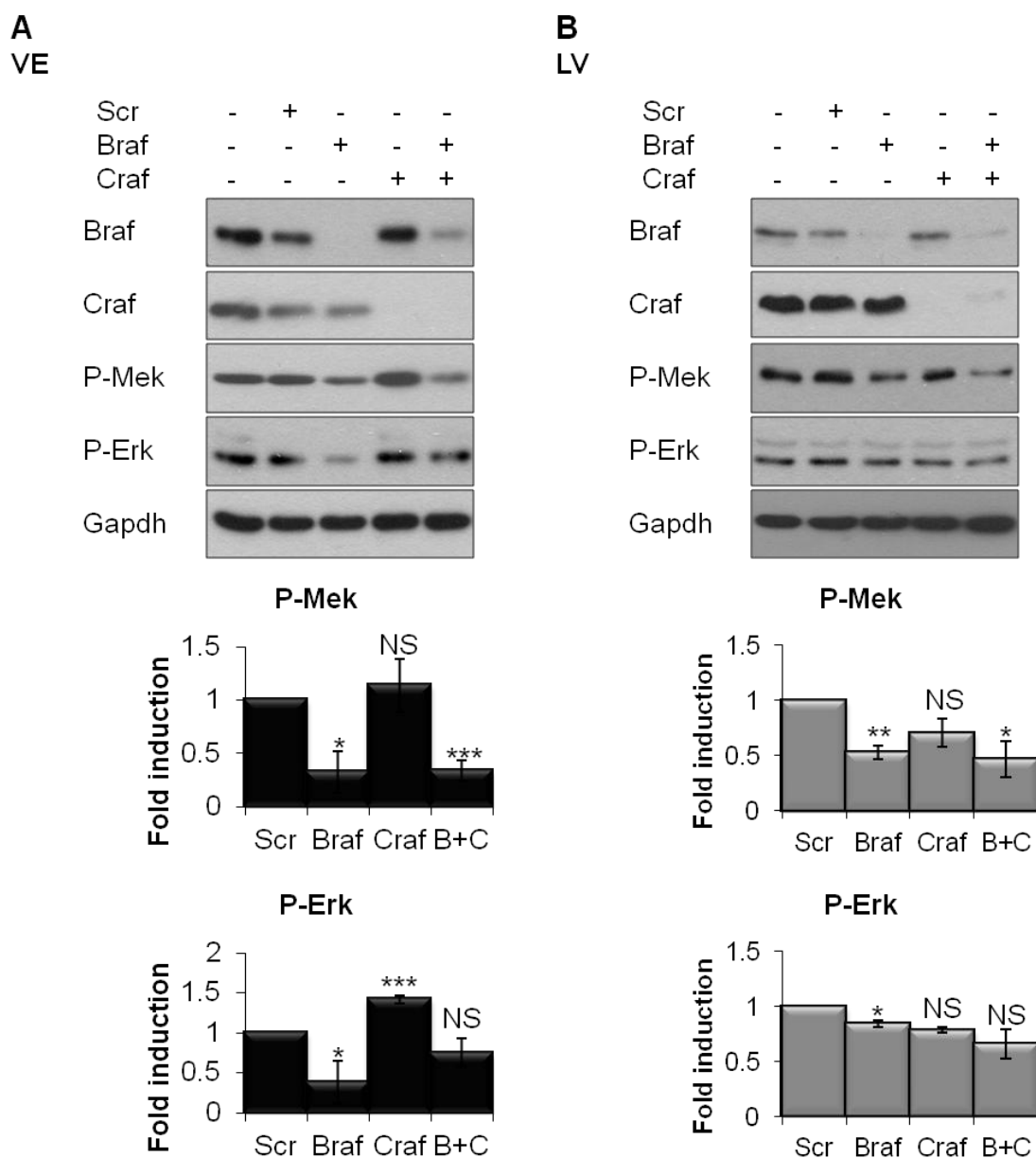
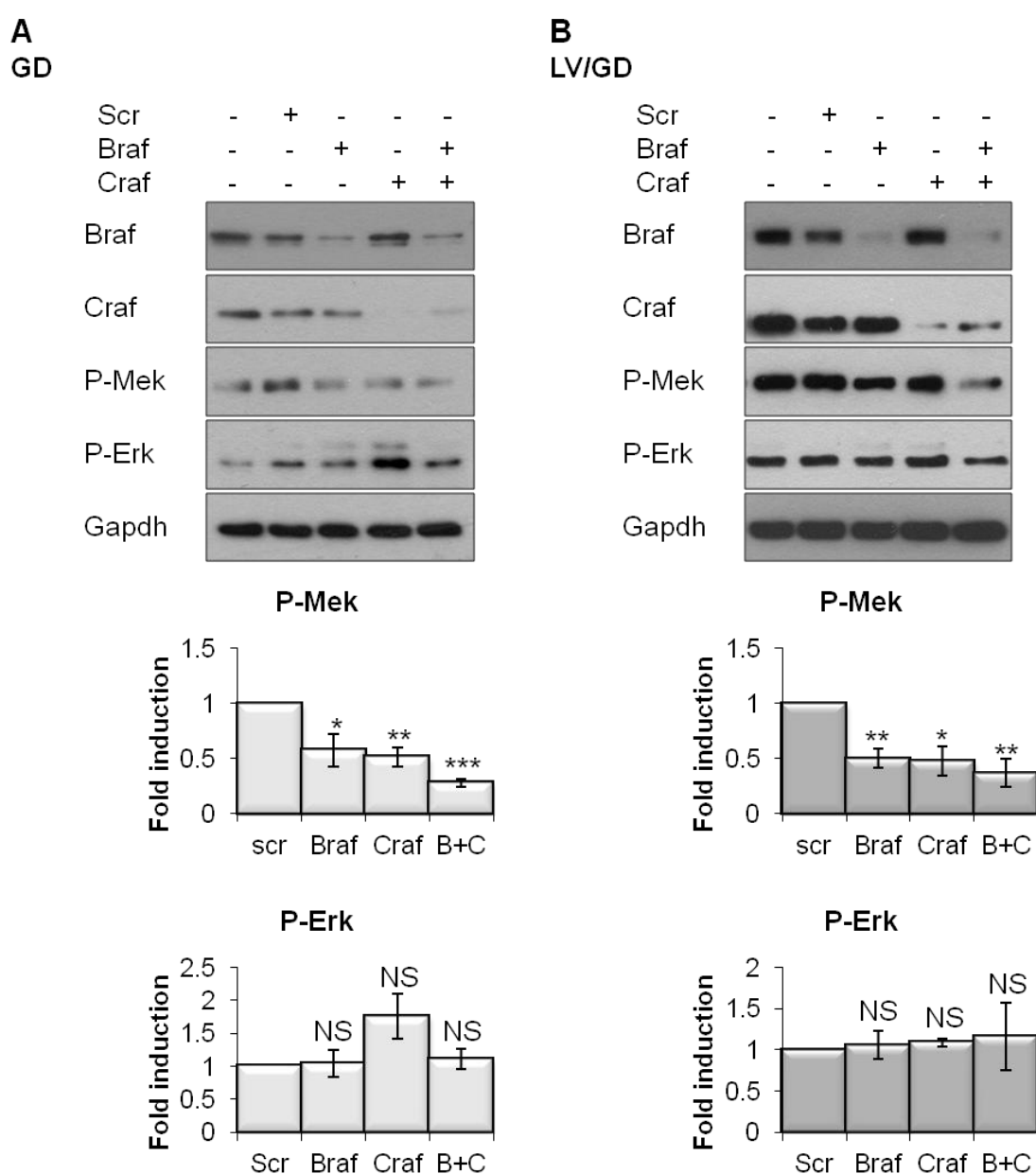


Figure 5.5. *Kras*^{+/-Lox-G12D} and double mutant MEFs signal through both *Braf* and *Craf*

Immortalised *Kras*^{+/-Lox-G12D} (GD) and double mutant (LV/GD) MEFs were either untransfected, or transfected with 100nM of Scrambled control (Scr), 100nM of *Braf* (*Braf*), 100nM of *Craf* (*Craf*), or 50nM of *Braf* and 50nM of *Craf* siRNA for 48 hours.

Protein expression was analysed by western blotting. Shown are representative blots (n=3). Bar charts show the levels of P-Mek and P-Erk quantitated using ImageJ and normalised with respect to Gapdh. Bars indicate mean of fold changes of 3 experiments with respect to scrambled control, error bars indicate standard error. (NS) Not significant (*) P<0.05 (**) P<0.01 (***) P<0.001 with respect to MEFs transfected with the scrambled control.



Braf siRNA and Cra siRNA individually in double mutant MEFs significantly reduced P-Mek levels to ~0.5-fold and ~0.4-fold respectively (Figure 5.5B). Braf and Cra siRNA together gave a greater reduction in P-Mek levels, again showing signalling through both Raf isoforms.

5.3.4. BRAF inhibitors increase P-Erk and P-Mek in $\text{Braf}^{+/Lox-L597V}$ and double mutant MEFs

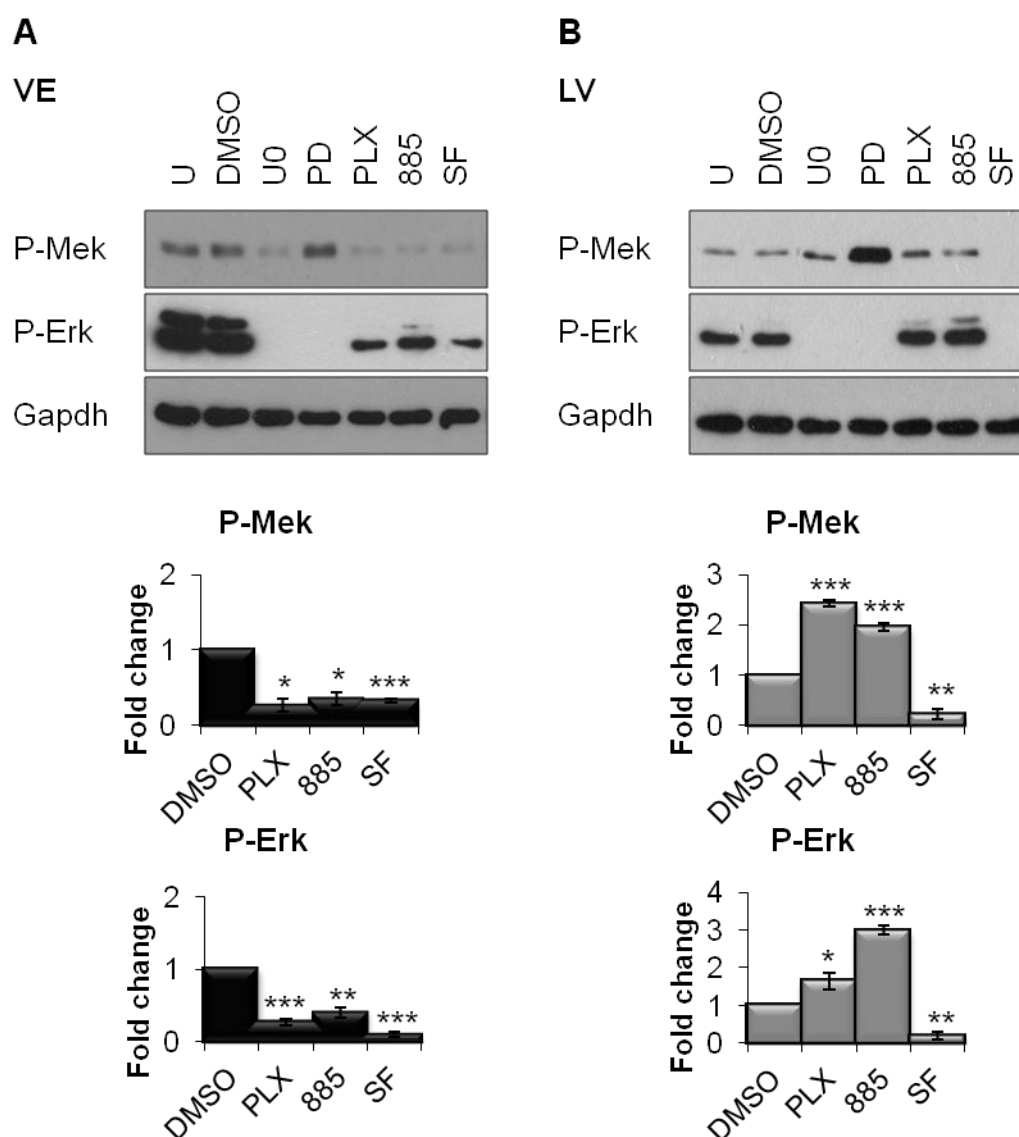
To test for efficiency of Raf and Mek inhibition, immortalised $\text{Braf}^{+/Lox-L597V}$, $\text{Kras}^{+/Lox-G12D}$ and double mutant MEFs were seeded to reach a confluency of ~95% on the day of treatment. MEFs were treated with the MEK inhibitors U0126 or PD184352, RAF inhibitors PLX4720 at 0.3 μ M or SB590885 at 1 μ M. At these concentrations PLX4720 and SB590885 are known to inhibit specifically BRAF, whereas Sorafenib at 10 μ M inhibits BRAF and CRAF. As controls, $\text{Braf}^{+/Lox-V600E}$ MEFs were included to test for successful inhibition, and all MEFs were treated with the carrier DMSO. Protein lysates were analysed by western blotting. DMSO treatment alone did not affect the protein levels in any of the treated cells.

The MEK inhibitors U0126 and PD184352 suppressed the levels of P-Erk in all MEF lines (Figure 5.6 and Figure 5.7), but raised the level of P-Mek, as expected. The negative regulators mirrored the levels of P-Mek and these data were not shown.

Figure 5.6 Inhibition of BRAF suppresses MAPK activity in *Braf*^{+/-Lox-V600E} MEFs but induces paradoxical activation in *Braf*^{+/-Lox-L597V} MEFs

Immortalised *Braf*^{+/-Lox-V600E} (VE) and *Braf*^{+/-Lox-L597V} (LV) MEFs were untreated (U), treated with DMSO (D), U0126 (U0), PD184352 (PD), PLX4720 (PLX), SB590885 (885) or Sorafenib (SF) for 4 hours.

Protein expression was analysed by western blotting. Shown are representative blots (n=3). Bar charts show the levels of P-Mek and P-Erk quantitated using ImageJ and normalised with respect to Gapdh. Bars indicate mean of fold changes of 3 experiments with respect to scrambled control, error bars indicate standard error. (*) P<0.05 (**) P<0.01 (***) P<0.001 with respect to DMSO control.



Consistent with previous studies (Heidorn *et al.*, 2010; Hatzivassiliou *et al.*, 2010; King *et al.*, 2006), the levels of P-Mek and P-Erk in $\text{Braf}^{+/Lox-V600E}$ MEFs were suppressed by the RAF inhibitors PLX4720, SB590885 and Sorafenib (Figure 5.6A).

By contrast, the levels of P-Mek and P-Erk in $\text{Braf}^{+/Lox-L597V}$ MEFs were increased by the BRAF inhibitors PLX4720 and SB590885, but reduced by Sorafenib treatment (Figure 5.6B). These results suggest that at concentrations that achieve specific inhibition of BRAF in $\text{Braf}^{+/Lox-L597V}$ MEFs, activation of the MAPK pathway is induced. These results also confirm that Cra has MAPK activation potential in $\text{Braf}^{+/Lox-L597V}$ MEFs as suggested by the knock-down experiments in Section 5.3.3.

Consistent with previous studies (Heidorn *et al.*, 2010; Hatzivassiliou *et al.*, 2010; King *et al.*, 2006), the levels of P-Mek and P-Erk were increased by PLX4720 and SB590885-treatment in $\text{Kras}^{+/Lox-G12D}$ MEFs, but suppressed by Sorafenib (Figure 5.7A).

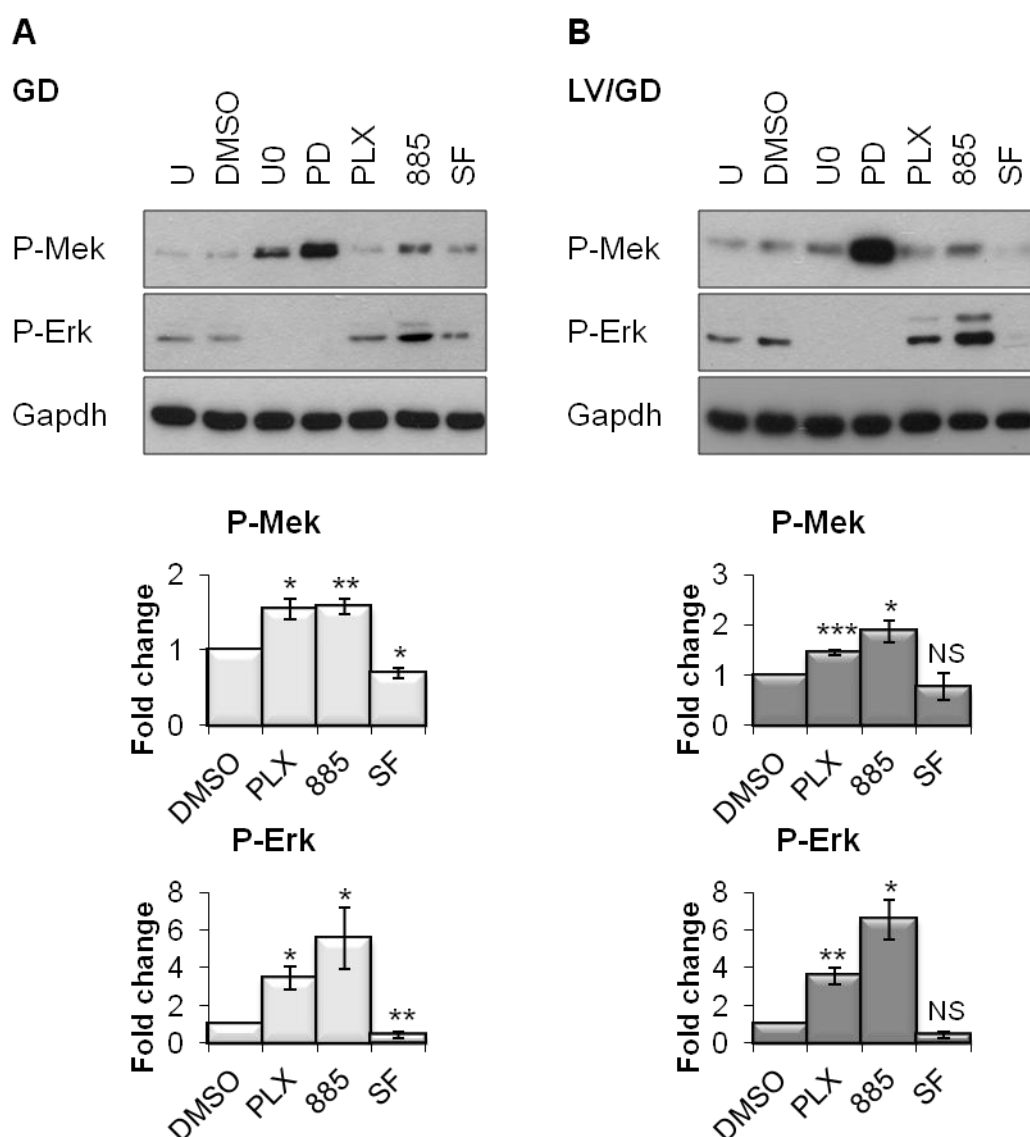
As in $\text{Kras}^{+/Lox-G12D}$ MEFs, the levels of P-Mek and P-Erk were induced by PLX4720 and SB590885 treatment in double mutant MEFs (Figure 5.7B). Sorafenib treatment inhibited both P-Mek and P-Erk.

RAF inhibitors induce BRAF:CRAF heterodimers. Previous studies have shown that BRAF inhibitors induced MEK/ERK activity in cells expressing ^{WT}BRAF and oncogenic RAS, and this was due to heterodimerisation of BRAF with CRAF (Heidorn *et al.*, 2010; Hatzivassiliou *et al.*, 2010). Therefore to determine

Figure 5.7 Inhibition of *Braf* in *Kras*^{+/-Lox-G12D} and double mutant MEFs induces paradoxical activation of the MAPK pathway

Immortalised *Kras*^{+/-Lox-G12D} (GD) and double mutant (LV/GD) MEFs were untreated (U), treated with DMSO (D), U0126 (U0), PD184352 (PD), PLX4720 (PLX), SB590885 (885) or Sorafenib (SF) for 4 hours.

Protein expression was analysed by western blotting. Shown are representative blots (n=3). Bar charts show the levels of P-Mek and P-Erk quantitated using ImageJ and normalised with respect to Gapdh. Bars indicate mean of fold changes of 3 experiments with respect to scrambled control, error bars indicate standard error. (NS) Not significant (*) P<0.05 (**) P<0.01 (***) P<0.001 with respect to DMSO control.

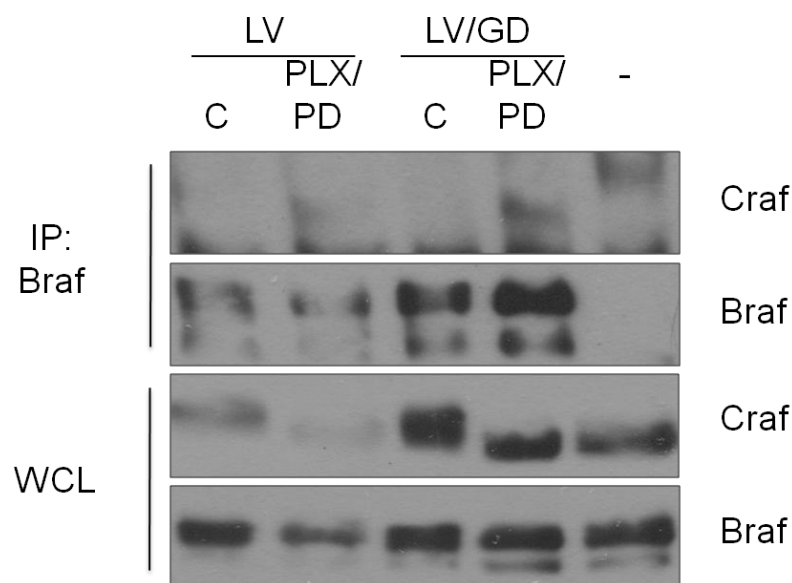


whether this was the mechanism of Mek/Erk activation in ^{L597V}Braf-expressing MEFs, Braf was immunoprecipitated from protein lysates of Braf^{+/Lox-L597V} and double mutant MEFs treated with PLX4720 and PD184352, and the immunoprecipitated proteins were analysed by western blotting (Figure 5.8). As controls, MEFs were treated with the carrier control DMSO, and as negative controls, the beads were conjugated to mouse IgG and incubated with protein lysates of the drug-treated double mutant MEFs. It has been shown that heterodimers cannot be observed when treated with PLX4720 alone (Heidorn *et al.*, 2010). This was suggested to be due to negative phosphorylation of BRAF by ERK, which could destabilise BRAF binding to CRAF (Rushworth *et al.*, 2006). Therefore, MEFs were treated simultaneously with PD184352 as well to inhibit the negative phosphorylatory effects of Erk.

Braf:Craf heterodimers were observed in ^{L597V}Braf-expressing MEFs treated with PLX4720 and PD184352 and not in DMSO-treated cells (Figure 5.8). Therefore inhibition of Braf induced Braf:Craf heterodimerisation. Interestingly, in the PLX4720 and PD184352-treated cell lysates Craf migrated faster than DMSO-treated cell lysates, suggesting feedback phosphorylation of Craf by Braf and/or Erk.

Figure 5.8 ^{L597V}Braf can heterodimerise with Cra

Immortalised Braf^{+/Lox-L597V} (LV) and double mutant (LV/GD) MEFs were treated with a carrier control (C) or PLX4270 and PD184352 (PLX/PD) for 4 hours. Protein lysates were immunoprecipitated for Braf (IP: Braf). Whole cell lysates (WCL) and the immunoprecipitated proteins were analysed with the antibodies indicated. As a negative control, the beads were conjugated to mouse IgG and incubated with protein lysates of the drug-treated double mutant MEFs.



5.4. Conclusion

In this Chapter, Cra activity was confirmed to be significantly increased in *L597V* Braf-expressing MEFs. In support of previous studies which showed that oncogenic RAS induces CRAF kinase activity (Dumaz *et al.*, 2006; Emuss *et al.*, 2005), *Kras*^{+/-Lox-G12D} MEFs also had higher Cra kinase activity than in wild-type MEFs^{WT} Cra. Interestingly, the Cra kinase activity of double mutant MEFs was much higher than the Cra kinase activity of *Braf*^{+/-Lox-L597V} and *Kras*^{+/-Lox-G12D} MEFs put together. Therefore *L597V* Braf not only induces Mek/Erk activity, but also enhances Cra activity in the presence of *G12D* Kras.

Unsurprisingly, Braf knock-down in *Braf*^{+/-Lox-V600E} MEFs reduced the MAPK activity as measured by a reduction in P-Mek and P-Erk levels. In support of previous studies which showed that CRAF inhibits *V600E* BRAF activity (Karreth *et al.*, 2009), knock-down of Cra enhanced the levels of P-Mek and P-Erk. Knock-down of Braf and Cra individually in *Braf*^{+/-Lox-L597V} MEFs reduced the MAPK activity, and knock-down of both Braf and Cra together further reduced the level of P-Mek. Therefore these results suggest that, although *L597V* Braf is the main activator of the Mek/Erk pathway, Cra contributes to some degree. This is in contrast to the results in Chapter 3, which showed a reduction in P-MEK and P-ERK levels in HEK 293^T cells overexpressing *L597V* BRAF and CRAF in comparison with cells overexpressing *L597V* BRAF only. The same was true in *Kras*^{+/-Lox-G12D} and double mutant MEFs.

The MEK inhibitors U0126 and PD184352 inhibited Erk signalling in all MEFs tested. The RAF inhibitors PLX4720 and SB590885, when used at a dose that

mainly inhibited BRAF, reduced P-Mek and P-Erk levels in Braf^{+/-Lox-V600E} MEFs, but induced Mek/Erk activation in Braf^{+/-Lox-L597V}, Kras^{+/-Lox-G12D} and double mutant MEFs. These results support previous studies showing paradoxical activation of MEK/ERK with BRAF inhibitor treatment in RAS-mutant cells (Heidorn *et al.*, 2010; Hatzivassiliou *et al.*, 2010; King *et al.*, 2006) but also show that the same mechanism operates in ^{L597V}Braf-expressing cells. Braf:Craf heterodimer formation in Braf^{+/-Lox-L597V} and double mutant MEFs treated with PLX4720 and PD184352 supported this theory. The importance of Craf in inhibitor-induced MAPK activation was supported by suppression of the MAPK pathway when both Braf and Craf were inhibited by Sorafenib. Thus, ^{L597V}Braf-expressing MEFs behave like Kras^{+/-G12D} cells in this regard.

Taken together, the data show that ^{L597V}Braf is the main activator of the MAPK pathway, but contribution from Craf can be observed through its intrinsic activity. Treatment with BRAF inhibitors is cautioned in ^{L597V}BRAF-expressing cancers and RASopathies.

6. **Braf^{+/Lox-L597V} mice develop tumours with age**

6.1. Introduction

As previously mentioned, ^{L597}BRAF mutations frequently co-exist with other mutations (<http://cancer.sanger.ac.uk/cosmic/gene/analysis?ln=BRAF>) in human cancers and, in Chapter 3, it was shown that ^{L597V}BRAF is not a driver oncogene. In Chapter 4, ^{L597V}Braf was shown to enhance the MAPK activity of G12D Kras. Therefore the weak MEK/ERK activity of ^{L597V}BRAF may contribute to cancer progression through enhancing the activity of other oncogenes. In theory, this would make Braf^{+/Lox-L597V} mice more prone to tumour development.

6.2. Aims

The aim of this chapter was to assess whether Braf^{+/Lox-L597V} mice were predisposed to tumour formation and whether mutations in other oncogenes were acquired in the process.

6.3. Results

The conditional knock-in mouse model was used for these experiments. Constitutive expression of ^{L597V}Braf from one allele was achieved by intercrossing Braf^{+/LSL-L597V} mice with mice heterozygous for the CMV-Cre transgene.

As mentioned in Chapter 1, it has been published by Andreadi et al (2012) that Braf^{+/Lox-L597V}; CMV-Cre mice have RASopathy hallmarks, and were born at the

expected Mendelian ratio, but some were lost after weaning and ~70% survived to adulthood (Andreadi *et al.*, 2012). To ensure that all Braf^{f+/Lox-L597V}; CMV-Cre mice were recombined to express the mutant allele and to remove the CMV-Cre transgene, Braf^{f+/Lox-L597V}; CMV-Cre mice were further intercrossed with Braf^{f+/+} mice, and the resulting offspring of Braf^{f+/Lox-L597V} mice that had lost the CMV-Cre transgene were analysed. These mice were fully recombined to express L597V Braf in all cells. Braf^{f+/+} siblings were used as controls.

6.3.1. Braf^{f+/Lox-L597V} mice had a shorter lifespan

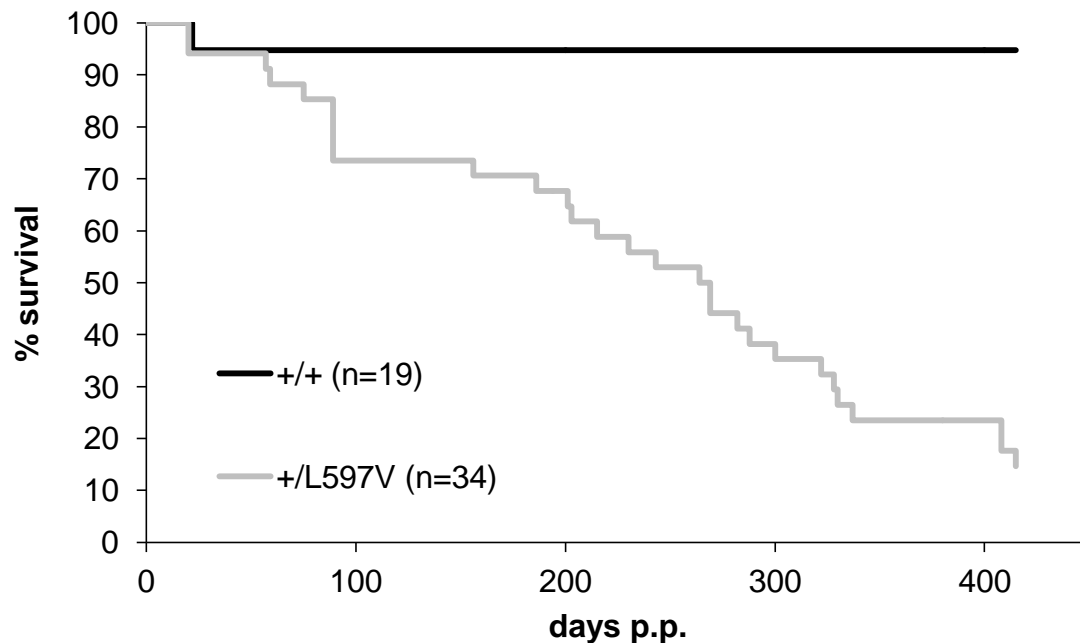
Survival curves were plotted. The age of the animals was recorded in a Kaplan-Meier survival curve (Figure 6.1). One Braf^{f+/+} animal died at 22 days old, but the rest survived for the duration of the study. 50% of Braf^{f+/Lox-L597V} mice survived for ~260 days, 25% of mice survived ~330 days and 15% of mice survived 415 days. Thus, they had reduced survival.

6.3.2. Summary of abnormal growths identified so far

Mice were sacrificed according to Home Office guidelines. Tissues were harvested and abnormalities recorded (Table 6.1). The most common abnormality was splenomegaly, with just over 50% of animals showing splenomegaly. 18% of the animals were sacrificed because they had two or more seizures. Although three of the animals (11%) that had seizures also had splenomegaly, they were not showing any other abnormalities.

Figure 6.1 Braf^{+/Lox-L597V} mice have a lower survival rate than controls

Braf^{+/Lox-L597V} mice were intercrossed with Braf^{+/+} mice. Mice were sacrificed according to Home Office guidelines to produce a Kaplan-Meier survival curve. As controls, the survival of Braf^{+/+} littermates was recorded.

**Table 6.1 Abnormalities**

Braf^{+/Lox-L597V} and Braf^{+/+} mice were sacrificed according to Home Office guidelines. Tissues were harvested and abnormalities recorded.

Pathology	Braf ^{+/Lox-L597V}	Braf ^{+/+}
Splenomegaly	15/28 (54%)	0/17 (0%)
Stroke	5/28 (18%)	0/17 (0%)
Growth in internal organs	4/28 (14%)	0/17 (0%)
Skin lesions	10/28 (36%)	0/17 (0%)
Uterine prolapse	3/28 (11%)	0/17 (0%)
Liver fibrosis	3/28 (11%)	0/17 (0%)

Braf^{+/Lox-L597V} animals developed growths that were reminiscent of early tumours. Braf^{+/+} animals did not develop tumours. 7% of animals had a growth on the small intestine, and 7% of animals had growths in the abdomen, which were confirmed to be hyperplasia of lymphoid tissue and hyperplasia of smooth muscle of the uterus respectively (see below). 36% of animals developed skin lesions, 21% were confirmed to be skin papillomas. 11% of the animals had uterine prolapse and splenomegaly but no other symptoms. 11% of animals also had liver fibrosis and splenomegaly.

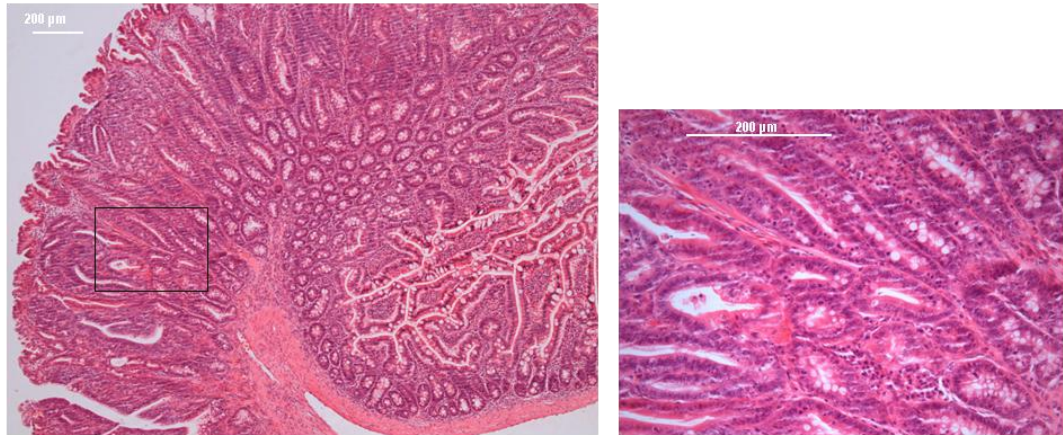
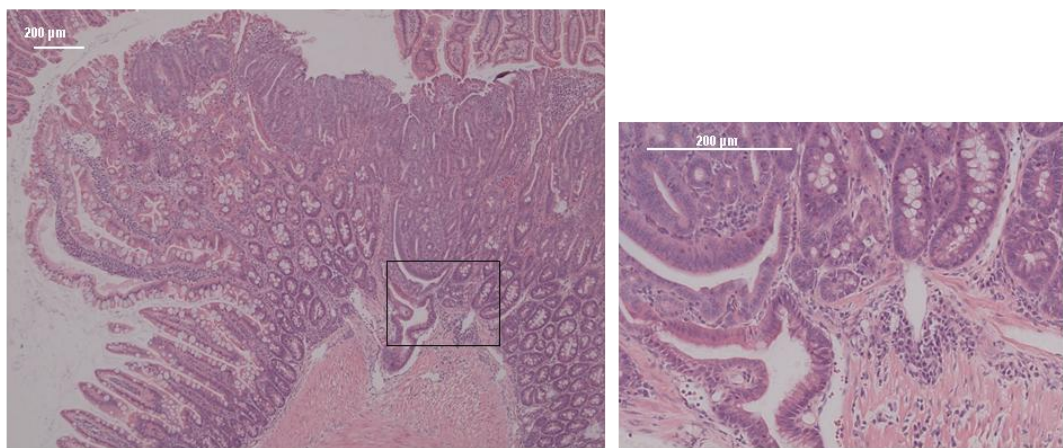
6.3.3. Histology of the abnormal growths

Organs and abnormal growths were dissected and then fixed in paraformaldehyde. The small intestine and large intestine were flushed out with PBS. The small intestine was divided into 6 sections. Both the large intestine and small intestine were opened up, swiss-rolled and then fixed in PFA. The fixed tissues were embedded into paraffin blocks and then cut into sections and transferred to glass slides by Susan Giblett (Biochemistry, Leicester). The tissue sections were stained with haematoxylin and eosin, and then photographed. All of the tumours were confirmed to be benign, since the cell morphology was normal and cells had not invaded neighbouring tissues.

The two growths on the small intestine were confirmed to be small intestinal adenomatous polyps (Figure 6.2). The crypts were irregular and formed a large overgrown mass of hyperplastic cells.

Figure 6.2 Small intestinal adenomatous polyps

H&E staining of small intestinal adenomatous polyps from two animals. Box represents area of enlargement.

A**B**

One of the growths in the abdomen was confirmed to be hyperplasia of lymphoid tissue (Figure 6.3). Although the cell morphology was normal, cells were hyperplastic. The other growth in the abdomen of another animal was confirmed to be hyperplasia of smooth muscle of the uterus (Figure 6.4). The muscle wall was unusually thick, but the cell morphology was normal and showed no signs of invasion.

The six skin growths were analysed histologically and confirmed to be skin papillomas (Figure 6.5). The cell morphology of the squamous cells was normal, and cells had not invaded into the dermal layer, but the thickness of the layer of squamous cells varied between samples.

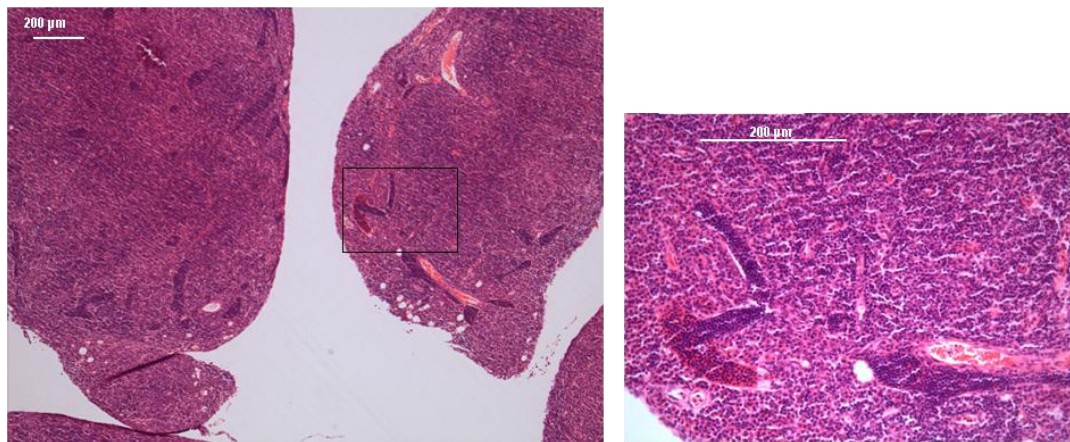
Three animals also had liver fibrosis (Figure 6.6). The liver had white or yellow lesions throughout. H&E staining showed lymphocyte infiltration, a sign of inflammation and fibrosis. The exact cause of inflammation under these settings is unknown, but was not found in wild-type animals.

6.3.4. Screening for mutations in *Raf* and *Ras*

As mentioned in Chapter 4, 10 human cancer samples have been found to harbour ^{L597V}*Braf* and other oncogenic mutations. The most frequently observed mutations were in *NRAS* or *BRAF*. To determine whether mutations in other oncogenes were acquired in ^{L597V}*Braf*-expressing tumours, DNA was extracted from paraffin-embedded blocks of tissue samples from tumours in *Braf*^{+/Lox-L597V} animals. The extracted DNA was amplified by PCR using primers designed to flank exons 11 and 15 in *Braf*, 7 and 10 in *Craf*, exons 1 and 2 in *Kras* and

Figure 6.3 Lymphoid hyperplasia

H&E staining of hyperplasia of lymphoid tissue. Box represents area of enlargement.

**Figure 6.4 Hyperplasia of smooth muscle of the uterus**

H&E staining of hyperplasia of smooth muscle of the uterus. Box represents area of enlargement.

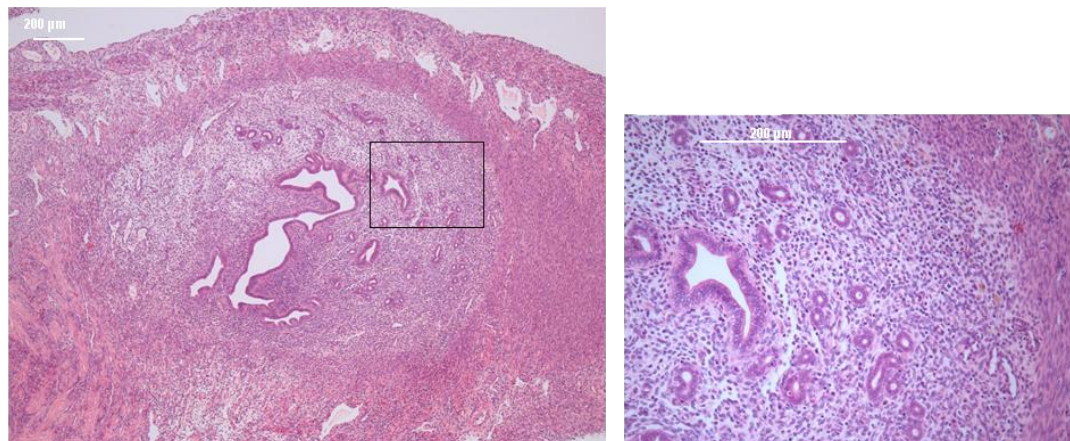


Figure 6.5 Skin papilloma

H&E staining of skin papilloma of six animals. Box represents area of enlargement.

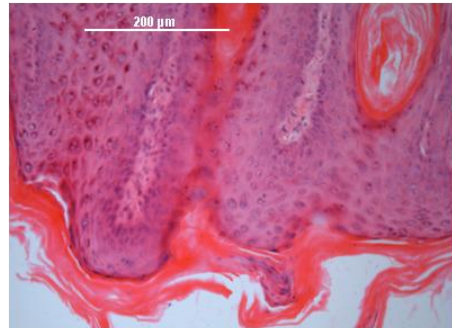
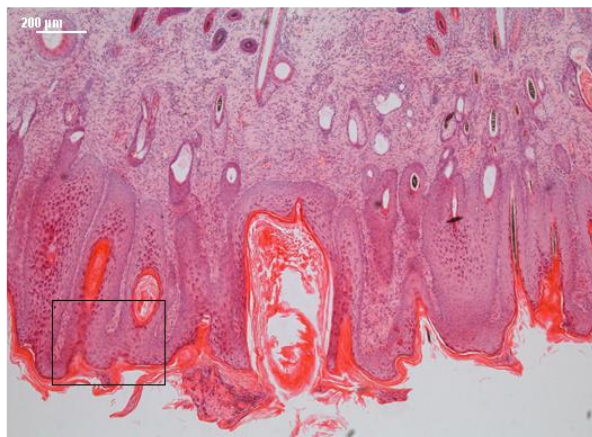
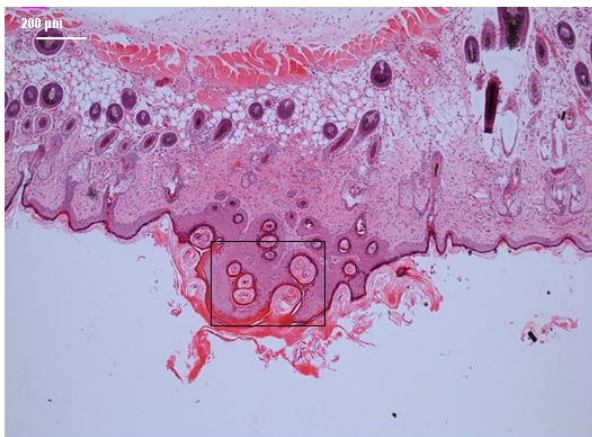
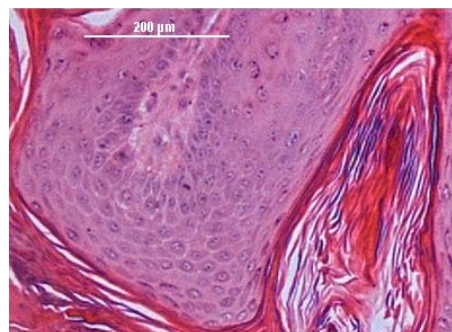
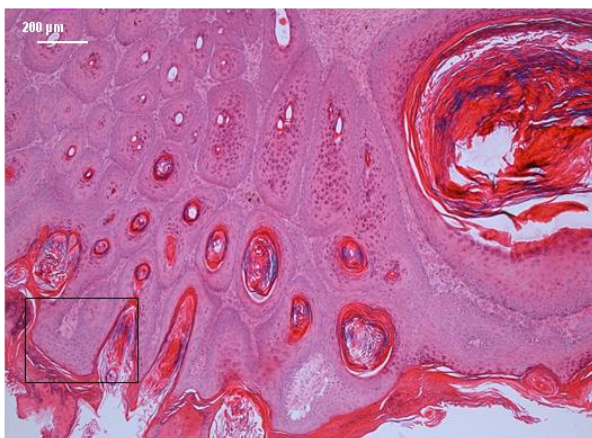
A**B****C**

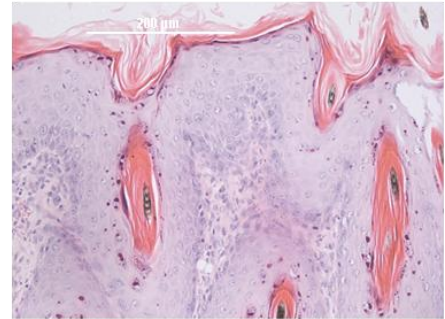
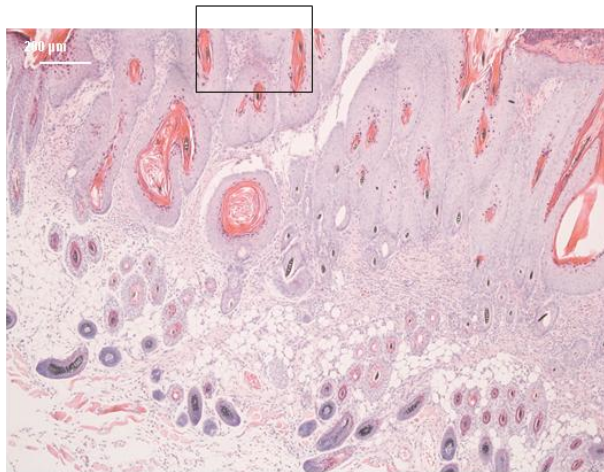
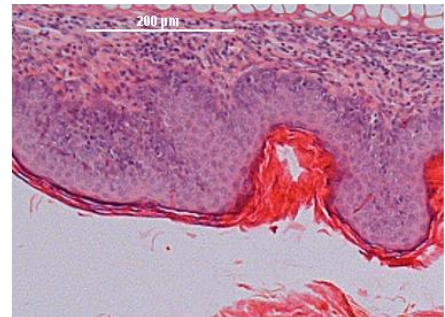
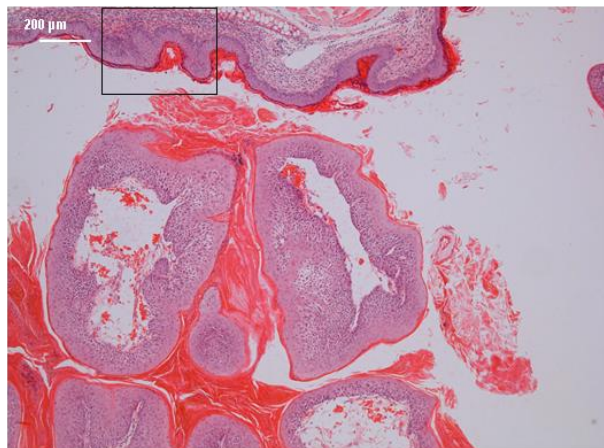
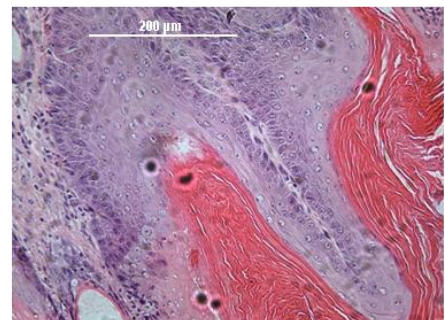
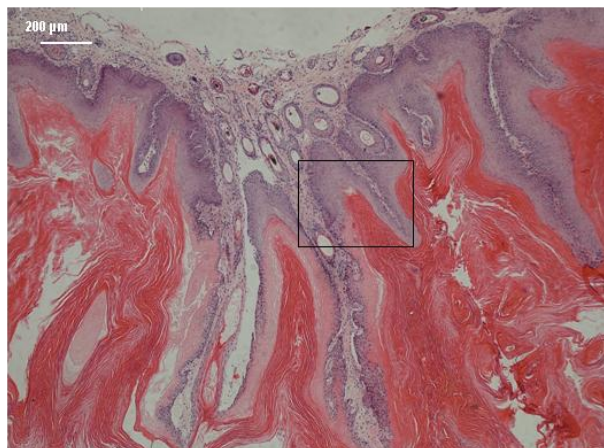
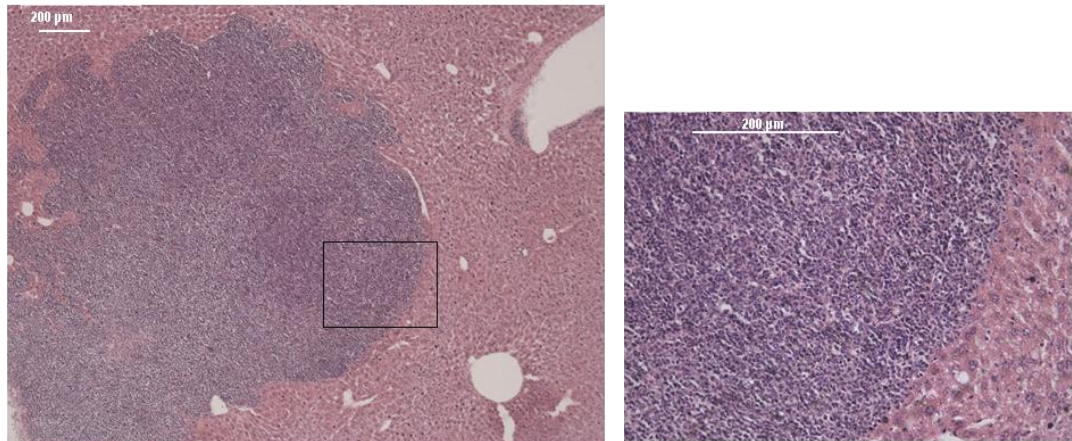
Figure 6.5 Skin papilloma continued**D****E****F**

Figure 6.6 Liver fibrosis

H&E staining of liver fibrosis. Box represents area of enlargement.



Hras, and exons 2 and 4 in *Nras*. The amplified DNA was purified and sent to The Protein Nucleic Acid Chemistry Laboratory (PNACL) for sequencing using the same primers. In total, the sequence of 13 samples were analysed, including two small intestinal adenomatous polyps, one lymphoid hyperplasia, one hyperplasia of the smooth muscle of uterus, six skin papillomas and three liver fibroses.

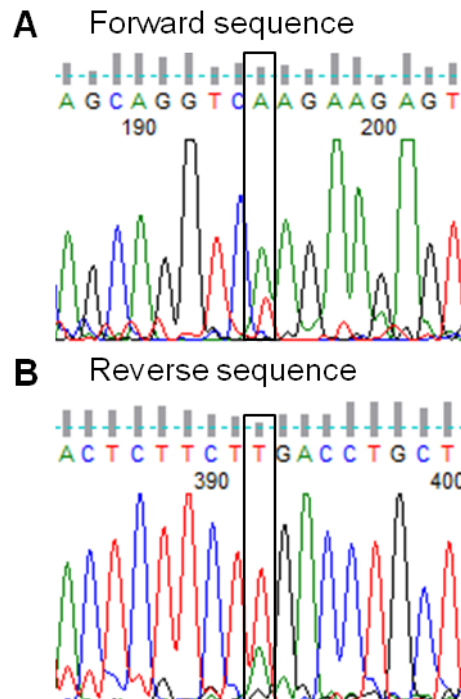
The nucleotide sequences were aligned with the wild-type sequence to scan for differences. The chromatogram of the forward and reverse sequences were manually analysed for double peaks, an indication of heterozygous mutations. All of the analysed tissues contained the 1789C>G transversion in *Braf* indicative of the ^{L597V}*Braf* mutation.

Mutations in *Braf*, *Craf*, *Kras* or *Nras* were not detected in any samples. However, one sample had a *Hras* mutation. 5 primer sets were used to sequence *Hras* exon 2. However, for technical reasons the sequence of only six samples was generated. This included three skin papillomas and three liver fibroses. Of the six samples analysed, one skin papilloma sample (histology represented by Figure 6.5F) contained a mutation in *Hras*. The chromatogram revealed a smaller T peak underneath A at base 182, representing heterozygosity for the Q61L mutation (Figure 6.7). The reverse sequence showed the same double peak, confirming the mutation. Q61L is the third most common nucleotide change in *HRAS* in human cancer, and is most commonly found in skin cancer

Figure 6.7 Chromatogram of Hras exon 2 sequence of skin papilloma sample

DNA was extracted from paraffin-embedded block of a skin papilloma sample. The DNA was amplified by PCR using primers flanking Hras exon 2. The products were purified and sent to PNACL for sequencing using the same primers.

- A) Chromatogram of the forward sequence.
- B) Chromatogram of the reverse sequence.



(<http://cancer.sanger.ac.uk/cosmic/gene/analysis?In=BRAF>). This result supports the hypothesis that mutations in other oncogenes contribute to tumour formation. The fact that nine out of 28 animals expressing ^{L597V}Braf have developed tumours, although all nine tumours were benign suggests a correlation between ^{L597V}BRAF and tumour formation. Furthermore, the identification of a known oncogenic mutation in *Hras* is consistent with the cooperation of ^{L597V}Braf with this oncogene in tumour development.

6.4. Conclusion

In Chapter 3 it was shown that ^{L597V}Braf is not a driver oncogene, and it is known that ^{L597V}BRAF mutations frequently co-exist with mutations in other driver oncogenes (<http://cancer.sanger.ac.uk/cosmic/gene/analysis?In=BRAF>). In Chapter 4, it was shown that ^{L597V}Braf cooperates with ^{G12D}Kras to drive hyperactivity of the MAPK pathway. Overall, these data confirm ^{L597V}Braf as a cooperating mutation.

Braf^{+/Lox-L597V} mice were bred on to remove the CMV-transgene. These mice were found to have a lower survival rate than control animals. 50% of animals survived for ~260 days, 25% of animals survived for ~330 days and 15% of animals survived for 415 days. This is a slightly lower overall rate than the first generation of Braf^{+/Lox-L597V} mice which had a higher survival rate, with ~70% of animals surviving 300 days (Andreadi *et al.*, 2012).

The most frequent but not life-threatening abnormality was splenomegaly, which was observed in ~50% of animals. Splenomegaly has been documented in many other RAS- and RAF-mutant mouse models including Kras^{+G12D} (Chan *et*

et al., 2004), Nras^{G12D/G12D} (Wang *et al.*, 2011), Braf^{f+/V600E} (Mercer *et al.*, 2005) and Braf^{f+/D594A} (Kamata *et al.*, 2010) mice. 14% of animals developed an internal growth. 36% of animals had skin lesions. 11% of animals had a uterine prolapse. These figures were consistent with work published by Andreadi *et al* (2012). In addition, 11% of animals had white or yellow growths throughout the liver which resembled fibrosis.

The tissue sections of growths in internal organs, skins lesions and liver fibrosis, were stained using haematoxylin and eosin. The cells of the lesions had not invaded neighbouring tissues. Therefore all of the observed lesions were benign. The growths in the small intestines were observed to be small intestinal adenomatous polyps. The cell morphology was normal but cells were hyperplastic, forming a large mass. One of the growths in the abdomen was a hyperproliferative lymph node. The cells were hyperplastic, but the cell morphology was normal. Another growth in the abdomen was in the uterus. The uterine wall was abnormally thick, but the cell morphology was normal and had not invaded into neighbouring tissues. It was confirmed to be hyperplasia of smooth muscle of the uterus. 60% of the skin lesions were benign skin papillomas. H&E staining of the abnormal livers showed lymphocyte infiltration, a sign of inflammation and fibrosis. Overall, these data show that Braf^{f+/Lox-L597V} mice are predisposed to formation of benign lesions when aged.

The abnormal tissues were also assessed for mutations in *Ras* and *Raf* oncogenes. Whole genome sequencing would have been ideal, but is prohibitively expensive and therefore targeted sequencing was undertaken.

DNA was extracted from paraffin-embedded blocks and sequenced for *Braf* exons 11 and 15, *Craf* exons 7 and 9, *Hras* and *Kras* exons 1 and 2, and *Nras* exons 2 and 4. All of the samples were confirmed to have the 1789 C>G transversion. In addition, one skin papilloma skin sample was heterozygous for the ^{Q61L}*Hras* mutation. This supports our hypothesis that mutations in other oncogenes arise and cooperate with ^{L597V}*Braf* in cancer development.

Only a small selection of oncogenes was sequenced, and it is likely that many other oncogenes or tumour suppressor genes were missed. Conceivably, mutations in *TP53*, *p19^{ARF}* and *EGFR* may also exist, as found in human cancers.

7. Summary and Discussion

7.1. ^{L597V}BRAF

Mutations in *BRAF* are detected in ~7% of human cancers (<http://cancer.sanger.ac.uk/cosmic/gene/analysis?ln=BRAF>). A mutation at Leu597 of *BRAF* is the fifth most common mutation in *BRAF* in human cancer, contributing to less than 0.5% of the total *BRAF* mutations (<http://cancer.sanger.ac.uk/cosmic/gene/analysis?ln=BRAF>). To date, a total of 59 cancer samples have been tested positive for a mutation at this residue, and 12 cancer samples have been identified to carry the ^{L597V}*BRAF* mutation (<http://cancer.sanger.ac.uk/cosmic/gene/analysis?ln=BRAF>). L597 is also mutated to glutamine, arginine and serine in human cancers (<http://cancer.sanger.ac.uk/cosmic/gene/analysis?ln=BRAF>).

The L597V mutation involves a 1789C>G transversion resulting in a leucine being substituted for a valine at residue 597. It is intriguing how this mutation is acquired in cancer even though both leucine and valine have similar properties, in that both amino acids have an aliphatic nonpolar side chain and both are hydrophobic, and are therefore on the inside of folded proteins. However, valine has one less methyl group in its side chain in comparison with leucine and is more hydrophobic. Therefore it can be speculated that valine disrupts the inactive conformation by causing the glycine-rich P-loop to become more compact, disrupting the contact with Gly463-Val470, and opening up the catalytic cleft for ATP. This may be why the mutant is more easily activated or is more active.

Leu597 is more commonly substituted to glutamine or arginine in human cancers. The latter mutant has never been examined in terms of its biological activity. However, as mentioned, a substitution to glutamine or serine were shown to have similar MAPK-inducing activity and foci-inducing capability to the V600E mutant (Hou *et al.*, 2007; Daniotti *et al.*, 2004), unlike L597V, which induced low levels of P-ERK (Wan *et al.*, 2004) and did not induce foci formation. Therefore it is clear that ^{L597V}BRAF has a different level of activity in comparison to other mutants at this residue, and thus the results obtained for ^{L597V}BRAF may not be indicative of the biological activity of the other mutants. In spite of this, the unique aspect of ^{L597V}BRAF is that it is detected in cancer and RASopathies and so the aim of this project was to further study ^{L597V}BRAF and unravel how it can contribute to RASopathies and cancer.

7.2. Comparison of the overexpression and endogenous system

Both overexpression and endogenous systems were utilised in this study. Overexpression, as used by previous studies that have examined ^{L597V}BRAF (Ritt *et al.*, 2010; Sarkozy *et al.*, 2009; Wan *et al.*, 2004) is a quick and useful system to introduce rare mutations into cells, but cells in culture accumulate additional mutations that may or may not have been tested for, and cells may behave differently due to long-term cultivation. More importantly, overexpression may perturb the system and not give results that are reflective of those *in vivo*. This was clearly shown in this study whereby overexpression of CRAF inhibited ^{L597V}BRAF-induced MAPK activity, but in the endogenous system, CraF was induced by ^{L597V}Braf and actually contributed to MAPK signalling. Contrasting results from overexpression has also been shown in the

literature. For example, foci formation was observed in ^{WT}BRAF-transfected cells, but not in non-transfected cells that also express ^{WT}BRAF (Sheu *et al.*, 2012). Moreover, in the same study, ^{V600E}BRAF-overexpression was observed to induce DNA damage and cell-cycle arrest (Sheu *et al.*, 2012), whereas previous work by Hong Jin (Biochemistry, Leicester) and in Chapter 3 of this study have shown that endogenous expression of ^{V600E}Braf confers a growth advantage, although MEFs enter a stage of senescence.

A human ^{L597V}BRAF-harboured lung cancer cell line was available through ATCC and was obtained by our lab, but it failed to grow. The cell line also carried other mutations, and was therefore not an ideal model to study ^{L597V}BRAF. Thus, a transgenic mouse model was the best alternative. Cancers harbouring ^{L597V}BRAF are cancers of the epithelium (<http://cancer.sanger.ac.uk/cosmic/gene/analysis?ln=BRAF>). However, it is almost impossible to culture primary epithelial cells, and therefore mouse embryonic fibroblasts were studied predominantly although *in vivo* phenotypes were also assessed by a postdoctoral researcher in our laboratory and published in Andreadi *et al* (2012).

Endogenous mouse systems are not without their disadvantage, and in particular it takes a long time to generate knock-in mice. To induce expression of the mutated protein, Cre recombinase is introduced. It is known that Cre can induce DNA damage, and introduction of Cre has been previously shown to suppress proliferation (Loonstra *et al.*, 2001; Silver & Livingston, 2001). Results were also complicated by individual variation between MEFs, which has been

discussed in Chapter 3. Lastly, MEFs enter a stage of senescence, where cells fail to grow, and during this stage, the MEFs cannot be used for experiments. Therefore only primary cells at an early passage and immortalised cells can be used for experiments. Mutations are accumulated during immortalisation. Therefore the use of immortalised cells can pose the same problem as using cells in long-term culture.

Consistent with previous data (Wan *et al.*, 2004), western blots of HEK 293^T cells overexpressing ^{L597V}BRAF and Braf^{+/Lox-L597V} MEFs show that ^{L597V}BRAF has intermediate kinase activity and has weak Mek/Erk signalling. However, the weak Mek/Erk activity failed to transform cells, failed to provide a growth advantage and did not induce early immortalisation. Therefore ^{L597V}Braf was not deemed to be a driver oncogene. Previous studies have suggested that weak MAPK activity causes the symptoms of RASopathies, as shown by development of RASopathy characteristics in mouse models that have weak MAPK activation (Schuhmacher *et al.*, 2008; Urosevic *et al.*, 2011), and inhibition of MEK prevented abnormal development in zebrafish (Anastasaki *et al.*, 2009; Anastasaki *et al.*, 2012). These studies suggest that the weak Mek/Erk activity of ^{L597V}BRAF is the cause of abnormal development and RASopathy hallmarks in mice as reported by Andreadi *et al.* (2012). Overall, the endogenous system provides a better understanding and provides additional information that simple overexpression cannot provide and has the added advantage that *in vivo* phenotypes can be assessed.

7.3. ^{L597V}Braf is an epistatic modifier of ^{G12D}Kras

Epistasis is the interaction between genes of a different locus (Cordell, 2002). This was documented in chicken combs and flower colour in pea plants as early as 1906 (Bateson, 1906). Epistasis is now researched in causes of human diseases including sickle cell anaemia (Nagel & Steinberg, 2001), systemic lupus erythematosus (Reviewed by Nagel, 2005), cystic fibrosis (Reviewed by Nagel, 2005) and asthma (Freimuth *et al.*, 2012). In sickle cell anaemia, the level of foetal Haemoglobin (HbF) was found to be the most powerful modulator of the clinical and haematological features, by inhibition of polymerisation of deoxy sickle haemoglobin, and prevention of Haemoglobin S (HbS) polymer-induced cellular damage (Nagel & Steinberg, 2001). Genotyping revealed that the level of HbF, encoded on Chromosome 11 was modulated by a single nucleotide polymorphism in BCL11A on Chromosome 2 (Alsultan *et al.*, 2011).

It has been estimated that up to 20 gene mutations are involved in tumourigenesis (Beerenwinkel *et al.*, 2007). The remaining gene mutations are “passenger mutations”. However, it has been suggested that some are epistatic modifiers (Ashworth *et al.*, 2011). Screens have identified potential epistatic modifiers involved in cancer (March *et al.*, 2011). An enrichment of novel modulators of the Wnt pathway were modulated in Apc-mutant mice that developed tumours (March *et al.*, 2011). Although screens have speculated the involvement of epistatically modifying genes in cancer, no studies to date have actually proven their interaction. In this study, it is shown that MEFs with both ^{L597V}Braf and ^{G12D}Kras behave differently to ^{L597V}Braf or ^{G12D}Kras single mutant

MEFs, suggesting epistatic modification. The *in vivo* effects of the mutations in combination were reported by Andreadi et al (2012).

As mentioned, we observed that ^{L597V}BRAF cannot initiate cancer, and ^{L597V}BRAF-expressing cells behave like wild-type cells. Therefore, it is predicted that ^{L597V}BRAF is not a founder mutation, but the frequency of this mutation suggests that it is correlated with cancer (<http://cancer.sanger.ac.uk/cosmic/gene/analysis?ln=BRAF>). Many of these cancers also have other driver mutations, including ^{Q61K}NRAS, ^{Q61R}NRAS, ^{G12S}NRAS, and ^{R759Q}FGFR2 mutations as well as other BRAF mutations including ^{V600E}BRAF and ^{K601E}BRAF (<http://cancer.sanger.ac.uk/cosmic/gene/analysis?ln=BRAF>).

Interestingly, ^{V600E}BRAF is the most frequently observed mutation coincident with Leu597 mutations in human cancer (<http://cancer.sanger.ac.uk/cosmic/gene/analysis?ln=BRAF>). However, cooperation of these two mutations was not examined in this study since it was impossible to obtain live mice containing both the LSL-L597V and LSL-V600E alleles. This is due to inefficient splicing of the LSL cassette which results in expression of only ~10% of the normal protein levels from the LSL alleles and embryos died due to organ failure from a lack of Braf protein (Catrin Pritchard., Unpublished data). However, following Cre recombination, normal levels of protein are expressed. Therefore, one way to circumvent this problem would be to intercross $\text{Braf}^{f+/Lox-L597V}$ animals with $\text{Braf}^{f+/LSL-V600E}$ animals. Since our study has shown that ^{L597V}Braf behaves similarly to ^{WT}Braf, it is safe to speculate that

$Braf^{+/Lox-L597V}$; $Braf^{+/LSL-V600E}$ double mutant animals will be born alive. However, to assess whether $L597V$ BRAF epistatically modifies $V600E$ BRAF, Cre will have to be introduced to induce recombination and expression of $V600E$ Braf. This was not examined due to time restraints and the complication of introducing Cre twice into the animals may make this experiment difficult. An alternative method would be to create a conditional knock-in mouse model that expresses both $L597V$ Braf and $V600E$ Braf on one allele and wild-type Braf, on the other. However, this is time-consuming and could not have materialised in time for his project.

Three different *NRAS* mutations were observed to co-exist with Leu597 mutations in human cancer. However, Nras mouse models were not available in the lab. Instead, the effect of $L597V$ Braf in combination with $G12D$ Kras was assessed. $Braf^{+/LSL-L597V}$ mice were intercrossed with $Kras^{+/LSL-G12D}$ mice to produce double mutants, and data shows that $L597V$ Braf epistatically modifies $G12D$ Kras.

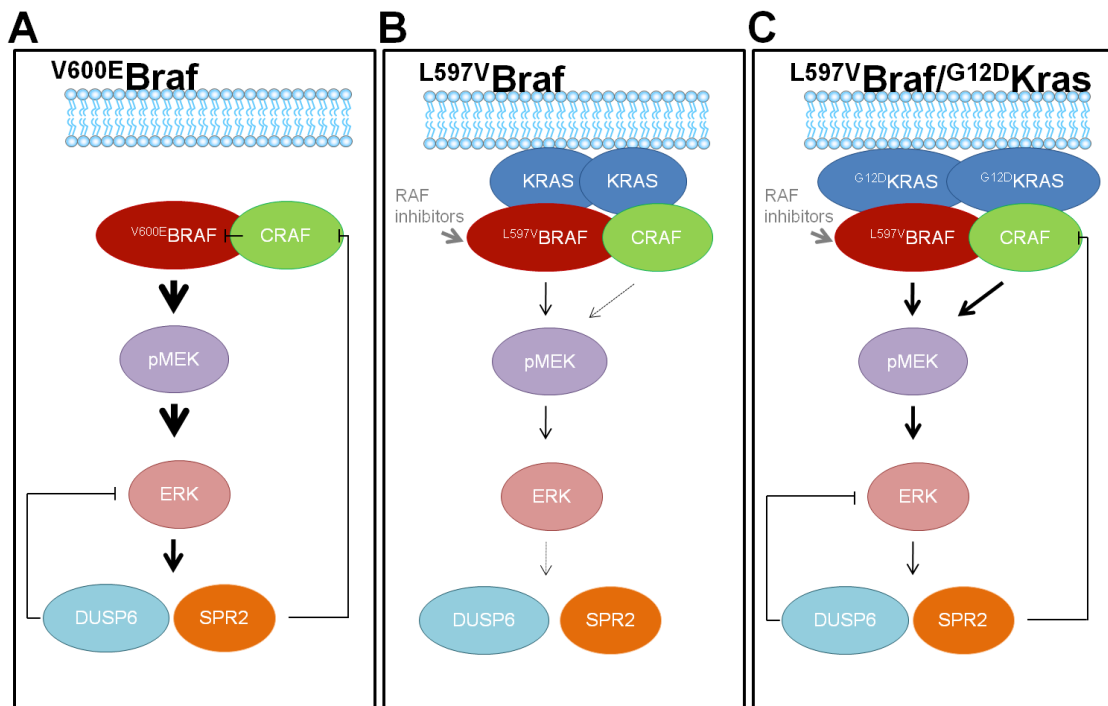
In this study, $L597V$ Braf on Chromosome 7 was found to modify $G12D$ Kras on Chromosome 12. The Braf activity of double mutant MEFs was slightly elevated in comparison with $Kras^{+/Lox-G12D}$ MEFs, but more importantly, the Craf kinase activity was elevated to levels higher than $Braf^{+/Lox-L597V}$ and $Kras^{+/Lox-G12D}$ together. This translated to elevated Mek/Erk activity, and cells were more transformed than $Kras^{+/Lox-G12D}$ MEFs. Transcriptome profiling revealed that double mutant MEFs shared the most gene changes with $Braf^{+/Lox-V600E}$ MEFs, which was more than $Braf^{+/Lox-L597V}$ and $Kras^{+/Lox-G12D}$ MEFs together. This suggests that $L597V$ Braf directs Kras signalling through Mek/Erk, since

V600E BRAF has been shown to signal exclusively through the MAPK pathway (Packer *et al.*, 2009). Double mutant MEFs also had gene changes that were not observed in $\text{Braf}^{+/Lox-L597V}$, $\text{Kras}^{+/Lox-G12D}$ or $\text{Braf}^{+/Lox-V600E}$ MEFs, suggesting that $\text{L}^{597V}\text{Braf}$ induces additional Mek-dependent and independent gene changes in $\text{Kras}^{+/Lox-G12D}$ MEFs. As suggested by kinase assays, this could be through hyperactivation of Crf, which has been previously shown to activate MAPK-dependent and MAPK-independent pathways (Broustas *et al.*, 2002; Ehrenreiter *et al.*, 2005; Jesenberger *et al.*, 2001; Chen *et al.*, 2001; Nantel *et al.*, 1999; Wang *et al.*, 1996). These results are summarised in Figure 7.1. Comparison of gene changes in MEFs transfected with Crf siRNA could be used to confirm whether the gene changes were due to hyperactivation of Crf or not. Treatment of the cells with MEK inhibitors followed by microarray could also be used to identify MEK-dependent and independent effects. Comparison of the two gene sets could be used to identify CRAF-induced MEK-independent pathways.

We tried to identify more cooperating mutations by sequencing tumours arising in $\text{Braf}^{+/Lox-L597V}$ mice. Indeed a $\text{Q}^{61L}\text{Hras}$ mutation was identified in one of the skin papillomas, which is found most commonly in melanomas (<http://cancer.sanger.ac.uk/cosmic/gene/analysis?ln=BRAF>). In this study, only the mutation hotspots in *RAF* and *RAS* were sequenced. Additional mutations could have been exposed if other oncogenes or tumour suppressor proteins had been sequenced or whole genome sequencing had been performed. However, as mentioned before, whole genome sequencing was too expensive

Figure 7.1 A schematic of mechanism of Mek/Erk pathway activation in $\text{Braf}^{+/Lox-L597V}$ and $\text{Braf}^{+/Lox-L597V}; \text{Kras}^{+/Lox-G12D}$ double mutant cells

- A) V600E Braf induces high levels of P-Mek and P-Erk independently of Ras, which leads to activation of negative regulators including Dusp6 and Spry2. Crf inhibits V600E Braf-induced MAPK signalling.
- B) L597V Braf signals through Braf and Crf, but the level of Mek/Erk activation is weak. L597V Braf is able to form a heterodimer with Crf when treated with Braf-specific inhibitors. This leads to transactivation of Crf, and enhanced MAPK signalling.
- C) In the presence of L597V Braf and G12D Kras, L597V Braf and G12D Kras synergise to enhance Mek/Erk-dependent and independent signalling pathways through Crf.



to perform in this particular study but the data provide additional evidence for cooperation between ^{L597V}Braf and ^{G12D}Kras.

7.4. ^{L597V}Braf signals through Braf and Crf

Previous studies have shown the importance of CRAF activity in MEK/ERK signalling of oncogenic RAS (Dumaz *et al.*, 2006), and activation of CRAF was suggested to be involved in paradoxical activation of the MAPK pathway in response to BRAF inhibitors (Heidorn *et al.*, 2010; Poulikakos *et al.*, 2010). It was therefore important to assess the relative contribution of BRAF and CRAF in ^{L597V}BRAF-induced MEK/ERK signalling, and to assess the response of ^{Braf^{+/L597V}} cells to BRAF inhibitors, to determine the effectiveness of these drugs in ^{L597V}BRAF-harbouring cancers and RASopathies.

Kamata *et al* (2010) have shown that the impaired activity ^{D594A}Braf mutant induced early immortalisation linked to induction of aneuploidy, and this was attributed to high Crf activity. Although ^{Braf^{+/Lox-L597V}} MEFs had slightly elevated Crf kinase activity, and siRNA knock-down showed evidence of signalling through Crf, the MEFs did not undergo early immortalisation, and so a role of ^{L597V}Braf in aneuploidy induction was ruled out. Since the ^{Braf^{+/Lox-L597V}}, ^{Kras^{+/Lox-G2D}} double mutant MEFs had excessively high Crf activity and underwent early immortalisation, aneuploidy induction may be more apparent. Therefore, a future goal would be to assess aneuploidy induction in the double mutant MEFs.

7.5. RAF inhibitors induce paradoxical activation of the Mek/Erk pathway in ^{L597V}Braf-expressing cells

Results from inhibitor studies in Chapter 5 show that RAF inhibitors induce heterodimerisation of BRAF and CRAF in ^{L597V}Braf-expressing cells, inducing paradoxical activation of the MAPK pathway. Therefore RAF inhibitors are likely to worsen cancer or RASopathy patients with the ^{L597V}BRAF mutation. It is possible that similar results would be obtained with other intermediate activity mutants such as G464V, G469E and N581S, but this would need to be examined further.

It is intriguing that BRAF inhibitors deplete MEK signalling in cells expressing the high kinase activity mutant ^{V600E}BRAF, but induce paradoxical MEK activation in wild-type cells (data not shown), and in cells expressing the intermediate kinase activity mutant ^{L597V}BRAF. This suggests that RAF inhibitors only inhibit the MAPK activity of high kinase activity mutants, but this leads to the question of what level of BRAF kinase activity is needed for inhibition to be achieved. This question needs to be solved before cancer of RASopathy patients who have non-^{V600E}BRAF are treated with RAF inhibitors. This issue could be resolved by using MEK inhibitors but these have not yet been FDA approved despite multiple clinical trials, as mentioned in Chapter 1.

In this study, we have concentrated on the involvement of the MAPK pathway, but as suggested by transcriptome profiling, MEK-independent activity may also be involved, particularly mediated by CRAF. As mentioned in Chapter 1, CRAF has been found to induce changes independently of MEK by direct binding.

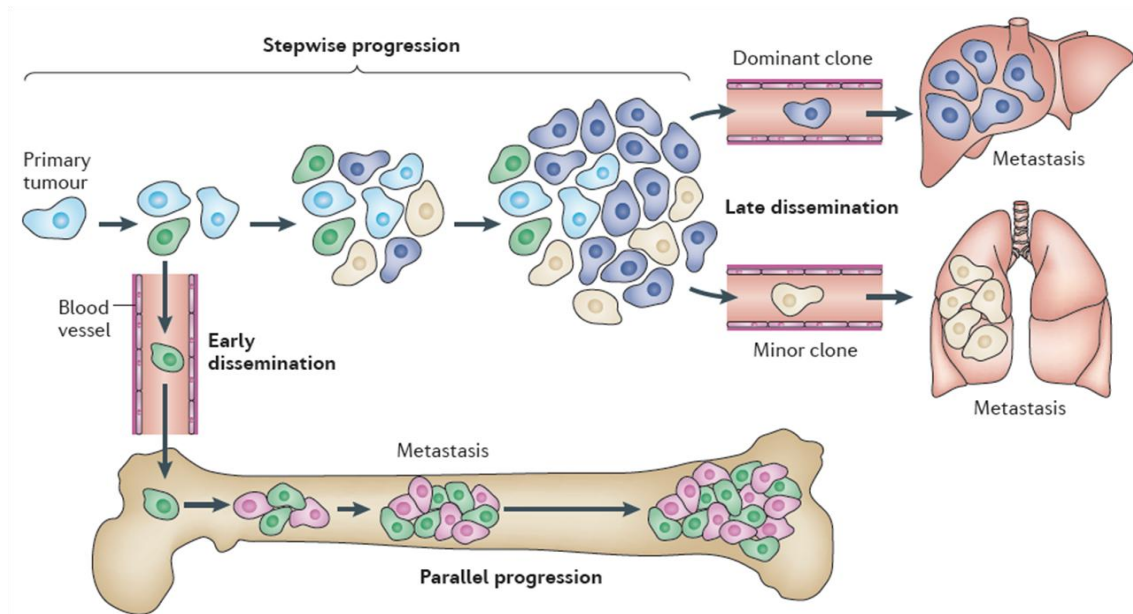
Previous studies have suggested that CRAF directly binds to pRb (Wang *et al.*, 1998), BAD (Wang *et al.*, 1996) and Grb10 (Nantel *et al.*, 1999) to prevent cell death. CRAF has also been shown to induce cell migration by binding to Rok- α (Ehrenreiter *et al.*, 2005) and myosin-binding subunit (Broustas *et al.*, 2002). Binding to MEKK1 was found to enhance NF- κ B expression and cell transformation (Baumann *et al.*, 2000). The high CRAF activity therefore could induce MEK-independent as well as -dependent pathways. In theory, alternative inhibitors will need to be sought to prevent the MEK-independent effects.

7.6. Genetic heterogeneity of tumours with the ^{L597V}BRAF mutation

A previously established model of cancer proposes this to be through survival of genetically unstable cells that accumulate genetic alterations and are presented with a biological fitness advantage (Nowell, 1976). More recently, the extent of tumour genetic heterogeneity has been revealed. A study of renal carcinoma showed that only ~34% of all mutations were detected in all regions of the primary tumour and this was reduced to 31% if pretreatment and metastatic lesions were included (Gerlinger *et al.*, 2012). The observation that some mutations were found solely in the primary or metastatic lesion suggested that further genetic divergence occurred at both sites after tumour dissemination, producing a branching evolutionary pattern of tumour growth (Gerlinger *et al.*, 2012). Two models of tumour progression have been proposed (Figure 7.2) (Reviewed by Marusyk *et al.*, 2012). The stepwise progression model suggested that intra-tumour heterogeneity occurs by accumulation of additional mutations during cell proliferation and increase in tumour mass, and metastasis occurs at the latest stage. The parallel progression model suggests that tumour

Figure 7.2 Two models of tumour progression and heterogeneity (Taken from Marusyk *et al.*, 2012)

Two models of tumour progression have been proposed. In the stepwise progression model, mutations accumulate during growth of the tumour, suggesting intra-tumour heterogeneity and tumour in-semination occurs at the very last stage. Therefore the metastatic lesion contains cells identical to the single clone. In the parallel progression model, tumour in-semination occurs early. Therefore the mutations accumulated in metastatic lesions are diverse and varied.



dissemination occurs early, and therefore differences between metastatic lesions occur. Both of these models suggest tumour heterogeneity and therefore, the primary lesion is unsuitable for diagnostic purposes because of intra-tumour heterogeneity or heterogeneity between metastatic lesions respectively (Reviewed by Marusyk *et al.*, 2012). Understanding heterogeneity is important, since this had been suggested to be one of the causes of drug resistance, as observed in melanoma cells that developed *KRAS* mutations to overcome Vemurafenib-induced apoptosis (Nazarian *et al.*, 2010).

We have shown that ^{L597V}BRAF acts as an epistatic modifier of ^{G12D}KRAS. ^{L597V}BRAF is not a driver mutation, but the enrichment of ^{L597V}BRAF with other mutations suggests that ^{L597V}BRAF acts as a cooperating event. This is likely to indicate that it is acquired as a secondary event rather than being a primary driver. It will be interesting to see if ^{L597V}BRAF mutations are uncovered in more extensive sequencing projects that address genetic heterogeneity. For example, if it is found in particular subclones or metastatic clones.

7.7. Future work

Transcriptome profiling and kinase assays suggest that ^{L597V}Braf in combination with ^{G12D}Kras signal through alternative pathways, and this may be through Crf-induced MEK-independent pathways. Thus future work would be to examine the role of Crf in these cells. To determine whether the gene changes were due to hyperactivation of Crf, the first step would be to use microarray analysis of double mutant MEFs with knock-down of Crf and compare the data with MEFs that have not had Crf knocked-down. Gene profiles could be

compared to MEK inhibitor treatment samples to differentiate between MEK-dependent and MEK-independent activities. It would also be important to examine other effectors of CRAF, which would be revealed by microarray analysis.

It would be important to further understand the role of ^{L597V}BRAF in cancer progression, and to understand at what stage the ^{L597V}BRAF mutation is acquired in tumour development. This could be achieved by sequencing the primary and metastatic tumours.

We have shown that the CraF kinase activity in $Kras^{+/Lox-G12D}$ MEFs is significantly higher than in wild-type MEFs, and the same level of CraF kinase activity in $Braf^{+/Lox-D594A}$ MEFs had been observed to induce aneuploidy (Kamata *et al.*, 2010). Therefore, it is possible that aneuploidy, a key cancer hallmark can be observed in $Kras^{+/Lox-G12D}$ and, in particular, $Braf^{+/Lox-L597V}$; $Kras^{+/Lox-G12D}$ MEFs. Since we have shown that ^{L597V}BRAF epistatically modified ^{G12D}Kras, and one of the effects was an increase in CRAF kinase activity, this suggests that the point at which the ^{L597V}BRAF mutation is acquired may reflect the point at which aneuploidy is induced.

We have suggested that cancer and RASopathy patients harbouring the ^{L597V}BRAF mutation will not benefit from BRAF inhibition as a result of transactivation of CRAF. Therefore CRAF inhibitors, such as GW5074 which are currently in preclinical studies (De La Garza *et al.*, 2012) may be useful for

these patients. Future work will therefore include testing the response of ^{L597V}BRAF-mutant cells to CRAF inhibitors.

8. Appendix

Publications

Andreadi, C., Cheung, L.K., Giblett, S., Patel, B., Jin, H., Mercer, K., Kamata, T., Lee, P., Williams, A., McMahon, M., Marais, R., Pritchard, C., 2012a. **The intermediate-activity (L597V) BRAF mutant acts as an epistatic modifier of oncogenic RAS by enhancing signaling through the RAF/MEK/ERK pathway.** *Genes & Development*. **26**, 1945-1958.

9. References

- Ackermann, J., Frutschi, M., Kaloulis, K., McKee, T., Trumpp, A., Beermann, F., 2005. Metastasizing melanoma formation caused by expression of activated N-RasQ61K on an INK4a-deficient background. *Cancer Research*. **65**, 4005-4011.
- Adjei, A.A., 2005. The role of mitogen-activated ERK-kinase inhibitors in lung cancer therapy. *Clinical Lung Cancer*. **7**, 221-223.
- Agazie, Y.M. & Hayman, M.J., 2003. Molecular mechanism for a role of SHP2 in epidermal growth factor receptor signaling. *Molecular and Cellular Biology*. **23**, 7875-7886.
- Ahmad, I., Iwata, T., Leung, H.Y., 2012. Mechanisms of FGFR-mediated carcinogenesis. *Biochimica Et Biophysica Acta*. **1823**, 850-860.
- Aksamitiene, E., Kholodenko, B.N., Kolch, W., Hoek, J.B., Kiyatkin, A., 2010. PI3K/Akt-sensitive MEK-independent compensatory circuit of ERK activation in ER-positive PI3K-mutant T47D breast cancer cells. *Cellular Signalling*. **22**, 1369-1378.
- Albanese, C., Johnson, J., Watanabe, G., Eklund, N., Vu, D., Arnold, A., Pestell, R.G., 1995. Transforming p21ras mutants and c-Ets-2 activate the cyclin D1 promoter through distinguishable regions. *The Journal of Biological Chemistry*. **270**, 23589-23597.
- Alessi, D.R., Saito, Y., Campbell, D.G., Cohen, P., Sithanandam, G., Rapp, U., Ashworth, A., Marshall, C.J., Cowley, S., 1994. Identification of the sites in MAP kinase kinase-1 phosphorylated by p74raf-1. *The EMBO Journal*. **13**, 1610-1619.
- Allanson, J.E., 2007. Noonan syndrome. *American Journal of Medical Genetics. Part C, Seminars in Medical Genetics*. **145C**, 274-279.
- Al-Mulla, F., Milner-White, E.J., Going, J.J., Birnie, G.D., 1999. Structural differences between valine-12 and aspartate-12 Ras proteins may modify carcinoma aggression. *The Journal of Pathology*. **187**, 433-438.
- Alsultan, A., Solovieff, N., Aleem, A., AlGahtani, F.H., Al-Shehri, A., Osman, M.E., Kurban, K., Bahakim, H., Al-Momen, A.K., Baldwin, C.T., Chui, D.H., Steinberg, M.H., 2011. Fetal hemoglobin in sickle cell anemia: Saudi patients from the Southwestern province have similar HBB haplotypes but higher HbF levels than African Americans. *American Journal of Hematology*. **86**, 612-614.
- Alvarez, E., Northwood, I.C., Gonzalez, F.A., Latour, D.A., Seth, A., Abate, C., Curran, T., Davis, R.J., 1991. Pro-Leu-Ser/Thr-Pro is a consensus primary sequence for substrate protein phosphorylation. Characterization of the phosphorylation of c-myc and c-jun proteins by an epidermal growth factor

receptor threonine 669 protein kinase. *The Journal of Biological Chemistry*. **266**, 15277-15285.

Ameyar, M., Wisniewska, M., Weitzman, J.B., 2003. A role for AP-1 in apoptosis: the case for and against. *Biochimie*. **85**, 747-752.

Anastasaki, C., Estep, A.L., Marais, R., Rauen, K.A., Patton, E.E., 2009. Kinase-activating and kinase-impaired cardio-facio-cutaneous syndrome alleles have activity during zebrafish development and are sensitive to small molecule inhibitors. *Human Molecular Genetics*. **18**, 2543-2554.

Anastasaki, C., Rauen, K.A., Patton, E.E., 2012. Continual low-level MEK inhibition ameliorates cardio-facio-cutaneous phenotypes in zebrafish. *Disease Models & Mechanisms*. **5**, 546-552.

Andreadi, C., Cheung, L.K., Giblett, S., Patel, B., Jin, H., Mercer, K., Kamata, T., Lee, P., Williams, A., McMahon, M., Marais, R., Pritchard, C., 2012a. The intermediate-activity (L597V) BRAF mutant acts as an epistatic modifier of oncogenic RAS by enhancing signaling through the RAF/MEK/ERK pathway. *Genes & Development*. **26**, 1945-1958.

Angel, P. & Karin, M., 1991. The role of Jun, Fos and the AP-1 complex in cell-proliferation and transformation. *Biochimica Et Biophysica Acta*. **1072**, 129-157.

Araki, T., Mohi, M.G., Ismat, F.A., Bronson, R.T., Williams, I.R., Kutok, J.L., Yang, W., Pao, L.I., Gilliland, D.G., Epstein, J.A., Neel, B.G., 2004. Mouse model of Noonan syndrome reveals cell type- and gene dosage-dependent effects of Ptpn11 mutation. *Nature Medicine*. **10**, 849-857.

Arnault, J.P., Mateus, C., Escudier, B., Tomasic, G., Wechsler, J., Hollville, E., Soria, J.C., Malka, D., Sarasin, A., Larcher, M., Andre, J., Kamsu-Kom, N., Boussemart, L., Lacroix, L., Spatz, A., Eggermont, A.M., Druillennec, S., Vagner, S., Eychene, A., Dumaz, N., Robert, C., 2012. Skin tumors induced by sorafenib; paradoxical RAS-RAF pathway activation and oncogenic mutations of HRAS, TP53, and TGFBR1. *Clinical Cancer Research : An Official Journal of the American Association for Cancer Research*. **18**, 263-272.

Ashworth, A., Lord, C.J., Reis-Filho, J.S., 2011. Genetic interactions in cancer progression and treatment. *Cell*. **145**, 30-38.

Atkins, M.B., Hsu, J., Lee, S., Cohen, G.I., Flaherty, L.E., Sosman, J.A., Sondak, V.K., Kirkwood, J.M., Eastern Cooperative Oncology Group, 2008. Phase III trial comparing concurrent biochemotherapy with cisplatin, vinblastine, dacarbazine, interleukin-2, and interferon alfa-2b with cisplatin, vinblastine, and dacarbazine alone in patients with metastatic malignant melanoma (E3695): a trial coordinated by the Eastern Cooperative Oncology Group. *Journal of Clinical Oncology : Official Journal of the American Society of Clinical Oncology*. **26**, 5748-5754.

- Bader, J.L. & Miller, R.W., 1978. Neurofibromatosis and childhood leukemia. *The Journal of Pediatrics*. **92**, 925-929.
- Balan, V., Leicht, D.T., Zhu, J., Balan, K., Kaplun, A., Singh-Gupta, V., Qin, J., Ruan, H., Comb, M.J., Tzivion, G., 2006. Identification of novel in vivo Raf-1 phosphorylation sites mediating positive feedback Raf-1 regulation by extracellular signal-regulated kinase. *Molecular Biology of the Cell*. **17**, 1141-1153.
- Balmanno, K., Chell, S.D., Gillings, A.S., Hayat, S., Cook, S.J., 2009. Intrinsic resistance to the MEK1/2 inhibitor AZD6244 (ARRY-142886) is associated with weak ERK1/2 signalling and/or strong PI3K signalling in colorectal cancer cell lines. *International Journal of Cancer. Journal International Du Cancer*. **125**, 2332-2341.
- Balmanno, K. & Cook, S.J., 1999. Sustained MAP kinase activation is required for the expression of cyclin D1, p21Cip1 and a subset of AP-1 proteins in CCL39 cells. *Oncogene*. **18**, 3085-3097.
- Barnier, J.V., Papin, C., Eychene, A., Lecoq, O., Calothy, G., 1995. The mouse B-raf gene encodes multiple protein isoforms with tissue-specific expression. *The Journal of Biological Chemistry*. **270**, 23381-23389.
- Bar-Sagi, D. & Hall, A., 2000. Ras and Rho GTPases: a family reunion. *Cell*. **103**, 227-238.
- Bates, S., Phillips, A.C., Clark, P.A., Stott, F., Peters, G., Ludwig, R.L., Vousden, K.H., 1998. p14ARF links the tumour suppressors RB and p53. *Nature*. **395**, 124-125.
- Baumann, B., Weber, C.K., Troppmair, J., Whiteside, S., Israel, A., Rapp, U.R., Wirth, T., 2000. Raf induces NF-kappaB by membrane shuttle kinase MEKK1, a signaling pathway critical for transformation. *Proceedings of the National Academy of Sciences of the United States of America*. **97**, 4615-4620.
- Beerenwinkel, N., Antal, T., Dingli, D., Traulsen, A., Kinzler, K.W., Velculescu, V.E., Vogelstein, B., Nowak, M.A., 2007. Genetic progression and the waiting time to cancer. *PLoS Computational Biology*. **3**, e225.
- Bentires-Alj, M., Kontaridis, M.I., Neel, B.G., 2006. Stops along the RAS pathway in human genetic disease. *Nature Medicine*. **12**, 283-285.
- Berger, D.H., Jardines, L.A., Chang, H., Ruggeri, B., 1997. Activation of Raf-1 in human pancreatic adenocarcinoma. *The Journal of Surgical Research*. **69**, 199-204.
- Bermudez, O., Marchetti, S., Pages, G., Gimond, C., 2008. Post-translational regulation of the ERK phosphatase DUSP6/MKP3 by the mTOR pathway. *Oncogene*. **27**, 3685-3691.

- Blasco, R.B., Francoz, S., Santamaria, D., Canamero, M., Dubus, P., Charron, J., Baccarini, M., Barbacid, M., 2011. c-Raf, but not B-Raf, is essential for development of K-Ras oncogene-driven non-small cell lung carcinoma. *Cancer Cell*. **19**, 652-663.
- Blivet-Van Eggelpoel, M.J., Chettouh, H., Fartoux, L., Aoudjehane, L., Barbu, V., Rey, C., Priam, S., Housset, C., Rosmorduc, O., Desbois-Mouthon, C., 2012. Epidermal growth factor receptor and HER-3 restrict cell response to sorafenib in hepatocellular carcinoma cells. *Journal of Hepatology*. **57**, 108-115.
- Boasberg, P.D., Redfern, C.H., Daniels, G.A., Bodkin, D., Garrett, C.R., Ricart, A.D., 2011. Pilot study of PD-0325901 in previously treated patients with advanced melanoma, breast cancer, and colon cancer. *Cancer Chemotherapy and Pharmacology*. **68**, 547-552.
- Bos, J.L., 1989. Ras Oncogenes in Human Cancer: a Review. *Cancer Research*. **49**, 4682-4689.
- Bos, J.L., Rehmann, H., Wittinghofer, A., 2007. GEFs and GAPs: critical elements in the control of small G proteins. *Cell*. **129**, 865-877.
- Bosch, E., Cherwinski, H., Peterson, D., McMahon, M., 1997. Mutations of critical amino acids affect the biological and biochemical properties of oncogenic A-Raf and Raf-1. *Oncogene*. **15**, 1021-1033.
- Boutros, T., Chevet, E., Metrakos, P., 2008. Mitogen-activated protein (MAP) kinase/MAP kinase phosphatase regulation: roles in cell growth, death, and cancer. *Pharmacological Reviews*. **60**, 261-310.
- Bowe, D.B., Kenney, N.J., Adereth, Y., Maroulakou, I.G., 2002. Suppression of Neu-induced mammary tumor growth in cyclin D1 deficient mice is compensated for by cyclin E. *Oncogene*. **21**, 291-298.
- Brady, S.C., Coleman, M.L., Munro, J., Feller, S.M., Morrice, N.A., Olson, M.F., 2009. Sprouty2 association with B-Raf is regulated by phosphorylation and kinase conformation. *Cancer Research*. **69**, 6773-6781.
- Brondello, J.M., Brunet, A., Pouyssegur, J., McKenzie, F.R., 1997. The dual specificity mitogen-activated protein kinase phosphatase-1 and -2 are induced by the p42/p44MAPK cascade. *The Journal of Biological Chemistry*. **272**, 1368-1376.
- Brondello, J.M., Pouyssegur, J., McKenzie, F.R., 1999. Reduced MAP kinase phosphatase-1 degradation after p42/p44MAPK-dependent phosphorylation. *Science (New York, N.Y.)*. **286**, 2514-2517.
- Broustas, C.G., Grammatikakis, N., Eto, M., Dent, P., Brautigan, D.L., Kasid, U., 2002. Phosphorylation of the myosin-binding subunit of myosin phosphatase by Raf-1 and inhibition of phosphatase activity. *The Journal of Biological Chemistry*. **277**, 3053-3059.

- Brown, J.R., Nigh, E., Lee, R.J., Ye, H., Thompson, M.A., Saudou, F., Pestell, R.G., Greenberg, M.E., 1998. Fos family members induce cell cycle entry by activating cyclin D1. *Molecular and Cellular Biology*. **18**, 5609-5619.
- Cabrita, M.A. & Christofori, G., 2008. Sprouty proteins, masterminds of receptor tyrosine kinase signaling. *Angiogenesis*. **11**, 53-62.
- Camps, M., Nichols, A., Arkinstall, S., 2000. Dual specificity phosphatases: a gene family for control of MAP kinase function. *FASEB Journal : Official Publication of the Federation of American Societies for Experimental Biology*. **14**, 6-16.
- Cargnello, M. & Roux, P.P., 2011. Activation and function of the MAPKs and their substrates, the MAPK-activated protein kinases. *Microbiology and Molecular Biology Reviews : MMBR*. **75**, 50-83.
- Carragher, L.A., Snell, K.R., Giblett, S.M., Aldridge, V.S., Patel, B., Cook, S.J., Winton, D.J., Marais, R., Pritchard, C.A., 2010. V600EBraf induces gastrointestinal crypt senescence and promotes tumour progression through enhanced CpG methylation of p16INK4a. *EMBO Molecular Medicine*. **2**, 458-471.
- Casar, B., Arozarena, I., Sanz-Moreno, V., Pinto, A., Agudo-Ibanez, L., Marais, R., Lewis, R.E., Berciano, M.T., Crespo, P., 2009a. Ras subcellular localization defines extracellular signal-regulated kinase 1 and 2 substrate specificity through distinct utilization of scaffold proteins. *Molecular and Cellular Biology*. **29**, 1338-1353.
- Casar, B., Pinto, A., Crespo, P., 2009b. ERK dimers and scaffold proteins: unexpected partners for a forgotten (cytoplasmic) task. *Cell Cycle (Georgetown, Tex.)*. **8**, 1007-1013.
- Casci, T., Vinos, J., Freeman, M., 1999. Sprouty, an intracellular inhibitor of Ras signaling. *Cell*. **96**, 655-665.
- Catling, A.D., Schaeffer, H.J., Reuter, C.W., Reddy, G.R., Weber, M.J., 1995. A proline-rich sequence unique to MEK1 and MEK2 is required for raf binding and regulates MEK function. *Molecular and Cellular Biology*. **15**, 5214-5225.
- Champion, K.J., Bunag, C., Estep, A.L., Jones, J.R., Bolt, C.H., Rogers, R.C., Rauen, K.A., Everman, D.B., 2011. Germline mutation in BRAF codon 600 is compatible with human development: de novo p.V600G mutation identified in a patient with CFC syndrome. *Clinical Genetics*. **79**, 468-474.
- Chan, D.W., Liu, V.W., Tsao, G.S., Yao, K.M., Furukawa, T., Chan, K.K., Ngan, H.Y., 2008. Loss of MKP3 mediated by oxidative stress enhances tumorigenicity and chemoresistance of ovarian cancer cells. *Carcinogenesis*. **29**, 1742-1750.

- Chan, J.M., Stampfer, M.J., Giovannucci, E., Gann, P.H., Ma, J., Wilkinson, P., Hennekens, C.H., Pollak, M., 1998. Plasma insulin-like growth factor-I and prostate cancer risk: a prospective study. *Science (New York, N.Y.)*. **279**, 563-566.
- Chapman, P.B., Einhorn, L.H., Meyers, M.L., Saxman, S., Destro, A.N., Panageas, K.S., Begg, C.B., Agarwala, S.S., Schuchter, L.M., Ernstoff, M.S., Houghton, A.N., Kirkwood, J.M., 1999. Phase III multicenter randomized trial of the Dartmouth regimen versus dacarbazine in patients with metastatic melanoma. *Journal of Clinical Oncology : Official Journal of the American Society of Clinical Oncology*. **17**, 2745-2751.
- Chapman, P.B., Hauschild, A., Robert, C., Haanen, J.B., Ascierto, P., Larkin, J., Dummer, R., Garbe, C., Testori, A., Maio, M., Hogg, D., Lorigan, P., Lebbe, C., Jouary, T., Schadendorf, D., Ribas, A., O'Day, S.J., Sosman, J.A., Kirkwood, J.M., Eggermont, A.M., Dreno, B., Nolop, K., Li, J., Nelson, B., Hou, J., Lee, R.J., Flaherty, K.T., McArthur, G.A., BRIM-3 Study Group, 2011. Improved survival with vemurafenib in melanoma with BRAF V600E mutation. *The New England Journal of Medicine*. **364**, 2507-2516.
- Chen, J., Fujii, K., Zhang, L., Roberts, T., Fu, H., 2001. Raf-1 promotes cell survival by antagonizing apoptosis signal-regulating kinase 1 through a MEK-ERK independent mechanism. *Proceedings of the National Academy of Sciences of the United States of America*. **98**, 7783-7788.
- Chen, K.F., Chen, H.L., Tai, W.T., Feng, W.C., Hsu, C.H., Chen, P.J., Cheng, A.L., 2011. Activation of phosphatidylinositol 3-kinase/Akt signaling pathway mediates acquired resistance to sorafenib in hepatocellular carcinoma cells. *The Journal of Pharmacology and Experimental Therapeutics*. **337**, 155-161.
- Chen, P.C., Wakimoto, H., Conner, D., Araki, T., Yuan, T., Roberts, A., Seidman, C., Bronson, R., Neel, B., Seidman, J.G., Kucherlapati, R., 2010. Activation of multiple signaling pathways causes developmental defects in mice with a Noonan syndrome-associated Sos1 mutation. *The Journal of Clinical Investigation*. **120**, 4353-4365.
- Cheung, M., Sharma, A., Madhunapantula, S.V., Robertson, G.P., 2008. Akt3 and mutant V600E B-Raf cooperate to promote early melanoma development. *Cancer Research*. **68**, 3429-3439.
- Choi, Y.J., Li, X., Hydbring, P., Sanda, T., Stefano, J., Christie, A.L., Signoretti, S., Look, A.T., Kung, A.L., von Boehmer, H., Sicinski, P., 2012. The requirement for cyclin d function in tumor maintenance. *Cancer Cell*. **22**, 438-451.
- Chong, H., Lee, J., Guan, K.L., 2001. Positive and negative regulation of Raf kinase activity and function by phosphorylation. *The EMBO Journal*. **20**, 3716-3727.

- Choong, K., Freedman, M.H., Chitayat, D., Kelly, E.N., Taylor, G., Zipursky, A., 1999. Juvenile myelomonocytic leukemia and Noonan syndrome. *Journal of Pediatric hematology/oncology*. **21**, 523-527.
- Cin, H., Meyer, C., Herr, R., Janzarik, W.G., Lambert, S., Jones, D.T., Jacob, K., Benner, A., Witt, H., Remke, M., Bender, S., Falkenstein, F., Van Anh, T.N., Olbrich, H., von Deimling, A., Pekrun, A., Kulozik, A.E., Gnekow, A., Scheurlen, W., Witt, O., Omran, H., Jabado, N., Collins, V.P., Brummer, T., Marschalek, R., Lichter, P., Korshunov, A., Pfister, S.M., 2011. Oncogenic FAM131B-BRAF fusion resulting from 7q34 deletion comprises an alternative mechanism of MAPK pathway activation in pilocytic astrocytoma. *Acta Neuropathologica*. **121**, 763-774.
- Corbalan-Garcia, S., Yang, S.S., Degenhardt, K.R., Bar-Sagi, D., 1996. Identification of the mitogen-activated protein kinase phosphorylation sites on human Sos1 that regulate interaction with Grb2. *Molecular and Cellular Biology*. **16**, 5674-5682.
- Corcoran, R.B., Dias-Santagata, D., Bergethon, K., Iafrate, A.J., Settleman, J., Engelman, J.A., 2010. BRAF gene amplification can promote acquired resistance to MEK inhibitors in cancer cells harboring the BRAF V600E mutation. *Science Signaling*. **3**, ra84.
- Corcoran, R.B., Ebi, H., Turke, A.B., Coffee, E.M., Nishino, M., Cogdill, A.P., Brown, R.D., Pelle, P.D., Dias-Santagata, D., Hung, K.E., Flaherty, K.T., Piris, A., Wargo, J.A., Settleman, J., Mino-Kenudson, M., Engelman, J.A., 2012. EGFR-mediated re-activation of MAPK signaling contributes to insensitivity of BRAF mutant colorectal cancers to RAF inhibition with vemurafenib. *Cancer Discovery*. **2**, 227-235.
- Cordell, H.J., 2002. Epistasis: what it means, what it doesn't mean, and statistical methods to detect it in humans. *Human Molecular Genetics*. **11**, 2463-2468.
- Costello, J.M., 1977. A new syndrome: mental subnormality and nasal papillomata. *Australian Paediatric Journal*. **13**, 114-118.
- Cruz, F., 3rd, Rubin, B.P., Wilson, D., Town, A., Schroeder, A., Haley, A., Bainbridge, T., Heinrich, M.C., Corless, C.L., 2003. Absence of BRAF and NRAS mutations in uveal melanoma. *Cancer Research*. **63**, 5761-5766.
- Dadzie, O.E., Yang, S., Emley, A., Keady, M., Bhawan, J., Mahalingam, M., 2009. RAS and RAF mutations in banal melanocytic aggregates contiguous with primary cutaneous melanoma: clues to melanomagenesis. *The British Journal of Dermatology*. **160**, 368-375.
- Dail, M., Li, Q., McDaniel, A., Wong, J., Akagi, K., Huang, B., Kang, H.C., Kogan, S.C., Shokat, K., Wolff, L., Braun, B.S., Shannon, K., 2010. Mutant Irf1, KrasG12D, and Notch1 cooperate in T lineage leukemogenesis and

modulate responses to targeted agents. *Proceedings of the National Academy of Sciences of the United States of America*. **107**, 5106-5111.

Dalby, K.N., Morrice, N., Caudwell, F.B., Avruch, J., Cohen, P., 1998. Identification of regulatory phosphorylation sites in mitogen-activated protein kinase (MAPK)-activated protein kinase-1a/p90rsk that are inducible by MAPK. *The Journal of Biological Chemistry*. **273**, 1496-1505.

Daniotti, M., Oggionni, M., Ranzani, T., Vallacchi, V., Campi, V., Di Stasi, D., Torre, G.D., Perrone, F., Luoni, C., Suardi, S., Frattini, M., Pilotti, S., Anichini, A., Tragni, G., Parmiani, G., Pierotti, M.A., Rodolfo, M., 2004. BRAF alterations are associated with complex mutational profiles in malignant melanoma. *Oncogene*. **23**, 5968-5977.

Dankort, D., Filenova, E., Collado, M., Serrano, M., Jones, K., McMahon, M., 2007. A new mouse model to explore the initiation, progression, and therapy of BRAFV600E-induced lung tumors. *Genes & Development*. **21**, 379-384.

Davie, J.R. & Spencer, V.A., 1999. Control of histone modifications. *Journal of Cellular Biochemistry*. **Suppl 32-33**, 141-148.

Davies, B.R., Logie, A., McKay, J.S., Martin, P., Steele, S., Jenkins, R., Cockerill, M., Cartlidge, S., Smith, P.D., 2007. AZD6244 (ARRY-142886), a potent inhibitor of mitogen-activated protein kinase/extracellular signal-regulated kinase 1/2 kinases: mechanism of action in vivo, pharmacokinetic/pharmacodynamic relationship, and potential for combination in preclinical models. *Molecular Cancer Therapeutics*. **6**, 2209-2219.

Davies, H., Bignell, G.R., Cox, C., Stephens, P., Edkins, S., Clegg, S., Teague, J., Woffendin, H., Garnett, M.J., Bottomley, W., Davis, N., Dicks, E., Ewing, R., Floyd, Y., Gray, K., Hall, S., Hawes, R., Hughes, J., Kosmidou, V., Menzies, A., Mould, C., Parker, A., Stevens, C., Watt, S., Hooper, S., Wilson, R., Jayatilake, H., Gusterson, B.A., Cooper, C., Shipley, J., Hargrave, D., Pritchard-Jones, K., Maitland, N., Chenevix-Trench, G., Riggins, G.J., Bigner, D.D., Palmieri, G., Cossu, A., Flanagan, A., Nicholson, A., Ho, J.W., Leung, S.Y., Yuen, S.T., Weber, B.L., Seigler, H.F., Darrow, T.L., Paterson, H., Marais, R., Marshall, C.J., Wooster, R., Stratton, M.R., Futreal, P.A., 2002. Mutations of the BRAF gene in human cancer. *Nature*. **417**, 949-954.

Davis, I.J., Hazel, T.G., Chen, R.H., Blenis, J., Lau, L.F., 1993. Functional domains and phosphorylation of the orphan receptor Nur77. *Molecular Endocrinology (Baltimore, Md.)*. **7**, 953-964.

De La Garza, E.M., Binkley, P.A., Ganapathy, M., Krishnegowda, N.K., Tekmal, R.R., Schenken, R.S., Kirma, N.B., 2012. Raf-1, a potential therapeutic target, mediates early steps in endometriosis lesion development by endometrial epithelial and stromal cells. *Endocrinology*. **153**, 3911-3921.

- Deng, X., Ruvolo, P., Carr, B., May, W.S., Jr, 2000. Survival function of ERK1/2 as IL-3-activated, staurosporine-resistant Bcl2 kinases. *Proceedings of the National Academy of Sciences of the United States of America*. **97**, 1578-1583.
- Denkert, C., Schmitt, W.D., Berger, S., Reles, A., Pest, S., Siegert, A., Lichtenegger, W., Dietel, M., Hauptmann, S., 2002. Expression of mitogen-activated protein kinase phosphatase-1 (MKP-1) in primary human ovarian carcinoma. *International Journal of Cancer. Journal International Du Cancer*. **102**, 507-513.
- Dhawan, P., Singh, A.B., Ellis, D.L., Richmond, A., 2002. Constitutive activation of Akt/protein kinase B in melanoma leads to up-regulation of nuclear factor- κ B and tumor progression. *Cancer Research*. **62**, 7335-7342.
- Dhomen, N., Reis-Filho, J.S., da Rocha Dias, S., Hayward, R., Savage, K., Delmas, V., Larue, L., Pritchard, C., Marais, R., 2009. Oncogenic Braf induces melanocyte senescence and melanoma in mice. *Cancer Cell*. **15**, 294-303.
- Diaz, L.A., Jr, Williams, R.T., Wu, J., Kinde, I., Hecht, J.R., Berlin, J., Allen, B., Bozic, I., Reiter, J.G., Nowak, M.A., Kinzler, K.W., Oliner, K.S., Vogelstein, B., 2012. The molecular evolution of acquired resistance to targeted EGFR blockade in colorectal cancers. *Nature*. **486**, 537-540.
- Dibb, N.J., Dilworth, S.M., Mol, C.D., 2004. Switching on kinases: oncogenic activation of BRAF and the PDGFR family. *Nature Reviews. Cancer*. **4**, 718-727.
- Dickinson, R.J., Williams, D.J., Slack, D.N., Williamson, J., Seternes, O.M., Keyse, S.M., 2002. Characterization of a murine gene encoding a developmentally regulated cytoplasmic dual-specificity mitogen-activated protein kinase phosphatase. *The Biochemical Journal*. **364**, 145-155.
- Digilio, M.C., Sarkozy, A., de Zorzi, A., Pacileo, G., Limongelli, G., Mingarelli, R., Calabro, R., Marino, B., Dallapiccola, B., 2006. LEOPARD syndrome: clinical diagnosis in the first year of life. *American Journal of Medical Genetics. Part A*. **140**, 740-746.
- Ding, Q., Gros, R., Gray, I.D., Taussig, R., Ferguson, S.S., Feldman, R.D., 2004. Raf kinase activation of adenylyl cyclases: isoform-selective regulation. *Molecular Pharmacology*. **66**, 921-928.
- Dougherty, M.K., Muller, J., Ritt, D.A., Zhou, M., Zhou, X.Z., Copeland, T.D., Conrads, T.P., Veenstra, T.D., Lu, K.P., Morrison, D.K., 2005. Regulation of Raf-1 by direct feedback phosphorylation. *Molecular Cell*. **17**, 215-224.
- Dowd, S., Sneddon, A.A., Keyse, S.M., 1998. Isolation of the human genes encoding the pyst1 and Pyst2 phosphatases: characterisation of Pyst2 as a cytosolic dual-specificity MAP kinase phosphatase and its catalytic activation by both MAP and SAP kinases. *Journal of Cell Science*. **111 (Pt 22)**, 3389-3399.

- Downward, J., 2003. Targeting RAS signalling pathways in cancer therapy. *Nature Reviews.Cancer*. **3**, 11-22.
- Dugan, L.L., Kim, J.S., Zhang, Y., Bart, R.D., Sun, Y., Holtzman, D.M., Gutmann, D.H., 1999. Differential effects of cAMP in neurons and astrocytes. Role of B-raf. *The Journal of Biological Chemistry*. **274**, 25842-25848.
- Dumaz, N., Hayward, R., Martin, J., Ogilvie, L., Hedley, D., Curtin, J.A., Bastian, B.C., Springer, C., Marais, R., 2006. In melanoma, RAS mutations are accompanied by switching signaling from BRAF to CRAF and disrupted cyclic AMP signaling. *Cancer Research*. **66**, 9483-9491.
- Easty, D.J., Gray, S.G., O'Byrne, K.J., O'Donnell, D., Bennett, D.C., 2011. Receptor tyrosine kinases and their activation in melanoma. *Pigment Cell & Melanoma Research*. **24**, 446-461.
- Eblen, S.T., Slack-Davis, J.K., Tarcsafalvi, A., Parsons, J.T., Weber, M.J., Catling, A.D., 2004. Mitogen-activated protein kinase feedback phosphorylation regulates MEK1 complex formation and activation during cellular adhesion. *Molecular and Cellular Biology*. **24**, 2308-2317.
- Ehrenreiter, K., Piazzolla, D., Velamoor, V., Sobczak, I., Small, J.V., Takeda, J., Leung, T., Baccarini, M., 2005. Raf-1 regulates Rho signaling and cell migration. *The Journal of Cell Biology*. **168**, 955-964.
- Ekerot, M., Stavridis, M.P., Delavaine, L., Mitchell, M.P., Staples, C., Owens, D.M., Keenan, I.D., Dickinson, R.J., Storey, K.G., Keyse, S.M., 2008. Negative-feedback regulation of FGF signalling by DUSP6/MKP-3 is driven by ERK1/2 and mediated by Ets factor binding to a conserved site within the DUSP6/MKP-3 gene promoter. *The Biochemical Journal*. **412**, 287-298.
- Emery, C.M., Vijayendran, K.G., Zipser, M.C., Sawyer, A.M., Niu, L., Kim, J.J., Hatton, C., Chopra, R., Oberholzer, P.A., Karpova, M.B., MacConaill, L.E., Zhang, J., Gray, N.S., Sellers, W.R., Dummer, R., Garraway, L.A., 2009. MEK1 mutations confer resistance to MEK and B-RAF inhibition. *Proceedings of the National Academy of Sciences of the United States of America*. **106**, 20411-20416.
- Emuss, V., Garnett, M., Mason, C., Marais, R., 2005. Mutations of C-RAF are rare in human cancer because C-RAF has a low basal kinase activity compared with B-RAF. *Cancer Research*. **65**, 9719-9726.
- Engelman, J.A., Chen, L., Tan, X., Crosby, K., Guimaraes, A.R., Upadhyay, R., Maira, M., McNamara, K., Perera, S.A., Song, Y., Chirieac, L.R., Kaur, R., Lightbown, A., Simendinger, J., Li, T., Padera, R.F., Garcia-Echeverria, C., Weissleder, R., Mahmood, U., Cantley, L.C., Wong, K.K., 2008. Effective use of PI3K and MEK inhibitors to treat mutant Kras G12D and PIK3CA H1047R murine lung cancers. *Nature Medicine*. **14**, 1351-1356.

Escudier, B., Eisen, T., Stadler, W.M., Szczyluk, C., Oudard, S., Siebels, M., Negrier, S., Chevreau, C., Solska, E., Desai, A.A., Rolland, F., Demkow, T., Hutson, T.E., Gore, M., Freeman, S., Schwartz, B., Shan, M., Simantov, R., Bukowski, R.M., TARGET Study Group, 2007. Sorafenib in advanced clear-cell renal-cell carcinoma. *The New England Journal of Medicine*. **356**, 125-134.

Falkson, C.I., Ibrahim, J., Kirkwood, J.M., Coates, A.S., Atkins, M.B., Blum, R.H., 1998. Phase III trial of dacarbazine versus dacarbazine with interferon alpha-2b versus dacarbazine with tamoxifen versus dacarbazine with interferon alpha-2b and tamoxifen in patients with metastatic malignant melanoma: an Eastern Cooperative Oncology Group study. *Journal of Clinical Oncology : Official Journal of the American Society of Clinical Oncology*. **16**, 1743-1751.

Farooq, A. & Zhou, M.M., 2004. Structure and regulation of MAPK phosphatases. *Cellular Signalling*. **16**, 769-779.

Farrar, M.A., Alberol-Ila, J., Perlmutter, R.M., 1996. Activation of the Raf-1 kinase cascade by coumermycin-induced dimerization. *Nature*. **383**, 178-181.

FAU, L.A., et al, 1116. Premature senescence involving p53 and p16 is activated in response to constitutive MEK/MAPK mitogenic signaling.

Favata, M.F., Horiuchi, K.Y., Manos, E.J., Daulerio, A.J., Stradley, D.A., Feeser, W.S., Van Dyk, D.E., Pitts, W.J., Earl, R.A., Hobbs, F., Copeland, R.A., Magolda, R.L., Scherle, P.A., Trzaskos, J.M., 1998. Identification of a novel inhibitor of mitogen-activated protein kinase kinase. *The Journal of Biological Chemistry*. **273**, 18623-18632.

Ferlay, J., Shin, H.R., Bray, F., Forman, D., Mathers, C., Parkin, D.M., 2010. Estimates of worldwide burden of cancer in 2008: GLOBOCAN 2008. *International Journal of Cancer. Journal International Du Cancer*. **127**, 2893-2917.

Fischer, A., Hekman, M., Kuhlmann, J., Rubio, I., Wiese, S., Rapp, U.R., 2007. B- and C-RAF display essential differences in their binding to Ras: the isotype-specific N terminus of B-RAF facilitates Ras binding. *The Journal of Biological Chemistry*. **282**, 26503-26516.

Fischmann, T.O., Smith, C.K., Mayhood, T.W., Myers, J.E., Reichert, P., Mannarino, A., Carr, D., Zhu, H., Wong, J., Yang, R.S., Le, H.V., Madison, V.S., 2009. Crystal structures of MEK1 binary and ternary complexes with nucleotides and inhibitors. *Biochemistry*. **48**, 2661-2674.

Flaherty, K.T., Infante, J.R., Daud, A., Gonzalez, R., Kefford, R.F., Sosman, J., Hamid, O., Schuchter, L., Cebon, J., Ibrahim, N., Kudchadkar, R., Burris, H.A., 3rd, Falchook, G., Algazi, A., Lewis, K., Long, G.V., Puzanov, I., Lebowitz, P., Singh, A., Little, S., Sun, P., Allred, A., Ouellet, D., Kim, K.B., Patel, K., Weber, J., 2012. Combined BRAF and MEK inhibition in melanoma with BRAF V600 mutations. *The New England Journal of Medicine*. **367**, 1694-1703.

- Flaherty, K.T., Puzanov, I., Kim, K.B., Ribas, A., McArthur, G.A., Sosman, J.A., O'Dwyer, P.J., Lee, R.J., Grippo, J.F., Nolop, K., Chapman, P.B., 2010. Inhibition of mutated, activated BRAF in metastatic melanoma. *The New England Journal of Medicine*. **363**, 809-819.
- Folkman, J., 1971. Tumor angiogenesis: therapeutic implications. *The New England Journal of Medicine*. **285**, 1182-1186.
- Fong, C.W., Chua, M.S., McKie, A.B., Ling, S.H., Mason, V., Li, R., Yusoff, P., Lo, T.L., Leung, H.Y., So, S.K., Guy, G.R., 2006. Sprouty 2, an inhibitor of mitogen-activated protein kinase signaling, is down-regulated in hepatocellular carcinoma. *Cancer Research*. **66**, 2048-2058.
- Forsheaw, T., Tatevossian, R.G., Lawson, A.R., Ma, J., Neale, G., Ogunkolade, B.W., Jones, T.A., Aarum, J., Dalton, J., Bailey, S., Chaplin, T., Carter, R.L., Gajjar, A., Broniscer, A., Young, B.D., Ellison, D.W., Sheer, D., 2009. Activation of the ERK/MAPK pathway: a signature genetic defect in posterior fossa pilocytic astrocytomas. *The Journal of Pathology*. **218**, 172-181.
- Franklin, C.C. & Kraft, A.S., 1997. Conditional expression of the mitogen-activated protein kinase (MAPK) phosphatase MKP-1 preferentially inhibits p38 MAPK and stress-activated protein kinase in U937 cells. *The Journal of Biological Chemistry*. **272**, 16917-16923.
- Freed, E., Symons, M., Macdonald, S.G., McCormick, F., Ruggieri, R., 1994. Binding of 14-3-3 proteins to the protein kinase Raf and effects on its activation. *Science (New York, N.Y.)*. **265**, 1713-1716.
- Freimuth, J., Clermont, F.F., Huang, X., DeSapio, A., Tokuyasu, T.A., Sheppard, D., Akhurst, R.J., 2012. Epistatic interactions between *Tgfb1* and genetic loci, *Tgfbm2* and *Tgfbm3*, determine susceptibility to an asthmatic stimulus. *Proceedings of the National Academy of Sciences of the United States of America*. **109**, 18042-18047.
- Frodin, M., Jensen, C.J., Merienne, K., Gammeltoft, S., 2000. A phosphoserine-regulated docking site in the protein kinase RSK2 that recruits and activates PDK1. *The EMBO Journal*. **19**, 2924-2934.
- Furukawa, T., Sunamura, M., Motoi, F., Matsuno, S., Horii, A., 2003. Potential tumor suppressive pathway involving DUSP6/MKP-3 in pancreatic cancer. *The American Journal of Pathology*. **162**, 1807-1815.
- Galli, S., Jahn, O., Hitt, R., Hesse, D., Opitz, L., Plessmann, U., Urlaub, H., Poderoso, J.J., Jares-Erijman, E.A., Jovin, T.M., 2009. A new paradigm for MAPK: structural interactions of hERK1 with mitochondria in HeLa cells. *PloS One*. **4**, e7541.
- Garnett, M.J. & Marais, R., 2004. Guilty as charged: B-RAF is a human oncogene. *Cancer Cell*. **6**, 313-319.

- Garnett, M.J., Rana, S., Paterson, H., Barford, D., Marais, R., 2005. Wild-type and mutant B-RAF activate C-RAF through distinct mechanisms involving heterodimerization. *Molecular Cell*. **20**, 963-969.
- Gerlinger, M., Rowan, A.J., Horswell, S., Larkin, J., Endesfelder, D., Gronroos, E., Martinez, P., Matthews, N., Stewart, A., Tarpey, P., Varela, I., Phillimore, B., Begum, S., McDonald, N.Q., Butler, A., Jones, D., Raine, K., Latimer, C., Santos, C.R., Nohadani, M., Eklund, A.C., Spencer-Dene, B., Clark, G., Pickering, L., Stamp, G., Gore, M., Szallasi, Z., Downward, J., Futreal, P.A., Swanton, C., 2012. Intratumor heterogeneity and branched evolution revealed by multiregion sequencing. *The New England Journal of Medicine*. **366**, 883-892.
- Gibbs, J.B., Sigal, I.S., Poe, M., Scolnick, E.M., 1984. Intrinsic GTPase activity distinguishes normal and oncogenic ras p21 molecules. *Proceedings of the National Academy of Sciences of the United States of America*. **81**, 5704-5708.
- Gille, H., Sharrocks, A.D., Shaw, P.E., 1992. Phosphorylation of transcription factor p62TCF by MAP kinase stimulates ternary complex formation at c-fos promoter. *Nature*. **358**, 414-417.
- Ginty, D.D., Bonni, A., Greenberg, M.E., 1994. Nerve growth factor activates a Ras-dependent protein kinase that stimulates c-fos transcription via phosphorylation of CREB. *Cell*. **77**, 713-725.
- Gonzalez-Garcia, A., Pritchard, C.A., Paterson, H.F., Mavria, G., Stamp, G., Marshall, C.J., 2005. RalGDS is required for tumor formation in a model of skin carcinogenesis. *Cancer Cell*. **7**, 219-226.
- Gorlin, R.J., Anderson, R.C., Moller, J.H., 1971. The Leopard (multiple lentiginos) syndrome revisited. *Birth Defects Original Article Series*. **07**, 110-115.
- Gowrishankar, K., Snoyman, S., Pupo, G.M., Becker, T.M., Kefford, R.F., Rizos, H., 2012. Acquired Resistance to BRAF Inhibition Can Confer Cross-Resistance to Combined BRAF/MEK Inhibition. *The Journal of Investigative Dermatology*.
- Greene, L.A. & Tischler, A.S., 1976. Establishment of a noradrenergic clonal line of rat adrenal pheochromocytoma cells which respond to nerve growth factor. *Proceedings of the National Academy of Sciences of the United States of America*. **73**, 2424-2428.
- Groom, L.A., Sneddon, A.A., Alessi, D.R., Dowd, S., Keyse, S.M., 1996. Differential regulation of the MAP, SAP and RK/p38 kinases by Pyst1, a novel cytosolic dual-specificity phosphatase. *The EMBO Journal*. **15**, 3621-3632.
- Gross, I., Bassit, B., Benezra, M., Licht, J.D., 2001. Mammalian sprouty proteins inhibit cell growth and differentiation by preventing ras activation. *The Journal of Biological Chemistry*. **276**, 46460-46468.

- Guerra, C., Mijimolle, N., Dhawahir, A., Dubus, P., Barradas, M., Serrano, M., Campuzano, V., Barbacid, M., 2003. Tumor induction by an endogenous K-ras oncogene is highly dependent on cellular context. *Cancer Cell*. **4**, 111-120.
- Gustafsson, B., Angelini, S., Sander, B., Christensson, B., Hemminki, K., Kumar, R., 2005. Mutations in the BRAF and N-ras genes in childhood acute lymphoblastic leukaemia. *Leukemia : Official Journal of the Leukemia Society of America, Leukemia Research Fund, U.K.* **19**, 310-312.
- Hacohen, N., Kramer, S., Sutherland, D., Hiromi, Y., Krasnow, M.A., 1998. sprouty encodes a novel antagonist of FGF signaling that patterns apical branching of the *Drosophila* airways. *Cell*. **92**, 253-263.
- Hainsworth, J.D., Cebotaru, C.L., Kanarev, V., Ciuleanu, T.E., Damyanov, D., Stella, P., Ganchev, H., Pover, G., Morris, C., Tzekova, V., 2010. A phase II, open-label, randomized study to assess the efficacy and safety of AZD6244 (ARRY-142886) versus pemetrexed in patients with non-small cell lung cancer who have failed one or two prior chemotherapeutic regimens. *Journal of Thoracic Oncology : Official Publication of the International Association for the Study of Lung Cancer*. **5**, 1630-1636.
- Hanafusa, H., Torii, S., Yasunaga, T., Nishida, E., 2002. Sprouty1 and Sprouty2 provide a control mechanism for the Ras/MAPK signalling pathway. *Nature Cell Biology*. **4**, 850-858.
- Hanahan, D. & Weinberg, R.A., 2011. Hallmarks of cancer: the next generation. *Cell*. **144**, 646-674.
- Hankinson, S.E., Willett, W.C., Colditz, G.A., Hunter, D.J., Michaud, D.S., Deroo, B., Rosner, B., Speizer, F.E., Pollak, M., 1998. Circulating concentrations of insulin-like growth factor-I and risk of breast cancer. *Lancet*. **351**, 1393-1396.
- Hatzivassiliou, G., Song, K., Yen, I., Brandhuber, B.J., Anderson, D.J., Alvarado, R., Ludlam, M.J., Stokoe, D., Gloor, S.L., Vigers, G., Morales, T., Aliagas, I., Liu, B., Sideris, S., Hoefflich, K.P., Jaiswal, B.S., Seshagiri, S., Koeppen, H., Belvin, M., Friedman, L.S., Malek, S., 2010. RAF inhibitors prime wild-type RAF to activate the MAPK pathway and enhance growth. *Nature*.
- Haura, E.B., Ricart, A.D., Larson, T.G., Stella, P.J., Bazhenova, L., Miller, V.A., Cohen, R.B., Eisenberg, P.D., Selaru, P., Wilner, K.D., Gadgeel, S.M., 2010. A phase II study of PD-0325901, an oral MEK inhibitor, in previously treated patients with advanced non-small cell lung cancer. *Clinical Cancer Research : An Official Journal of the American Association for Cancer Research*. **16**, 2450-2457.
- Hayes, D.N., Lucas, A.S., Tanvetyanon, T., Krzyzanowska, M.K., Chung, C.H., Murphy, B.A., Gilbert, J., Mehra, R., Moore, D.T., Sheikh, A., Hoskins, J., Hayward, M.C., Zhao, N., O'Connor, W., Weck, K.E., Cohen, R.B., Cohen, E.E., 2012. Phase II efficacy and pharmacogenomic study of Selumetinib (AZD6244;

- ARRY-142886) in iodine-131 refractory papillary thyroid carcinoma with or without follicular elements. *Clinical Cancer Research : An Official Journal of the American Association for Cancer Research*. **18**, 2056-2065.
- Heidorn, S.J., Milagre, C., Whittaker, S., Nourry, A., Niculescu-Duvas, I., Dhomen, N., Hussain, J., Reis-Filho, J.S., Springer, C.J., Pritchard, C., Marais, R., 2010. Kinase-Dead BRAF and Oncogenic RAS Cooperate to Drive Tumor Progression through CRAF. *Cell*. **140**, 209-221.
- Hekman, M., Fischer, A., Wennogle, L.P., Wang, Y.K., Campbell, S.L., Rapp, U.R., 2005. Novel C-Raf phosphorylation sites: serine 296 and 301 participate in Raf regulation. *FEBS Letters*. **579**, 464-468.
- Henderson, Y.C., Chen, Y., Frederick, M.J., Lai, S.Y., Clayman, G.L., 2010. MEK inhibitor PD0325901 significantly reduces the growth of papillary thyroid carcinoma cells in vitro and in vivo. *Molecular Cancer Therapeutics*. **9**, 1968-1976.
- Hennekam, R.C., 2003. Costello syndrome: an overview. *American Journal of Medical Genetics. Part C, Seminars in Medical Genetics*. **117C**, 42-48.
- Herber, B., Truss, M., Beato, M., Muller, R., 1994. Inducible regulatory elements in the human cyclin D1 promoter. *Oncogene*. **9**, 1295-1304.
- Hipskind, R.A., Buscher, D., Nordheim, A., Baccarini, M., 1994. Ras/MAP kinase-dependent and -independent signaling pathways target distinct ternary complex factors. *Genes & Development*. **8**, 1803-1816.
- Hodgkin, J., 1980. More sex-determination mutants of *Caenorhabditis elegans*. *Genetics*. **96**, 649-664.
- Hou, P., Liu, D., Xing, M., 2007. The T1790A BRAF mutation (L597Q) in childhood acute lymphoblastic leukemia is a functional oncogene. *Leukemia : Official Journal of the Leukemia Society of America, Leukemia Research Fund, U.K.* **21**, 2216-2218.
- Hu, C.D., Kariya, K., Kotani, G., Shirouzu, M., Yokoyama, S., Kataoka, T., 1997. Coassociation of Rap1A and Ha-Ras with Raf-1 N-terminal region interferes with ras-dependent activation of Raf-1. *The Journal of Biological Chemistry*. **272**, 11702-11705.
- Huff, K., End, D., Guroff, G., 1981. Nerve growth factor-induced alteration in the response of PC12 pheochromocytoma cells to epidermal growth factor. *The Journal of Cell Biology*. **88**, 189-198.
- Huser, M., Luckett, J., Chiloeches, A., Mercer, K., Iwobi, M., Giblett, S., Sun, X.M., Brown, J., Marais, R., Pritchard, C., 2001. MEK kinase activity is not necessary for Raf-1 function. *The EMBO Journal*. **20**, 1940-1951.

- Huynh, H., Soo, K.C., Chow, P.K., Tran, E., 2007. Targeted inhibition of the extracellular signal-regulated kinase pathway with AZD6244 (ARRY-142886) in the treatment of hepatocellular carcinoma. *Molecular Cancer Therapeutics*. **6**, 138-146.
- International Human Genome Sequencing Consortium, 2004. Finishing the euchromatic sequence of the human genome. *Nature*. **431**, 931-945.
- Jackson, E.L., Willis, N., Mercer, K., Bronson, R.T., Crowley, D., Montoya, R., Jacks, T., Tuveson, D.A., 2001. Analysis of lung tumor initiation and progression using conditional expression of oncogenic K-ras. *Genes & Development*. **15**, 3243-3248.
- Jessenberger, V., Procyk, K.J., Ruth, J., Schreiber, M., Theussl, H.C., Wagner, E.F., Baccarini, M., 2001. Protective role of Raf-1 in Salmonella-induced macrophage apoptosis. *The Journal of Experimental Medicine*. **193**, 353-364.
- Jiang, C.C., Lai, F., Thorne, R.F., Yang, F., Liu, H., Hersey, P., Zhang, X.D., 2011. MEK-independent survival of B-RAFV600E melanoma cells selected for resistance to apoptosis induced by the RAF inhibitor PLX4720. *Clinical Cancer Research : An Official Journal of the American Association for Cancer Research*. **17**, 721-730.
- Johannessen, C.M., Boehm, J.S., Kim, S.Y., Thomas, S.R., Wardwell, L., Johnson, L.A., Emery, C.M., Stransky, N., Cogdill, A.P., Barretina, J., Caponigro, G., Hieronymus, H., Murray, R.R., Salehi-Ashtiani, K., Hill, D.E., Vidal, M., Zhao, J.J., Yang, X., Alkan, O., Kim, S., Harris, J.L., Wilson, C.J., Myer, V.E., Finan, P.M., Root, D.E., Roberts, T.M., Golub, T., Flaherty, K.T., Dummer, R., Weber, B.L., Sellers, W.R., Schlegel, R., Wargo, J.A., Hahn, W.C., Garraway, L.A., 2010. COT drives resistance to RAF inhibition through MAP kinase pathway reactivation. *Nature*. **468**, 968-972.
- Johnson, L., Mercer, K., Greenbaum, D., Bronson, R.T., Crowley, D., Tuveson, D.A., Jacks, T., 2001. Somatic activation of the K-ras oncogene causes early onset lung cancer in mice. *Nature*. **410**, 1111-1116.
- Jones, D.T., Kocialkowski, S., Liu, L., Pearson, D.M., Backlund, L.M., Ichimura, K., Collins, V.P., 2008. Tandem duplication producing a novel oncogenic BRAF fusion gene defines the majority of pilocytic astrocytomas. *Cancer Research*. **68**, 8673-8677.
- Joseph, E.W., Pratilas, C.A., Poulikakos, P.I., Tadi, M., Wang, W., Taylor, B.S., Halilovic, E., Persaud, Y., Xing, F., Viale, A., Tsai, J., Chapman, P.B., Bollag, G., Solit, D.B., Rosen, N., 2010. The RAF inhibitor PLX4032 inhibits ERK signaling and tumor cell proliferation in a V600E BRAF-selective manner.
- Lin, A.W., Barradas, M., Stone, J.C., van Aelst, L., Serrano, M., Lowe, S.W., 1998. Premature senescence involving p53 and p16 is activated in response to constitutive MEK/MAPK mitogenic signaling. *Genes & Development*. **12**, 3008-3019.

Proceedings of the National Academy of Sciences of the United States of America. **107**, 14903-14908.

Kamata, T., Hussain, J., Giblett, S., Hayward, R., Marais, R., Pritchard, C., 2010. BRAF inactivation drives aneuploidy by deregulating CRAF. *Cancer Research.* **70**, 8475-8486.

Kamijo, T., Weber, J.D., Zambetti, G., Zindy, F., Roussel, M.F., Sherr, C.J., 1998. Functional and physical interactions of the ARF tumor suppressor with p53 and Mdm2. *Proceedings of the National Academy of Sciences of the United States of America.* **95**, 8292-8297.

Karasarides, M., Chloeches, A., Hayward, R., Niculescu-Duvaz, D., Scanlon, I., Friedlos, F., Ogilvie, L., Hedley, D., Martin, J., Marshall, C.J., Springer, C.J., Marais, R., 2004. B-RAF is a therapeutic target in melanoma. *Oncogene.* **23**, 6292-6298.

Karlsson, M., Mathers, J., Dickinson, R.J., Mandl, M., Keyse, S.M., 2004. Both nuclear-cytoplasmic shuttling of the dual specificity phosphatase MKP-3 and its ability to anchor MAP kinase in the cytoplasm are mediated by a conserved nuclear export signal. *The Journal of Biological Chemistry.* **279**, 41882-41891.

Karreth, F.A., DeNicola, G.M., Winter, S.P., Tuveson, D.A., 2009. C-Raf inhibits MAPK activation and transformation by B-Raf(V600E). *Molecular Cell.* **36**, 477-486.

Karreth, F.A., Frese, K.K., DeNicola, G.M., Baccarini, M., Tuveson, D.A., 2011. C-Raf is required for the initiation of lung cancer by K-Ras(G12D). *Cancer Discovery.* **1**, 128-136.

Keilhack, H., David, F.S., McGregor, M., Cantley, L.C., Neel, B.G., 2005. Diverse biochemical properties of Shp2 mutants. Implications for disease phenotypes. *The Journal of Biological Chemistry.* **280**, 30984-30993.

Kerr, B., Allanson, J., Delrue, M.A., Gripp, K.W., Lacombe, D., Lin, A.E., Rauen, K.A., 2008. The diagnosis of Costello syndrome: nomenclature in Ras/MAPK pathway disorders. *American Journal of Medical Genetics.Part A.* **146A**, 1218-1220.

Keyse, S.M., 2008. Dual-specificity MAP kinase phosphatases (MKPs) and cancer. *Cancer Metastasis Reviews.* **27**, 253-261.

Keyse, S.M. & Emslie, E.A., 1992. Oxidative stress and heat shock induce a human gene encoding a protein-tyrosine phosphatase. *Nature.* **359**, 644-647.

King, A.J., Patrick, D.R., Batorsky, R.S., Ho, M.L., Do, H.T., Zhang, S.Y., Kumar, R., Rusnak, D.W., Takle, A.K., Wilson, D.M., Hugger, E., Wang, L., Karreth, F., Loughheed, J.C., Lee, J., Chau, D., Stout, T.J., May, E.W., Rominger, C.M., Schaber, M.D., Luo, L., Lakdawala, A.S., Adams, J.L., Contractor, R.G., Smalley, K.S., Herlyn, M., Morrissey, M.M., Tuveson, D.A.,

- Huang, P.S., 2006. Demonstration of a genetic therapeutic index for tumors expressing oncogenic BRAF by the kinase inhibitor SB-590885. *Cancer Research*. **66**, 11100-11105.
- King, A.J., Sun, H., Diaz, B., Barnard, D., Miao, W., Bagrodia, S., Marshall, M.S., 1998. The protein kinase Pak3 positively regulates Raf-1 activity through phosphorylation of serine 338. *Nature*. **396**, 180-183.
- Kirkwood, J.M., Bastholt, L., Robert, C., Sosman, J., Larkin, J., Hersey, P., Middleton, M., Cantarini, M., Zazulina, V., Kemsley, K., Dummer, R., 2012. Phase II, open-label, randomized trial of the MEK1/2 inhibitor selumetinib as monotherapy versus temozolomide in patients with advanced melanoma. *Clinical Cancer Research : An Official Journal of the American Association for Cancer Research*. **18**, 555-567.
- Kolch, W., 2000. Meaningful relationships: the regulation of the Ras/Raf/MEK/ERK pathway by protein interactions. *The Biochemical Journal*. **351 Pt 2**, 289-305.
- Koudova, M., Seemanova, E., Zenker, M., 2009. Novel BRAF mutation in a patient with LEOPARD syndrome and normal intelligence. *European Journal of Medical Genetics*. **52**, 337-340.
- Kovary, K. & Bravo, R., 1991. The jun and fos protein families are both required for cell cycle progression in fibroblasts. *Molecular and Cellular Biology*. **11**, 4466-4472.
- Kramer, S., Okabe, M., Hacohen, N., Krasnow, M.A., Hiromi, Y., 1999. Sprouty: a common antagonist of FGF and EGF signaling pathways in *Drosophila*. *Development (Cambridge, England)*. **126**, 2515-2525.
- Kratz, C.P., Rapisuwon, S., Reed, H., Hasle, H., Rosenberg, P.S., 2011. Cancer in Noonan, Costello, cardiofaciocutaneous and LEOPARD syndromes. *American Journal of Medical Genetics. Part C, Seminars in Medical Genetics*. **157**, 83-89.
- Kubicek, M., Pacher, M., Abraham, D., Podar, K., Eulitz, M., Baccarini, M., 2002. Dephosphorylation of Ser-259 regulates Raf-1 membrane association. *The Journal of Biological Chemistry*. **277**, 7913-7919.
- Kuburovic, V., Vukomanovic, V., Carcavilla, A., Ezquieta-Zubicaray, B., Kuburovic, N., 2011. Two cases of LEOPARD syndrome--RAF1 mutations firstly described in children. *The Turkish Journal of Pediatrics*. **53**, 687-691.
- Kwabi-Addo, B., Wang, J., Erdem, H., Vaid, A., Castro, P., Ayala, G., Ittmann, M., 2004. The expression of Sprouty1, an inhibitor of fibroblast growth factor signal transduction, is decreased in human prostate cancer. *Cancer Research*. **64**, 4728-4735.

- Kwak, S.P., Hakes, D.J., Martell, K.J., Dixon, J.E., 1994. Isolation and characterization of a human dual specificity protein-tyrosine phosphatase gene. *The Journal of Biological Chemistry*. **269**, 3596-3604.
- Landis, M.W., Pawlyk, B.S., Li, T., Sicinski, P., Hinds, P.W., 2006. Cyclin D1-dependent kinase activity in murine development and mammary tumorigenesis. *Cancer Cell*. **9**, 13-22.
- Lee, H.Y., Suh, Y.A., Lee, J.I., Hassan, K.A., Mao, L., Force, T., Gilbert, B.E., Jacks, T., Kurie, J.M., 2002. Inhibition of oncogenic K-ras signaling by aerosolized gene delivery in a mouse model of human lung cancer. *Clinical Cancer Research : An Official Journal of the American Association for Cancer Research*. **8**, 2970-2975.
- Levy-Nissenbaum, O., Sagi-Assif, O., Kapon, D., Hantisteanu, S., Burg, T., Raanani, P., Avigdor, A., Ben-Bassat, I., Witz, I.P., 2003a. Dual-specificity phosphatase Pyst2-L is constitutively highly expressed in myeloid leukemia and other malignant cells. *Oncogene*. **22**, 7649-7660.
- Levy-Nissenbaum, O., Sagi-Assif, O., Raanani, P., Avigdor, A., Ben-Bassat, I., Witz, I.P., 2003b. Overexpression of the dual-specificity MAPK phosphatase PYST2 in acute leukemia. *Cancer Letters*. **199**, 185-192.
- Light, Y., Paterson, H., Marais, R., 2002. 14-3-3 antagonizes Ras-mediated Raf-1 recruitment to the plasma membrane to maintain signaling fidelity. *Molecular and Cellular Biology*. **22**, 4984-4996.
- Liu, D., Liu, Z., Condouris, S., Xing, M., 2007a. BRAF V600E maintains proliferation, transformation, and tumorigenicity of BRAF-mutant papillary thyroid cancer cells. *The Journal of Clinical Endocrinology and Metabolism*. **92**, 2264-2271.
- Liu, Y., Lagowski, J., Sundholm, A., Sundberg, A., Kulesz-Martin, M., 2007b. Microtubule disruption and tumor suppression by mitogen-activated protein kinase phosphatase 4. *Cancer Research*. **67**, 10711-10719.
- Lo, T.L., Yusoff, P., Fong, C.W., Guo, K., McCaw, B.J., Phillips, W.A., Yang, H., Wong, E.S., Leong, H.F., Zeng, Q., Putti, T.C., Guy, G.R., 2004. The ras/mitogen-activated protein kinase pathway inhibitor and likely tumor suppressor proteins, sprouty 1 and sprouty 2 are deregulated in breast cancer. *Cancer Research*. **64**, 6127-6136.
- Loda, M., Capodiceci, P., Mishra, R., Yao, H., Corless, C., Grigioni, W., Wang, Y., Magi-Galluzzi, C., Stork, P.J., 1996. Expression of mitogen-activated protein kinase phosphatase-1 in the early phases of human epithelial carcinogenesis. *The American Journal of Pathology*. **149**, 1553-1564.
- Loonstra, A., Vooijs, M., Beverloo, H.B., Allak, B.A., van Drunen, E., Kanaar, R., Berns, A., Jonkers, J., 2001. Growth inhibition and DNA damage induced by

Cre recombinase in mammalian cells. *Proceedings of the National Academy of Sciences of the United States of America*. **98**, 9209-9214.

Lorusso, P.M., Adjei, A.A., Varterasian, M., Gadgeel, S., Reid, J., Mitchell, D.Y., Hanson, L., DeLuca, P., Bruzek, L., Piens, J., Asbury, P., Van Becelaere, K., Herrera, R., Sebolt-Leopold, J., Meyer, M.B., 2005. Phase I and pharmacodynamic study of the oral MEK inhibitor CI-1040 in patients with advanced malignancies. *Journal of Clinical Oncology : Official Journal of the American Society of Clinical Oncology*. **23**, 5281-5293.

Luo, Z., Diaz, B., Marshall, M.S., Avruch, J., 1997. An intact Raf zinc finger is required for optimal binding to processed Ras and for ras-dependent Raf activation in situ. *Molecular and Cellular Biology*. **17**, 46-53.

Luo, Z., Tzivion, G., Belshaw, P.J., Vavvas, D., Marshall, M., Avruch, J., 1996. Oligomerization activates c-Raf-1 through a Ras-dependent mechanism. *Nature*. **383**, 181-185.

Madhunapantula, S.V., Sharma, A., Robertson, G.P., 2007. PRAS40 deregulates apoptosis in malignant melanoma. *Cancer Research*. **67**, 3626-3636.

Maemondo, M., Inoue, A., Kobayashi, K., Sugawara, S., Oizumi, S., Isobe, H., Gemma, A., Harada, M., Yoshizawa, H., Kinoshita, I., Fujita, Y., Okinaga, S., Hirano, H., Yoshimori, K., Harada, T., Ogura, T., Ando, M., Miyazawa, H., Tanaka, T., Saijo, Y., Hagiwara, K., Morita, S., Nukiwa, T., North-East Japan Study Group, 2010. Gefitinib or chemotherapy for non-small-cell lung cancer with mutated EGFR. *The New England Journal of Medicine*. **362**, 2380-2388.

Mandl, M., Slack, D.N., Keyse, S.M., 2005. Specific inactivation and nuclear anchoring of extracellular signal-regulated kinase 2 by the inducible dual-specificity protein phosphatase DUSP5. *Molecular and Cellular Biology*. **25**, 1830-1845.

Marais, R., Light, Y., Paterson, H.F., Marshall, C.J., 1995. Ras recruits Raf-1 to the plasma membrane for activation by tyrosine phosphorylation. *The EMBO Journal*. **14**, 3136-3145.

Marais, R., Light, Y., Paterson, H.F., Mason, C.S., Marshall, C.J., 1997. Differential regulation of Raf-1, A-Raf, and B-Raf by oncogenic ras and tyrosine kinases. *The Journal of Biological Chemistry*. **272**, 4378-4383.

Marais, R., Wynne, J., Treisman, R., 1993. The SRF accessory protein Elk-1 contains a growth factor-regulated transcriptional activation domain. *Cell*. **73**, 381-393.

March, H.N., Rust, A.G., Wright, N.A., ten Hoeve, J., de Ridder, J., Eldridge, M., van der Weyden, L., Berns, A., Gadiot, J., Uren, A., Kemp, R., Arends, M.J., Wessels, L.F., Winton, D.J., Adams, D.J., 2011. Insertional mutagenesis

identifies multiple networks of cooperating genes driving intestinal tumorigenesis. *Nature Genetics*. **43**, 1202-1209.

Marchetti, S., Gimond, C., Chambard, J.C., Touboul, T., Roux, D., Pouyssegur, J., Pages, G., 2005. Extracellular signal-regulated kinases phosphorylate mitogen-activated protein kinase phosphatase 3/DUSP6 at serines 159 and 197, two sites critical for its proteasomal degradation. *Molecular and Cellular Biology*. **25**, 854-864.

Marin, T.M., Keith, K., Davies, B., Conner, D.A., Guha, P., Kalaitzidis, D., Wu, X., Lauriol, J., Wang, B., Bauer, M., Bronson, R., Franchini, K.G., Neel, B.G., Kontaridis, M.I., 2011. Rapamycin reverses hypertrophic cardiomyopathy in a mouse model of LEOPARD syndrome-associated PTPN11 mutation. *The Journal of Clinical Investigation*. **121**, 1026-1043.

Marquette, A., Andre, J., Bagot, M., Bensussan, A., Dumaz, N., 2011. ERK and PDE4 cooperate to induce RAF isoform switching in melanoma. *Nature Structural & Molecular Biology*. **18**, 584-591.

Marshall, C.J., 1995. Specificity of receptor tyrosine kinase signaling: transient versus sustained extracellular signal-regulated kinase activation. *Cell*. **80**, 179-185.

Marusyk, A., Almendro, V., Polyak, K., 2012. Intra-tumour heterogeneity: a looking glass for cancer? *Nature Reviews.Cancer*. **12**, 323-334.

Mason, C.S., Springer, C.J., Cooper, R.G., Superti-Furga, G., Marshall, C.J., Marais, R., 1999. Serine and tyrosine phosphorylations cooperate in Raf-1, but not B-Raf activation. *The EMBO Journal*. **18**, 2137-2148.

Masuda, K., Shima, H., Watanabe, M., Kikuchi, K., 2001. MKP-7, a novel mitogen-activated protein kinase phosphatase, functions as a shuttle protein. *The Journal of Biological Chemistry*. **276**, 39002-39011.

McCubrey, J.A., Milella, M., Tafuri, A., Martelli, A.M., Lunghi, P., Bonati, A., Cervello, M., Lee, J.T., Steelman, L.S., 2008. Targeting the Raf/MEK/ERK pathway with small-molecule inhibitors. *Current Opinion in Investigational Drugs* (London, England : 2000). **9**, 614-630.

McGrath, J.P., Capon, D.J., Goeddel, D.V., Levinson, A.D., 1984. Comparative biochemical properties of normal and activated human ras p21 protein. *Nature*. **310**, 644-649.

McKie, A.B., Douglas, D.A., Olijslagers, S., Graham, J., Omar, M.M., Heer, R., Gnanapragasam, V.J., Robson, C.N., Leung, H.Y., 2005. Epigenetic inactivation of the human sprouty2 (hSPRY2) homologue in prostate cancer. *Oncogene*. **24**, 2166-2174.

- Mebratu, Y. & Tesfaigzi, Y., 2009. How ERK1/2 activation controls cell proliferation and cell death: Is subcellular localization the answer? *Cell Cycle* (Georgetown, Tex.). **8**, 1168-1175.
- Mercer, K., Giblett, S., Green, S., Lloyd, D., DaRocha Dias, S., Plumb, M., Marais, R., Pritchard, C., 2005. Expression of endogenous oncogenic V600E-B-raf induces proliferation and developmental defects in mice and transformation of primary fibroblasts. *Cancer Research*. **65**, 11493-11500.
- Mercer, K.E. & Pritchard, C.A., 2003. Raf proteins and cancer: B-Raf is identified as a mutational target. *Biochimica Et Biophysica Acta*. **1653**, 25-40.
- Middleton, M.R., Grob, J.J., Aaronson, N., Fierlbeck, G., Tilgen, W., Seiter, S., Gore, M., Aamdal, S., Cebon, J., Coates, A., Dreno, B., Henz, M., Schadendorf, D., Kapp, A., Weiss, J., Fraass, U., Statkevich, P., Muller, M., Thatcher, N., 2000. Randomized phase III study of temozolomide versus dacarbazine in the treatment of patients with advanced metastatic malignant melanoma. *Journal of Clinical Oncology : Official Journal of the American Society of Clinical Oncology*. **18**, 158-166.
- Mielgo, A., Seguin, L., Huang, M., Camargo, M.F., Anand, S., Franovic, A., Weis, S.M., Advani, S.J., Murphy, E.A., Cheresch, D.A., 2011. A MEK-independent role for CRAF in mitosis and tumor progression. *Nature Medicine*. **17**, 1641-1645.
- Mikula, M., Schreiber, M., Husak, Z., Kucerova, L., Ruth, J., Wieser, R., Zatloukal, K., Beug, H., Wagner, E.F., Baccarini, M., 2001. Embryonic lethality and fetal liver apoptosis in mice lacking the c-raf-1 gene. *The EMBO Journal*. **20**, 1952-1962.
- Milagre, C., Dhomen, N., Geyer, F.C., Hayward, R., Lambros, M., Reis-Filho, J.S., Marais, R., 2010. A mouse model of melanoma driven by oncogenic KRAS. *Cancer Research*. **70**, 5549-5557.
- Mitsudomi, T., Morita, S., Yatabe, Y., Negoro, S., Okamoto, I., Tsurutani, J., Seto, T., Satouchi, M., Tada, H., Hirashima, T., Asami, K., Katakami, N., Takada, M., Yoshioka, H., Shibata, K., Kudoh, S., Shimizu, E., Saito, H., Toyooka, S., Nakagawa, K., Fukuoka, M., West Japan Oncology Group, 2010. Gefitinib versus cisplatin plus docetaxel in patients with non-small-cell lung cancer harbouring mutations of the epidermal growth factor receptor (WJTOG3405): an open label, randomised phase 3 trial. *The Lancet Oncology*. **11**, 121-128.
- Monick, M.M., Powers, L.S., Barrett, C.W., Hinde, S., Ashare, A., Groskreutz, D.J., Nyunoya, T., Coleman, M., Spitz, D.R., Hunninghake, G.W., 2008. Constitutive ERK MAPK activity regulates macrophage ATP production and mitochondrial integrity. *Journal of Immunology (Baltimore, Md.: 1950)*. **180**, 7485-7496.

Montagut, C., Sharma, S.V., Shioda, T., McDermott, U., Ulman, M., Ulkus, L.E., Dias-Santagata, D., Stubbs, H., Lee, D.Y., Singh, A., Drew, L., Haber, D.A., Settleman, J., 2008. Elevated CRAF as a potential mechanism of acquired resistance to BRAF inhibition in melanoma. *Cancer Research*. **68**, 4853-4861.

Mott, H.R., Carpenter, J.W., Zhong, S., Ghosh, S., Bell, R.M., Campbell, S.L., 1996. The solution structure of the Raf-1 cysteine-rich domain: a novel ras and phospholipid binding site. *Proceedings of the National Academy of Sciences of the United States of America*. **93**, 8312-8317.

Muda, M., Boschert, U., Smith, A., Antonsson, B., Gillieron, C., Chabert, C., Camps, M., Martinou, I., Ashworth, A., Arkinstall, S., 1997. Molecular cloning and functional characterization of a novel mitogen-activated protein kinase phosphatase, MKP-4. *The Journal of Biological Chemistry*. **272**, 5141-5151.

Muda, M., Theodosiou, A., Rodrigues, N., Boschert, U., Camps, M., Gillieron, C., Davies, K., Ashworth, A., Arkinstall, S., 1996. The dual specificity phosphatases M3/6 and MKP-3 are highly selective for inactivation of distinct mitogen-activated protein kinases. *The Journal of Biological Chemistry*. **271**, 27205-27208.

Muroya, K., Hattori, S., Nakamura, S., 1992. Nerve growth factor induces rapid accumulation of the GTP-bound form of p21ras in rat pheochromocytoma PC12 cells. *Oncogene*. **7**, 277-281.

Murphy, L.O., MacKeigan, J.P., Blenis, J., 2004. A network of immediate early gene products propagates subtle differences in mitogen-activated protein kinase signal amplitude and duration. *Molecular and Cellular Biology*. **24**, 144-153.

Murphy, L.O., Smith, S., Chen, R.H., Fingar, D.C., Blenis, J., 2002. Molecular interpretation of ERK signal duration by immediate early gene products. *Nature Cell Biology*. **4**, 556-564.

Murphy, T., Hori, S., Sewell, J., Gnanapragasam, V.J., 2010. Expression and functional role of negative signalling regulators in tumour development and progression. *International Journal of Cancer*. *Journal International Du Cancer*. **127**, 2491-2499.

Muslin, A.J., Tanner, J.W., Allen, P.M., Shaw, A.S., 1996. Interaction of 14-3-3 with signaling proteins is mediated by the recognition of phosphoserine. *Cell*. **84**, 889-897.

Muss, H.B., Thor, A.D., Berry, D.A., Kute, T., Liu, E.T., Koerner, F., Cirrincione, C.T., Budman, D.R., Wood, W.C., Barcos, M., 1994. c-erbB-2 expression and response to adjuvant therapy in women with node-positive early breast cancer. *The New England Journal of Medicine*. **330**, 1260-1266.

Nagase, T., Kikuno, R., Nakayama, M., Hirosawa, M., Ohara, O., 2000. Prediction of the coding sequences of unidentified human genes. XVIII. The

complete sequences of 100 new cDNA clones from brain which code for large proteins in vitro. *DNA Research : An International Journal for Rapid Publication of Reports on Genes and Genomes*. **7**, 273-281.

Nagel, R.L., 2005. Epistasis and the genetics of human diseases. *Comptes Rendus Biologies*. **328**, 606-615.

Nagel, R.L. & Steinberg, M.H., 2001. Role of epistatic (modifier) genes in the modulation of the phenotypic diversity of sickle cell anemia. *Pediatric Pathology & Molecular Medicine*. **20**, 123-136.

Nagy, A., 2000. Cre recombinase: the universal reagent for genome tailoring. *Genesis (New York, N.Y.: 2000)*. **26**, 99-109.

Nahta, R., Yu, D., Hung, M.C., Hortobagyi, G.N., Esteva, F.J., 2006. Mechanisms of disease: understanding resistance to HER2-targeted therapy in human breast cancer. *Nature Clinical Practice.Oncology*. **3**, 269-280.

Nakamura, T., Colbert, M., Krenz, M., Molkentin, J.D., Hahn, H.S., Dorn, G.W., 2nd, Robbins, J., 2007. Mediating ERK 1/2 signaling rescues congenital heart defects in a mouse model of Noonan syndrome. *The Journal of Clinical Investigation*. **117**, 2123-2132.

Nantel, A., Huber, M., Thomas, D.Y., 1999. Localization of endogenous Grb10 to the mitochondria and its interaction with the mitochondrial-associated Raf-1 pool. *The Journal of Biological Chemistry*. **274**, 35719-35724.

Nazarian, R., Shi, H., Wang, Q., Kong, X., Koya, R.C., Lee, H., Chen, Z., Lee, M.K., Attar, N., Sazegar, H., Chodon, T., Nelson, S.F., McArthur, G., Sosman, J.A., Ribas, A., Lo, R.S., 2010. Melanomas acquire resistance to B-RAF(V600E) inhibition by RTK or N-RAS upregulation. *Nature*. **468**, 973-977.

Neel, B.G., Gu, H., Pao, L., 2003. The 'Shp'ing news: SH2 domain-containing tyrosine phosphatases in cell signaling. *Trends in Biochemical Sciences*. **28**, 284-293.

Nichols, A., Camps, M., Gillieron, C., Chabert, C., Brunet, A., Wilsbacher, J., Cobb, M., Pouyssegur, J., Shaw, J.P., Arkinstall, S., 2000. Substrate recognition domains within extracellular signal-regulated kinase mediate binding and catalytic activation of mitogen-activated protein kinase phosphatase-3. *The Journal of Biological Chemistry*. **275**, 24613-24621.

Noguchi, T., Metz, R., Chen, L., Mattei, M.G., Carrasco, D., Bravo, R., 1993. Structure, mapping, and expression of erp, a growth factor-inducible gene encoding a nontransmembrane protein tyrosine phosphatase, and effect of ERP on cell growth. *Molecular and Cellular Biology*. **13**, 5195-5205.

Noonan, J.A., 1994. Noonan syndrome. An update and review for the primary pediatrician. *Clinical Pediatrics*. **33**, 548-555.

- Noonan, J.A., 1968. Hypertelorism with Turner phenotype. A new syndrome with associated congenital heart disease. *American Journal of Diseases of Children* (1960). **116**, 373-380.
- Nowell, P.C., 1976. The clonal evolution of tumor cell populations. *Science* (New York, N.Y.). **194**, 23-28.
- Ogawa, T., Takayama, K., Takakura, N., Kitano, S., Ueno, H., 2002. Anti-tumor angiogenesis therapy using soluble receptors: enhanced inhibition of tumor growth when soluble fibroblast growth factor receptor-1 is used with soluble vascular endothelial growth factor receptor. *Cancer Gene Therapy*. **9**, 633-640.
- Ohren, J.F., Chen, H., Pavlovsky, A., Whitehead, C., Zhang, E., Kuffa, P., Yan, C., McConnell, P., Spessard, C., Banotai, C., Mueller, W.T., Delaney, A., Omer, C., Sebolt-Leopold, J., Dudley, D.T., Leung, I.K., Flamme, C., Warmus, J., Kaufman, M., Barrett, S., Tecle, H., Hasemann, C.A., 2004. Structures of human MAP kinase kinase 1 (MEK1) and MEK2 describe novel noncompetitive kinase inhibition. *Nature Structural & Molecular Biology*. **11**, 1192-1197.
- Okudela, K., Yazawa, T., Woo, T., Sakaeda, M., Ishii, J., Mitsui, H., Shimoyamada, H., Sato, H., Tajiri, M., Ogawa, N., Masuda, M., Takahashi, T., Sugimura, H., Kitamura, H., 2009. Down-regulation of DUSP6 expression in lung cancer: its mechanism and potential role in carcinogenesis. *The American Journal of Pathology*. **175**, 867-881.
- Omerovic, J., Hammond, D.E., Clague, M.J., Prior, I.A., 2008. Ras isoform abundance and signalling in human cancer cell lines. *Oncogene*. **27**, 2754-2762.
- Ostman, A., 2004. PDGF receptors-mediators of autocrine tumor growth and regulators of tumor vasculature and stroma. *Cytokine & Growth Factor Reviews*. **15**, 275-286.
- Ozaki, K., Kadomoto, R., Asato, K., Tanimura, S., Itoh, N., Kohno, M., 2001. ERK pathway positively regulates the expression of Sprouty genes. *Biochemical and Biophysical Research Communications*. **285**, 1084-1088.
- Packer, L.M., East, P., Reis-Filho, J.S., Marais, R., 2009. Identification of direct transcriptional targets of (V600E)BRAF/MEK signalling in melanoma. *Pigment Cell & Melanoma Research*. **22**, 785-798.
- Packer, L.M., Rana, S., Hayward, R., O'Hare, T., Eide, C.A., Rebocho, A., Heidorn, S., Zabriskie, M.S., Niculescu-Duvaz, I., Druker, B.J., Springer, C., Marais, R., 2011. Nilotinib and MEK inhibitors induce synthetic lethality through paradoxical activation of RAF in drug-resistant chronic myeloid leukemia. *Cancer Cell*. **20**, 715-727.
- Paik, S., Bryant, J., Park, C., Fisher, B., Tan-Chiu, E., Hyams, D., Fisher, E.R., Lippman, M.E., Wickerham, D.L., Wolmark, N., 1998. *erbB-2* and response to

doxorubicin in patients with axillary lymph node-positive, hormone receptor-negative breast cancer. *Journal of the National Cancer Institute*. **90**, 1361-1370.

Palmero, I., Pantoja, C., Serrano, M., 1998. p19ARF links the tumour suppressor p53 to Ras. *Nature*. **395**, 125-126.

Pandit, B., Sarkozy, A., Pennacchio, L.A., Carta, C., Oishi, K., Martinelli, S., Pogna, E.A., Schackwitz, W., Ustaszewska, A., Landstrom, A., Bos, J.M., Ommen, S.R., Esposito, G., Lepri, F., Faul, C., Mundel, P., Lopez Siguero, J.P., Tenconi, R., Selicorni, A., Rossi, C., Mazzanti, L., Torrente, I., Marino, B., Digilio, M.C., Zampino, G., Ackerman, M.J., Dallapiccola, B., Tartaglia, M., Gelb, B.D., 2007. Gain-of-function RAF1 mutations cause Noonan and LEOPARD syndromes with hypertrophic cardiomyopathy. *Nature Genetics*. **39**, 1007-1012.

Papin, C., Denouel-Galy, A., Laugier, D., Calothy, G., Eychene, A., 1998. Modulation of kinase activity and oncogenic properties by alternative splicing reveals a novel regulatory mechanism for B-Raf. *The Journal of Biological Chemistry*. **273**, 24939-24947.

Paraiso, K.H., Fedorenko, I.V., Cantini, L.P., Munko, A.C., Hall, M., Sondak, V.K., Messina, J.L., Flaherty, K.T., Smalley, K.S., 2010. Recovery of phospho-ERK activity allows melanoma cells to escape from BRAF inhibitor therapy. *British Journal of Cancer*. **102**, 1724-1730.

Patel, S.P., Lazar, A.J., Papadopoulos, N.E., Liu, P., Infante, J.R., Glass, M.R., Vaughn, C.S., Lorusso, P.M., Cohen, R.B., Davies, M.A., Kim, K.B., 2012. Clinical responses to selumetinib (AZD6244; ARRY-142886)-based combination therapy stratified by gene mutations in patients with metastatic melanoma. *Cancer*.

Pavey, T., Hoyle, M., Ciani, O., Crathorne, L., Jones-Hughes, T., Cooper, C., Osipenko, L., Venkatachalam, M., Rudin, C., Ukoumunne, O., Garside, R., Anderson, R., 2012. Dasatinib, nilotinib and standard-dose imatinib for the first-line treatment of chronic myeloid leukaemia: systematic reviews and economic analyses. *Health Technology Assessment (Winchester, England)*. **16**, 1-277.

Pawson, T., 1995. Protein modules and signalling networks. *Nature*. **373**, 573-580.

Peyssonnaud, C., Provot, S., Felder-Schmittbuhl, M.P., Calothy, G., Eychene, A., 2000. Induction of postmitotic neuroretina cell proliferation by distinct Ras downstream signaling pathways. *Molecular and Cellular Biology*. **20**, 7068-7079.

Pierpont, E.I., Pierpont, M.E., Mendelsohn, N.J., Roberts, A.E., Tworog-Dube, E., Rauen, K.A., Seidenberg, M.S., 2010. Effects of germline mutations in the Ras/MAPK signaling pathway on adaptive behavior: cardiofaciocutaneous syndrome and Noonan syndrome. *American Journal of Medical Genetics. Part A*. **152A**, 591-600.

Plotnikov, A., Zehorai, E., Procaccia, S., Seger, R., 2011. The MAPK cascades: signaling components, nuclear roles and mechanisms of nuclear translocation. *Biochimica Et Biophysica Acta*. **1813**, 1619-1633.

Pollock, P.M., Harper, U.L., Hansen, K.S., Yudt, L.M., Stark, M., Robbins, C.M., Moses, T.Y., Hostetter, G., Wagner, U., Kakareka, J., Salem, G., Pohida, T., Heenan, P., Duray, P., Kallioniemi, O., Hayward, N.K., Trent, J.M., Meltzer, P.S., 2003. High frequency of BRAF mutations in nevi. *Nature Genetics*. **33**, 19-20.

Pomerantz, J., Schreiber-Agus, N., Liegeois, N.J., Silverman, A., Alland, L., Chin, L., Potes, J., Chen, K., Orlow, I., Lee, H.W., Cordon-Cardo, C., DePinho, R.A., 1998. The *Ink4a* tumor suppressor gene product, p19Arf, interacts with MDM2 and neutralizes MDM2's inhibition of p53. *Cell*. **92**, 713-723.

Poulikakos, P.I., Persaud, Y., Janakiraman, M., Kong, X., Ng, C., Moriceau, G., Shi, H., Atefi, M., Titz, B., Gabay, M.T., Salton, M., Dahlman, K.B., Tadi, M., Wargo, J.A., Flaherty, K.T., Kelley, M.C., Misteli, T., Chapman, P.B., Sosman, J.A., Graeber, T.G., Ribas, A., Lo, R.S., Rosen, N., Solit, D.B., 2011. RAF inhibitor resistance is mediated by dimerization of aberrantly spliced BRAF(V600E). *Nature*. **480**, 387-390.

Poulikakos, P.I., Zhang, C., Bollag, G., Shokat, K.M., Rosen, N., 2010. RAF inhibitors transactivate RAF dimers and ERK signalling in cells with wild-type BRAF. *Nature*.

Powell, M.B., Hyman, P., Bell, O.D., Balmain, A., Brown, K., Alberts, D., Bowden, G.T., 1995. Hyperpigmentation and melanocytic hyperplasia in transgenic mice expressing the human T24 Ha-ras gene regulated by a mouse tyrosinase promoter. *Molecular Carcinogenesis*. **12**, 82-90.

Pratilas, C.A., Taylor, B.S., Ye, Q., Viale, A., Sander, C., Solit, D.B., Rosen, N., 2009. (V600E)BRAF is associated with disabled feedback inhibition of RAF-MEK signaling and elevated transcriptional output of the pathway. *Proceedings of the National Academy of Sciences of the United States of America*. **106**, 4519-4524.

Preger, E., Ziv, I., Shabtay, A., Sher, I., Tsang, M., Dawid, I.B., Altuvia, Y., Ron, D., 2004. Alternative splicing generates an isoform of the human Sef gene with altered subcellular localization and specificity. *Proceedings of the National Academy of Sciences of the United States of America*. **101**, 1229-1234.

Prehoda, K.E., Lee, D.J., Lim, W.A., 1999. Structure of the enabled/VASP homology 1 domain-peptide complex: a key component in the spatial control of actin assembly. *Cell*. **97**, 471-480.

Prior, I.A. & Hancock, J.F., 2012. Ras trafficking, localization and compartmentalized signalling. *Seminars in Cell & Developmental Biology*. **23**, 145-153.

Pritchard, C.A., Bolin, L., Slattey, R., Murray, R., McMahon, M., 1996. Post-natal lethality and neurological and gastrointestinal defects in mice with targeted disruption of the A-Raf protein kinase gene. *Current Biology : CB*. **6**, 614-617.

Pritchard, C.A., Samuels, M.L., Bosch, E., McMahon, M., 1995. Conditionally oncogenic forms of the A-Raf and B-Raf protein kinases display different biological and biochemical properties in NIH 3T3 cells. *Molecular and Cellular Biology*. **15**, 6430-6442.

Pumiglia, K.M. & Decker, S.J., 1997a. Cell cycle arrest mediated by the MEK/mitogen-activated protein kinase pathway. *Proceedings of the National Academy of Sciences of the United States of America*. **94**, 448-452.

Pumiglia, K.M. & Decker, S.J., 1997b. Cell cycle arrest mediated by the MEK/mitogen-activated protein kinase pathway. *Proceedings of the National Academy of Sciences of the United States of America*. **94**, 448-452.

Pursiheimo, J.P., Kieksi, A., Jalkanen, M., Salmivirta, M., 2002. Protein kinase A balances the growth factor-induced Ras/ERK signaling. *FEBS Letters*. **521**, 157-164.

Qin, J., Xin, H., Nickoloff, B.J., 2012. Specifically targeting ERK1 or ERK2 kills melanoma cells. *Journal of Translational Medicine*. **10**, 15.

Rajagopalan, H., Bardelli, A., Lengauer, C., Kinzler, K.W., Vogelstein, B., Velculescu, V.E., 2002. Tumorigenesis: RAF/RAS oncogenes and mismatch-repair status. *Nature*. **418**, 934.

Rajakulendran, T., Sahmi, M., Lefrancois, M., Sicheri, F., Therrien, M., 2009. A dimerization-dependent mechanism drives RAF catalytic activation. *Nature*. **461**, 542-545.

Ranganathan, A., Pearson, G.W., Chrestensen, C.A., Sturgill, T.W., Cobb, M.H., 2006. The MAP kinase ERK5 binds to and phosphorylates p90 RSK. *Archives of Biochemistry and Biophysics*. **449**, 8-16.

Ratain, M.J., Eisen, T., Stadler, W.M., Flaherty, K.T., Kaye, S.B., Rosner, G.L., Gore, M., Desai, A.A., Patnaik, A., Xiong, H.Q., Rowinsky, E., Abbruzzese, J.L., Xia, C., Simantov, R., Schwartz, B., O'Dwyer, P.J., 2006. Phase II placebo-controlled randomized discontinuation trial of sorafenib in patients with metastatic renal cell carcinoma. *Journal of Clinical Oncology : Official Journal of the American Society of Clinical Oncology*. **24**, 2505-2512.

Rauen, K.A., 2006. Distinguishing Costello versus cardio-facio-cutaneous syndrome: BRAF mutations in patients with a Costello phenotype. *American Journal of Medical Genetics.Part A*. **140**, 1681-1683.

Rauen, K.A., Banerjee, A., Bishop, W.R., Lauchle, J.O., McCormick, F., McMahon, M., Melese, T., Munster, P.N., Nadaf, S., Packer, R.J., Sebolt-Leopold, J., Viskochil, D.H., 2011. Costello and cardio-facio-cutaneous

syndromes: Moving toward clinical trials in RASopathies. *American Journal of Medical Genetics. Part C, Seminars in Medical Genetics*. **157**, 136-146.

Rauhala, H.E., Porkka, K.P., Tolonen, T.T., Martikainen, P.M., Tammela, T.L., Visakorpi, T., 2005. Dual-specificity phosphatase 1 and serum/glucocorticoid-regulated kinase are downregulated in prostate cancer. *International Journal of Cancer. Journal International Du Cancer*. **117**, 738-745.

Ray, L.B. & Sturgill, T.W., 1988. Insulin-stimulated microtubule-associated protein kinase is phosphorylated on tyrosine and threonine in vivo. *Proceedings of the National Academy of Sciences of the United States of America*. **85**, 3753-3757.

Razzaque, M.A., Nishizawa, T., Komoike, Y., Yagi, H., Furutani, M., Amo, R., Kamisago, M., Momma, K., Katayama, H., Nakagawa, M., Fujiwara, Y., Matsushima, M., Mizuno, K., Tokuyama, M., Hirota, H., Muneuchi, J., Higashinakagawa, T., Matsuoka, R., 2007. Germline gain-of-function mutations in RAF1 cause Noonan syndrome. *Nature Genetics*. **39**, 1013-1017.

Rebocho, A.P. & Marais, R., 2012. ARAF acts as a scaffold to stabilize BRAF:CRAF heterodimers. *Oncogene*.

Ren, Y., Cheng, L., Rong, Z., Li, Z., Li, Y., Li, H., Wang, Z., Chang, Z., 2006. hSef co-localizes and interacts with Ras in the inhibition of Ras/MAPK signaling pathway. *Biochemical and Biophysical Research Communications*. **347**, 988-993.

Ries, S., Biederer, C., Woods, D., Shifman, O., Shirasawa, S., Sasazuki, T., McMahon, M., Oren, M., McCormick, F., 2000. Opposing effects of Ras on p53: transcriptional activation of mdm2 and induction of p19ARF. *Cell*. **103**, 321-330.

Rinehart, J., Adjei, A.A., Lorusso, P.M., Waterhouse, D., Hecht, J.R., Natale, R.B., Hamid, O., Varterasian, M., Asbury, P., Kaldjian, E.P., Gulyas, S., Mitchell, D.Y., Herrera, R., Sebolt-Leopold, J.S., Meyer, M.B., 2004. Multicenter phase II study of the oral MEK inhibitor, CI-1040, in patients with advanced non-small-cell lung, breast, colon, and pancreatic cancer. *Journal of Clinical Oncology : Official Journal of the American Society of Clinical Oncology*. **22**, 4456-4462.

Ritt, D.A., Monson, D.M., Specht, S.I., Morrison, D.K., 2010. Impact of feedback phosphorylation and Raf heterodimerization on normal and mutant B-Raf signaling. *Molecular and Cellular Biology*. **30**, 806-819.

Robbins, D.J., Zhen, E., Owaki, H., Vanderbilt, C.A., Ebert, D., Geppert, T.D., Cobb, M.H., 1993. Regulation and properties of extracellular signal-regulated protein kinases 1 and 2 in vitro. *The Journal of Biological Chemistry*. **268**, 5097-5106.

Roberts, A., Allanson, J., Jadico, S.K., Kavamura, M.I., Noonan, J., Opitz, J.M., Young, T., Neri, G., 2006. The cardiofaciocutaneous syndrome. *Journal of Medical Genetics*. **43**, 833-842.

Roberts, A.E., Araki, T., Swanson, K.D., Montgomery, K.T., Schiripo, T.A., Joshi, V.A., Li, L., Yassin, Y., Tamburino, A.M., Neel, B.G., Kucherlapati, R.S., 2007. Germline gain-of-function mutations in *SOS1* cause Noonan syndrome. *Nature Genetics*. **39**, 70-74.

Rodriguez-Viciano, P., Tetsu, O., Tidyman, W.E., Estep, A.L., Conger, B.A., Cruz, M.S., McCormick, F., Rauen, K.A., 2006. Germline mutations in genes within the MAPK pathway cause cardio-facio-cutaneous syndrome. *Science (New York, N.Y.)*. **311**, 1287-1290.

Rodriguez-Viciano, P., Warne, P.H., Dhand, R., Vanhaesebroeck, B., Gout, I., Fry, M.J., Waterfield, M.D., Downward, J., 1994. Phosphatidylinositol-3-OH kinase as a direct target of Ras. *Nature*. **370**, 527-532.

Roring, M., Herr, R., Fiala, G.J., Heilmann, K., Braun, S., Eisenhardt, A.E., Halbach, S., Capper, D., von Deimling, A., Schamel, W.W., Saunders, D.N., Brummer, T., 2012. Distinct requirement for an intact dimer interface in wild-type, V600E and kinase-dead B-Raf signalling. *The EMBO Journal*.

Rosell, R., Carcereny, E., Gervais, R., Vergnenegre, A., Massuti, B., Felip, E., Palmero, R., Garcia-Gomez, R., Pallares, C., Sanchez, J.M., Porta, R., Cobo, M., Garrido, P., Longo, F., Moran, T., Insa, A., De Marinis, F., Corre, R., Bover, I., Illiano, A., Dansin, E., de Castro, J., Milella, M., Reguart, N., Altavilla, G., Jimenez, U., Provencio, M., Moreno, M.A., Terrasa, J., Munoz-Langa, J., Valdivia, J., Isla, D., Domine, M., Molinier, O., Mazieres, J., Baize, N., Garcia-Campelo, R., Robinet, G., Rodriguez-Abreu, D., Lopez-Vivanco, G., Gebbia, V., Ferrera-Delgado, L., Bombaron, P., Bernabe, R., Bearz, A., Artal, A., Cortesi, E., Rolfo, C., Sanchez-Ronco, M., Drozdowskyj, A., Queralt, C., de Aguirre, I., Ramirez, J.L., Sanchez, J.J., Molina, M.A., Taron, M., Paz-Ares, L., Spanish Lung Cancer Group in collaboration with Groupe Francais de Pneumo-Cancerologie and Associazione Italiana Oncologia Toracica, 2012. Erlotinib versus standard chemotherapy as first-line treatment for European patients with advanced EGFR mutation-positive non-small-cell lung cancer (EURTAC): a multicentre, open-label, randomised phase 3 trial. *The Lancet Oncology*. **13**, 239-246.

Roskoski, R., Jr, 2012a. ERK1/2 MAP kinases: Structure, function, and regulation. *Pharmacological Research : The Official Journal of the Italian Pharmacological Society*.

Roskoski, R., Jr, 2012b. MEK1/2 dual-specificity protein kinases: structure and regulation. *Biochemical and Biophysical Research Communications*. **417**, 5-10.

Rosty, C., Aubriot, M.H., Cappellen, D., Bourdin, J., Cartier, I., Thiery, J.P., Sastre-Garau, X., Radvanyi, F., 2005. Clinical and biological characteristics of cervical neoplasias with FGFR3 mutation. *Molecular Cancer*. **4**, 15.

- Roth, F.P., Lipshitz, H.D., Andrews, B.J., 2009. Q&A: epistasis. *Journal of Biology*. **8**, 35.
- Rousseau, B., Larrieu-Lahargue, F., Javerzat, S., Guilhem-Ducleon, F., Beermann, F., Bikfalvi, A., 2004. The *tyrp1*-Tag/*tyrp1*-FGFR1-DN bigenic mouse: a model for selective inhibition of tumor development, angiogenesis, and invasion into the neural tissue by blockade of fibroblast growth factor receptor activity. *Cancer Research*. **64**, 2490-2495.
- Roy, S., Lane, A., Yan, J., McPherson, R., Hancock, J.F., 1997. Activity of plasma membrane-recruited Raf-1 is regulated by Ras via the Raf zinc finger. *The Journal of Biological Chemistry*. **272**, 20139-20145.
- Rushworth, L.K., Hindley, A.D., O'Neill, E., Kolch, W., 2006. Regulation and role of Raf-1/B-Raf heterodimerization. *Molecular and Cellular Biology*. **26**, 2262-2272.
- Sahai, E., Olson, M.F., Marshall, C.J., 2001. Cross-talk between Ras and Rho signalling pathways in transformation favours proliferation and increased motility. *The EMBO Journal*. **20**, 755-766.
- Sarkozy, A., Carta, C., Moretti, S., Zampino, G., Digilio, M.C., Pantaleoni, F., Scioletti, A.P., Esposito, G., Cordeddu, V., Lepri, F., Petrangeli, V., Dentici, M.L., Mancini, G.M., Selicorni, A., Rossi, C., Mazzanti, L., Marino, B., Ferrero, G.B., Silengo, M.C., Memo, L., Stanzial, F., Faravelli, F., Stuppia, L., Puxeddu, E., Gelb, B.D., Dallapiccola, B., Tartaglia, M., 2009. Germline BRAF mutations in Noonan, LEOPARD, and cardiofaciocutaneous syndromes: molecular diversity and associated phenotypic spectrum. *Human Mutation*. **30**, 695-702.
- Sasaki, A., Taketomi, T., Kato, R., Saeki, K., Nonami, A., Sasaki, M., Kuriyama, M., Saito, N., Shibuya, M., Yoshimura, A., 2003. Mammalian Sprouty4 suppresses Ras-independent ERK activation by binding to Raf1. *Nature Cell Biology*. **5**, 427-432.
- Sasaki, A., Taketomi, T., Wakioka, T., Kato, R., Yoshimura, A., 2001. Identification of a dominant negative mutant of Sprouty that potentiates fibroblast growth factor- but not epidermal growth factor-induced ERK activation. *The Journal of Biological Chemistry*. **276**, 36804-36808.
- Sauer, B. & Henderson, N., 1988. Site-specific DNA recombination in mammalian cells by the Cre recombinase of bacteriophage P1. *Proceedings of the National Academy of Sciences of the United States of America*. **85**, 5166-5170.
- Scheffler, J.E., Waugh, D.S., Bekesi, E., Kiefer, S.E., LoSardo, J.E., Neri, A., Prinzo, K.M., Tsao, K.L., Wegrzynski, B., Emerson, S.D., 1994. Characterization of a 78-residue fragment of c-Raf-1 that comprises a minimal binding domain for the interaction with Ras-GTP. *The Journal of Biological Chemistry*. **269**, 22340-22346.

- Schlessinger, J., 1994. SH2/SH3 signaling proteins. *Current Opinion in Genetics & Development*. **4**, 25-30.
- Schneider, T.C., Abdulrahman, R.M., Corssmit, E.P., Morreau, H., Smit, J.W., Kapiteijn, E., 2012. Long-term analysis of the efficacy and tolerability of sorafenib in advanced radio-iodine refractory differentiated thyroid carcinoma: final results of a phase II trial. *European Journal of Endocrinology / European Federation of Endocrine Societies*. **167**, 643-650.
- Schubbert, S., Zenker, M., Rowe, S.L., Boll, S., Klein, C., Bollag, G., van der Burgt, I., Musante, L., Kalscheuer, V., Wehner, L.E., Nguyen, H., West, B., Zhang, K.Y., Sistermans, E., Rauch, A., Niemeyer, C.M., Shannon, K., Kratz, C.P., 2006. Germline KRAS mutations cause Noonan syndrome. *Nature Genetics*. **38**, 331-336.
- Schuhmacher, A.J., Guerra, C., Sauzeau, V., Canamero, M., Bustelo, X.R., Barbacid, M., 2008. A mouse model for Costello syndrome reveals an Ang II-mediated hypertensive condition. *The Journal of Clinical Investigation*. **118**, 2169-2179.
- Sebolt-Leopold, J.S., 2004. MEK inhibitors: a therapeutic approach to targeting the Ras-MAP kinase pathway in tumors. *Current Pharmaceutical Design*. **10**, 1907-1914.
- Sebolt-Leopold, J.S., Dudley, D.T., Herrera, R., Van Becelaere, K., Wiland, A., Gowan, R.C., Tecle, H., Barrett, S.D., Bridges, A., Przybranowski, S., Leopold, W.R., Saltiel, A.R., 1999. Blockade of the MAP kinase pathway suppresses growth of colon tumors in vivo. *Nature Medicine*. **5**, 810-816.
- Serrano, M., Lin, A.W., McCurrach, M.E., Beach, D., Lowe, S.W., 1997. Oncogenic ras provokes premature cell senescence associated with accumulation of p53 and p16INK4a. *Cell*. **88**, 593-602.
- Sewing, A., Wiseman, B., Lloyd, A.C., Land, H., 1997. High-intensity Raf signal causes cell cycle arrest mediated by p21Cip1. *Molecular and Cellular Biology*. **17**, 5588-5597.
- Shao, Y. & Aplin, A.E., 2010. Akt3-mediated resistance to apoptosis in B-RAF-targeted melanoma cells. *Cancer Research*. **70**, 6670-6681.
- Sharma, A., Tran, M.A., Liang, S., Sharma, A.K., Amin, S., Smith, C.D., Dong, C., Robertson, G.P., 2006. Targeting mitogen-activated protein kinase/extracellular signal-regulated kinase kinase in the mutant (V600E) B-Raf signaling cascade effectively inhibits melanoma lung metastases. *Cancer Research*. **66**, 8200-8209.
- Sharp, L.L., Schwarz, D.A., Bott, C.M., Marshall, C.J., Hedrick, S.M., 1997. The influence of the MAPK pathway on T cell lineage commitment. *Immunity*. **7**, 609-618.

- Shaul, Y.D. & Seger, R., 2006. ERK1c regulates Golgi fragmentation during mitosis. *The Journal of Cell Biology*. **172**, 885-897.
- Shaulian, E. & Karin, M., 2001. AP-1 in cell proliferation and survival. *Oncogene*. **20**, 2390-2400.
- Shaw, A.T., Meissner, A., Dowdle, J.A., Crowley, D., Magendantz, M., Ouyang, C., Parisi, T., Rajagopal, J., Blank, L.J., Bronson, R.T., Stone, J.R., Tuveson, D.A., Jaenisch, R., Jacks, T., 2007. Sprouty-2 regulates oncogenic K-ras in lung development and tumorigenesis. *Genes & Development*. **21**, 694-707.
- Sherr, C.J., 1996. Cancer cell cycles. *Science (New York, N.Y.)*. **274**, 1672-1677.
- Sherr, C.J. & Roberts, J.M., 2004. Living with or without cyclins and cyclin-dependent kinases. *Genes & Development*. **18**, 2699-2711.
- Sherr, C.J. & Weber, J.D., 2000. The ARF/p53 pathway. *Current Opinion in Genetics & Development*. **10**, 94-99.
- Sheu, J.J., Guan, B., Tsai, F.J., Hsiao, E.Y., Chen, C.M., Seruca, R., Wang, T.L., Shih, I., 2012. Mutant BRAF induces DNA strand breaks, activates DNA damage response pathway, and up-regulates glucose transporter-1 in nontransformed epithelial cells. *The American Journal of Pathology*. **180**, 1179-1188.
- Shields, J.M., Pruitt, K., McFall, A., Shaub, A., Der, C.J., 2000. Understanding Ras: 'it ain't over 'til it's over'. *Trends in Cell Biology*. **10**, 147-154.
- Sicinska, E., Aifantis, I., Le Cam, L., Swat, W., Borowski, C., Yu, Q., Ferrando, A.A., Levin, S.D., Geng, Y., von Boehmer, H., Sicinski, P., 2003. Requirement for cyclin D3 in lymphocyte development and T cell leukemias. *Cancer Cell*. **4**, 451-461.
- Sievert, A.J., Jackson, E.M., Gai, X., Hakonarson, H., Judkins, A.R., Resnick, A.C., Sutton, L.N., Storm, P.B., Shaikh, T.H., Biegel, J.A., 2009. Duplication of 7q34 in pediatric low-grade astrocytomas detected by high-density single-nucleotide polymorphism-based genotype arrays results in a novel BRAF fusion gene. *Brain Pathology (Zurich, Switzerland)*. **19**, 449-458.
- Silver, D.P. & Livingston, D.M., 2001. Self-excising retroviral vectors encoding the Cre recombinase overcome Cre-mediated cellular toxicity. *Molecular Cell*. **8**, 233-243.
- Slack, D.N., Seternes, O.M., Gabrielsen, M., Keyse, S.M., 2001. Distinct binding determinants for ERK2/p38alpha and JNK map kinases mediate catalytic activation and substrate selectivity of map kinase phosphatase-1. *The Journal of Biological Chemistry*. **276**, 16491-16500.

- Slamon, D.J., Clark, G.M., Wong, S.G., Levin, W.J., Ullrich, A., McGuire, W.L., 1987. Human breast cancer: correlation of relapse and survival with amplification of the HER-2/neu oncogene. *Science (New York, N.Y.)*. **235**, 177-182.
- Smalley, K.S., Haass, N.K., Brafford, P.A., Lioni, M., Flaherty, K.T., Herlyn, M., 2006. Multiple signaling pathways must be targeted to overcome drug resistance in cell lines derived from melanoma metastases. *Molecular Cancer Therapeutics*. **5**, 1136-1144.
- Smalley, K.S., Xiao, M., Villanueva, J., Nguyen, T.K., Flaherty, K.T., Letrero, R., Van Belle, P., Elder, D.E., Wang, Y., Nathanson, K.L., Herlyn, M., 2009. CRAF inhibition induces apoptosis in melanoma cells with non-V600E BRAF mutations. *Oncogene*. **28**, 85-94.
- Solit, D.B., Garraway, L.A., Pratilas, C.A., Sawai, A., Getz, G., Basso, A., Ye, Q., Lobo, J.M., She, Y., Osman, I., Golub, T.R., Sebolt-Leopold, J., Sellers, W.R., Rosen, N., 2006. BRAF mutation predicts sensitivity to MEK inhibition. *Nature*. **439**, 358-362.
- Sondergaard, J.N., Nazarian, R., Wang, Q., Guo, D., Hsueh, T., Mok, S., Sazegar, H., MacConaill, L.E., Barretina, J.G., Kehoe, S.M., Attar, N., von Euw, E., Zuckerman, J.E., Chmielowski, B., Comin-Anduix, B., Koya, R.C., Mischel, P.S., Lo, R.S., Ribas, A., 2010. Differential sensitivity of melanoma cell lines with BRAFV600E mutation to the specific Raf inhibitor PLX4032. *Journal of Translational Medicine*. **8**, 39.
- Sosman, J.A., Kim, K.B., Schuchter, L., Gonzalez, R., Pavlick, A.C., Weber, J.S., McArthur, G.A., Hutson, T.E., Moschos, S.J., Flaherty, K.T., Hersey, P., Kefford, R., Lawrence, D., Puzanov, I., Lewis, K.D., Amaravadi, R.K., Chmielowski, B., Lawrence, H.J., Shyr, Y., Ye, F., Li, J., Nolop, K.B., Lee, R.J., Joe, A.K., Ribas, A., 2012. Survival in BRAF V600-mutant advanced melanoma treated with vemurafenib. *The New England Journal of Medicine*. **366**, 707-714.
- Stahl, J.M., Sharma, A., Cheung, M., Zimmerman, M., Cheng, J.Q., Bosenberg, M.W., Kester, M., Sandirasegarane, L., Robertson, G.P., 2004. Deregulated Akt3 activity promotes development of malignant melanoma. *Cancer Research*. **64**, 7002-7010.
- Stancato, L.F., Sakatsume, M., David, M., Dent, P., Dong, F., Petricoin, E.F., Krolewski, J.J., Silvennoinen, O., Saharinen, P., Pierce, J., Marshall, C.J., Sturgill, T., Finbloom, D.S., Lerner, A.C., 1997. Beta interferon and oncostatin M activate Raf-1 and mitogen-activated protein kinase through a JAK1-dependent pathway. *Molecular and Cellular Biology*. **17**, 3833-3840.
- Sternberg, N., Hamilton, D., Hoess, R., 1981. Bacteriophage P1 site-specific recombination. II. Recombination between loxP and the bacterial chromosome. *Journal of Molecular Biology*. **150**, 487-507.

- Stiller, C.A., Chessells, J.M., Fitchett, M., 1994. Neurofibromatosis and childhood leukaemia/lymphoma: a population-based UKCCSG study. *British Journal of Cancer*. **70**, 969-972.
- Storm, S.M., Brennscheidt, U., Sithanandam, G., Rapp, U.R., 1990. Raf Oncogenes in Carcinogenesis. *Critical Reviews in Oncogenesis*. **2**, 1-8.
- Stott, F.J., Bates, S., James, M.C., McConnell, B.B., Starborg, M., Brookes, S., Palmero, I., Ryan, K., Hara, E., Vousden, K.H., Peters, G., 1998. The alternative product from the human CDKN2A locus, p14(ARF), participates in a regulatory feedback loop with p53 and MDM2. *The EMBO Journal*. **17**, 5001-5014.
- Su, F., Bradley, W.D., Wang, Q., Yang, H., Xu, L., Higgins, B., Kolinsky, K., Packman, K., Kim, M.J., Trunzer, K., Lee, R.J., Schostack, K., Carter, J., Albert, T., Germer, S., Rosinski, J., Martin, M., Simcox, M.E., Lestini, B., Heimbrook, D., Bollag, G., 2012a. Resistance to Selective BRAF Inhibition Can Be Mediated by Modest Upstream Pathway Activation. *Cancer Research*. **72**, 969-978.
- Su, F., Viros, A., Milagre, C., Trunzer, K., Bollag, G., Spleiss, O., Reis-Filho, J.S., Kong, X., Koya, R.C., Flaherty, K.T., Chapman, P.B., Kim, M.J., Hayward, R., Martin, M., Yang, H., Wang, Q., Hilton, H., Hang, J.S., Noe, J., Lambros, M., Geyer, F., Dhomen, N., Niculescu-Duvaz, I., Zambon, A., Niculescu-Duvaz, D., Preece, N., Robert, L., Otte, N.J., Mok, S., Kee, D., Ma, Y., Zhang, C., Habets, G., Burton, E.A., Wong, B., Nguyen, H., Kockx, M., Andries, L., Lestini, B., Nolop, K.B., Lee, R.J., Joe, A.K., Troy, J.L., Gonzalez, R., Hutson, T.E., Puzanov, I., Chmielowski, B., Springer, C.J., McArthur, G.A., Sosman, J.A., Lo, R.S., Ribas, A., Marais, R., 2012b. RAS mutations in cutaneous squamous-cell carcinomas in patients treated with BRAF inhibitors. *The New England Journal of Medicine*. **366**, 207-215.
- Sugiura, K., Ozawa, S., Kitagawa, Y., Ueda, M., Kitajima, M., 2007. Co-expression of aFGF and FGFR-1 is predictive of a poor prognosis in patients with esophageal squamous cell carcinoma. *Oncology Reports*. **17**, 557-564.
- Sun, H., King, A.J., Diaz, H.B., Marshall, M.S., 2000. Regulation of the protein kinase Raf-1 by oncogenic Ras through phosphatidylinositol 3-kinase, Cdc42/Rac and Pak. *Current Biology : CB*. **10**, 281-284.
- Sundberg-Smith, L.J., Doherty, J.T., Mack, C.P., Taylor, J.M., 2005. Adhesion stimulates direct PAK1/ERK2 association and leads to ERK-dependent PAK1 Thr212 phosphorylation. *The Journal of Biological Chemistry*. **280**, 2055-2064.
- Sweet, R.W., Yokoyama, S., Kamata, T., Feramisco, J.R., Rosenberg, M., Gross, M., 1984. The product of ras is a GTPase and the T24 oncogenic mutant is deficient in this activity. *Nature*. **311**, 273-275.
- Takahashi, T., Yamaguchi, S., Chida, K., Shibuya, M., 2001. A single autophosphorylation site on KDR/Flk-1 is essential for VEGF-A-dependent

- activation of PLC-gamma and DNA synthesis in vascular endothelial cells. *The EMBO Journal*. **20**, 2768-2778.
- Takano, Y., Shiota, G., Kawasaki, H., 2000. Analysis of genomic imprinting of insulin-like growth factor 2 in colorectal cancer. *Oncology*. **59**, 210-216.
- Takehara, N., Kawabe, J., Aizawa, Y., Hasebe, N., Kikuchi, K., 2000. High glucose attenuates insulin-induced mitogen-activated protein kinase phosphatase-1 (MKP-1) expression in vascular smooth muscle cells. *Biochimica Et Biophysica Acta*. **1497**, 244-252.
- Tamura, Y., Simizu, S., Osada, H., 2004. The phosphorylation status and anti-apoptotic activity of Bcl-2 are regulated by ERK and protein phosphatase 2A on the mitochondria. *FEBS Letters*. **569**, 249-255.
- Tang, C.M. & Yu, J., 2012. Hypoxia-inducible factor-1 as a therapeutic target in cancer. *Journal of Gastroenterology and Hepatology*.
- Taniguchi, K., Kohno, R., Ayada, T., Kato, R., Ichiyama, K., Morisada, T., Oike, Y., Yonemitsu, Y., Maehara, Y., Yoshimura, A., 2007. Spreads are essential for embryonic lymphangiogenesis by regulating vascular endothelial growth factor receptor 3 signaling. *Molecular and Cellular Biology*. **27**, 4541-4550.
- Tanoue, T., Adachi, M., Moriguchi, T., Nishida, E., 2000. A conserved docking motif in MAP kinases common to substrates, activators and regulators. *Nature Cell Biology*. **2**, 110-116.
- Tanoue, T., Moriguchi, T., Nishida, E., 1999. Molecular cloning and characterization of a novel dual specificity phosphatase, MKP-5. *The Journal of Biological Chemistry*. **274**, 19949-19956.
- Tao, W. & Levine, A.J., 1999. P19(ARF) stabilizes p53 by blocking nucleocytoplasmic shuttling of Mdm2. *Proceedings of the National Academy of Sciences of the United States of America*. **96**, 6937-6941.
- Tartaglia, M., Martinelli, S., Stella, L., Bocchinfuso, G., Flex, E., Cordeddu, V., Zampino, G., Burgt, I., Palleschi, A., Petrucci, T.C., Sorcini, M., Schoch, C., Foa, R., Emanuel, P.D., Gelb, B.D., 2006. Diversity and functional consequences of germline and somatic PTPN11 mutations in human disease. *American Journal of Human Genetics*. **78**, 279-290.
- Tartaglia, M., Pennacchio, L.A., Zhao, C., Yadav, K.K., Fodale, V., Sarkozy, A., Pandit, B., Oishi, K., Martinelli, S., Schackwitz, W., Ustaszewska, A., Martin, J., Bristow, J., Carta, C., Lepri, F., Neri, C., Vasta, I., Gibson, K., Curry, C.J., Sigüero, J.P., Digilio, M.C., Zampino, G., Dallapiccola, B., Bar-Sagi, D., Gelb, B.D., 2007. Gain-of-function SOS1 mutations cause a distinctive form of Noonan syndrome. *Nature Genetics*. **39**, 75-79.
- Thor, A.D., Berry, D.A., Budman, D.R., Muss, H.B., Kute, T., Henderson, I.C., Barcos, M., Cirrincione, C., Edgerton, S., Allred, C., Norton, L., Liu, E.T., 1998.

erbB-2, p53, and efficacy of adjuvant therapy in lymph node-positive breast cancer. Journal of the National Cancer Institute. **90**, 1346-1360.

Tidyman, W.E. & Rauen, K.A., 2009. The RASopathies: developmental syndromes of Ras/MAPK pathway dysregulation. *Current Opinion in Genetics & Development.* **19**, 230-236.

Tidyman, W.E. & Rauen, K.A., 2008. Noonan, Costello and cardio-facio-cutaneous syndromes: dysregulation of the Ras-MAPK pathway. *Expert Reviews in Molecular Medicine.* **10**, e37.

Torii, S., Kusakabe, M., Yamamoto, T., Maekawa, M., Nishida, E., 2004. Sef is a spatial regulator for Ras/MAP kinase signaling. *Developmental Cell.* **7**, 33-44.

Trejo, C.L., Juan, J., Vicent, S., Sweet-Cordero, A., McMahon, M., 2012. MEK1/2 inhibition blocks development of autochthonous lung tumors induced by KRASG12D or BRAFV600E. *Cancer Research.*

Trimarchi, J.M. & Lees, J.A., 2002. Sibling rivalry in the E2F family. *Nature Reviews.Molecular Cell Biology.* **3**, 11-20.

Tsai, J., Lee, J.T., Wang, W., Zhang, J., Cho, H., Mamo, S., Bremer, R., Gillette, S., Kong, J., Haass, N.K., Sproesser, K., Li, L., Smalley, K.S., Fong, D., Zhu, Y.L., Marimuthu, A., Nguyen, H., Lam, B., Liu, J., Cheung, I., Rice, J., Suzuki, Y., Luu, C., Settachatgul, C., Shellooe, R., Cantwell, J., Kim, S.H., Schlessinger, J., Zhang, K.Y., West, B.L., Powell, B., Habets, G., Zhang, C., Ibrahim, P.N., Hirth, P., Artis, D.R., Herlyn, M., Bollag, G., 2008. Discovery of a selective inhibitor of oncogenic B-Raf kinase with potent antimelanoma activity. *Proceedings of the National Academy of Sciences of the United States of America.* **105**, 3041-3046.

Tsang, M., Friesel, R., Kudoh, T., Dawid, I.B., 2002. Identification of Sef, a novel modulator of FGF signalling. *Nature Cell Biology.* **4**, 165-169.

Tsao, H., Atkins, M.B., Sober, A.J., 2004. Management of cutaneous melanoma. *The New England Journal of Medicine.* **351**, 998-1012.

Tsavachidou, D., Coleman, M.L., Athanasiadis, G., Li, S., Licht, J.D., Olson, M.F., Weber, B.L., 2004. SPRY2 is an inhibitor of the ras/extracellular signal-regulated kinase pathway in melanocytes and melanoma cells with wild-type BRAF but not with the V599E mutant. *Cancer Research.* **64**, 5556-5559.

Turner, N. & Grose, R., 2010. Fibroblast growth factor signalling: from development to cancer. *Nature Reviews.Cancer.* **10**, 116-129.

Tuveson, D.A., Shaw, A.T., Willis, N.A., Silver, D.P., Jackson, E.L., Chang, S., Mercer, K.L., Grochow, R., Hock, H., Crowley, D., Hingorani, S.R., Zaks, T., King, C., Jacobetz, M.A., Wang, L., Bronson, R.T., Orkin, S.H., DePinho, R.A., Jacks, T., 2004. Endogenous oncogenic K-ras(G12D) stimulates proliferation

and widespread neoplastic and developmental defects. *Cancer Cell*. **5**, 375-387.

Tzivion, G., Luo, Z., Avruch, J., 1998. A dimeric 14-3-3 protein is an essential cofactor for Raf kinase activity. *Nature*. **394**, 88-92.

Urosevic, J., Sauzeau, V., Soto-Montenegro, M.L., Reig, S., Desco, M., Wright, E.M., Canamero, M., Mulero, F., Ortega, S., Bustelo, X.R., Barbacid, M., 2011. Constitutive activation of B-Raf in the mouse germ line provides a model for human cardio-facio-cutaneous syndrome. *Proceedings of the National Academy of Sciences of the United States of America*. **108**, 5015-5020.

van der Burgt, I., 2007. Noonan syndrome. *Orphanet Journal of Rare Diseases*. **2**, 4.

Vartanian, A.A., 2012. Signaling pathways in tumor vasculogenic mimicry. *Biochemistry.Biokhimiia*. **77**, 1044-1055.

Vasudev, N.S. & Larkin, J.M., 2011. Tyrosine kinase inhibitors in the treatment of advanced renal cell carcinoma: focus on pazopanib. *Clinical Medicine Insights.Oncology*. **5**, 333-342.

Vik, T.A. & Ryder, J.W., 1997. Identification of serine 380 as the major site of autophosphorylation of *Xenopus* pp90rsk. *Biochemical and Biophysical Research Communications*. **235**, 398-402.

Villanueva, J., Vultur, A., Lee, J.T., Somasundaram, R., Fukunaga-Kalabis, M., Cipolla, A.K., Wubbenhorst, B., Xu, X., Gimotty, P.A., Kee, D., Santiago-Walker, A.E., Letrero, R., D'Andrea, K., Pushparajan, A., Hayden, J.E., Brown, K.D., Laquerre, S., McArthur, G.A., Sosman, J.A., Nathanson, K.L., Herlyn, M., 2010. Acquired resistance to BRAF inhibitors mediated by a RAF kinase switch in melanoma can be overcome by cotargeting MEK and IGF-1R/PI3K. *Cancer Cell*. **18**, 683-695.

Vogt, P.K. & Bos, T.J., 1990. Jun: Oncogene and Transcription Factor. *Advances in Cancer Research*. **55**, 1-35.

Voice, J.K., Klemke, R.L., Le, A., Jackson, J.H., 1999. Four human ras homologs differ in their abilities to activate Raf-1, induce transformation, and stimulate cell motility. *The Journal of Biological Chemistry*. **274**, 17164-17170.

Wagle, N., Emery, C., Berger, M.F., Davis, M.J., Sawyer, A., Pochanard, P., Kehoe, S.M., Johannessen, C.M., Macconail, L.E., Hahn, W.C., Meyerson, M., Garraway, L.A., 2011. Dissecting therapeutic resistance to RAF inhibition in melanoma by tumor genomic profiling. *Journal of Clinical Oncology : Official Journal of the American Society of Clinical Oncology*. **29**, 3085-3096.

Wakioka, T., Sasaki, A., Kato, R., Shouda, T., Matsumoto, A., Miyoshi, K., Tsuneoka, M., Komiya, S., Baron, R., Yoshimura, A., 2001. Spry is a Sprouty-related suppressor of Ras signalling. *Nature*. **412**, 647-651.

Wan, P.T., Garnett, M.J., Roe, S.M., Lee, S., Niculescu-Duvaz, D., Good, V.M., Jones, C.M., Marshall, C.J., Springer, C.J., Barford, D., Marais, R., Cancer Genome Project, 2004. Mechanism of activation of the RAF-ERK signaling pathway by oncogenic mutations of B-RAF. *Cell*. **116**, 855-867.

Wang, H.G., Rapp, U.R., Reed, J.C., 1996. Bcl-2 targets the protein kinase Raf-1 to mitochondria. *Cell*. **87**, 629-638.

Wang, J., Liu, Y., Li, Z., Wang, Z., Tan, L.X., Ryu, M.J., Meline, B., Du, J., Young, K.H., Ranheim, E., Chang, Q., Zhang, J., 2011. Endogenous oncogenic Nras mutation initiates hematopoietic malignancies in a dose- and cell type-dependent manner. *Blood*. **118**, 368-379.

Wang, S., Ghosh, R.N., Chellappan, S.P., 1998. Raf-1 physically interacts with Rb and regulates its function: a link between mitogenic signaling and cell cycle regulation. *Molecular and Cellular Biology*. **18**, 7487-7498.

Wang, Y. & Becker, D., 1997. Antisense targeting of basic fibroblast growth factor and fibroblast growth factor receptor-1 in human melanomas blocks intratumoral angiogenesis and tumor growth. *Nature Medicine*. **3**, 887-893.

Wang, Y., Van Becelaere, K., Jiang, P., Przybranowski, S., Omer, C., Sebolt-Leopold, J., 2005. A role for K-ras in conferring resistance to the MEK inhibitor, CI-1040. *Neoplasia* (New York, N.Y.). **7**, 336-347.

Wartmann, M. & Davis, R.J., 1994. The native structure of the activated Raf protein kinase is a membrane-bound multi-subunit complex. *The Journal of Biological Chemistry*. **269**, 6695-6701.

Weber, C.K., Slupsky, J.R., Kalmes, H.A., Rapp, U.R., 2001a. Active Ras induces heterodimerization of cRaf and BRaf. *Cancer Research*. **61**, 3595-3598.

Weber, C.K., Slupsky, J.R., Kalmes, H.A., Rapp, U.R., 2001b. Active Ras induces heterodimerization of cRaf and BRaf. *Cancer Research*. **61**, 3595-3598.

Wellbrock, C., Karasarides, M., Marais, R., 2004. The RAF proteins take centre stage. *Nature Reviews.Molecular Cell Biology*. **5**, 875-885.

Wesche, J., Haglund, K., Haugsten, E.M., 2011. Fibroblast growth factors and their receptors in cancer. *The Biochemical Journal*. **437**, 199-213.

Whalen, A.M., Galasinski, S.C., Shapiro, P.S., Nahreini, T.S., Ahn, N.G., 1997. Megakaryocytic differentiation induced by constitutive activation of mitogen-activated protein kinase kinase. *Molecular and Cellular Biology*. **17**, 1947-1958.

Wickenden, J.A., Jin, H., Johnson, M., Gillings, A.S., Newson, C., Austin, M., Chell, S.D., Balmano, K., Pritchard, C.A., Cook, S.J., 2008. Colorectal cancer cells with the BRAF(V600E) mutation are addicted to the ERK1/2 pathway for

- growth factor-independent survival and repression of BIM. *Oncogene*. **27**, 7150-7161.
- Williams, V.C., Lucas, J., Babcock, M.A., Gutmann, D.H., Korf, B., Maria, B.L., 2009. Neurofibromatosis type 1 revisited. *Pediatrics*. **123**, 124-133.
- Willumsen, B.M., Christensen, A., Hubbert, N.L., Papageorge, A.G., Lowy, D.R., 1984. The p21 ras C-terminus is required for transformation and membrane association. *Nature*. **310**, 583-586.
- Wilson, T.R., Fridlyand, J., Yan, Y., Penuel, E., Burton, L., Chan, E., Peng, J., Lin, E., Wang, Y., Sosman, J., Ribas, A., Li, J., Moffat, J., Sutherlin, D.P., Koeppen, H., Merchant, M., Neve, R., Settleman, J., 2012. Widespread potential for growth-factor-driven resistance to anticancer kinase inhibitors. *Nature*. **487**, 505-509.
- Wojnowski, L., Stancato, L.F., Larner, A.C., Rapp, U.R., Zimmer, A., 2000. Overlapping and specific functions of Braf and Craf-1 proto-oncogenes during mouse embryogenesis. *Mechanisms of Development*. **91**, 97-104.
- Wojnowski, L., Stancato, L.F., Zimmer, A.M., Hahn, H., Beck, T.W., Larner, A.C., Rapp, U.R., Zimmer, A., 1998. Craf-1 protein kinase is essential for mouse development. *Mechanisms of Development*. **76**, 141-149.
- Wojnowski, P. & Patkowski, J., 1997. The significance of leukotrienes in pathophysiology of bronchial asthma--therapy perspectives. *Postepy Higieny i Medycyny Doswiadczalnej*. **51**, 499-514.
- Won, J.K., Yang, H.W., Shin, S.Y., Lee, J.H., Heo, W.D., Cho, K.H., 2012. The cross regulation between ERK and PI3K signaling pathways determines the tumoricidal efficacy of MEK inhibitor. *Journal of Molecular Cell Biology*.
- Woods, D., Parry, D., Cherwinski, H., Bosch, E., Lees, E., McMahon, M., 1997a. Raf-induced proliferation or cell cycle arrest is determined by the level of Raf activity with arrest mediated by p21Cip1. *Molecular and Cellular Biology*. **17**, 5598-5611.
- Woods, D., Parry, D., Cherwinski, H., Bosch, E., Lees, E., McMahon, M., 1997b. Raf-induced proliferation or cell cycle arrest is determined by the level of Raf activity with arrest mediated by p21Cip1. *Molecular and Cellular Biology*. **17**, 5598-5611.
- Workman, P., Clarke, P.A., Guillard, S., Raynaud, F.I., 2006. Drugging the PI3 kinome. *Nature Biotechnology*. **24**, 794-796.
- Wu, J.J., Zhang, L., Bennett, A.M., 2005. The noncatalytic amino terminus of mitogen-activated protein kinase phosphatase 1 directs nuclear targeting and serum response element transcriptional regulation. *Molecular and Cellular Biology*. **25**, 4792-4803.

- Wu, S., Wang, Y., Sun, L., Zhang, Z., Jiang, Z., Qin, Z., Han, H., Liu, Z., Li, X., Tang, A., Gui, Y., Cai, Z., Zhou, F., 2011. Decreased expression of dual-specificity phosphatase 9 is associated with poor prognosis in clear cell renal cell carcinoma. *BMC Cancer*. **11**, 413.
- Xia, K., Mukhopadhyay, N.K., Inhorn, R.C., Barber, D.L., Rose, P.E., Lee, R.S., Narsimhan, R.P., D'Andrea, A.D., Griffin, J.D., Roberts, T.M., 1996. The cytokine-activated tyrosine kinase JAK2 activates Raf-1 in a p21ras-dependent manner. *Proceedings of the National Academy of Sciences of the United States of America*. **93**, 11681-11686.
- Xie, P., Streu, C., Qin, J., Bregman, H., Pagano, N., Meggers, E., Marmorstein, R., 2009. The crystal structure of BRAF in complex with an organoruthenium inhibitor reveals a mechanism for inhibition of an active form of BRAF kinase. *Biochemistry*. **48**, 5187-5198.
- Xu, S., Furukawa, T., Kanai, N., Sunamura, M., Horii, A., 2005. Abrogation of DUSP6 by hypermethylation in human pancreatic cancer. *Journal of Human Genetics*. **50**, 159-167.
- Xue, C., Huang, Y., Huang, P.Y., Yu, Q.T., Pan, J.J., Liu, L.Z., Song, X.Q., Lin, S.J., Wu, J.X., Zhang, J.W., Zhao, H.Y., Xu, F., Liu, J.L., Hu, Z.H., Zhao, L.P., Zhao, Y.Y., Wu, X., Zhang, J., Ma, Y.X., Zhang, L., 2012. Phase II study of sorafenib in combination with cisplatin and 5-fluorouracil to treat recurrent or metastatic nasopharyngeal carcinoma. *Annals of Oncology : Official Journal of the European Society for Medical Oncology / ESMO*.
- Yan, J., Roy, S., Apolloni, A., Lane, A., Hancock, J.F., 1998. Ras isoforms vary in their ability to activate Raf-1 and phosphoinositide 3-kinase. *The Journal of Biological Chemistry*. **273**, 24052-24056.
- Yan, M. & Templeton, D.J., 1994. Identification of 2 serine residues of MEK-1 that are differentially phosphorylated during activation by raf and MEK kinase. *The Journal of Biological Chemistry*. **269**, 19067-19073.
- Yang, H., Higgins, B., Kolinsky, K., Packman, K., Bradley, W.D., Lee, R.J., Schostack, K., Simcox, M.E., Kopetz, S., Heimbrosk, D., Lestini, B., Bollag, G., Su, F., 2012. Antitumor activity of BRAF inhibitor vemurafenib in preclinical models of BRAF-mutant colorectal cancer. *Cancer Research*. **72**, 779-789.
- Yang, H., Higgins, B., Kolinsky, K., Packman, K., Go, Z., Iyer, R., Kolis, S., Zhao, S., Lee, R., Grippo, J.F., Schostack, K., Simcox, M.E., Heimbrosk, D., Bollag, G., Su, F., 2010. RG7204 (PLX4032), a selective BRAFV600E inhibitor, displays potent antitumor activity in preclinical melanoma models. *Cancer Research*. **70**, 5518-5527.
- Yang, J., Yu, Y., Duerksen-Hughes, P.J., 2003a. Protein kinases and their involvement in the cellular responses to genotoxic stress. *Mutation Research*. **543**, 31-58.

- Yang, R.B., Ng, C.K., Wasserman, S.M., Komuves, L.G., Gerritsen, M.E., Topper, J.N., 2003b. A novel interleukin-17 receptor-like protein identified in human umbilical vein endothelial cells antagonizes basic fibroblast growth factor-induced signaling. *The Journal of Biological Chemistry*. **278**, 33232-33238.
- Yazdi, A.S., Palmedo, G., Flaig, M.J., Puchta, U., Reckwerth, A., Rutten, A., Mentzel, T., Hugel, H., Hantschke, M., Schmid-Wendtner, M.H., Kutzner, H., Sander, C.A., 2003. Mutations of the BRAF gene in benign and malignant melanocytic lesions. *The Journal of Investigative Dermatology*. **121**, 1160-1162.
- Yee, D., 2012. Insulin-like growth factor receptor inhibitors: baby or the bathwater? *Journal of the National Cancer Institute*. **104**, 975-981.
- Yeh, T.C., Marsh, V., Bernat, B.A., Ballard, J., Colwell, H., Evans, R.J., Parry, J., Smith, D., Brandhuber, B.J., Gross, S., Marlow, A., Hurley, B., Lyssikatos, J., Lee, P.A., Winkler, J.D., Koch, K., Wallace, E., 2007. Biological characterization of ARRY-142886 (AZD6244), a potent, highly selective mitogen-activated protein kinase kinase 1/2 inhibitor. *Clinical Cancer Research : An Official Journal of the American Association for Cancer Research*. **13**, 1576-1583.
- Yeung, K., Seitz, T., Li, S., Janosch, P., McFerran, B., Kaiser, C., Fee, F., Katsanakis, K.D., Rose, D.W., Mischak, H., Sedivy, J.M., Kolch, W., 1999. Suppression of Raf-1 kinase activity and MAP kinase signalling by RKIP. *Nature*. **401**, 173-177.
- Yigzaw, Y., Cartin, L., Pierre, S., Scholich, K., Patel, T.B., 2001. The C terminus of sprouty is important for modulation of cellular migration and proliferation. *The Journal of Biological Chemistry*. **276**, 22742-22747.
- Yoshida, T., Hisamoto, T., Akiba, J., Koga, H., Nakamura, K., Tokunaga, Y., Hanada, S., Kumemura, H., Maeyama, M., Harada, M., Ogata, H., Yano, H., Kojiro, M., Ueno, T., Yoshimura, A., Sata, M., 2006. Spreds, inhibitors of the Ras/ERK signal transduction, are dysregulated in human hepatocellular carcinoma and linked to the malignant phenotype of tumors. *Oncogene*. **25**, 6056-6066.
- Yu, H., Spitz, M.R., Mistry, J., Gu, J., Hong, W.K., Wu, X., 1999. Plasma levels of insulin-like growth factor-I and lung cancer risk: a case-control analysis. *Journal of the National Cancer Institute*. **91**, 151-156.
- Yu, Q., Geng, Y., Sicinski, P., 2001. Specific protection against breast cancers by cyclin D1 ablation. *Nature*. **411**, 1017-1021.
- Yuen, S.T., Davies, H., Chan, T.L., Ho, J.W., Bignell, G.R., Cox, C., Stephens, P., Edkins, S., Tsui, W.W., Chan, A.S., Futreal, P.A., Stratton, M.R., Wooster, R., Leung, S.Y., 2002. Similarity of the phenotypic patterns associated with BRAF and KRAS mutations in colorectal neoplasia. *Cancer Research*. **62**, 6451-6455.

- Yusoff, P., Lao, D.H., Ong, S.H., Wong, E.S., Lim, J., Lo, T.L., Leong, H.F., Fong, C.W., Guy, G.R., 2002. *Sprouty2 inhibits the Ras/MAP kinase pathway by inhibiting the activation of Raf. The Journal of Biological Chemistry.* **277**, 3195-3201.
- Zhang, B.H. & Guan, K.L., 2000. *Activation of B-Raf kinase requires phosphorylation of the conserved residues Thr598 and Ser601. The EMBO Journal.* **19**, 5429-5439.
- Zheng, C.F. & Guan, K.L., 1994. *Activation of MEK family kinases requires phosphorylation of two conserved Ser/Thr residues. The EMBO Journal.* **13**, 1123-1131.
- Zhou, C., Wu, Y.L., Chen, G., Feng, J., Liu, X.Q., Wang, C., Zhang, S., Wang, J., Zhou, S., Ren, S., Lu, S., Zhang, L., Hu, C., Hu, C., Luo, Y., Chen, L., Ye, M., Huang, J., Zhi, X., Zhang, Y., Xiu, Q., Ma, J., Zhang, L., You, C., 2011. *Erlotinib versus chemotherapy as first-line treatment for patients with advanced EGFR mutation-positive non-small-cell lung cancer (OPTIMAL, CTONG-0802): a multicentre, open-label, randomised, phase 3 study. The Lancet Oncology.* **12**, 735-742.
- Zhu, J., Woods, D., McMahon, M., Bishop, J.M., 1998. *Senescence of human fibroblasts induced by oncogenic Raf. Genes & Development.* **12**, 2997-3007.
- Zimmermann, S. & Moelling, K., 1999. *Phosphorylation and regulation of Raf by Akt (protein kinase B). Science (New York, N.Y.).* **286**, 1741-1744.
- Zipser, M.C., Eichhoff, O.M., Widmer, D.S., Schlegel, N.C., Schoenewolf, N.L., Stuart, D., Liu, W., Gardner, H., Smith, P.D., Nuciforo, P., Dummer, R., Hoek, K.S., 2011. *A proliferative melanoma cell phenotype is responsive to RAF/MEK inhibition independent of BRAF mutation status. Pigment Cell & Melanoma Research.* **24**, 326-333.